USAARL Report No. 2003-09

Analysis of Head Motion in Rotary-Wing Flight Using Various Helmet-Mounted Display Configurations (Part II. Elevation)

By Ryan J. Rostad, Clarence E. Rash, and John S. Crowley

Aircrew Health and Performance Division
and
Aircrew Protection Division

May 2003

U S A A R L

U.S. Army
Aeromedical Research
Laboratory

Notice

Qualified requesters

Qualified requesters may obtain copies from the Defense Technical Information Center (DTIC), Cameron Station, Alexandria, Virginia 22314. Orders will be expedited if placed through the librarian or other person designated to request documents from DTIC.

Change of address

Organizations receiving reports from the U.S. Army Aeromedical Research Laboratory on automatic mailing lists should confirm correct address when corresponding about laboratory reports.

Disposition

Destroy this document when it is no longer needed. Do not return it to the originator.

Disclaimer

The views, opinions, and/or findings contained in this report are those of the author(s) and should not be construed as an official Department of the Army position, policy, or decision, unless so designated by other official documentation. Citation of trade names in this report does not constitute an official Department of the Army endorsement or approval of the use of such commercial items.

REPORT DOCUMENTATION PAGE

Form Approved
OMB No. 0704-0188

1a. REPORT SECURITY CLASSIFICATION
Unclassified

1b. RESTRICTIVE MARKINGS

2a. SECURITY CLASSIFICATION

3. DISTRIBUTION / AVAILABILITY OF REPORT
Approved for public release, distribution unlimited

2b. DECLASSIFICATION / DOWNGRADING

4. PERFORMING ORGANIZATION REPORT NUMBER(S)
USAARL Report No. 2003-09

5. MONITORING ORGANIZATION REPORT NUMBER(S)

6a. NAME OF PERFORMING ORGANIZATION
U.S. Army Aeromedical Research Laboratory

6b. OFFICE SYMBOL (If
MCMR-UAD

7a. NAME OF MONITORING ORGANIZATION
U.S. Army Medical Research and Materiel Command

6c. ADDRESS (City, State, and ZIP Code)
P.O. Box 620577
Fort Rucker, AL 36362-0577

7b. ADDRESS (City, State, and ZIP Code)
504 Scott Street
Fort Detrick, MD 21702-5012

8a. NAME OF FUNDING / SPONSORING ORGANIZATION

8b. OFFICE SYMBOL (If

9. PROCUREMENT INSTRUMENT IDENTIFICATION NUMBER

8c. ADDRESS (City, State, and ZIP Code)

10. SOURCE OF FUNDING NUMBERS

PROGRAM ELEMENT NO.	PROJECT NO.	TASK NO.	WORK UNIT ACCESSION NO.
622787A	879	P	DA361539

11. TITLE (Include Security Classification)
(U) Analysis of Head Motion in Rotary-Wing Flight Using Various Helmet-Mounted Display Configurations (Part II-Elevation)

12. PERSONAL AUTHOR(S)
Ryan J. Rostad, Clarence E. Rash, John S. Crowley

13a. TYPE OF REPORT	13b. TIME COVERED FROM TO	14. DATE OF REPORT (Year, Month,	15. PAGE COUNT
Final		2003 May	144

16. SUPPLEMENTAL NOTATION

17. COSATI CODES		
FIELD	GROUP	SUB-GROUP

18. SUBJECT TERMS (Continue on reverse if necessary and identify by block number)
Helmet-mounted displays (HMDs), head motion, head position, head tracking, elevation

19. ABSTRACT (Continue on reverse if necessary and identify by block number)
In spite of an immense increase in interest in helmet-mounted displays (HMDs) over the past two decades, there have been few studies on head motion while using HMDs in operational flight. Rotary-wing flights conducted using a number of HMD configurations have resulted in a head position database that will be useful in filling this void. Various analysis techniques have been applied to investigate characteristics of elevation head position distributions for a slalom flight maneuver for four visual environments: good visual environment (daytime, unaided), night vision goggles, HMD with thermal imagery, and HMD with thermal imagery and symbology.

20. DISTRIBUTION / AVAILABILITY OF
☑ UNCLASSIFIED/UNLIMITED ☐ SAME AS RPT. ☐ DTIC USERS

21. ABSTRACT SECURITY CLASSIFICATION
Unclassified

22a. NAME OF RESPONSIBLE INDIVIDUAL
Supervisor, Science Information Center

22b. TELEPHONE (Include Area
(334) 255-6907

22c. OFFICE SYMBOL
MCMR-UAX-SI

Table of contents

Table of contents (continued)

Page

List of figures

List of figures (continued)

Page

Table of contents (continued)
List of figures (continued)

Page

List of tables

Introduction

From the mid to late 1990s, the Defence Evaluation and Research Agency (DERA), Farnborough, United Kingdom, conducted a rotary-wing (helicopter) research effort known as the Day/Night All Weather (D/NAW) program. The principal aim of this program was to enable safe tactical helicopter flight in severely limited visibility. The major focus of the program was advanced helmet- or head-mounted display (HMD) technologies and the associated symbology design issues (Crowley, 1998).

HMDs are devices or systems that present the pilot(s) with pilotage imagery, flight information, and/or fire control (weaponry) imagery and symbology (Rash (Ed.), 1999). They are, by definition, head- or helmet-mounted systems. Melzer and Moffitt (1997) describe an HMD as minimally consisting of "an image source and collimating optics in a head mount." Rash (1999) expands this description to include a visual coupling system which performs the function of slaving head and/or eye positions and motions to one or more aircraft systems. Examples of rotary-wing HMDs include the U. S. Army's fielded Integrated Helmet and Display Sighting System (IHADSS) used on the AH-64 Apache attack helicopter and the under-development Helmet Integrated Display and Sight System (HIDSS) to be used on the RAH-66 Comanche helicopter.

From March to September 1997, under the auspices of the D/NAW program, a series of flights was flown to establish baseline flight performance for future HMD performance comparisons. These flights consisted of several flight path maneuvers (e.g., slalom, rapid egress, side-step, etc.) and visual environments, defined by the mode of visual information presentation (i.e., unaided day, using night vision goggles (NVGs), and using two HMD configurations). For safety considerations, all flights except with NVGs were conducted during the day.

As an aside to the normal flight performance parameters measured during the flights, head azimuth, elevation, and roll position data also were collected, not as part of the experimental design but as standard practice. This paper reports the analysis of the elevation data for the slalom maneuver. An analysis of azimuth head motion was presented in Rostad et al., 2001. (Roll data analyses will be presented in a future report.)

The availability of this head position data is advantageous for two reasons. First, extremely limited operational head position data have been presented in the literature. And, very little of this has been collected in the operational flight environment using HMDs. Second, for the same flights for which head position data are presented here, measures of motion sickness symptoms, pre- and postflight, were made. In order to test the hypothesis that motion sickness symptoms may be correlated with differences in head motion attributed to the different visual environments (or conversely, head motion is affected by the onset of motion sickness symptoms due to different visual environments), it is necessary to be able to describe the different visual environment head position distributions using a set of parameters (e.g., central moments).

Background

A major operational characteristic of HMDs is their capability to allow the pilot to control external imaging sensors and weapons via head movement. This head slaving capability is achieved through the use of head trackers of various technologies, e.g., mechanical, electro-optical, magnetic, ultrasonic, etc. Most recently, magnetic systems have been the most widely used head tracking technology and are considered to be relatively mature for use in the aviation environment (Borah, 1998). The performance of a head tracking system (sometimes referred to as a visually coupled system [VCS]) is determined by a number of parameters, which include motion box size, pointing angle accuracy, pointing angle resolution, update rate, and jitter. Specifications for these parameters usually are affected by the aircraft platform (fixed wing and rotary-wing). A more detailed discussion of tracking performance parameters can be found in Kocian and Task (1995).

Despite the immense popularity of HMDs, there has been only a relatively small increase in studies investigating visually coupled systems. Most of these studies have looked at the performance of head (or eye) tracking technologies (Borah, 1989; Robinson and Wetzel, 1989; and Cameron, Trythall and Barton, 1995) or head motion prediction (Azuma and Bishop, 1995; Curtis and Sowizral, 1994). However, there has been very limited data collected and made available on head position and velocity within the operational flight environment, especially for flights using HMDs.

Several anatomical and biomechanical studies have reported values for range of head motion for elevation (up and down). The reported ranges of these values, as well as for peak velocity and acceleration, are presented in Table 1. Note that only a few of the cited studies indicated clearly as to whether or not neck and shoulder participation was included in the reported values. Caution must be taken when reviewing the values for head motion in Table 1. These values, based on laboratory anatomical and biomechanical measures, would most likely be reduced in an operational cockpit where seat, restraint system and cockpit design present physical obstructions and other limits to allowable ranges of motion. In addition, it has been shown that head motion is reduced by inertial loading such as that induced by the increased head supported weight of HMDs (Gauthier, Martin and Stark, 1986), and the increased neck muscle loading associated with the use of HMDs increases fatigue which may indirectly reduce the frequency and range of head motion (Phillips and Petrofsky, 1983).

The studies summarized in Table 1 do not represent a description of head motion values as would be encountered in actual flight scenarios. Only two studies could be found which collected and presented head motion data during actual flight conditions. Szoboszlay et al. (1995) investigated the effect of field of view (FOV) restriction on rotary-wing pilot workload and performance in an instrumented NAH-1S Cobra. In this study, pilots executed seven flight maneuvers adapted from the U.S. Army Aeronautical Design Standard (ADS) 33D (U.S. Army Aviation and Troop Command, 1994). The flight maneuvers were slalom, acceleration/deceleration, hover, bob-up/turn/bob-down,

Table 1.
Reported anatomical and biomechanical elevation head motion ranges.

	Allen and Webb (1983)	Zangemeister and Stark (1981)	Sherk (1989)	Glanville and Kreezer (1937); Hertzberg (1972)	Durlach and Mavor (1995)
Elevation (total)	-10° to 25° See note.	---	---	-60° to 60°	---
-flexion only	---	---	54°-74°	---	---
-extension only	---	---	39°-93°	---	---
Peak velocity	---	---	---	---	300°/sec
Peak acceleration	---	551°/sec^2 for 5° head movement 3300°/sec^2 for 60° head movement	---	---	---

Note. Values do not include neck participation.

hovering turn, pirouette, and precision landing. These maneuvers were executed in the daytime under good visual conditions with no precipitation. Cockpit instruments were covered in order to force the pilot to rely on the outside scene cues. Trials were flown for six FOV configurations ranging from 20 degrees to 100 degrees in 20-degree increments and for an unrestricted (natural) FOV condition. One of the performance parameters measured was time spent at specific azimuth and elevation positions. Figure 1 shows the resulting histograms of the elevation angle, respectively, of the head position for a typical pilot during one of the bob-up maneuvers. The elevation histograms (Figure 2) show an increase in head motion as the horizontal FOV was decreased.

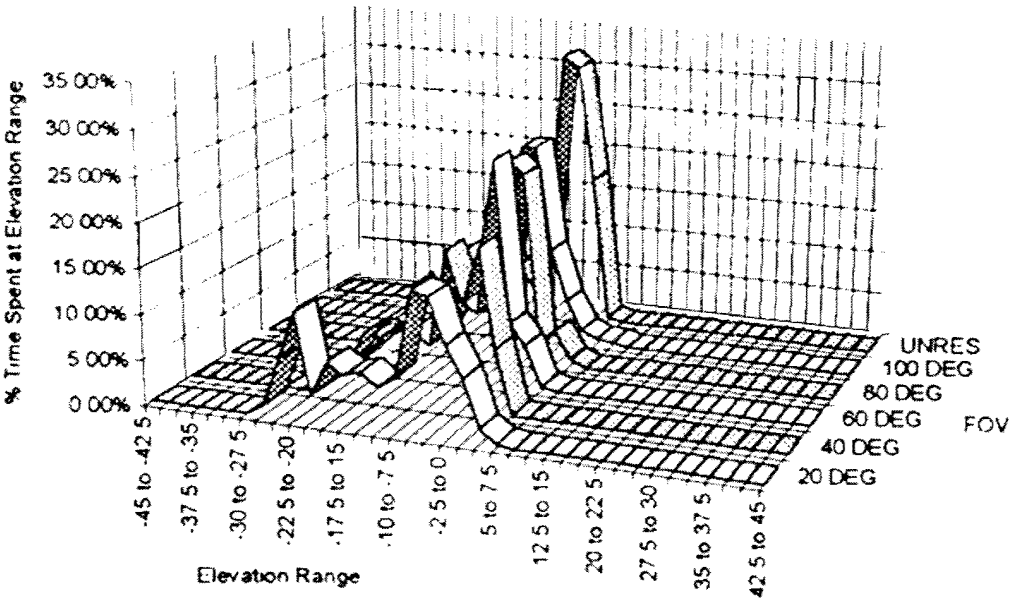

Figure 1. Head elevation angle histograms for a single pilot for the bob-up maneuver. (Szoboszlay et al., 1995).

Perhaps, the most pertinent study to this current paper was conducted by Verona et al. (1986), where head motion data were collected from six pilots as each flew a modified UH-1M Huey helicopter over a circular 15-mile contour course. (Data from one of the six pilots (#2) were not incorporated in the analysis due to loss of boresight.) All of the pilots were rated in the UH-1M aircraft, and pilot #4 was an Army MEDEVAC pilot with previous search and rescue experience. The pilots also were required to visually search for an "enemy" aircraft which could appear anywhere, while flying the contour coarse. A head tracking system was used to measure the pilot's head motion. The system provided coverage of ±180° azimuth and -90° to +30° elevation with 0.5° accuracy. The head tracking data were collected over two flights of 25-minute duration per pilot with head position samples taken every 40 milliseconds (ms). All of the flights and data acquisitions were conducted on the same day. Of the five remaining pilots, three flew in the morning and two flew in the afternoon. They were not told that head motion was the focus of the study; instead, they were advised that they were assessing a new helmet fit. The subject pilots sat in the left seat of the aircraft.

The first and last 3 minutes were not used in the analysis, which consisted of position and velocity frequency histograms for azimuth and elevation from the head tracking line-of-sight data. The elevation position histogram collapsed across the remaining five subjects is presented in Figure 2. Figure 3 shows the corresponding velocity histogram. The summary statistics for mean, median, standard deviation (SD), skewness and kurtosis, collapsed across the five pilots for elevation position, are presented in Table 2. Summary statistics for elevation velocities are presented in Table 3. Percent relative cumulative frequency curves for elevation velocities are presented in Figure 4.

The elevation position data and statistics, Figure 2 and Table 2, showed a range of -65° to +30°. (Note: 0° is directly in front of the left-seated pilot, not at the center of the aircraft.) The major peak occurred at -1°. The small hump at -40° corresponds to the position of the chin transparency in the lower front of the aircraft. The pilots spent 95 percent of their time between -14° and +14°; the pilots' heads remained essentially level. The standard deviations for elevation were not as large as for azimuth, as would be expected since elevation range of motion is more limited. The negative medians indicated the pilots were looking down more often than they were looking up.

Table 2.
Elevation position summary statistics.

Subject	Mean	Median	S.D.	Skewness	Kurtosis
Elevation position					
1	-3.73	-3.14	3.85	0.40	8.96
3	-3.03	-2.27	6.26	-2.64	20.00
4	-6.39	-3.24	12.31	-1.62	3.55
5	-2.32	0.47	7.25	-2.32	24.31
6	3.13	4.41	6.86	-3.67	26.32
All 5 subjects	-2.09	-1.08	8.46	-2.25	11.79

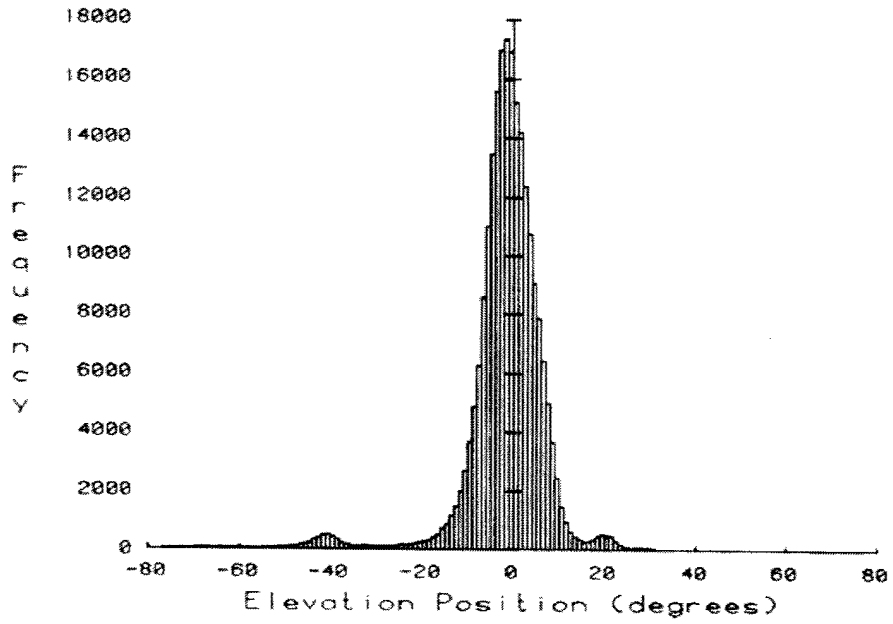

Figure 2. Frequency histograms for elevation position (Verona et al., 1986).

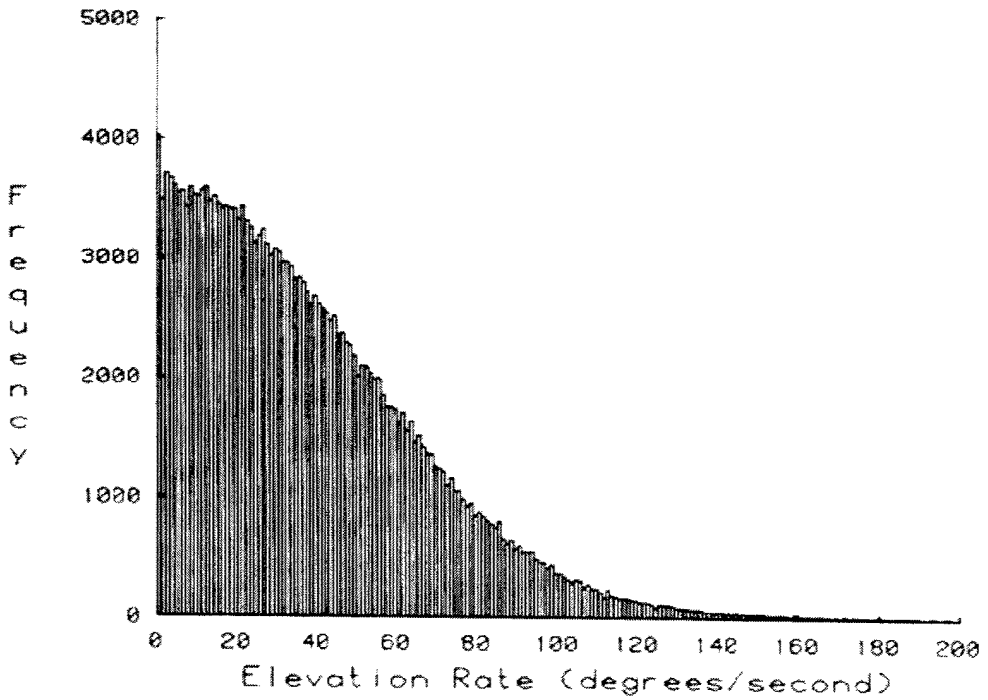

Figure 3. Frequency histogram for elevation velocity (Verona et al.,1986).

Table 3.
Elevation velocity summary statistics (Verona et al., 1986).

Subject	Mean	Median	S.D.	Skewness	Kurtosis
Elevation velocity					
1	36.23	30.91	28.10	1.11	1.52
3	37.08	32.10	28.11	0.99	1.07
4	35.78	29.71	29.57	1.45	2.96
5	43.69	38.73	32.15	1.04	1.37
6	37.16	32.08	28.81	1.19	1.98
All 5 subjects	37.93	32.50	29.46	1.17	1.81

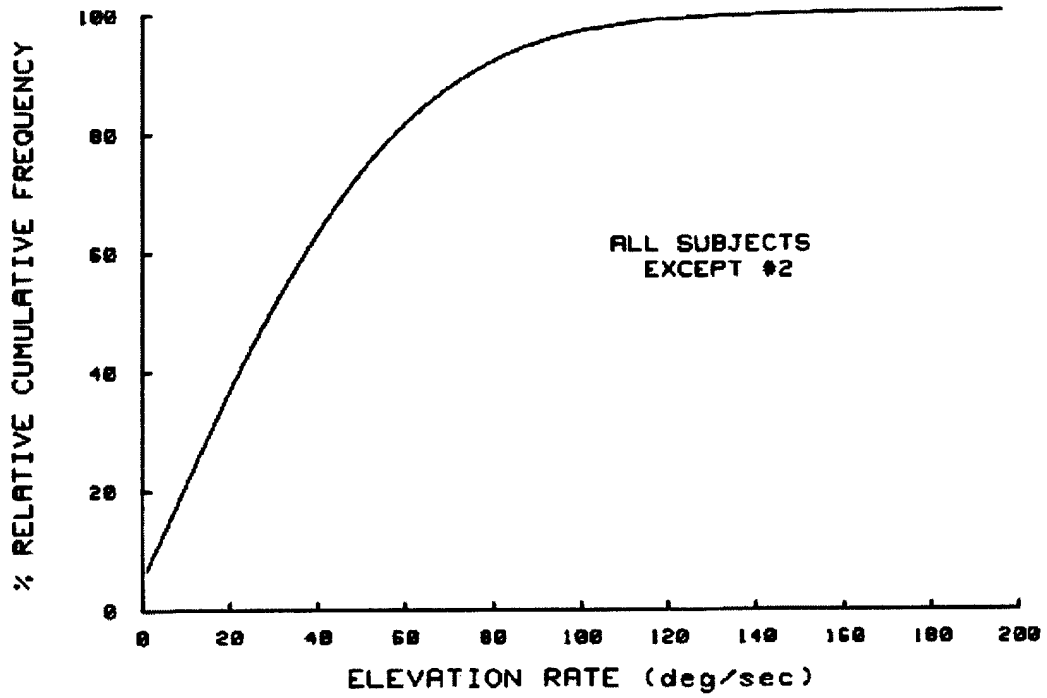

Figure 4. Percent relative cumulative frequency versus elevation velocity (Verona et al., 1986).

The summary of statistics for elevation velocities is presented in Table 3. The variability between subjects was greater than the variability within subjects, underlining the role of individual differences in search dynamics. The within-subject variability in the median ranged from approximately 1°/sec to 11°/sec, and between-subject differences in the median for all the pilots combined ranged from approximately 0°/sec to 9°/sec. In addition, the medians were again smaller than the means, indicating more data points at the lower velocities.

The relative cumulative frequency curves of the velocity data (Figure 4) indicated that 50 percent of the elevation velocities were less than or equal to 32°/sec. The curve also showed that 90 percent of the elevation velocities were less than or equal to 80°/sec. As an aside, approximately 98 percent of the elevation velocities were equal to or less than 120°/sec, the maximum slew rate of the thermal imaging system selected for the AH-64 Apache helicopter.

In a summary of Verona et al. (1986), it was found that the concentration of elevation head positions indicated that the pilots looked primarily forward, even though the flight scenario required a large range of head movements for the search task. In addition, this study supported a maximum slew rate of 120°/sec.

The findings presented herein attempt to expand the small database of elevation head position and velocity values for actual flight scenarios while wearing HMDs.

Experimental design

The original overall study design for the flights consisted of six flight maneuvers, two levels of aggressiveness (LOAs) and four visual conditions. Each of these factors is described in the sections below. A full flight trial was limited to approximately 90 minutes in duration. A flight was defined as consisting of a varying numbers of "runs" where a "run" was the completion of the full set of all six maneuvers at a given LOA by a single pilot for one of the four visual conditions. While the elements of the experimental design are briefly described in the following sections, detailed discussions can be found in Rostad et al., 2001.

Instrumentation

Aircraft

All flights were in a Lynx ZD285 helicopter (Figure 5), which is a standard Lynk AH Mk 7 airframe with Gem Mk 205 engines but modified to exclude infrared suppressors, missile mounts, or other role equipment. The aircraft was configured for two experimenters seated in the rear cabin; an evaluated pilot, who served as a subject, in the front left seat; and a safety pilot in the front right seat. The instrument panel was modified to provide the safety pilot with ready access to all normal cockpit instruments. The subject pilot was provided with a cut-down panel providing primary flight instruments only.

An additional aircraft modification was the outfitting of all forward cockpit windows (but not overhead windows) with custom amber-tinted panels. The purpose of this modification was to allow the day-use, simulated HMD visual environment.

Figure 5. The DERA Lynx research helicopter outfitted with custom amber-tinted panels.

Visually coupled system (VCS)

The VCS was comprised of a direct current (DC) electromagnetic head positioning system (HPS) with a transmitter affixed to the airframe close to the subject pilot's head with a sensor attached to his helmet. The HPS provided six degrees of freedom (DOF) output over a large range of head movements. The platform could be directed to the HPS line of sight over a range of ± 120° azimuth and +30° to -90° elevation at a maximum rate of 110°/sec. The platform also carried a thermal imager derived from the Class II Thermal Imaging Common Module (TICM) II with an FOV of 55° horizontal by 37° vertical, producing a raster output in a 625 line/50 Hz format. A Radstone symbol generator was used to produce symbology.

The HPS sampled head position approximately every 5 ms. However, to reduce the volume of the data for storage and analysis, the available head position data files were transformed to 100 ms (0.1 sec)-samples.

Helmet-mounted display (HMD)

The aircraft was equipped with an HMD, manufactured by GEC, which used 625 line/50 Hz miniature (1-inch diameter) monochrome cathode ray tubes (CRTs) as image sources (Figure 6). The optical train provided a fully overlapped 53° horizontal by 37° vertical FOV. Although capable of binocular operation, the HMD was driven by a single video channel in a biocular mode (same image in both eyes). The HMD could display symbology only (not used in this study), thermal imaging only (TIO), or combined thermal imaging and symbology. The HMD imagery was relatively dim and could not be seen easily under daylight conditions. For safety reasons, flights in this study were conducted only under daylight conditions. For this combination of reasons, a modification to the HMD was necessary.

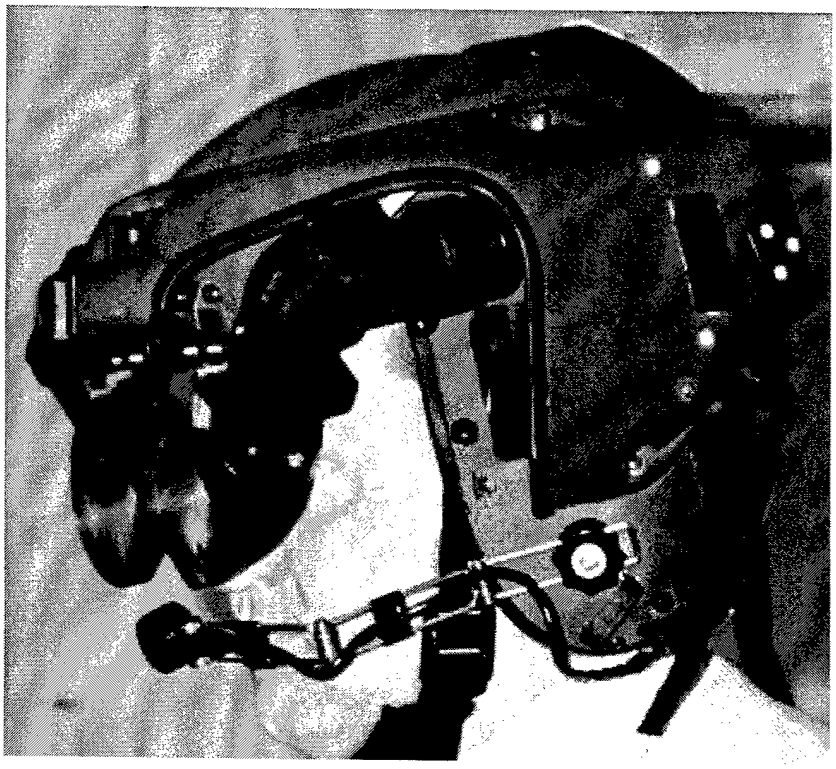

Figure 6. Flight helmet with 53-degree FOV HMD.

Simulated degraded visual environment (SDVE)

The daytime study flight requirement created several problems:

- The HMD imagery was difficult to see against the bright daytime sky.
- The flat surfaces of the HMD combiner optics resulted in numerous reflections that distracted and disoriented the pilot.
- The daytime visual environment was full of visual cues that were absent during night flight.

Therefore, to be able to use the HMD during the required daytime flights, a novel hood assembly referred to as a SDVE was developed (Crowley, 1998). The SDVE consisted of a full HMD hood assembly and a blue filter that was complementary to the amber screens already in place over all cockpit transparencies except the overhead panels. The combination of the amber and blue filters prevented exterior viewing by the subject pilot. The hood assembly consisted of a tailored fire-retardant black cloth hood worn over the pilot's helmeted head (Figure 7).

The subject pilot could not see anything directly outside the aircraft but was able to view his arms, the controls, most of the instrument panel, and the left side cockpit structure when looking ahead. The instrument panel was heavily tinted and darkened due to a dark blue filter. This made it so that pilots could not read any numbers on the gauges, but could make out the main needle on the bigger gauges.

Figure 7. SDVE system.

Night vision goggles (NVGs)

A single pair of Fenn NG600 (Gen III) NVGs was used for all flights. The Fenn NG600 was 3rd GEN and had a 47° circular FOV.

Subjects

There were 4 subject pilots, all male. Ages were 31, 33, 34 and 37 with 1500, 1830, 2000 and 2700 flight hours, respectively.

Visual environments

The study employed four types of visual environments. These environments were:

- Good visual environment (GVE)
- Night Vision Goggles (NVG)
- Thermal imaging only (TIO)
- Rotary-wing symbology (RWS)

GVE flight was conducted in a normal daytime environment only when "good visibility" was available. These flights served as a baseline to document a reference level of functional quality performance.

NVG flights were flown in a nighttime environment using the Fenn NG600 night vision goggle system. A mean ambient light level of 10 milliLux was the target illumination level. However, any illumination within the range 5-50 milliLux was deemed acceptable. Along with the GVE flights, these flights also were used to develop a baseline for evaluating the VCS.

TIO flights were flown in a daytime environment using the SDVE hood and amber filter windscreen systems. Under the SDVE, the subject pilots were presented with thermal imagery only on the 53° HMD. No symbology was presented.

RWS flights were flown in a daytime environment using the SDVE hood and amber filter windscreen systems. Under the SDVE, the subject pilots were presented with thermal imagery and symbology on the 53° HMD.

Flight maneuvers

Flights were flown during the period mid-March to late-September 1997. The subjects flew a total of six maneuvers: Slalom, curved approach, hovering (spot) turns, rapid egress, bob-up/down, and sidestep. The focus for this analysis is on the slalom maneuver due to its more consistent flight pattern and easily defined flight cycle.

All six maneuvers were performed successively in each run starting with the slalom and ending with the sidestep maneuver. Under ideal conditions, the maneuvers would be randomly presented. However, this counterbalancing design was not possible because the VCS was not available during the first two months of planned flights.

All flights were conducted during daytime hours, with the exception of the NVG flights. Flights occurred in the region of southern England known as the Salisbury Plain training area at a location known as Haxton Down, approximately 6.6 miles (11 kilometers) north of the Boscombe Down airfield. All flights approached the test area by originating from the Boscombe Down airfield via a set route flown by the safety pilot at 90 knots indicated airspeed (KIAS) at 200 feet above ground level (AGL), descending to 50 feet AGL on approach to the course. The safety pilot aligned the aircraft over the track and handed the controls over to the subject pilot at an appropriate ground speed, at 50 feet AGL, and at a point at least 200 m (650 feet) prior to the first slalom turn. Ground speed at release was to be approximately 30 knots for low LOA and 40 knots for moderate LOA.

There were two LOA: Low and moderate. Low LOA consisted of the use of up to a thirty-degree angle of bank (AOB), as required, and a moderate speed (> 0 knots, but 30 knots desired) to achieve an unhurried progression through the course. Pedal-assisted skidding turns were acceptable. There were no time constraints. The moderate LOA intended to exploit the full VCS flight envelope as far as possible and to target 30-degree

AOB in all turns with up to 45-degree transients (at safety pilot discretion). Speed was adjusted to achieve rapid progression through the course with an appropriate turn radius (>0 knots, 40 knots desired). Pedal-assisted skidding turns were again acceptable. The required slalom course maneuver completion time was less than 90 seconds.

The slalom segment of the test course consisted of a south to north transit through the Haxton Down area at nap of the earth (NOE) heights and speeds. At Haxton Down, a convenient group of south-north oriented woods labeled Woods One through Four (with "gates" between woods), with intervening east-west avenues, provided a serpentine (slalom) course. The directions of the progressive course turns were: Right, followed by two left turns, two more right turns, and ending with two left turns (Figure 8). Ground track was maintained as close as possible (but not less than 5 meters) from N-S edges of woods, and as close as possible to centerlines of E-W avenues.

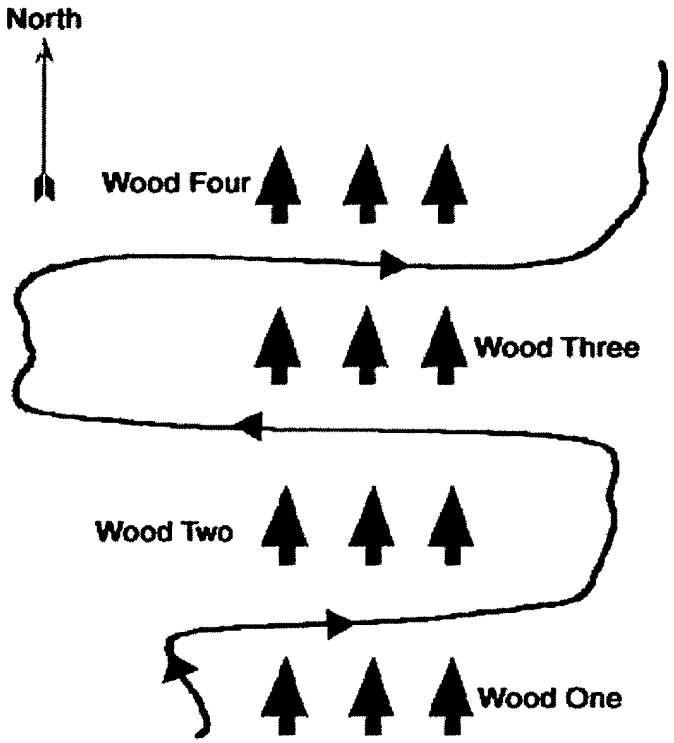

Figure 8. Representative flight path for slalom flight maneuver.

Six performance objectives were defined for the study: 1) Ability to maneuver with respect to ground features in NOE flight in the degraded visual environments (NVGs and HMDs), 2) Ability to maintain spatial awareness and obstacle clearance during a complex multi-axis maneuver, 3) Check for undesirable display dynamics when performing maneuvers representative of moderately aggressive NOE flight, 4) Ability to control height during turning flight, 5) Ability to adjust airspeed to maintain a ground track defined by obstacles, and 6) Ability to control sideslip in turns at moderate airspeed.

Database

The provided head motion database consisted of 628 files. The files were divided into 33 subdirectories, where each subdirectory contained the files for a given flight. A flight was defined as consisting of a varying numbers of "runs" where a "run" was the completion of the full set of all six maneuvers at a given LOA by a single pilot for one of the four visual conditions. A given file in the database contained data pertaining to a single subject for one combination of LOA, flight maneuver, visual environment, and type of run (practice, intermediate or full). There were 107 files for the slalom maneuver.

This analysis focused on head motion for the slalom maneuver. Of the 107 files provided in the database, four were eliminated from the analysis due to missing or corrupted data. This left 103 files for analysis.

Data analysis

The question to be answered by this analysis was: Were the distributions for head motion position (and velocity) different for the four visual environments? The head motion data files under analysis herein for the slalom maneuver were a time series of head elevation position values for four different visual environments, confounded by two levels of aggressiveness and three run types. In addition to analyses of position data, transformations on these data included construction of velocity, reversal and excursion distributions. Briefly, a reversal was defined as a change in head motion direction (e.g., turning from looking up to looking down) and an excursion was defined as the change in angular position between two reversal points.

Data preparation

The slalom files consisted of data collected for a flight pattern flown over a set course running north and south with the turns going east and west (Figure 8). In order to be able to compare across subjects and visual conditions, it was decided to equalize across files by using data over a defined section within the slalom maneuver. This section, referred to as a cycle, was defined as shown in Figure 9. A cycle consisted of two right hand turns and two left hand turns. We also wanted to include a small portion before and after the turns in order to capture pilot head movements during preparation for and recovery from turns. In order to do this consistently, the means of the minimum and the maximum values of the longitude both prior and following the four turns were calculated. The point where the longitude exceeded the mean before the first right hand turn was used as the start point of the cycle. Where the longitude fell below the mean after the last left hand turn was used as the end point of the cycle.

Once a cycle was defined for each file, the data were smoothed using a three-point moving average routine in preparation for analysis.

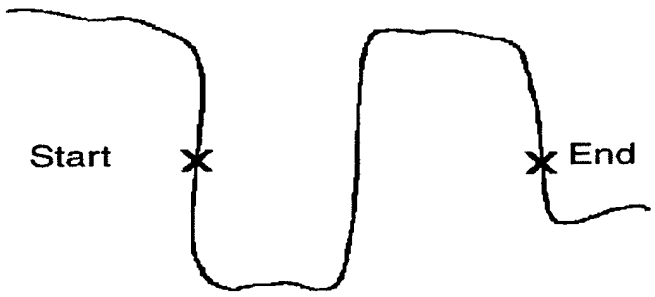

Figure 9. Definition of cycle used in analysis to equalize the slalom maneuver.

Data analysis methods

Multiple approaches were used to answer the research question. The first approach was to transform all of the position time series data into histograms that represented position distributions. Then, the distribution moments (and additional distribution statistics) were calculated for each distribution. The second approach was to construct graphical representations of the distributions in the form of box plots.

A distribution can be fully defined by four moments: Mean, variance (or standard deviation), skewness, and kurtosis. However, it is useful to calculate additional distribution statistics (e.g., minimum, maximum, median, interquartile range (IQR), etc.).

Position analyses

Position distribution histograms

The use of histograms to represent the position distributions is a fundamental technique to allow an overall appreciation of head motion. The histograms presented herein use 1-degree intervals. There were 103 elevation position distributions available for analysis. The resulting position histograms are presented in Appendix A. Subject #1 has a total of 25 histograms that represent the various combinations of LOA, run type and visual environment; subject #2 has 24 histograms; subject #3 has 34 histograms; and subject #4 has 20 histograms.

In the following sections, negative values are associated with the pilot looking downward and positive values are associated with the pilot looking upward.

Individual position distributions

These individual distributions are worth examining for general characteristics and trends for each subject and visual condition. Such an examination yields the following:

Subject #1. The individual head position distributions for subject #1 (Figures A-1 to A-4, Appendix A) present the following characteristics: a) The distributions were unimodal; b) for GVE and NVG, there appeared to be two distinct types of

distributions that had medians that clustered about either -15° or -25°; c) for GVE, all means and medians were negative, implying the pilots were always looking down as compared to the 0° straight-ahead direction; d) all distributions were fairly symmetrical; e) for TIO and RWS, there were well defined central modes, slightly negative of 0°, and all medians were clustered about -2°; and f) for TIO and RWS, the overall range appeared tighter than for the GVE and NVG visual environments.

Subject #2. The head position distributions for subject #2 (Figures A-5 to A-8, Appendix A) present the following characteristics: a) There appeared to be greater variability in overall range than for subject #1; b) for GVE and NVG, the distributions presented medians clustered between -15° and -20°; c) all means and medians were negative; d) all distributions were unimodal; and e) for TIO and RWS, the medians clustered about -5°.

Subject #3. The head position distributions for subject #3 (Figures A-9 to A-12, Appendix A) present the following characteristics: a) All distributions were unimodal; b) for GVE, the medians were clustered about either -15°; c) for NVG, all medians clustered about either -15° or -30°; d) for NVG, the range of position values had greater variability than for subjects #1 and #2; and e) for TIO and RWS, all medians were clustered about -5°.

Subject #4. The head position distributions for subject #4 (Figure A-13 to A-14, Appendix A) present the following characteristics: a) For GVE, the medians varied more than for all other subjects; b) for NVG, there was a higher range of position values, as for subject #3; and c) all means and medians were negative.

Note: Head position data for subject #4 were not available for TIO and RWS visual environments.

Combined distributions

This rather large aggregate of histograms makes it difficult to compare head motion across visual environments. To overcome this problem, the authors have argued that distribution comparisons can be based on combined distributions that are total data sets formed by combining data from all runs for a given visual environment (Rostad et al., In press). These combined distributions are not based on the average of individual runs but rather the summation of individual runs.

The general tenet of the argument for basing analyses on combined distributions is that the influence of the LOA and run type confounds, contributes to, but does not define, the general shape and characteristics of the head motion distribution for a given visual environment.

Based on this argument, Figures 10-13 present the combined elevation position distributions by subject and visual environment. Note that head position data for subject #4 were available for only two visual environments, GVE and NVG. As with the

individual distributions, these combined distributions also can be examined visually for general characteristics and trends, which should generally be similar to those found for the individual distributions. The following observations are made:

Subject #1. The combined GVE head position distribution for subject #1 (Figure 10) present the following characteristics: a) It is bimodal with modes at -15° and -27°, and b) the approximate range is -7° to -44° with an outlier near –52°.

The combined NVG head position distribution for subject #1 (Figure 10) present the following characteristics: a) It is bimodal with modes at -14° and -27°, and b) the approximate range is -7° to -46°.

The combined TIO head position distribution for subject #1 (Figure 10) present the following characteristics: a) There is a strong central mode at approximately 0°, and b) the approximate range is +9° to -11°.

The combined RWS head position distribution for subject #1 (Figure 10) present the following characteristics: a) There is a strong central mode at approximately +1°, and b) the approximate range is +8° to -11°.

Subject #2. The combined GVE head position distribution for subject #2 (Figure 11) present the following characteristics: a) There is a strong central mode at -16°, and b) the approximate range is -2° to -41°.

The combined NVG head position distribution for subject #2 (Figure 11) present the following characteristics: a) It is bimodal with modes at -12° and -21°, and b) the approximate range is +2° to -30° with an outlier at -35°.

The combined TIO head position distribution for subject #2 (Figure 11) present the following characteristics: a) There is a strong central mode at approximately -5°, and b) the approximate range is +7° to -17°.

The combined RWS head position distribution for subject #2 (Figure 11) present the following characteristics: a) There is a strong central mode at approximately -7°, and b) the approximate range is +3° to -18°.

Subject #3. The combined GVE head position distribution for subject #3 (Figure 12) present the following characteristics: a) There is a strong central mode at -15°, and b) the approximate range is -5° to -28°.

The combined NVG head position distribution for subject #3 (Figure 12) present the following characteristics: a) It is bimodal with modes at -14° and -30°, and b) the approximate range is +1° to -41° with an outlier at -45°.

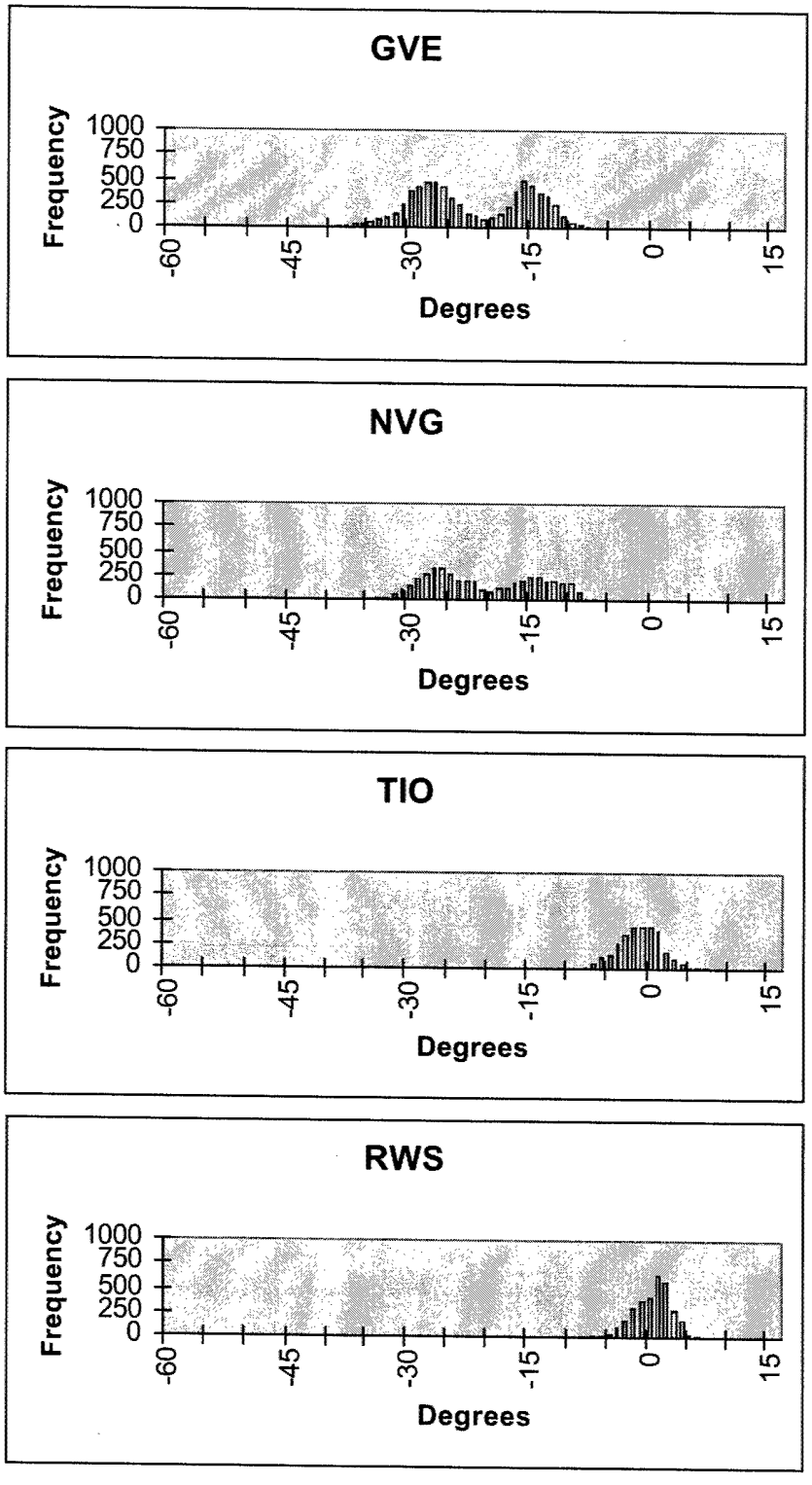

Figure 10. Combined position histograms for subject #1.

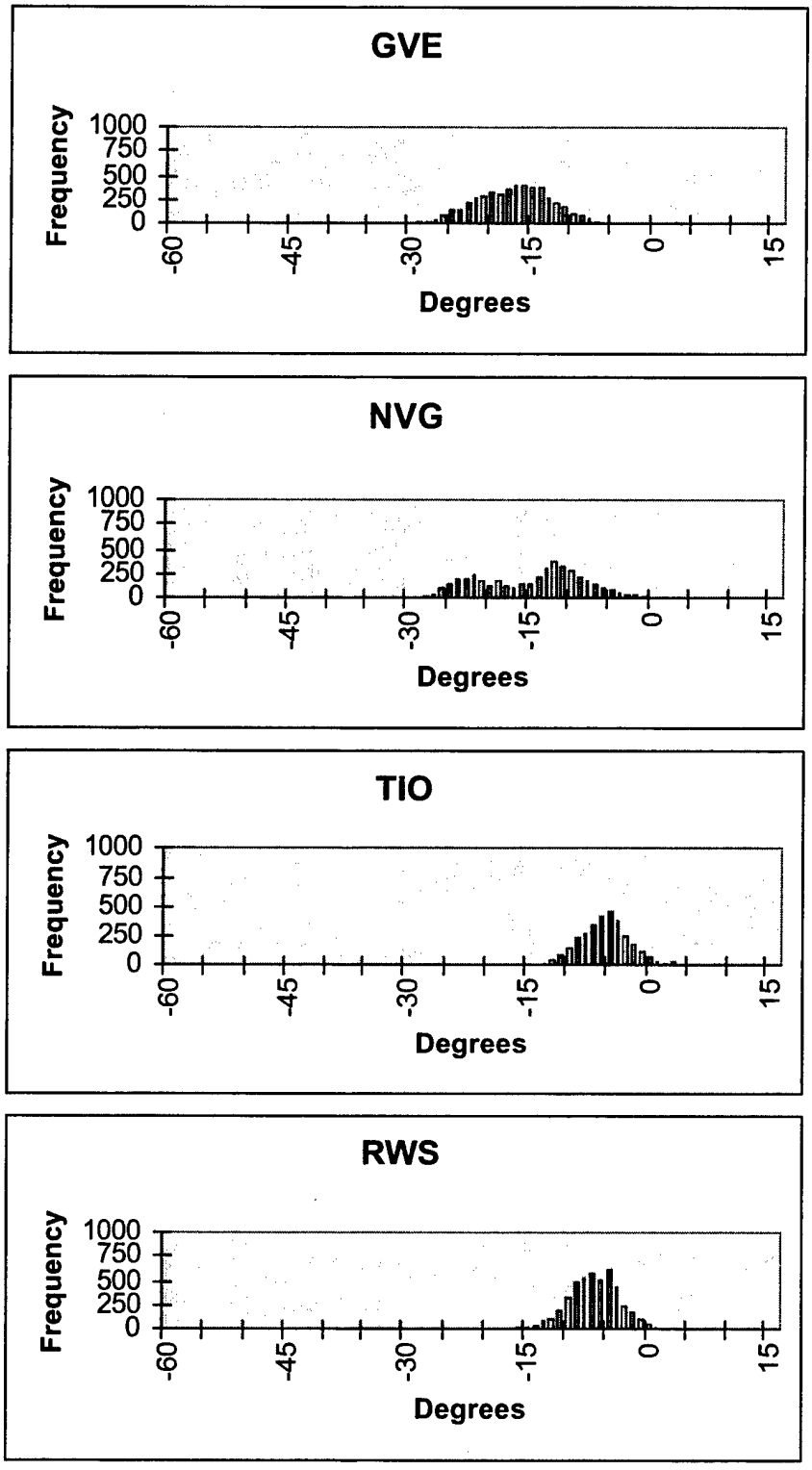

Figure 11. Combined position histograms for subject #2.

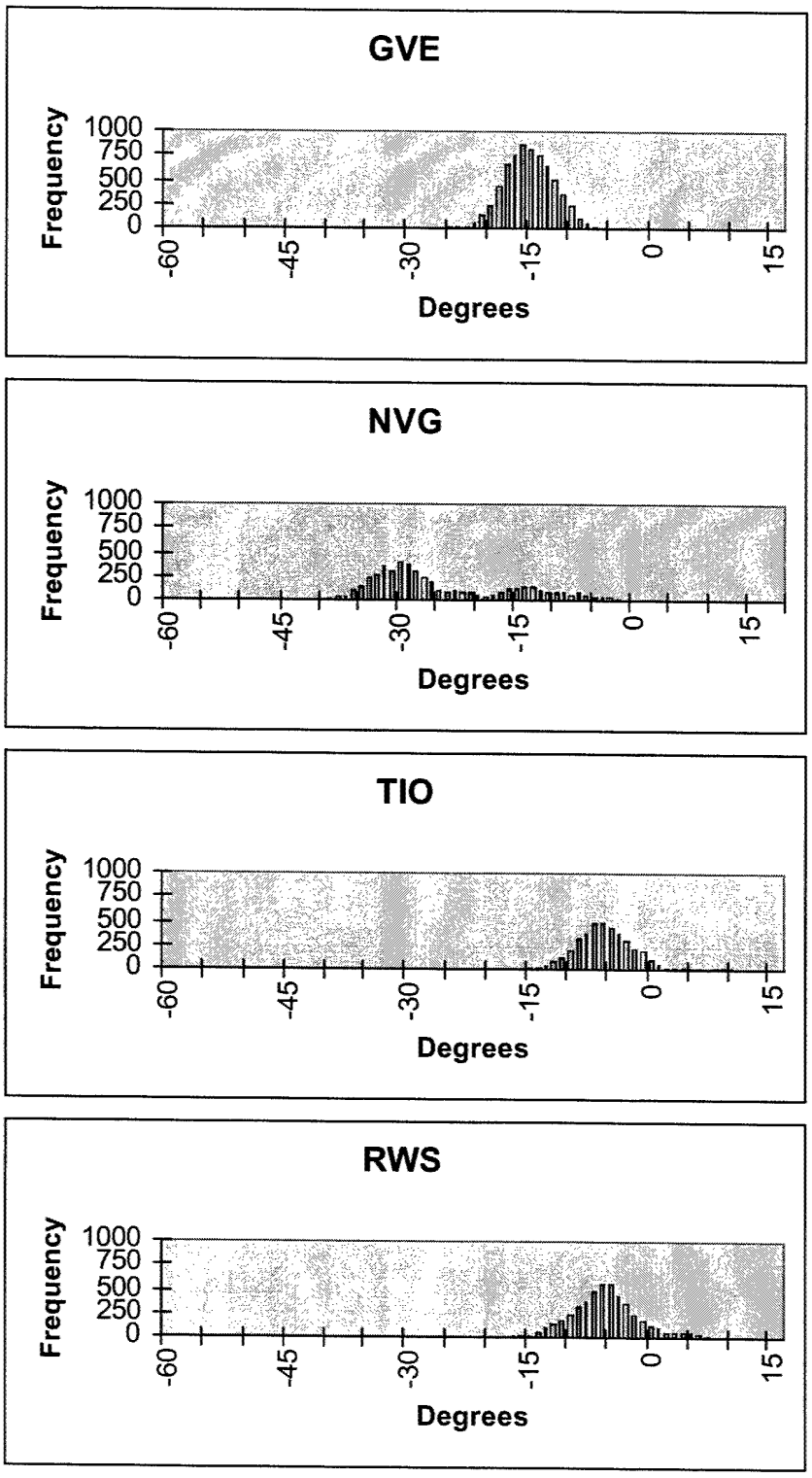

Figure 12. Combined position histograms for subject #3.

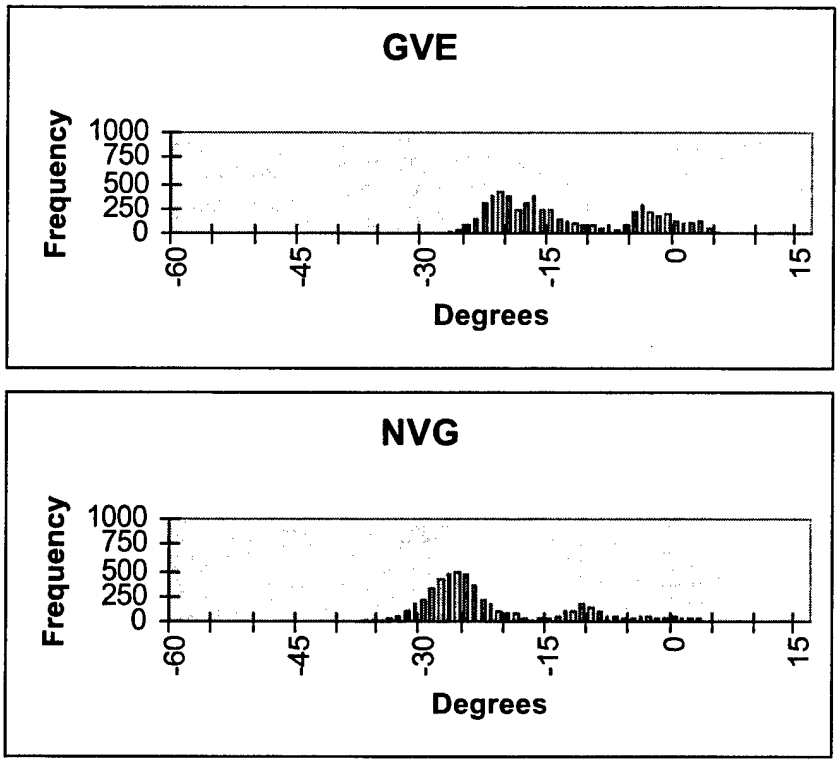

Figure 13. Combined position histograms for subject #4.

The combined TIO head position distribution for subject #3 (Figure 12) present the following characteristics: a) There is a strong central mode at approximately -6°, and b) the approximate range is +13° to -18°.

The combined RWS head position distribution for subject #3 (Figure 12) present the following characteristics: a) There is a strong central mode at approximately -5°, and b) the approximate range is +8° to -21°.

Subject #4. The combined GVE head position distribution for subject #4 (Figure 13) present the following characteristics: a) It is bimodal with modes at -2° and -17°, and b) the approximate range is +8° to -28°.

The combined NVG head position distribution for subject #4 (Figure 13) present the following characteristics: a) It is bimodal with a ill-defined mode at -10° and a well-defined mode at -27°, and b) the approximate range is +7° to -38°.

Note: Head position data for subject #4 were not available for TIO and RWS visual environments.

Having examined both the individual and combined position distributions, further discussion is required regarding the argument to base analyses on the combined rather than individual distributions. The combined GVE distributions for subjects #1 and #4 and

the NVG combined distributions for all subjects appear as bimodal. However, all of the individual distributions for these subjects and visual conditions are unimodal. An inspection of the individual distributions in Appendix A shows that this bimodal nature seen in the identified combined distributions arises from a dichotomy that exists in a grouping characteristic of the individual distributions. The authors are presented with a dilemma. This dilemma is whether to continue with the argument to base analyses on the combined distributions or to disengage this argument in light of the unimodal characteristic of all of the individual distributions.

In an attempt to explain the dichotomy, the authors looked for explanations for the bimodal characteristic. Discussions with pilots lead to the possible explanation that, for NVG flights, the NVG mount can often be positioned at different angles to the eyes. Since an examination of the individual distributions showed that the modes indeed were grouped by runs within a single flight, this was considered a rational explanation. However, this explanation does not extend to the GVE runs, since it is unlikely that a pilot would have a helmet fit which would vary by as much as 15°, the typical difference between the two elevation position modes. Continued discussions with pilots failed to produce any single reason why the subject pilots would exhibit the two varied head position modes.

The essence of the argument for basing analyses on combined distributions is that no distribution for any single run is identical to the distribution for another run, even for the same subject and visual condition. And, when position data from a large number of individual distributions are combined, a general pattern will emerge. Therefore, while in this instance, attention will be paid to the unimodal nature of the individual distributions, analyses will be based on the combined distributions since it is argued they represent the better picture of head motion exhibited by pilots while using HMDs.

Moments and additional distribution statistics

While distribution shape provides a basic understanding of the ongoing head motion, the semi-quantitative nature of distribution histograms does not allow for analytical comparison. For this reason, distributions often are described or defined by the distribution's moments. There are four such moments: First (mean), second (variance or standard deviation), third (skewness), and fourth (kurtosis). It is also useful to calculate additional distribution statistics, e.g., minimum, maximum, median, etc.

Summary individual and combined distribution moments and statistics tables for all subjects, grouped by visual environment, are provided in Appendix B. However, accepting the argument that comparisons can be based on the combined distributions, a summary of distribution moments and statistics by subject and visual environment for the combined distributions only is presented in Table 4. Examination of Appendix B and Table 4 lead to the identification of a number of characteristics and trends:

Table 4.
Combined elevation position summary by subject and visual environment.
(Time expressed in seconds; Other dimensional statistics expressed in degrees)

Subject	Visual Environment	Mean Time	Min	Max	Mean	Median	S.D.	IQR	Skew	Kurt
1	GVE	57.6	-52.7	-8.1	-22.9	-24.3	7.2	-28.8 to -16.2	0.0	-1.1
1	NVG	66.7	-46.0	-4.8	-21.3	-22.4	6.9	-27.2 to -15.1	0.1	-1.1
1	TIO	105.3	-11.9	7.0	-1.8	-1.7	2.8	-3.6 to 0.0	-0.1	0.3
1	RWS	109.4	-11.6	6.1	-0.2	0.2	2.4	-1.7 to 1.4	-0.6	0.7
2	GVE	60.5	-42.0	-2.7	-18.0	-17.7	4.7	-21.3 to -14.6	-0.2	0.2
2	NVG	75.3	-35.7	0.4	-15.5	-14.2	6.4	-21.4 to -10.8	-0.2	-0.9
2	TIO	80.2	-17.3	9.8	-6.0	-6.0	3.3	-8.1 to -4.2	0.4	1.3
2	RWS	77.6	-19.1	1.8	-7.3	-7.2	3.1	-9.3 to -5.1	-0.2	0.1
3	GVE	56.5	-29.7	-5.4	-15.8	-15.8	3.1	-17.9 to -13.6	0.0	0.0
3	NVG	58.3	-45.5	-0.3	-24.8	-28.2	9.1	-31.8 to -16.8	0.7	-0.7
3	TIO	82.8	-18.1	12.6	-5.9	-6.4	4.1	-8.5 to -3.9	1.0	2.4
3	RWS	62.2	-21.4	7.5	-6.0	-6.1	4.5	-8.8 to -3.6	0.3	0.4
4	GVE	52.9	-29.8	6.7	-13.5	-16.3	8.8	-20.9 to -4.8	0.4	-1.2
4	NVG	60.8	-39.1	5.7	-21.7	-25.2	9.2	-28.1 to -14.7	1.0	-0.1
4	TIO	None								
4	RWS									

Subject #1. The summary GVE head position distribution statistics for subject #1 present the following characteristics: a) The individual distributions could be grouped into those having medians of approximately -16° or -27°; b) the combined median was –24.3°; c) for the combined distribution, elevation head position was always below the straight-ahead line of sight, ranging from –8.1° to –22.9°; and d) the IQR was –28.8° to –16.2° (12.6°).

The combined NVG head position distribution statistics for subject #1 present the following characteristics: a) The individual distributions could be grouped into those having medians of approximately -15° or -26°; b) the combined median was –22.4°; c) for the combined distribution, elevation head position was always below the straight-ahead line of sight, ranging from –4.8° to –21.3°; and d) the IQR was –27.2° to –15.1° (12.1°).

The combined TIO head position distribution statistics for subject #1 present the following characteristics: a) The individual distributions were unimodal having a combined median of –1.7°; b) elevation head position ranged both below and above the straight-ahead line of sight, from –11.9° to +7.0°; and c) the IQR was –3.6° to 0.0° (3.6°).

The combined RWS head position distribution statistics for subject #1 present the following characteristics: a) The individual distributions were unimodal having a combined median of 0.2°; b) elevation head position ranged both below and above

the straight-ahead line of sight, from –11.6° to +6.1°; and c) the IQR was –1.7° to 1.4° (3.1°).

When these four visual environments characteristics are studied in comparison for subject #1, the following observations were made: a) The medians were negative, except RWS, which was barely positive at 0.2°; b) GVE had the largest IQR (12.6°) and SD (7.2°); c) TIO and RWS were very similar in characteristics and had the smallest ranges and IQRs; and d) both GVE and NVG individual distributions were grouped about two different modes.

Subject #2. The summary, GVE head position distribution statistics for subject #2 present the following characteristics: a) The individual and combined distributions were unimodal having a combined median of –17.7°; b) for the combined distribution, elevation head position was always below the straight-ahead line of sight, ranging from –42.0° to –2.7°, and c) the IQR was –21.3° to –14.6° (6.5°).

The combined NVG head position distribution statistics for subject #2 present the following characteristics: a) The individual distributions could be grouped into those having medians of approximately -11° or -22°; b) the combined median was –14.2°; c) for the combined distribution, elevation head position was mostly below the straight-ahead line of sight, ranging from –35.7° to 0.4°; and d) the IQR was –21.4° to –10.8° (10.6°).

The combined TIO head position distribution statistics for subject #2 present the following characteristics: a) The individual distributions were unimodal having a combined median of –6.0°; b) elevation head position ranged both below and above the straight-ahead line of sight, from –17.3° to +9.8°; and c) the IQR was –8.1° to –4.2° (3.9°).

The combined RWS head position distribution statistics for subject #2 present the following characteristics: a) The individual distributions were unimodal having a combined median of –7.2°; b) elevation head position ranged both below and above the straight-ahead line of sight, from –19.1° to +1.8°; and c) the IQR was –9.3° to –5.1° (4.2°).

When these four visual environments characteristics are studied in comparison for subject #2, the following observations were made: a) The medians were all negative, b) NVG had the largest IQR (10.6°) and SD (6.4°), c) TIO and RWS were very similar in characteristics and had the smallest ranges and IQRs, and d) the NVG individual distributions were grouped about two different modes.

Subject #3. The summary, GVE head position distribution statistics for subject #3 present the following characteristics: a) The individual and combined distributions were unimodal having a combined median of –15.8°; b) for the combined distribution, elevation head position was always below the straight-ahead line of sight, ranging from –29.7° to –5.4°; and c) the IQR was –17.9° to –13.6° (4.3°).

The combined NVG head position distribution statistics for subject #3 present the following characteristics: a) The individual distributions could be grouped into those having medians of approximately -13° or -29°; b) the combined median was –28.2°; c) for the combined distribution, elevation head position was always below the straight-ahead line of sight, ranging from –45.5° to -0.3°; and d) the IQR was –31.8° to –16.8° (15.0°).

The combined TIO head position distribution statistics for subject #3 present the following characteristics: a) The individual distributions were unimodal having a combined median of –6.4°; b) elevation head position ranged both below and above the straight-ahead line of sight, from –18.1° to +12.6°; and c) the IQR was –8.5° to –3.9° (4.6°).

The combined RWS head position distribution statistics for subject #3 present the following characteristics: a) The individual distributions were unimodal having a combined median of –6.1°; b) elevation head position ranged both below and above the straight-ahead line of sight, from –21.4° to +7.5°; and c) the IQR was –8.8° to –3.6° (5.2°).

When these four visual environments characteristics are studied in comparison for subject #3, the following observations were made: a) The medians were all negative; b) NVG had the largest IQR (15.0°) and SD (9.1°); c) TIO and RWS were very similar in characteristics and had the smallest ranges; and d) the NVG individual distributions were grouped about two different modes.

Subject #4. The summary GVE head position distribution statistics for subject #4 present the following characteristics: a) The individual distributions could be grouped into those having medians of approximately -3°, -15° or -22°; b) the combined median was –16.3°; c) for the combined distribution, elevation head position was both below and above the straight-ahead line of sight, ranging from –29.8° to +6.7°; and d) the IQR was –20.9° to –4.8° (16.1°).

The combined NVG head position distribution statistics for subject #4 present the following characteristics: a) The individual distributions could be grouped into those having medians of approximately -9° or -27°; b) the combined median was –25.2°; c) for the combined distribution, elevation head position was both below and above the straight-ahead line of sight, ranging from –39.1° to +5.7°; and d) the IQR was –28.1° to –14.7° (13.4°).

When these two visual environments characteristics are studied in comparison for subject #4, the following observations can be made: a) The medians were both negative; b) GVE had the larger IQR (16.1°), NVG had the larger SD (9.2°); and c) the NVG and GVE individual distributions were grouped about two different modes.

Note: Head position data for subject #4 were not available for TIO and RWS visual environments.

Graphical comparisons

While considerable information is available in Table 4 and several pages have been spent enumerating and comparing the distribution characteristics presented in Table 4, distributions are often better understood through graphical techniques. In addition, the shapes of the head position distributions under analysis generally appear to deviate from normality and are asymmetrical, which speaks against conventional parametric analysis. When this is the case, graphical techniques such as box plots can provide excellent methods of comparing distributions.

The box plot technique provides a visual summary of a data set by emphasizing a select set of statistic values, e.g., median, quartiles, and IQR. Box plots for combined elevation position distributions for all subjects are presented in Figures 14-17. Individual box plots for all subjects by visual environment are presented in Appendix C.

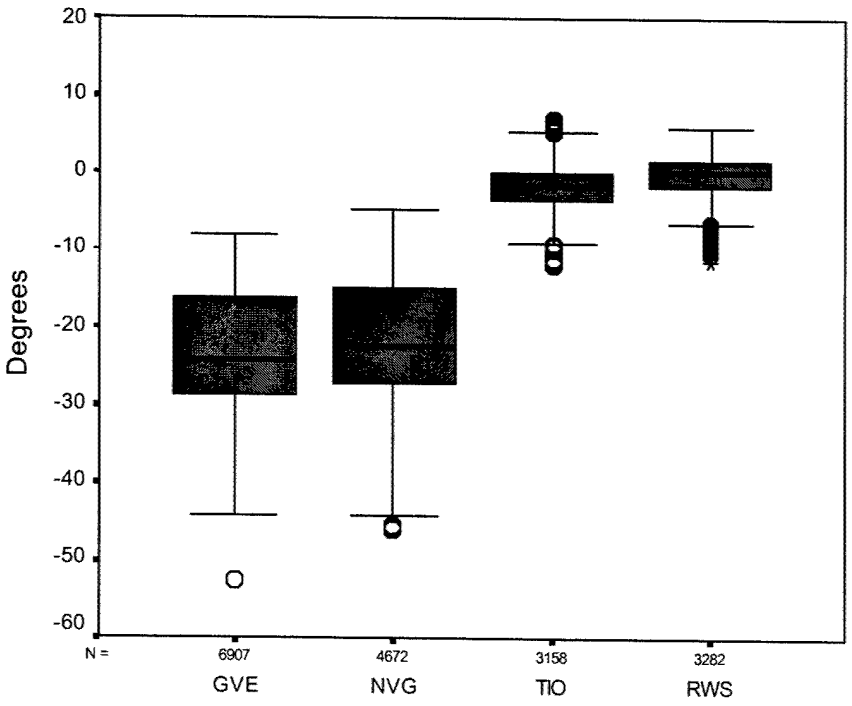

Figure 14. Combined elevation position box plots for subject #1.

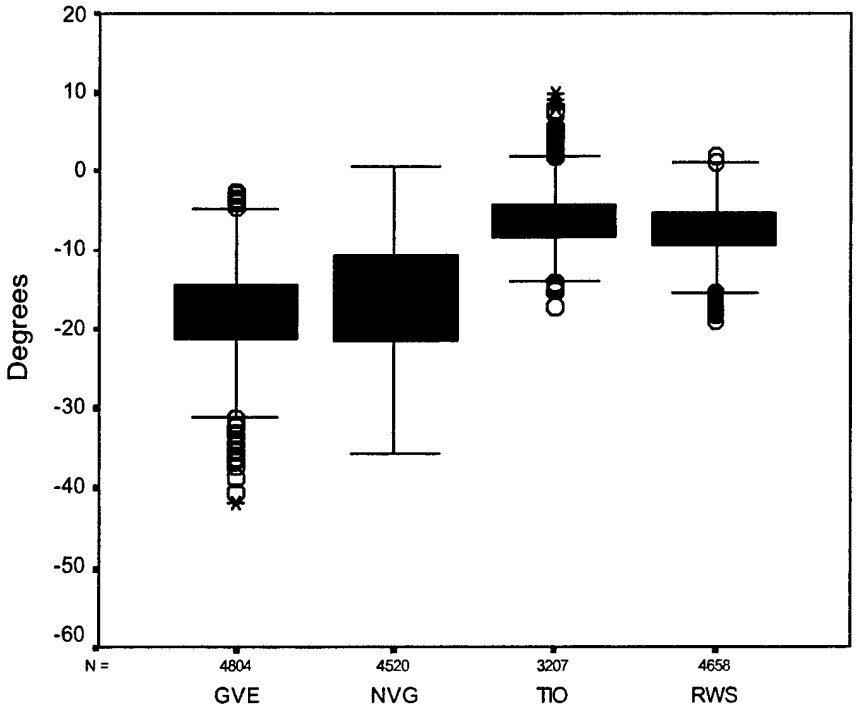

Figure 15. Combined elevation position box plots for subject #2.

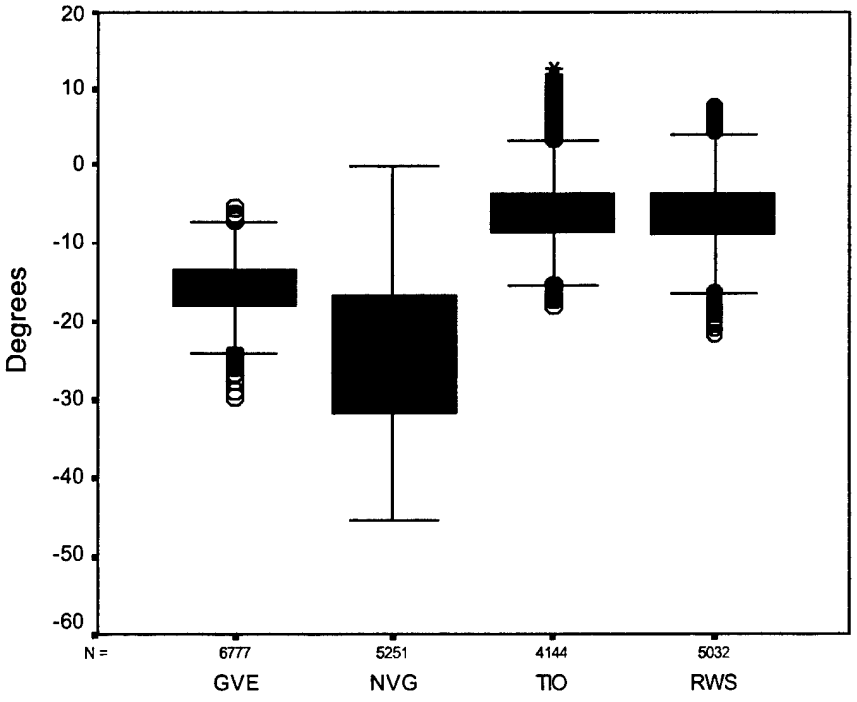

Figure 16. Combined elevation position box plots for subject #3.

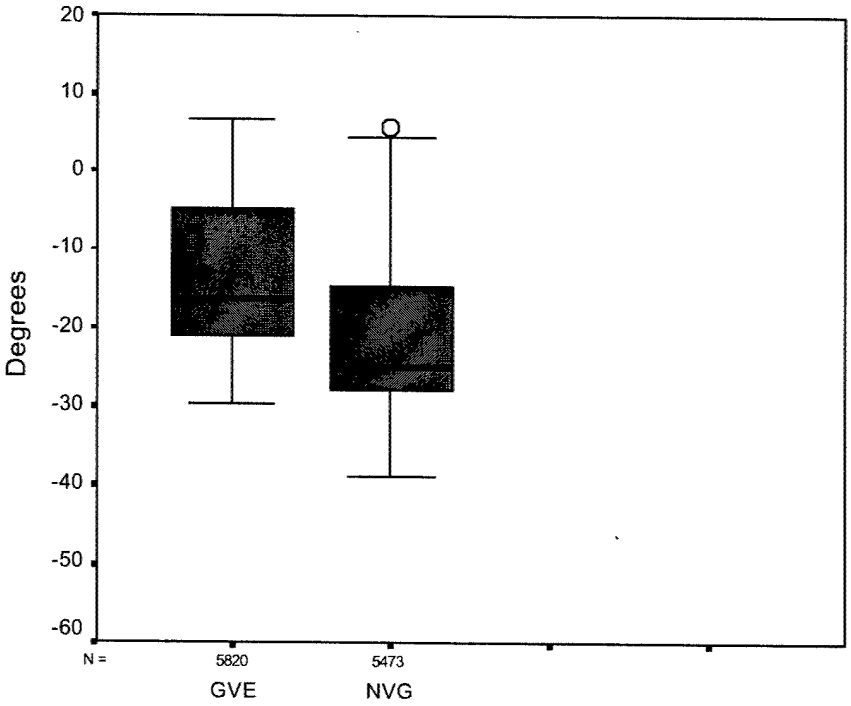

Figure 17. Combined elevation position box plots for subject #4.

From the combined box plots for subject #1 in Figure 14, the following characteristics and trends can be construed: a) The GVE and NVG have the largest IQRs and are similar in size; b) the IQRs for the TIO and RWS also are similar; c) the GVE and NVG medians are relatively the same, as are those for TIO and RWS; d) all positions for GVE and NVG were below level line of sight; e) elevation positions for TIO and RWS were generally symmetrical about the level line of sight; and f) the TIO and RWS had outlier values primarily in the down elevation direction.

When the individual box plots for subject #1 in Figures C-1 through C-4 are examined, the following characteristics and trends can be construed: a) For GVE, there are two distinctive groupings of the run distributions; the first four runs, having similar shapes, were flown during one flight; the remaining runs were associated with two additional flights; and, the first flight was separated by 5 days from the following flights, which were on consecutive days; b) for NVG, there was a similar trend; the first two runs occurred during the same flight and the resulting distributions were grouped; and, the next three runs were on the following day, and the last two runs were seven days later; c) for TIO and RWS, all runs were made during the same flight; the TIO medians and IQRs were very similar; and, the TIO runs possessed a large number of downward-looking outliers.

When both the combined and individual box plots for subject #1 are analyzed together, it can be seen that there is very likely some factor that is associated with the different flights for GVE and NVG that caused natural groupings of the elevation position distributions. Whatever this factor was, it does manifest itself in GVE and NVG runs

across flights. It is not possible to draw this conclusion for TIO and RWS runs since all of these runs for subject #1 were associated with a single flight.

As a consequence of the identification of a possible confounding factor in the elevation distributions, there is some concern over the authors' argument (presented in the previous azimuth analysis (Rostad et al., 2001)) that an understanding of head motion can be simplified by performing analyses on combined distributions rather than on collections of individual distributions. This possible confound needs to be kept in mind during the investigation of the combined and individual box plots for the remaining subjects.

From the combined box plots for subject #2 in Figure 15, the following characteristics and trends can be construed: a) The NVG has the largest IQR, b) all medians were negative (downward shifted), and c) the TIO and RWS are most similar in shape.

When the individual box plots for subject #2 in Figures C-5 through C-8 are examined, the following characteristics and trends can be construed: a) For GVE, the first five runs and the remaining four runs belonged to separate flights on consecutive days; there was only a minor grouping effect apparent across flights; all medians were negative and less than –15°; and, there was a high degree of symmetry among the distributions; b) for NVG, there were two distinct groupings of runs; these groupings were associated with separate flights; and, all medians were negative; c) for TIO, all medians were negative; while the four runs were across two separate flights, there was no apparent grouping effect; and, there were considerable position data above the straight ahead line of sight, i.e., upward; and d) for RWS, all medians were well clustered, even though the runs were divided across two flights on consecutive days; medians were between –5° and -8°; and, there was a higher frequency of negative (downward) outlier positions.

As with subject #1, a confound seems be present across flights for subject #2 for some visual conditions. The possible confound manifested itself only for GVE and NVG. TIO and RWS runs across flights did not present the grouping effect.

From the combined box plots for subject #3 in Figure 16, the following characteristics and trends can be construed: a) The NVG has the largest range and IQR, b) all the medians are negative (downward shifted), c) the TIO and RWS are most similar in shape, and d) the TIO and RWS have outlier values at top and bottom.

When the individual box plots for subject #3 in Figures C-9 through C-12 are examined, the following characteristics and trends can be construed: a) For GVE, all medians are well clustered about approximately -15°; this is in spite of the fact that the individual runs are spread across three flights; all medians are negative (downward); and, there are more negative (downward) outliers; b) for NVG, the runs are segregated into three distinct groupings; the groupings are associated with three separate flights; and all medians are negative (downward); c) TIO runs represent two flights but do not present any grouping characteristic; all distributions have a high degree of symmetry; there were considerable positive (upward) positions; and, all medians are negative (downward); and d) for RWS,

runs from three flights are presented; there is no grouping effect; there were considerable positive (upward) positions; and, all medians are negative (downward).

The possible grouping effect demonstratively manifested itself only for NVG.

From the combined box plots for subject #4 in Figure 17, the following characteristics and trends can be construed: a) The NVG range is greater, but the greater IQR is for GVE; b) the medians are both negative (downward); and c) the 3rd quartiles consistently have larger range than the 2nd quartiles.

When the individual box plots for subject #4 in Figures C-13 through C-14 are examined, the following characteristics and trends can be construed: a) For GVE, there were three distinct groupings associated with different flights; all medians were negative (downward); and positive (upward) positions were present; and b) for NVG, each set of three consecutive runs were associated with different flights; however, the first six runs (first two flights) did not exhibit the grouping effect; runs associated with the third flight did exhibit the grouping effect; and, all medians were negative (downward).

For subject #4, the grouping confound was very evident for GVE. It was also present to a degree for NVG. Subject #4 did not have any TIO or RWS runs.

When all runs for all subjects and visual conditions are scrutinized, some trends involving the possible confound are evident. First, the grouping effect across flights is present for NVG for all four subjects. For GVE, the grouping effect is present, to some degree, for three of the four subjects. Second, for TIO and RWS, for subjects where there is more than one flight, the grouping effect does not present itself.

After discussions with pilots familiar with HMD flight, the following explanation for the grouping effect is suggested. Repeatable head tracking data are dependent on the initial boresighting alignment of the helmet with the aircraft and head tracker. This alignment is strongly dependent on the reproducibility of the helmet fit. The greatest degree of freedom is in the vertical alignment of the helmet; e.g., it is more difficult to repeat the tilt of the helmet on the head from flight to flight than the lateral rotation of the helmet. For TIO and RWS runs, the limited exit pupil position of these HMD configurations forced the pilot to be more critical in reproducing the helmet fit and alignment in order to achieve the HMD's full field-of-view. Therefore, for HMD flights (even on different days), the pilot was more likely to reproduce the helmet position relative to the head, which reduced head tracking boresighting differences. For GVE flights, the helmet tilt had no similar driver for reproducibility of fit, and therefore was susceptible to alignment errors from flight to flight. This was also true for NVG runs. In addition, for NVG runs, there is another factor that can induce vertical helmet misalignment between flights. The NVG device has a special mounting bracket. This bracket has multiple tilt positions. It is possible that pilots did not always use the same mount tilt position and, instead, repositioned the helmet to achieve field-of-view with the NVG device. Therefore, based on this argument, it is reasonable to expect vertical shifts

in the elevation position medians for the GVE and NVG visual conditions but not for the two HMD visual conditions, TIO and RWS.

Distribution comparison

The comparison of distributions is generally accomplished using a Chi-square goodness of fit test. However, as was shown in the azimuth position study (Rostad et al., 2001), this test was not found to be meaningful. This finding was not surprising since the argument previously presented for comparing combined distributions rather than individual distributions pointed out the often considerable differences between the specific characteristics of individual head position distributions even for the same subject performing the same maneuver with same visual environment. For this reason, the validity of using the Chi-square statistic to test for differences in the combined distributions was compromised.

Because the chi-square statistic could not be used to meaningfully test for differences between combined head position distributions, another approach was investigated. In the azimuth analysis of the histograms, the distribution moments, and the graphical plots, a common trend was noticed. In each analysis, there seemed to be a strong indication that the spread of the head positions for the four visual environments exhibited a common rank order. It was concluded that the IQR was the best metric for comparing the position distributions. To investigate this conclusion for the current elevation data, Table 5 was constructed to allow comparison of various spread statistics, which included the IQR, the range and the standard deviation. Ranking within subjects is provided in parentheses.

Table 5, at first glance, does not suggest any trend in ranks of the various spread statistics within subjects for the four visual conditions. This observation is borne out in Table 6, where the Spearman rank-correlation values show extremely weak associations between the spread statistics and visual environments. However, remembering the issue of the multiple unimodal distribution groupings seen in the GVE and NVG individual elevation distributions of some subjects, it was decided to temporarily set aside the combined distribution analysis argument and look at, instead, the means of the spread statistics for the individual position distributions. This results in the values and ranks presented in Table 7. To restate, the values presented in Table 7 are those of the mean IQR, range, and S.D. computed using the IQRs, ranges, and S.D.s for all of the individual distributions (runs) for each subject for each visual environment.

A second use of the Spearman rank-correlation test to the new rankings based on the individual distributions produces the new correlation coefficients presented in Table 8. As was found with the combined distributions, there is no evidence for any strong association between any of the spread statistics and the visual environments. Remember that less weight must be assigned to correlations with subject #4 because only GVE and NVG data were available.

Table 5.
Comparison of IQR, range and standard deviation for combined distributions.
(expressed in degrees, ranks within subject given in ( ))

Subject	Visual environment	IQR	Range	S.D.
1	GVE	12.6 (1)	44.6 (1)	7.2 (1)
1	NVG	12.1 (2)	41.2 (2)	6.9 (2)
1	TIO	3.6 (3)	18.9 (3)	2.8 (3)
1	RWS	3.1 (4)	17.7 (4)	2.4 (4)
2	GVE	6.5 (2)	39.3 (1)	4.7 (2)
2	NVG	10.6 (1)	36.1 (2)	6.4 (1)
2	TIO	3.9 (4)	27.1 (3)	3.3 (3)
2	RWS	4.2 (3)	20.9 (4)	3.1 (4)
3	GVE	4.3 (4)	24.3 (4)	3.1 (4)
3	NVG	15.0 (1)	45.2 (1)	9.1 (1)
3	TIO	4.6 (3)	30.7 (2)	4.1 (3)
3	RWS	5.2 (2)	28.9 (3)	4.5 (2)
4	GVE	16.1 (1)	36.5 (2)	8.8 (2)
4	NVG	13.4 (2)	44.8 (1)	9.2 (1)

Table 6.
Spearman rank-correlation coefficients for IQR, range and standard deviation for combined distributions.

IQR					Range					S.D.				
	#1	#2	#3	#4		#1	#2	#3	#4		#1	#2	#3	#4
#1		+0.6	-0.4	+1	#1		+1	-0.2	+1	#1		+0.8	-0.4	-1
#2			+0.4	-1	#2			-0.2	-1	#2			+0.2	+1
#3				-1	#3				+1	#3				+1
#4					#4					#4				

In summary, the investigation of elevation head position fails to find any distribution spread statistic that can be used to discriminate between elevation position distributions for the four visual environments. However, the two measures of central tendency, the mean and median, are consistently greater in the downward direction for the GVE and NVG conditions than for the two HMD conditions, TIO and RWS.

Table 7.
Comparison of IQR, range and standard deviation means for individual distributions.
(expressed in degrees, ranks within subject given in ( ))

Subject	Visual environment	IQR	Range	S.D.
1	GVE	4.0 (2)	23.8 (1)	3.5 (2)
1	NVG	4.2 (1)	18.0 (2)	3.6 (1)
1	TIO	3.6 (3)	16.5 (3)	2.8 (3)
1	RWS	3.2 (4)	15.6 (4)	2.4 (4)
2	GVE	4.9 (1)	25.9 (1)	4.0 (2)
2	NVG	4.7 (2)	24.2 (2)	4.7 (1)
2	TIO	4.0 (3.5)	20.2 (3)	3.2 (3)
2	RWS	4.0 (3.5)	16.3 (4)	3.0 (4)
3	GVE	3.8 (4)	17.4 (4)	3.0 (4)
3	NVG	5.7 (1)	22.1 (3)	4.0 (2.5)
3	TIO	4.4 (3)	25.0 (1)	4.0 (2.5)
3	RWS	5.1 (2)	23.7 (2)	4.3 (1)
4	GVE	4.2 (2)	15.1 (2)	2.9 (2)
4	NVG	6.0 (1)	23.2 (1)	4.4 (1)

Table 8.
Spearman rank-correlation coefficients for means of IQR, range and standard deviations for individual distributions.

IQR					Range					S.D.				
	#1	#2	#3	#4		#1	#2	#3	#4		#1	#2	#3	#4
#1		+0.8	+0.2	+1	#1		+1	-0.8	-1	#1		+1	-0.6	+1
#2			-0.3	-1	#2			-0.8	-1	#2			-0.6	+1
#3				+1	#3				+1	#3				+1
#4					#4					#4				

Rate analyses

Up to this point, all of the characteristics of head motion that have been investigated have related to position. As was learned in the azimuth position analysis study (Rostad et al., In press), additional information regarding head motion can be obtained from investigating the frequencies, magnitudes and rates (velocities) of change in head position. Three characteristics for an investigation of change in head position are reversals, excursions, and head velocities. Reversals, which measure frequency of head movement, are defined as the number of times that the pilot changes movement from one direction to the other during the cycle. Excursions (magnitudes) are a measurement of the angular

distance that the pilot's head travels in degrees between reversals, and velocities are a measure of the rate of speed in which the pilot moves his head during excursions.

Reversals

This temporal characteristic is based on the number of times the pilot reverses head movement from one direction to the other, e.g., reversing from moving upward to moving downward. To account for the differences in run times, a reversal rate, expressed as the number of reversals per minute, was adopted. Tables D-1 to D-4 in Appendix D present the number of reversals and reversal rates for each run for all subjects by visual environment. Mean reversal rates were calculated and are presented in Table 9 with rank orders within subjects provided in parentheses. These mean reversal rates are plotted with ±1 standard deviation bars in Figure 18.

Table 9.
Mean elevation reversal rates.

	Subject #1	Subject #2	Subject #3	Subject #4
GVE	33.0(2)	36.5(2)	34.4(1)	27.2(2)
NVG	36.3(1)	37.2(1)	31.7(2)	29.6(1)
TIO	32.9(4)	30.1(3)	26.5(3)	
RWS	33.2(3)	28.4(4)	25.3(4)	

Note: Means expressed in reversals per minute.

In Rostad et al. (In press), mean reversal rate was found to be, at best, only a weak indicator of the difference in azimuth head motion within the four different visual environments. Similarly, an examination of Figure 18 shows considerable variability in the mean elevation reversal rates between visual environments for all of the subjects. As with the measures of dispersion, ranking of these rates appears to be the only meaningful analysis. For three of the four subjects, mean reversal rates for the GVE and NVG visual environments were ranked first and second, respectively. For the three subjects for which TIO and RWS data were present, these mean reversal rates were not well clustered in value but were always less than those rates for GVE and NVG.

As with the measures of dispersion, the Spearman rank-correlation was used to test correlation between subjects (Table 10). Due to the variation across subjects and the lack of sample size, mean reversal rate is, at best, only a weak indicator of the difference in head motion within the four different visual environments.

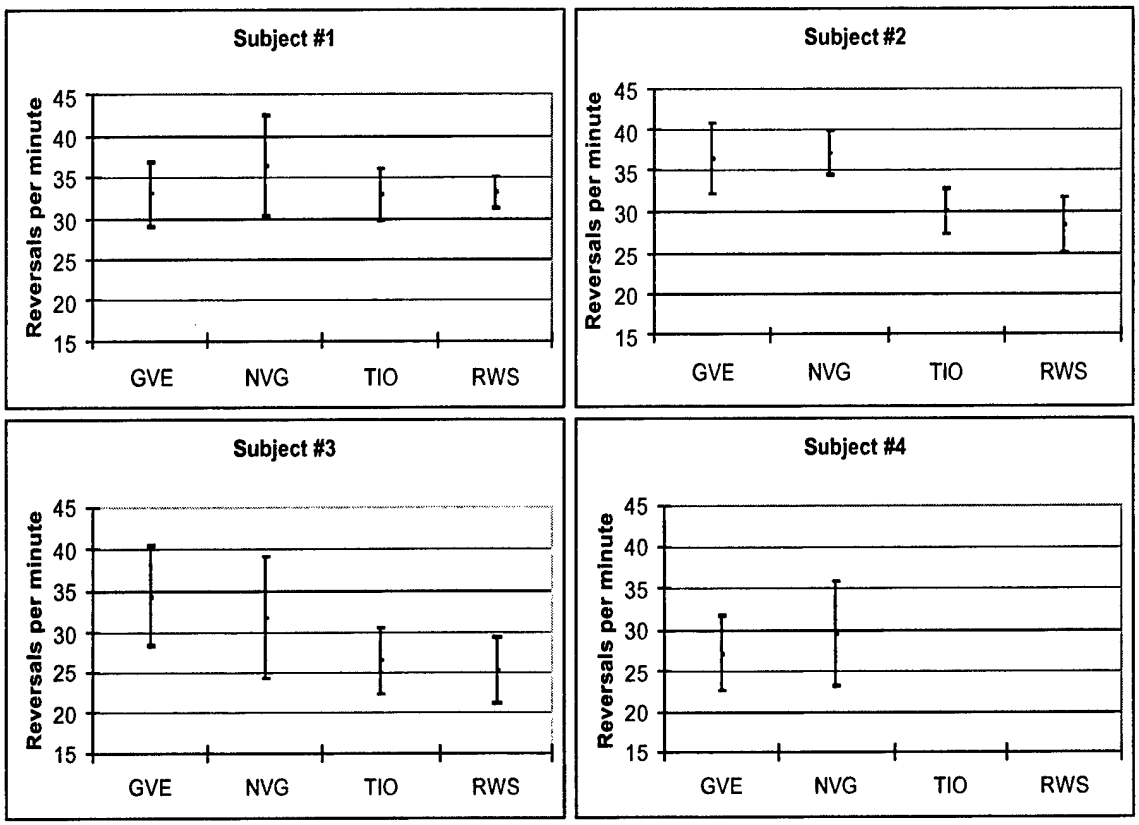

Figure 18. Reversal standard deviation charts showing ±1 standard deviation and means by subject, by visual environment.

Table 10.
Spearman ranking correlation for mean elevation reversal rates.

Reversal Rates				
	#1	#2	#3	#4
#1		+0.8	+0.6	+1
#2			+0.8	+1
#3				-1
#4				

Excursions

An additional temporal characteristic investigated was head excursions. An excursion is defined as the distance the pilot moved his head between reversals expressed in degrees. Distribution histograms for excursion values for individual runs for each subject and

visual environment are presented in Appendix E. Combined histograms overlaid with cumulative frequency curves are shown in Figures 19-22. Excursion values representing the 25^{th}-, 50^{th}-, 95^{th}-, and 99^{th}-percentile points are presented in Table 11 for the combined excursion distributions. Tables summarizing the elevation excursion data by subject and visual environment are presented Appendix F. Excursion box plots are presented in Appendix G.

Examining the histograms, tables and box plots (Appendices E-G, respectively), the following observations or features were noted. First, the distributions of excursions values varied greatly even for individual runs for a given subject and visual condition. Second, across all subjects and visual environments, the largest head excursion recorded was 27.4°. For all subjects, across all visual conditions, 95% of the excursions were 11° or less in size. From Table 11, the 25^{th}-percentile values typically were 2° for each subject for all visual conditions; the 50^{th}-percentile values were between 2° and 5°, with a typical value of 4°, regardless of visual condition. An inspection of 95^{th} and 99^{th}-percentile values showed no clear trend between visual conditions. Based on these values, the added head supported weight of the NVG and two HMD conditions appeared to have had little influence on the distribution of head excursions.

Overall, examination of the distribution of the head excursions provided no definitive differences between the four visual environments. The distribution shapes were not well defined for any visual environment.

In an attempt to obtain an overall sense of the range of excursions exhibited by all of the pilots, for all of the visual environments, a histogram of excursion size combining across all runs was constructed (Figure 23). This overall distribution has the following statistics: Mean of 4.2°, median of 3.4°, standard deviation of 3.5°, and IQR of 4.2°. An overlaid cumulative frequency curve indicates 50% of all excursions were 3° or less. The 95% and 99% excursion values were 11° and 17°, respectively. The largest (maximum) excursion exhibited by any pilot during any run was 27.4°.

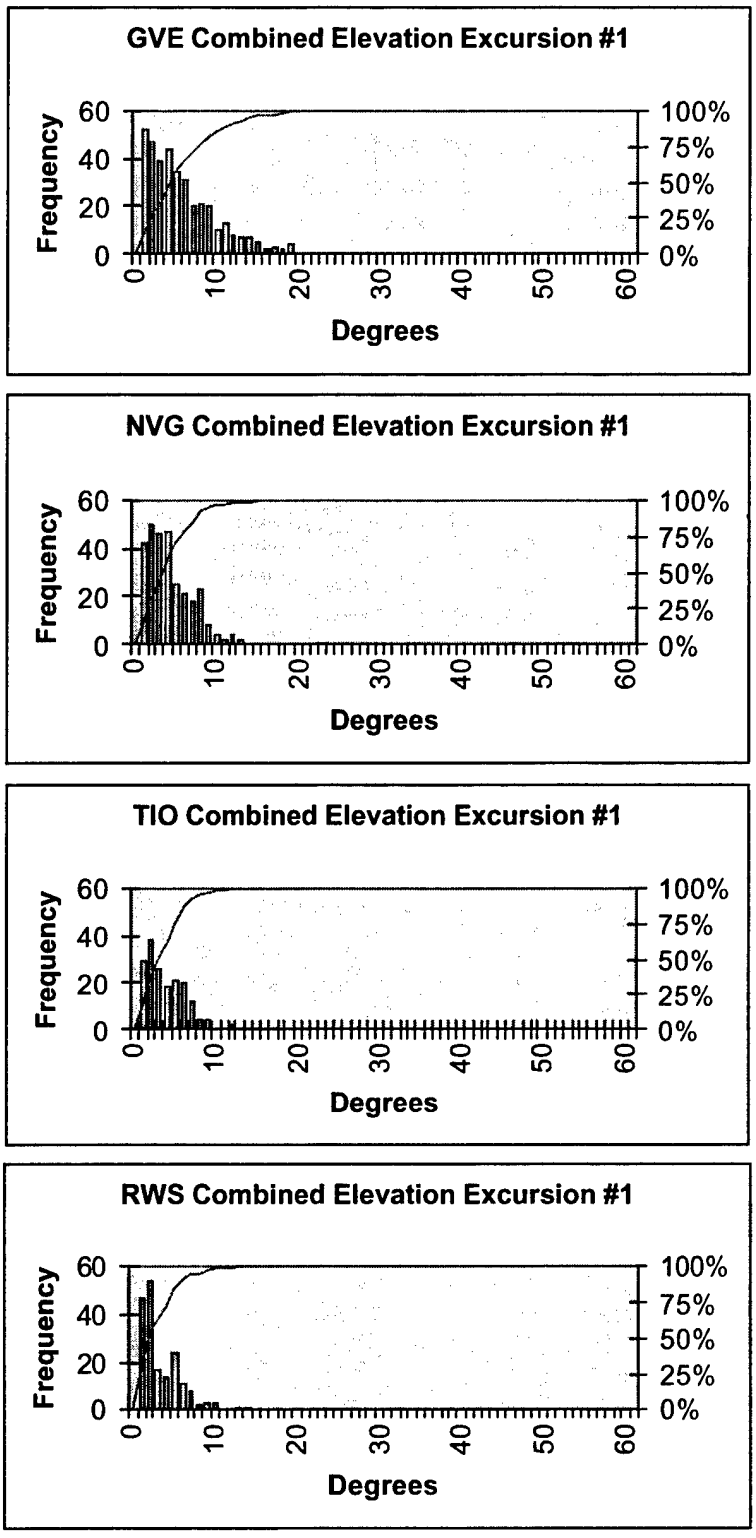

Figure 19. Subject #1 combined excursion histograms by flight type with cumulative frequency curve.

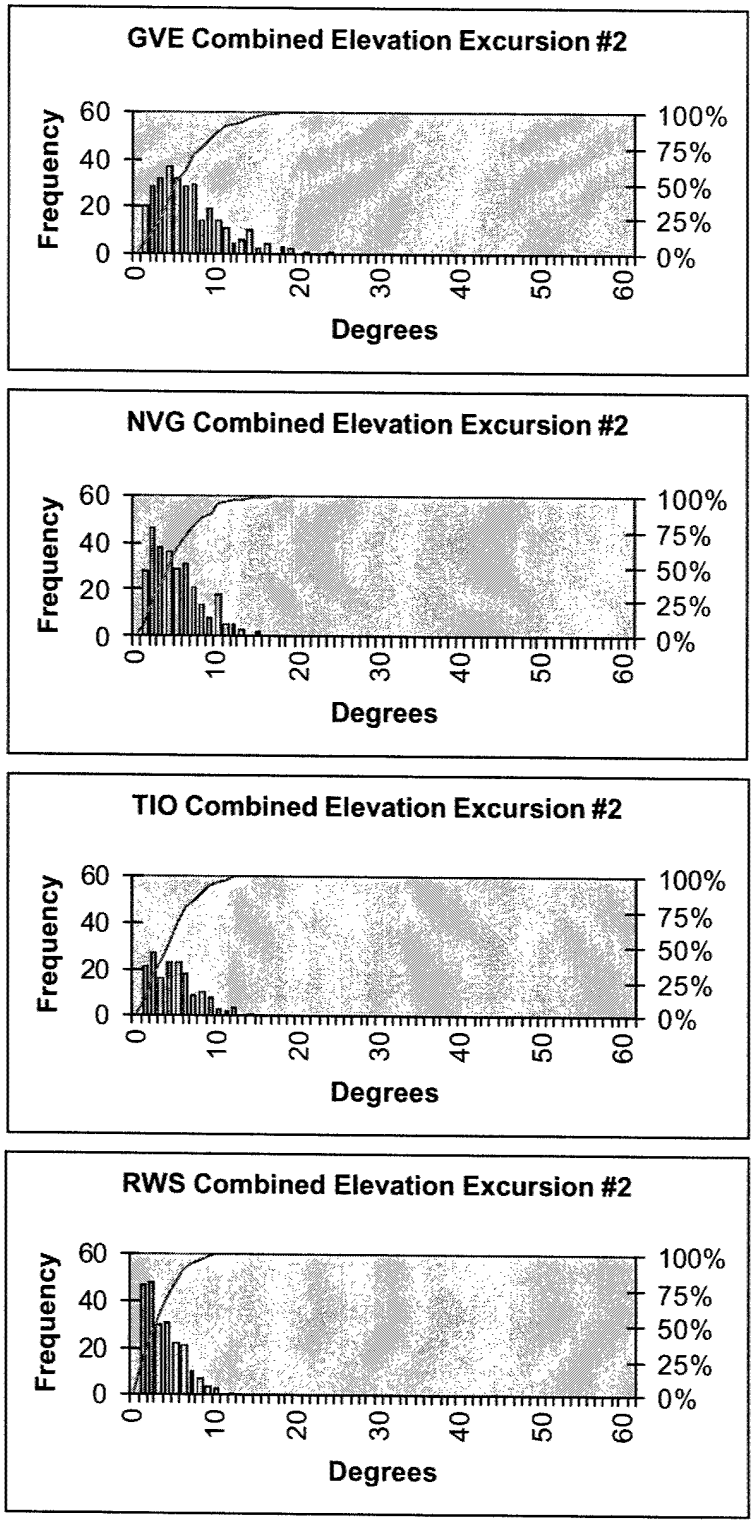

Figure 20. Subject #2 combined excursion histograms by flight type with cumulative frequency curve.

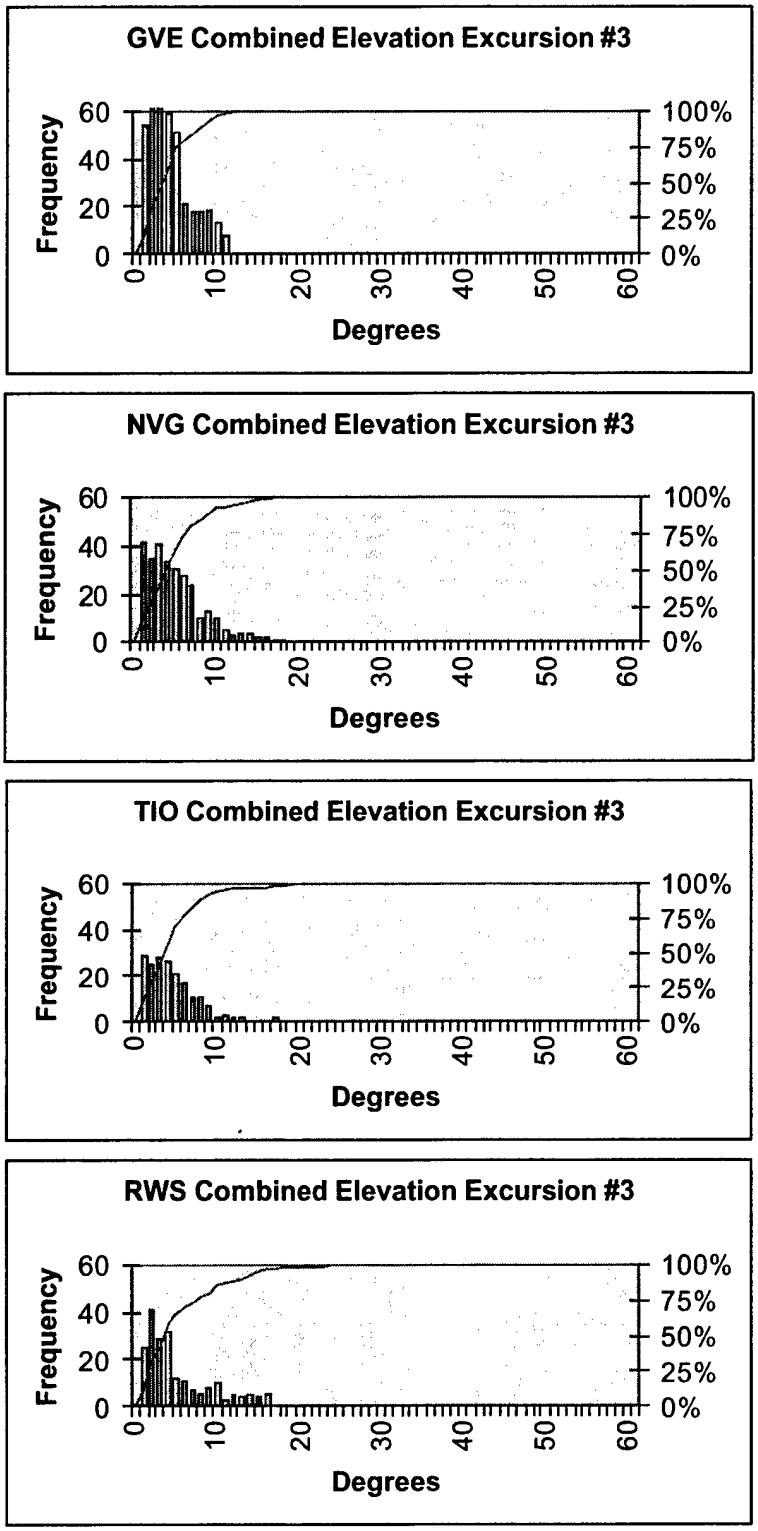

Figure 21. Subject #3 combined excursion histograms by flight type with cumulative frequency curve.

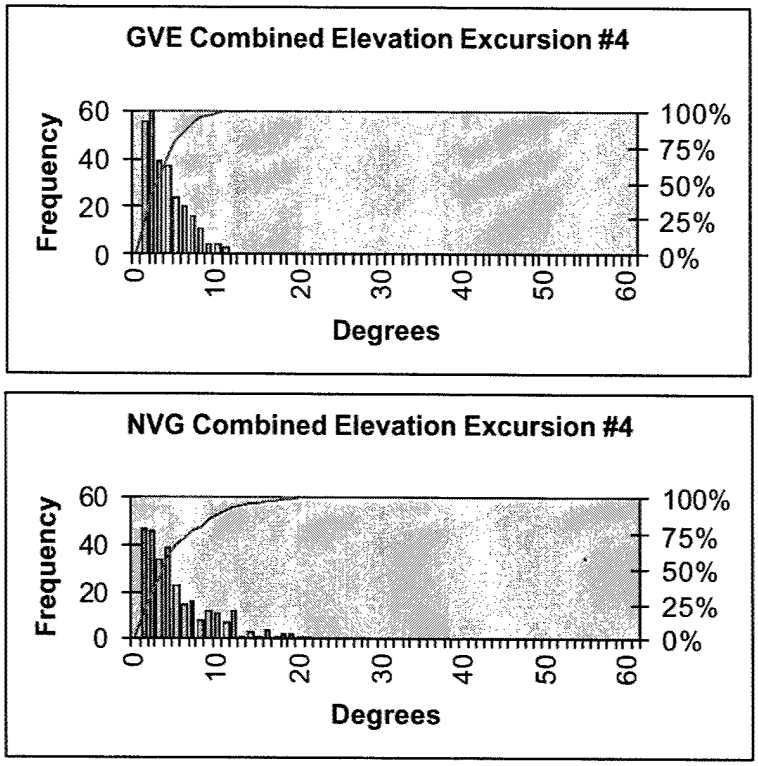

Figure 22. Subject #4 combined excursion histograms by flight type with cumulative frequency curve.

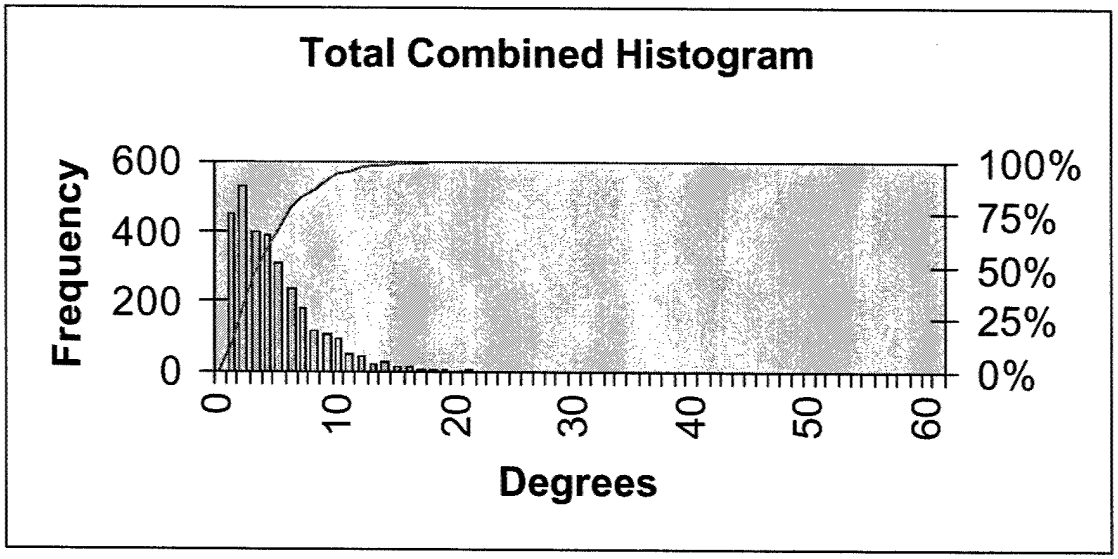

Figure 23. Overall excursion histogram for all subjects, for all visual environments.

Table 11.
Cumulative excursion percentile values.

Subject	Flight Environment	25%	50%	95%	99%
Subject #1	GVE	2	5	14	19
	NVG	2	4	9	13
	TIO	2	3	8	12
	RWS	1	2	8	13
Subject #2	GVE	3	5	14	19
	NVG	2	4	11	16
	TIO	2	4	10	12
	RWS	2	3	8	10
Subject #3	GVE	2	4	10	11
	NVG	2	4	12	16
	TIO	2	4	11	19
	RWS	2	4	16	19
Subject #4	GVE	2	3	8	11
	NVG	2	4	14	19
	TIO	None			
	RWS				

Note: All values expressed in degrees.

Velocity

Biomechanical and physiological data (Durluch and Mavor, 1995) support unloaded elevation head velocity values as high as 300°/sec. Larger peak velocity values are associated with increasing size of head motion excursions. It is very likely that when the head is supporting additional weights of HMDs, peak velocity values would be less.

For these analyses, all velocity values were expressed as positive in value. There was no attempt to separate velocities of motions upward from motions downward. Velocity values were calculated from the time-sequenced elevation position data using an algorithm based on the central derivative (Bloch, 2000). The algorithm calculated the instantaneous velocities at the middle of a moving three-point interval of the time-sequenced data. Velocities at the initial and final data points were not calculated. An inspection of the resulting velocities verified there were no artifacts introduced by the derivative process.

Velocity distribution histograms

As with head position data, the use of histograms to represent the velocity distributions is a fundamental technique in the understanding of head motion. The histograms presented herein use 1-degree per second (°/sec) intervals. Also, as with the position data,

for the combinations of four subjects, four visual environments and two LOAs, there were 103 elevation velocity distributions available for analysis.

Individual velocity distributions. Subject #1 has a total of 25 velocity histograms that represent the various combinations of LOA, run type and visual environment; subject #2 has 24 histograms; subject #3 has 34 histograms; and subject #4 has 20 histograms. The resulting individual velocity histograms, with cumulative frequency curves overlaid, are presented in Appendix H. Examining these individual histograms for general characteristics and trends for each subject and visual condition yields the following:

Subject #1. The individual GVE head velocity distributions for subject #1 (Figure H-1) present the following characteristics: a) Cumulative frequency curves become asymptotic at velocities approximately 20°/sec to 30°/sec; and b) the beginning slopes of the cumulative frequency curves generally are not very steep, implying that the low velocity values are spread out.

NVG head velocity distributions for subject #1 (Figure H-2) present the following characteristics: a) Cumulative frequency curves become asymptotic at velocities approximately 15°/sec to 25°/sec; and b) the beginning slopes of the cumulative frequency curves are steeper than for the GVE visual.

TIO head velocity distributions for subject #1 (Figure H-3) present the following characteristics: a) Cumulative frequency curves become asymptotic at velocities near 15°/sec; and b) the beginning slopes of the cumulative frequency curves are steeper than for the GVE and NVG visual conditions.

RWS head velocity distributions for subject #1 (Figure H-4) present the following characteristics: a) Cumulative frequency curves become asymptotic at velocities near 15°/sec; and b) the beginning slopes of the cumulative frequency curves are steeper than for the GVE and NVG visual conditions comparably as steep as the TIO visual environment.

Subject #2. The GVE head velocity distributions for subject #2 (Figure H-5) present the following characteristics: a) Cumulative frequency curves become asymptotic at velocities approximately 20°/sec to 40°/sec; and b) the beginning slopes of the cumulative frequency curves have a gradual rise implying that the frequency of the low velocity values are spread out over a larger range.

NVG head velocity distributions for subject #2 (Figure H-6) present the following characteristics: a) Cumulative frequency curves are not consistent and become asymptotic at velocities approximately 15°/sec to 25°/sec; and b) the beginning slopes of the cumulative frequency curves are steeper than for the GVE visual condition.

TIO head velocity distributions for subject #2 (Figure H-7) present the following characteristics: a) Cumulative frequency curves are not consistent and become asymptotic at velocities approximately 20°/sec, and b) the beginning slopes of the cumulative frequency curves are steeper than the GVE and NVG visual conditions.

RWS head velocity distributions for subject #2 (Figure H-8) present the following characteristics: a) Cumulative frequency curves become asymptotic at velocities approximately 15°/sec; and b) the beginning slopes of the cumulative frequency curves are steeper than for the GVE and NVG, but slightly steeper than TIO.

Subject #3. The GVE head velocity distributions for subject #3 (Figure H-9) present the following characteristics: a) Cumulative frequency curves are not consistent and become asymptotic at velocities between 15-24°/sec; and b) the beginning slopes of the cumulative frequency curves vary, but in general have a gradual rise implying that the frequency of the low velocity values are spread out over a larger range.

NVG head velocity distributions for subject #3 (Figure H-10) present the following characteristics: a) Cumulative frequency curves become asymptotic at velocities between 20°/sec and 25°/sec, with one exception at 35°/sec; and b) the beginning slopes of the cumulative frequency curves are even more gradual than for the GVE visual condition.

TIO head velocity distributions for subject #3 (Figure H-11) present the following characteristics: a) Cumulative frequency curves become asymptotic at velocities between 13-23°/sec; and b) the beginning slopes of the cumulative frequency curves vary greatly.

RWS head position distributions for subject #3 (Figure H-12) present the following characteristics: a) Cumulative frequency curves become asymptotic at velocities between 15-23°/sec; and b) the beginning slopes of the cumulative frequency curves vary greatly.

Subject #4. The GVE head velocity distributions for subject #4 (Figure H-13) present the following characteristics: a) Cumulative frequency curves are not consistent and become asymptotic at velocities between 12-25°/sec; and b) the beginning slopes of the cumulative frequency curves vary greatly from very seep to moderately gradual.

NVG head velocity distributions for subject #4 (Figure H-14) present the following characteristics: a) Cumulative frequency curves become asymptotic at velocities of between 15-25°/sec; and b) the beginning slopes of the cumulative frequency curves are more consistent than, but similar to, the GVE visual condition.

Note: Head position data for subject #4 were not available for TIO and RWS visual environments.

Combined velocity histograms. As with the position data, it is argued that combined velocity histograms are more useful in understanding the general (average) nature of head velocities present in the shalom course flown in this study. Figures 24-27 present the combined velocity distributions by subject and visual environment. Note that head velocity data for subject #4 were available for only two visual environments, GVE and NVG. As with the individual distributions, these combined distributions can be examined visually for general characteristics and trends. The following observations are made:

Subject #1. The combined GVE head velocity distribution for subject #1 (Figure 24) present the following characteristics: a) The cumulative frequency curve becomes asymptotic near 25°/sec, and b) the 50-percent velocity value is 5°/sec.

The combined NVG head velocity distribution for subject #1 (Figure 24) shows: a) The cumulative frequency curve becomes asymptotic at around 19°/sec, and b) the 50-percent velocity value is 4°/sec.

The combined TIO head velocity distribution for subject #1 (Figure 24) shows: a) The cumulative frequency curve becomes asymptotic near 15°/sec, and b) the 50-percent velocity value is 3°/sec.

The combined RWS head velocity distribution for subject #1 (Figure 24) shows: a) The cumulative frequency curve becomes asymptotic near 13°/sec, b) the 50-percent velocity value is 3°/sec.

Subject #2. The combined GVE head velocity distribution for subject #2 (Figure 25) present the following characteristics: a) The cumulative frequency curve becomes asymptotic near 30°/sec, and b) the 50-percent velocity value is 5°/sec.

The combined NVG head velocity distribution for subject #2 (Figure 25) present the following characteristics: a) The cumulative frequency curve become asymptotic near 20°/sec, and b) the 50-percent velocity value is 4°/sec.

The combined TIO head velocity distribution for subject #2 (Figure 25) shows: a) The cumulative frequency curve becomes asymptotic near 20°/sec, and b) the 50-percent velocity value is 4°/sec.

The combined RWS head velocity distribution for subject #2 (Figure 25) shows: a) The cumulative frequency curve becomes asymptotic near 15°/sec, and b) the 50-percent velocity value is 3°/sec.

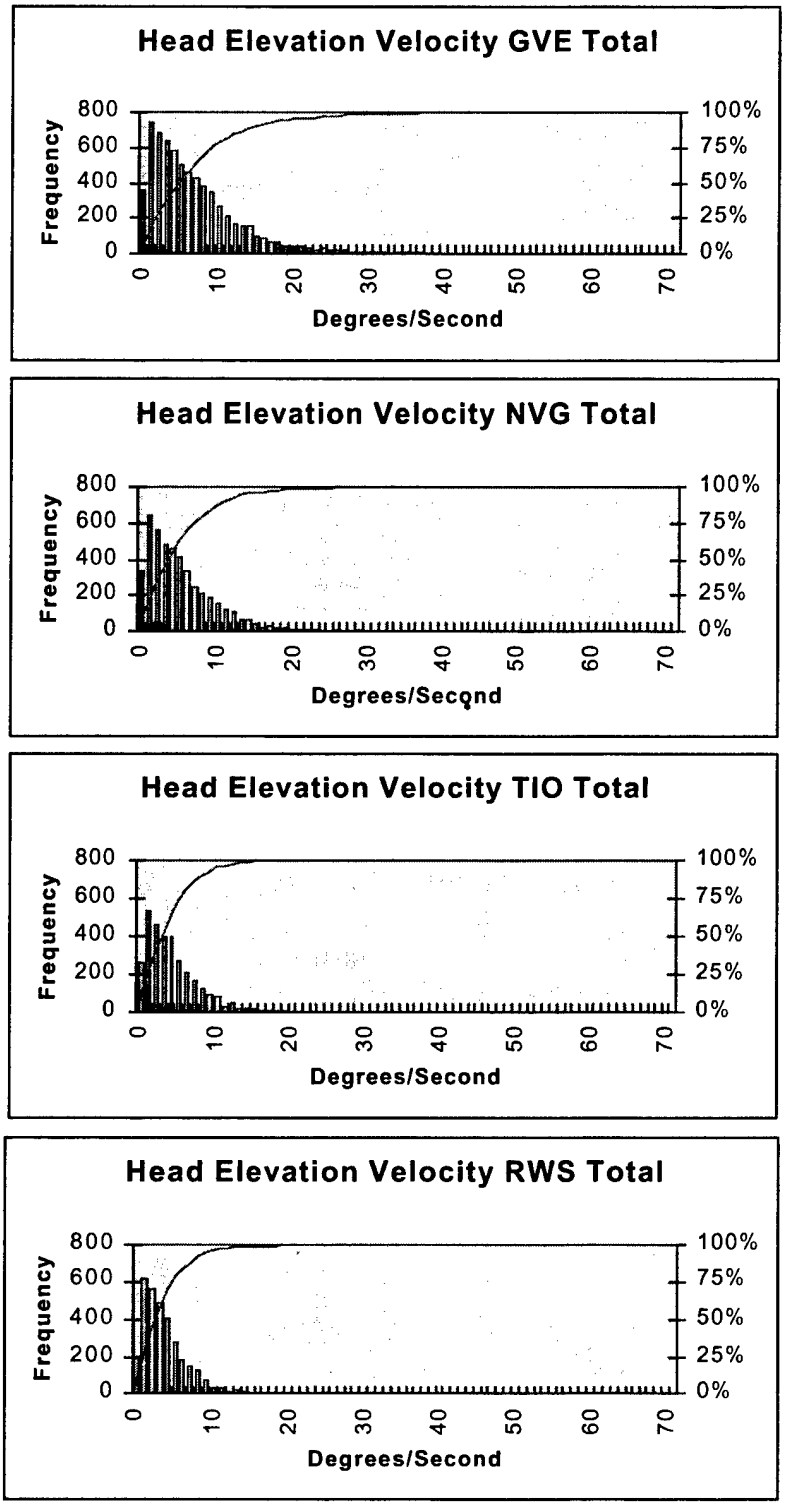

Figure 24. Combined velocity histograms for subject #1.

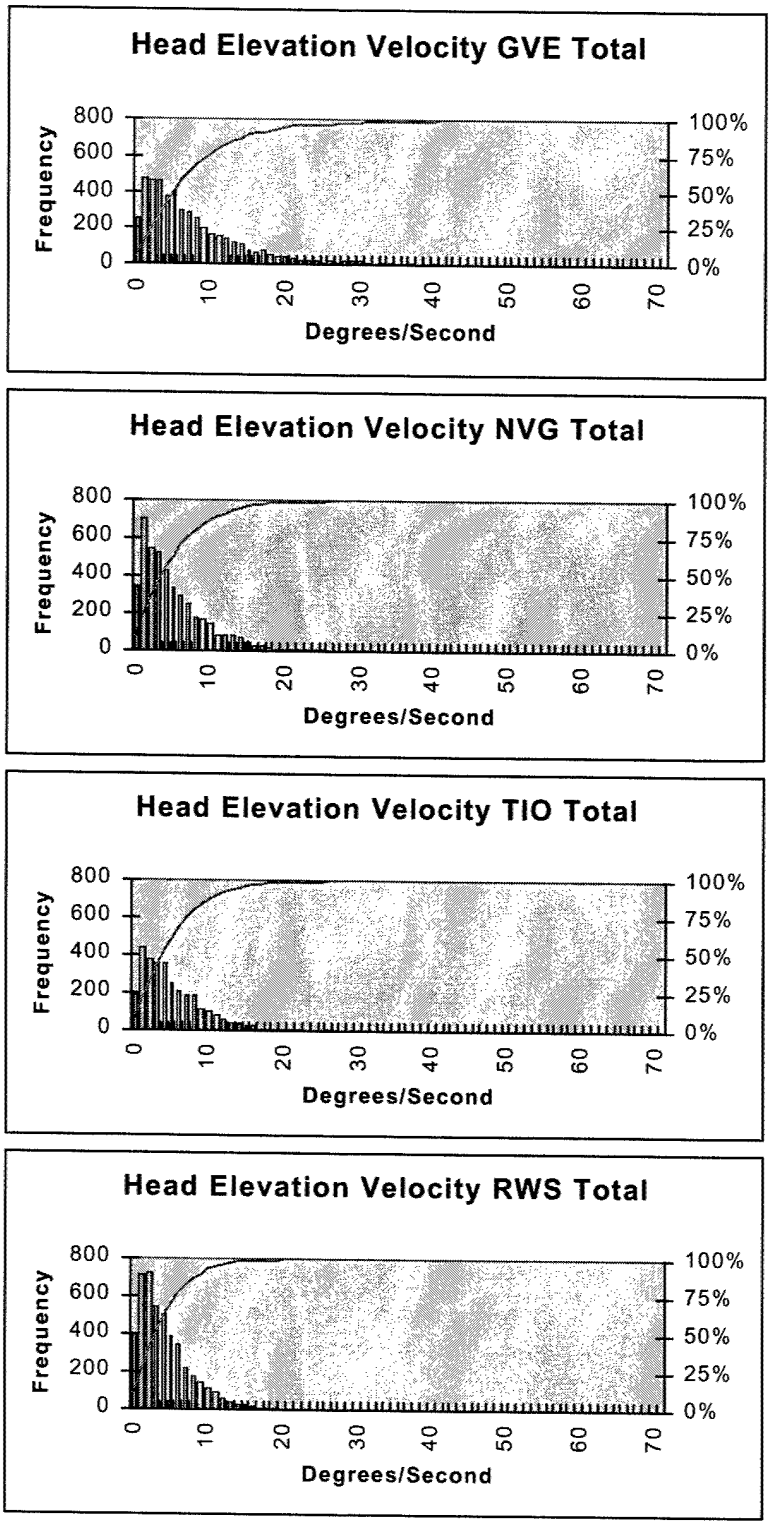

Figure 25. Combined velocity histograms for subject #2.

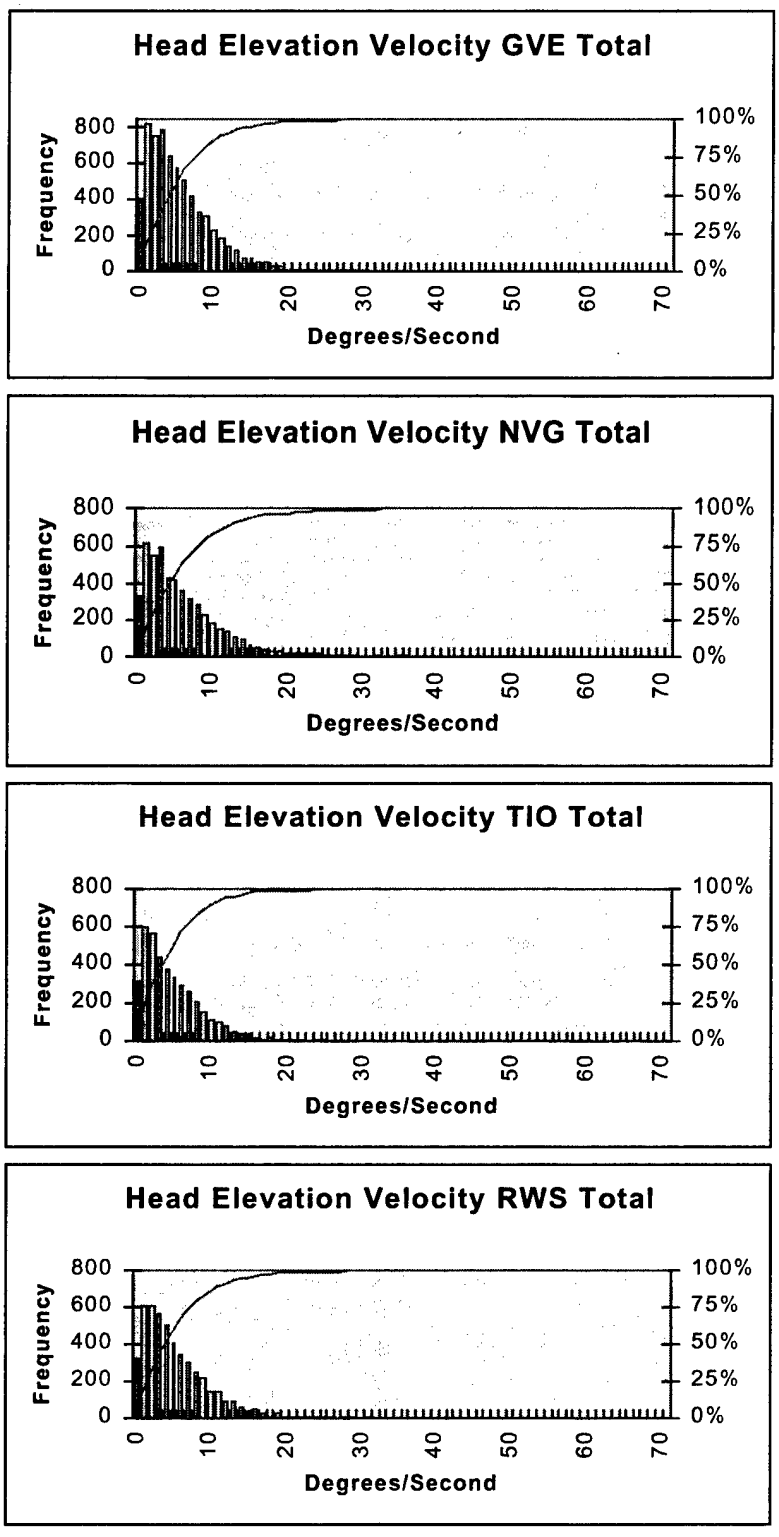

Figure 26. Combined velocity histograms for subject #3.

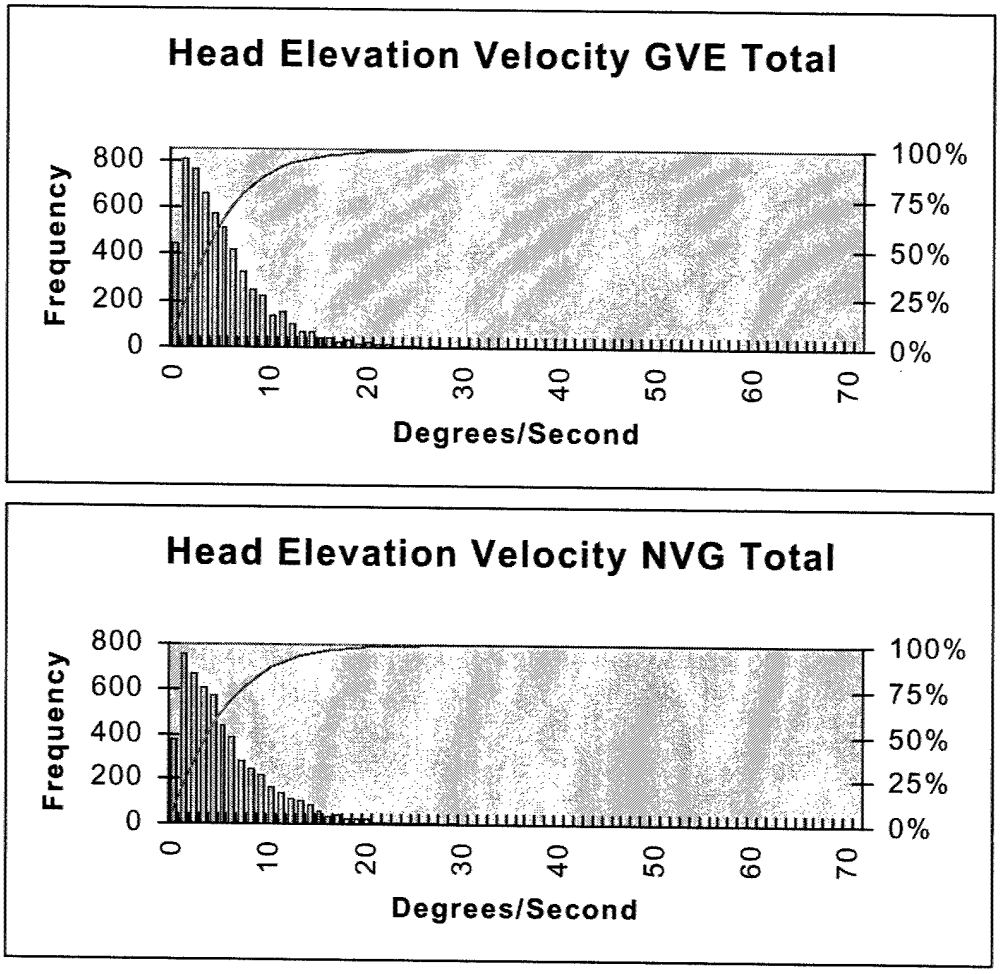

Figure 27. Combined velocity histograms for subject #4.

Subject #3. The combined GVE head velocity distribution for subject #3 (Figure 26) present the following characteristics: a) The cumulative frequency curve becomes asymptotic near 22°/sec, and b) the 50-percent velocity value is 4°/sec.

The combined NVG head velocity distribution for subject #3 (Figure 26) present the following characteristics: a) The cumulative frequency curve becomes asymptotic near 23°/sec, and b) the 50-percent velocity value is 5°/sec.

The combined TIO head velocity distribution for subject #3 (Figure 26) shows: a) The cumulative frequency curve becomes asymptotic near 18°/sec, and b) the 50-percent velocity value is 4°/sec.

The combined RWS head velocity distribution for subject #3 (Figure 26) shows: a) The cumulative frequency curve asymptotic near 20°/sec, and b) the 50-percent velocity value is 4°/sec.

Subject #4. The combined GVE head velocity distribution for subject #4 (Figure 27) present the following characteristics: a) The cumulative frequency becomes asymptotic at around 19°/sec, and b) the 50-percent velocity value is 5°/sec.

The combined NVG head velocity distribution for subject #4(Figure 27) present the following characteristics: a) The cumulative frequency curve becomes asymptotic at around 18°/sec, and b) the 50-percent velocity value is 4°/sec.

When the above observations are examined across subjects, the 50-percent velocity values range from 3-5°/sec for all visual conditions. In general, the asymptotic velocity values are greater for the GVE and NVG visual conditions, and in general, for subjects #1-3, the standard deviations in the elevation velocity values are slightly greater for the GVE and NVG conditions than for the two HMD conditions (TIO and RWS).

As with excursions, it was useful to construct a histogram that represents all velocities exhibited by all pilots during all runs (Figure 28). This overall distribution has the following statistics: Mean of 5.5°/sec, median of 4°/sec, standard deviation of 5.3°/sec, and IQR of 6°/sec. An overlaid cumulative frequency curve indicates that 50% of all velocities were 4°/sec or less. The 95% and 99% velocity values were 14°/sec and 24°/sec, respectively. The largest (maximum) elevation velocity exhibited by any pilot during any run was 111°/sec.

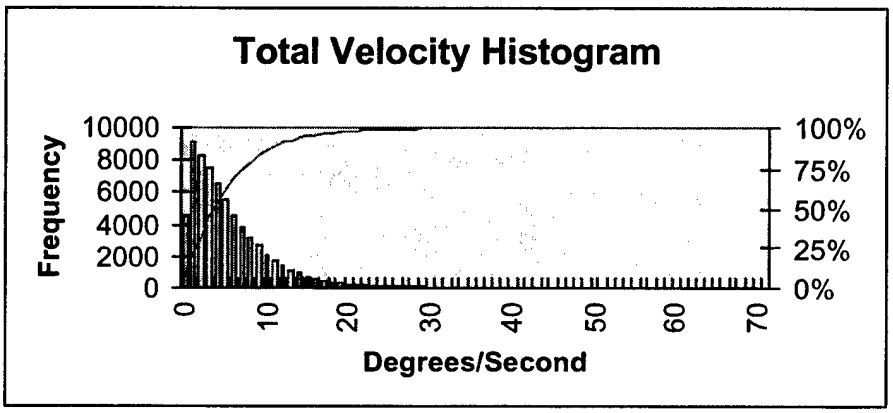

Figure 28. Overall velocity histogram for all subjects, for all visual environments.

Velocity distribution statistics

While distribution shape provides a basic understanding of the ongoing head motion, the semi-quantitative nature of distribution histograms does not allow for comprehensive comparison. For this reason, distributions often are described further by the distribution's moments and other additional statistics. For the velocity distributions presented herein, the maximum, mean, median, standard deviation, and IQR have been calculated.

Summary individual and combined distribution moments and statistics tables for all subjects, grouped by visual environment, are provided in Appendix I. However, following

the previous arguments that comparisons can be based on the combined distributions, a summary of the calculated distribution moments and statistics by subject and visual environment for the combined distributions only is presented in Table 12. Provided in parentheses beside each value is the within subject rank of that value for the selected statistic.

Table 12.

Combined elevation velocity summary by subject and visual environment. Time expressed in seconds; other dimensional statistics expressed in °/sec, ranks within subject given in ( ).

Subject	Visual Environment	Time	Max	Mean	Median	S.D.	IQR
1	GVE	690.6	57.0	7.0(1)	5.0(1)	6.6(1)	2.0 to 9.0(1)
1	NVG	467.2	46.0	5.3(2)	4.0(4)	4.8(2)	2.0 to 7.0(2.5)
1	TIO	315.8	29.0	4.1(3)	3.0(2.5)	3.6(3)	1.0 to 6.0(2.5)
1	RWS	328.2	47.0	3.7(4)	3.0(2.5)	3.5(4)	1.0 to 5.0(4)
2	GVE	480.4	111.0	7.6(1)	5.0(1)	7.5(1)	2.0 to 8.0(2)
2	NVG	452.0	48.0	5.2(3)	4.0(2.5)	5.1(2)	2.0 to 7.0(4)
2	TIO	320.7	45.0	5.4(2)	4.0(2.5)	4.9(3)	2.0 to 8.0(2)
2	RWS	465.8	39.0	4.4(4)	3.0(4)	3.9(4)	2.0 to 8.0(2)
3	GVE	677.7	41.0	5.7(2)	4.0(3)	5.4(2)	2.0 to 8.0(2.5)
3	NVG	525.1	66.0	6.3(1)	5.0(1)	5.9(1)	2.0 to 9.0(1)
3	TIO	414.4	41.0	5.0(4)	4.0(3)	4.5(4)	2.0 to 7.0(4)
3	RWS	497.8	51.0	5.6(3)	4.0(3)	5.0(3)	2.0 to 8.0(2.5)
4	GVE	582.0	39.0	5.1(2)	4.0(1.5)	4.8(2)	2.0 to 7.0(2)
4	NVG	557.3	45.0	5.4(1)	4.0(1.5)	4.9(1)	2.0 to 8.0(1)
4	TIO	None					
4	RWS						

To investigate the trend in ranking amongst the various velocity statistics, Tables 13 and 14 present the Spearman rank-correlation coefficients for two measures of central tendency, mean and median, and two measures of dispersion, standard deviation and IQR. While remembering that correlation coefficients involving subject #4 should be given less weight because only GVE and NVG data were available, the Spearman rank-correlation tests showed virtually no association between the visual environment and the mean, median, standard deviation, and IQR. In other words, elevation velocity distributions failed to provide a methodology for discriminating elevation head motion between the four visual environments.

Graphical comparison

Graphical comparisons are based on a 5-number summary box plot employed in the SPSS for Windows™ statistical software. The box plot technique provides a visual summary of a data set by emphasizing a select set of statistic values, e.g., median,

Table 13.
Spearman rank-correlation coefficients for velocity mean and median.

Mean					Median				
	#1	#2	#3	#4		#1	#2	#3	#4
#1		+0.80	+0.60	-1	#1		+0.85	+0.20	+0.50
#2			0.00	-1	#2			+0.25	+0.50
#3				+0.60	#3				+0.50
#4					#4				

Table 14.
Spearman rank-correlation coefficients for velocity standard deviation and IQR.

S.D.					IQR				
	#1	#2	#3	#4		#1	#2	#3	#4
#1		+1	+0.60	-1	#1		+0.25	+0.10	-1
#2			+0.60	-1	#2			-0.35	-1
#3				+1	#3				+1
#4					#4				

quartiles, and IQR. Box plots for combined elevation velocity distributions for all subjects are presented in Figures 29-32. Individual box plots for all subjects by visual environment are presented in Appendix J. It should also be noted that extreme values have been removed to provide a less cluttered graphical representation.

From the box plots for subject #1 in Figure 29, the following characteristics and trends can be observed: a) the GVE box plot has the largest IQR; b) NVG and TIO have similar IQRs; and c) median followed by NVG, and then TIO and RWS (which are equal); however, differences were small.

From the box plots for subject #2 in Figure 30, the following characteristics and trends can be observed: a) GVE box plot has the largest IQR and range; and b) GVE has the largest median; however, there were only small differences between the medians for all four visual environments.

From the box plots for subject #3 in Figure 31, the following characteristic and trend can be construed: NVG has the largest IQR median and range; however, there were only small differences in the box plots between all four visual environments.

From the box plots for subject #4 in Figure 32, the following characteristic and trend can be construed: Box plots for GVE and NVG are virtually identical.

Across all subjects, a graphical comparison via box plots for the four visual conditions failed to show any differences.

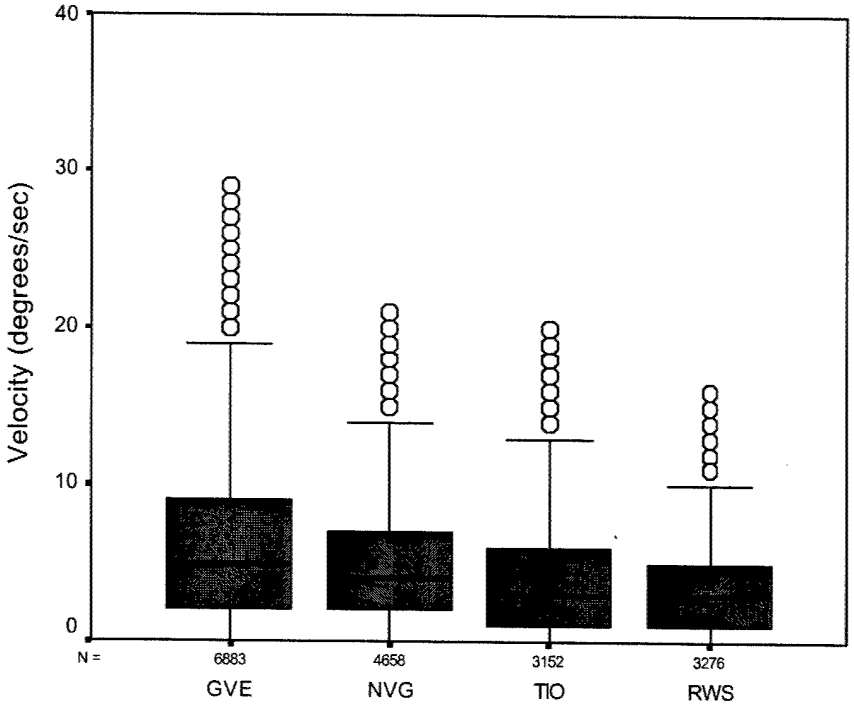

*Note: Extreme values are excluded to allow for better visual representation.

Figure 29. Combined elevation velocity box plots for subject #1.

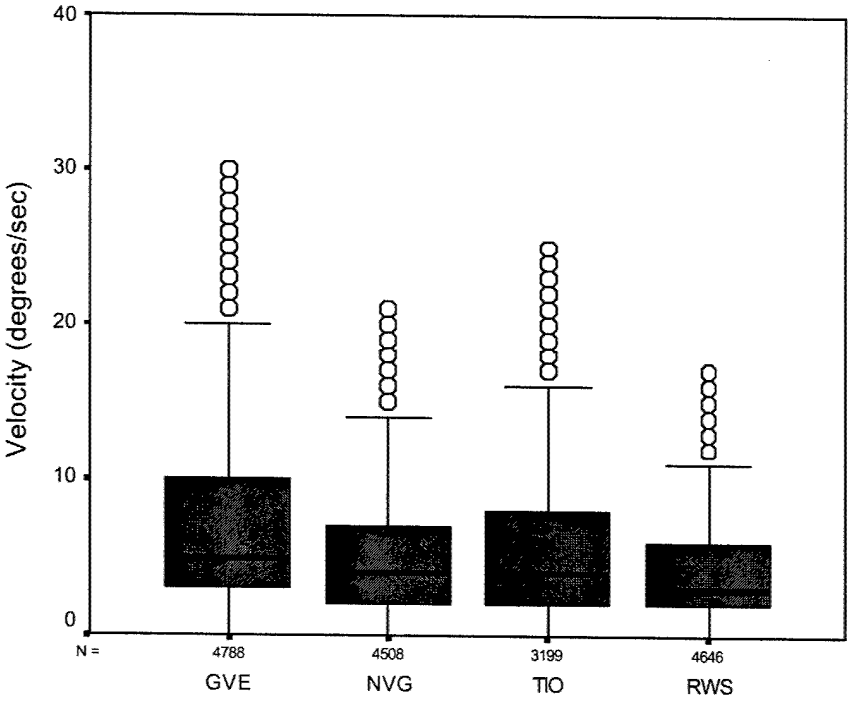

*Note: Extreme values are excluded to allow for better visual representation.

Figure 30. Combined elevation velocity box plots for subject #2.

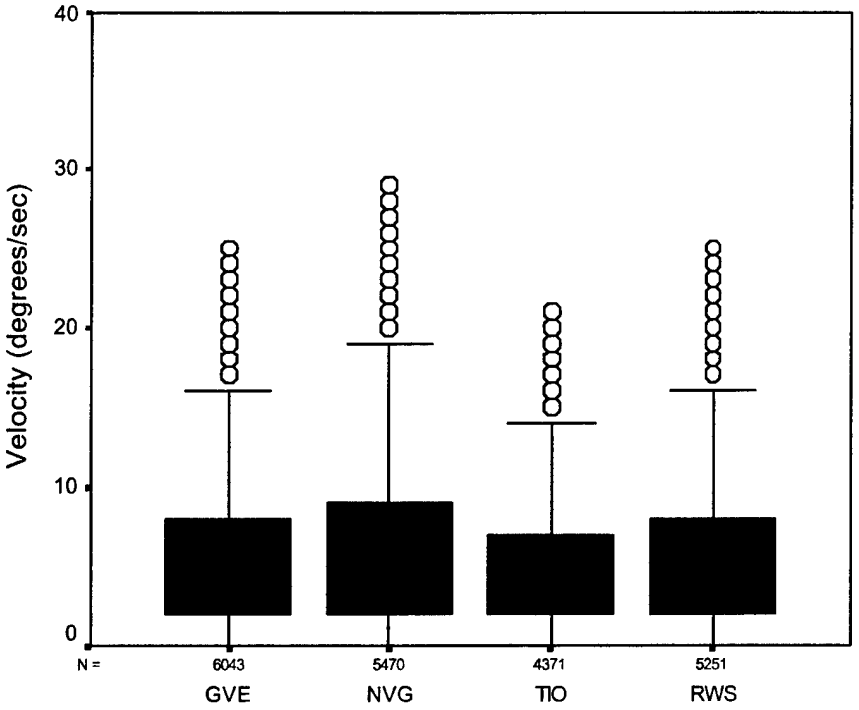

*Note: Extreme values are excluded to allow for better visual representation.
Figure 31. Combined elevation velocity box plots for subject #3.

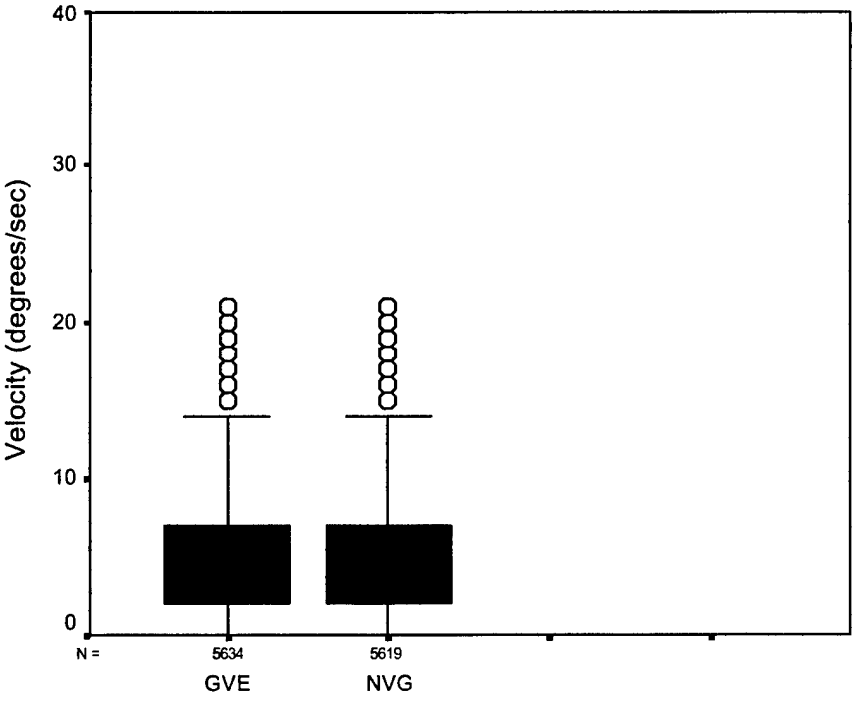

*Note: Extreme values are excluded to allow for better visual representation.
Figure 32. Combined elevation velocity box plots for subject #4.

Discussion

Verona et al. (1986) identified two major factors that influence head motion characteristics in rotary-wing flight. The first factor is aircraft configuration, which encompasses crewstation design, seating configuration (tandem vs. side-by-side), seat adjustment (fore/aft and up/down), and transparency (window) locations. The second factor is the flight task/environment, which encompasses the flight maneuver, terrain/route familiarity, and threat level. The introduction of HMDs (to include NVGs) into the cockpit with their reduced FOVs is an additional element of the flight task/environment factor.

For the data analyzed herein, the aircraft had side-by-side seating and the subject was in the left seat; 0° in elevation was associated with the level direction directly in front of subject. The exact vertical angular subtense of the transparencies is not available. However, an inspection of Figure 5 leads to the following observations: While dependent on seat height adjustment and pilot height, the upward vertical visibility is extremely limited. The lower forward vertical visibility is limited by the extended nose of the aircraft and the forward-looking infrared (FLIR) sensor mount. Two small rectangular side windows, one on each side, are located approximately at the position of the pilot's feet.

The flight course was well known to the subjects, and overall, the slalom maneuver task was relatively benign.

Considering the preceding discussion, several characteristics of the resulting head motion for the data herein might be predicted. First, the slalom maneuver over a familiar course with a zero threat level was not a very demanding flight task requiring large head movements. Except for standard safety reasons, the subject might be expected to look primarily forward. However, it would be expected that the use of HMDs would result in an increase in the range of head motion in an attempt to compensate for the reduced HMD FOV. Another predicted characteristic is the effect of the subject being seated in the left seat of a side-by-side aircraft with the added vision blockage by the right-seated pilot (for GVE and NVG). The subject had the advantage of (unmeasured) eye movement out of the left side, but was required to rely on head motion to view right.

The impact on head motion due to the reduced FOVs for NVG, TIO and RWS visual environments is worth exploring further. When the 47° FOV NVGs were worn, the pilot was required to exercise a head movement in order to see an object more than approximately 24° upward or downward from his current line of sight. For the 53° horizontal by 37° vertical HMD used for TIO and RWS, additional head movement must have occurred in order for the pilot to see an object more than approximately 19° from his current line of sight. For unaided, daytime flight (GVE), the human eye has an instantaneous FOV of roughly 120° (vertical (V)) by 150° (horizontal (H)). When both eyes are considered, the overall binocular FOV measures approximately 120° (V) by 200° (H) (Zucherman, 1954). Humans have the option of both eye and head rotation to assist in viewing. However, in a static scenario, it is generally accepted that humans will use eye movements to view objects up to approximately 15° beyond the current line of sight

direction, beyond which head movement will occur (Bahill, Adler and Stark, 1975). It would be reasonable to predict that between the NVG, TIO and RWS HMD visual environments, that NVG, with the smallest instantaneous FOV, would have the greatest "extent" of head motion. When GVE is considered, the 15° value must not be interpreted as a value beyond which one "must" invoke head movement. While NVG, TIO and RWS visual environments force head movements to look beyond their respective FOVs, GVE allows for peripheral vision and head/eye combination movements, precluding forced head movement in many situations. As a result, speculation on head movement for GVE is difficult. In fact, it is more logical to use head motion in the GVE visual environment as a baseline to which head motion in the NVG, TIO, and RWS visual environments are compared.

The GVE visual environment provides the greatest FOV, that of the human visual system, with only small losses due to the presence of the subjects flight helmet. The NVG visual environment results in the additional head supported weight of the NVG system, produces a forward offset center of gravity (CG), and reduces the FOV to 47°. These factors are opposite in their anticipated impact on head motion. The additional head-supported weight and CG offset would be expected to reduce both range of head positions and velocities through the impact of fatigue and moment of inertia. The two HMD visual environments, TIO and RWS, also are influenced by additional head-supported weight and offset CG. The FOV for these two environments, at 37° vertically, is reduced with respect to the GVE environment and slightly smaller than the 47° NVG environment. Head motion for these two environments is further affected by the inherent delays associated with the head tracking system and the sensor/turret gimbal.

One final factor, and initial driver for this study, is the possible influence of motion sickness on head motion. The actual HMD design used in this study had look-under, look-around capability. However, this capability was offset by the use of the SDVE system, restricting external visual input to that solely provided by the FLIR imagery (and symbology for RWS). This produced a near full-immersion system that has been linked to the phenomenon of "cybersickness." Cybersickness is similar to simulator sickness in that the symptoms of motion sickness (e.g., nausea, sweating, pallor, etc.) can result from lack of correlation between visual and vestibular sensory inputs. Of course, in this study both inputs were present. However, imagery presented by HMDs has a measurable delay in its presentation due to lag times and update rates. This may manifest itself as cybersickness (Melzer and Moffitt, 1997; Rash (Ed.), 1999).

As a final part of the discussion, it is worthwhile to compare the results of this current investigation of head motion with the previous Verona et al. study (1986). This comparison, while valid only for the GVE environment, would be based on the only other head motion database available that represents operational, military, rotary-wing flight. In Verona et al. (1986), six male U.S. Army aviators flew a modified UH-1M Huey helicopter over a circular 15-mile contour course while wearing a prototype AH-64 Apache helmet, which allowed measurement of head position. In both studies, the aircraft had side-by-side seating with the subject pilot in the left seat. The most significant difference between the two studies was the level of aggression. In the study reported

herein, the subjects were flying a well-known flight pattern in a no-threat environment. In Verona et al. (1986), subjects were instructed to look for a threat aircraft that would appear somewhere in their FOV during the flight.

In Verona et al. (1986), for what would be analogous to the GVE condition in the study reported herein, an elevation position range (across all subjects) of -65° to 35° was reported with 95% of the time spent looking between –14° and +14°. A maximum elevation velocity of 160°/sec deg/sec was reported. Fifty percent of the elevation velocity values were less than 33°/sec; 90% were less than 80°/sec.

For the current investigation, the GVE condition across all subjects (Figure 33) resulted in an elevation position range of approximately –53° to +7°, with 95% of the time spent looking between –31° and 0°. The elevation position range is smaller than found by Verona et al (1986); this reduction is not surprising and is in line with the reduced flight threat and aggression level, i.e., reduced ground speed (~30 knots versus 50 knots), in the most recent investigation.

The major peak in elevation position in the current investigation occurred at –17°; the pilot's head remained essentially in a below level direction. This is in contrast to the near level direction (-1°) peak position found by Verona et al. (1986). The most reasonable explanation for this difference is again the reduced flight threat and aggression level in the most recent investigation. The previous investigations required an aggressive search pattern for a threat aircraft.

The maximum GVE elevation velocity for the current investigation was 111° /sec. Fifty percent of the elevation velocity values were less than 3°/sec; 90% were less than 14° /sec. A combined GVE velocity distribution for all subjects is presented in Figure 34. These values were much smaller than reported by Verona et al. (1986), as would be expected.

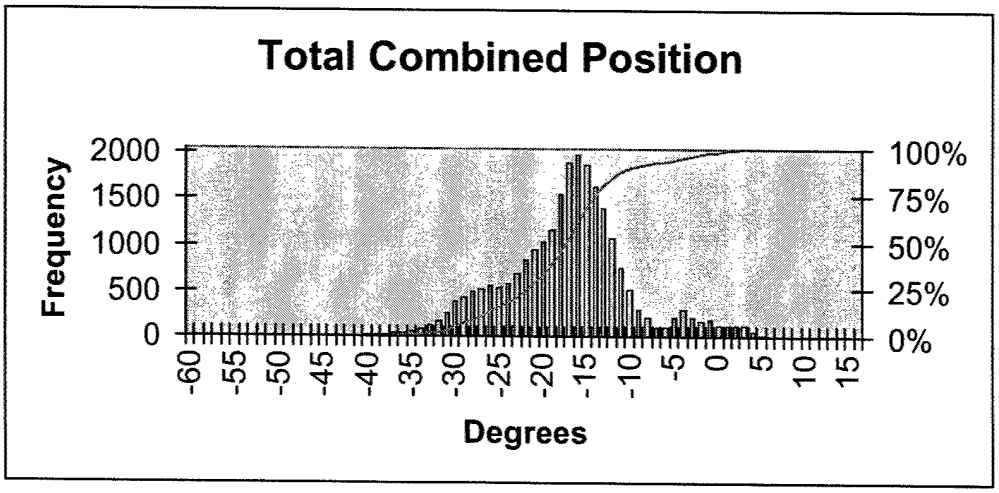

Figure 33. Frequency histogram for current study GVE elevation position combined for all subjects.

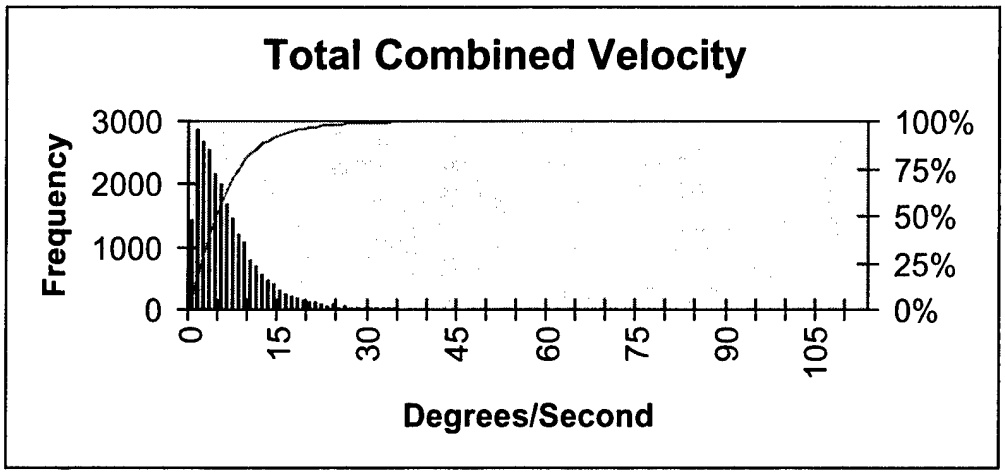

Figure 34. Frequency histogram for current study GVE elevation velocity combined for all subjects.

Summary

Position analyses

As was found with the analysis of azimuth head motion (Rostad et al., 2001), there was great variability in head position data, both within and between subjects. This is not a surprising finding in view of the many factors involved in rotary-wing flight. Both this study and the one conducted by Verona et al. (1986) validate the assertion that even for the same pilot flying the same course back-to-back under the same conditions, head motion will be different. However, it is reasonable to expect that certain trends in head motion may be present for a given set of conditions. This is the argument put forth herein and in the previous azimuth analyses (Rostad et al., 2001).

Perhaps the most significant finding in this investigation of elevation position was the failure to identify any distribution statistic that would serve as a discriminator between visual environments. Rostad et al. (2001) had shown that the IQR spread statistic was a useful discriminator between visual environments for azimuth head position. The authors suggest that this failure is due to the sensitivity of elevation position data to the repeatability of helmet fit. Another possibility is that the decreased vertical FOV through the aircraft windscreen limits the range of elevation head motion.

However, there were some general characteristics and trends in the elevation head position data that could be noted:

- The GVE and NVG distributions have the greater IQRs and ranges.
- The GVE and NVG means and medians are consistently greater in the downward direction than for the two HMD conditions, TIO and RWS.

- The two HMD conditions, TIO and RWS, have the most similar distribution characteristics. These include median, range and IQR.
- Repeatability of helmet fit greatly affects elevation head position. This impact is most apparent for the NVG visual environment where, in addition to variation in the positioning of the helmet vertically on the head, there are multiple NVG mounting bracket tilt positions.

Rate analyses

With regard to rate of change in head position across the four visual environments, three parameters were investigated: reversal rates, excursions, and velocities. Reversal rates, which attempted to quantify the number of times pilots reversed head motion direction, failed to show significant differences between the visual environments. However, in general, there was a trend for higher reversal rates in the GVE and NVG (nonHMD) visual environments.

Excursions were used as an additional measure of the angular elevation movement of the head by the pilots between reversal points, expressed in degrees. Histograms of excursion sizes showed elevation movements as large as 27.4°. However, none of the distribution histograms, for any of the pilots, for any of the visual environments, showed any high degree of similarities. All pilots had relatively large frequencies of smaller head excursions (<5°). An analysis of all excursions collapsed across all runs indicated that 50% of all excursions were less than 3° in size; 95% were less than 11°.

Velocities exhibited for the four visual environments failed to show any differences. Neither the mean, median or IQR statistics could be used to discriminate between the visual environments. In addition, there was no clear trend between subjects for which visual environments exhibited the highest velocities. However, the standard deviation for the GVE and NVG environments were higher than for the two nonHMD environments (TIO and RWS).

An analysis of all velocity values collapsed across all runs (Figure 28) indicated that 50% of all velocities were less than 3°/sec; 95% were less than 14°/sec. The largest velocity exhibited by any pilot during any run was 111°/sec.

The Spearman rank-correlation tests failed to show more than a weak association between the visual environment and the mean, median, standard deviation and IQR. Therefore, none of these statistics could be used for discriminating between visual environments.

Conclusions

This investigation had two objectives. The first was to expand the understanding of the head motion of (Army) pilots in an operational rotary-wing environment, especially while wearing various HMD configurations. The second objective was to identify which

characteristics of head motion position and velocity data could be used to differentiate between head motion distributions (e.g., different visual flight environments).

The first objective was met via the construction of frequency histograms for the measured head positions, excursions, and velocities for four different visual flight conditions, i.e., GVE, NVG, TIO, and RWS. These distributions were defined by the calculation of their moments (i.e., mean, standard deviation, skewness, and kurtosis) as well as additional statistics (e.g., minimum, maximum, median, IQR, etc).

The position distributions for elevation did not show any strong trends as were found in the previous azimuth analysis. Head position was fully contained within the range of approximately -53° (down) and +13° (up), for a total of 66°. When the spread of head position values was examined by visual environment, the GVE and NVG environments generally produced the greatest IQR, range and standard deviation for each subject.

Similarly, the elevation velocity data showed no trends. The maximum velocity exhibited by any pilot for any visual environment was 111°/sec. The mean and median velocities were 5.5°/sec and 4°/sec, respectively. For all velocity distributions combined, 50% of all velocities were 3°/sec or less; 95% were 14°/sec or less; and over 99% of all velocities were less than 24°/sec. When velocity distributions were compared by visual environment, no single visual environment consistently produced any predominant characteristics.

The second objective to identify one or more distribution statistics to allow discrimination between head motion in the various visual environments was achieved indirectly by the finding that none of the distribution statistics could be used to differentiate between head velocity distributions.

In conclusion, while the previous investigation of azimuth head motion demonstrated the usefulness of one or more distribution spread statistics as a mechanism to discriminate between head motion in various visual environments, the current investigation seems to indicate that characteristics of elevation head motion do not vary enough to allow a similar discrimination.

References

Allen, J. H., and Webb, R. C. 1983. Helmet mounted display feasibility model. Orlando, FL: Naval Training Equipment Center. NAVTRAEQUIPCEN IH-338.

Azuma, R., and Bishop, G. 1995. A frequency-domain analysis of head-motion prediction. Computer Graphics Proceedings, SIGGRAPH 95, Los Angeles, CA, August 6-11 401-408.

Bahill, A. T., Adler, D., and Stark, L. 1975. Most naturally occurring human saccades have magnitudes of 15 degrees or less. *Investigative Ophthalmology*, June, Vol. 14/6, 468-469.

Bloch, S. C. 2000. Excel for engineers and scientists. New York: John Wiley and Sons. 69-74.

Borah, J. 1989. Helmet mounted eye tracking for virtual panoramic display systems. Vol. II: Eye tracker specification and design approach. Wright Patterson Air Force Base, OH: Armstrong Aerospace Medical Research Laboratory. AAMRL-TR-89-019.

Borah, J. 1998. Technology and application of head based control. Proceedings of Research and Technology Organization, Lecture Series 215, Alternative Control Technologies: Human Factors Issues, RTO-EN-3, 6-1 to 6-12.

Cameron, A. A., Trythall, S., and Barton, A. M. 1995. Helmet trackers – The future. Helmet- and Head-Mounted Displays and Symbology Design Requirements II, Proceedings of SPIE, Vol. 2465, 281-295.

Crowley, J. S. 1998. Simulating a degraded visual environment in the Lynx helicopter. Farnborough: DERA. DERA Report No. DERA/CHS/PP5/CR9780005/1.0.

Curtis, W., and Sowizral, H. 1994. A note on dynamics of human head motions and on predictive filtering of head-set orientations. SPIE Proceedings: Telemanipulator and telepresence technologies, vol. 2351. Boston, MA. 23-58.

Durlach, N. J. and Mavor, A. S. 1995. Virtual reality scientific and techno logical challenges. Washington D.C., National Academy Press 188-204.

Glanville, A. D., and Kreezer, G. 1937. The maximum amplitude and velocity of joint movements in normal male human adults. Human Biology, 9: 197.

Gauthier, G. M., Martin, B. J., and Stark, L. W. 1986. Adapted head- and eye-movement responses to head inertia. Aviation, Space, and Environmental Medicine. 57:336-42.

Hertzberg, H. T. E. 1972. Human anthropology. In VanCott, H. P. and Kinkade, R. G. (Eds). Human engineering guide to equipment design. Washington D.C.: American Institutes for Research.

Kocian, D. F., and Task, H. L. 1995 "Visually coupled systems hardware and the human interface" In Barfield, W., and Furness, T. A., (Eds) Virtual environments and advanced interface design. New York: Oxford University Press.

Melzer, J. E., and Moffitt, K. 1997. Head mounted displays: Designing for the user. New York: McGraw Hill.

Phillips, C. A., and Petrofsky, J. S. 1983. Neck muscle loading and fatigue: Systematic variation of headgear weight center-of-gravity. Aviation, space, and environmental medicine. 54(10):901-905.

Rash, C. E. Editor. 1999. Helmet-mounted display: Design issues for rotary-wing aircraft. Fort Rucker, AL: U. S. Army Aeromedical Research Laboratory.

Robinson, R. M. , and Wetzel, P. A. 1989. Eye tracker development in the fiber optic helmet mounted display. Helmet-Mounted Displays, Proceedings of SPIE Vol. 1116, 102-108.

Rostad, R. J. , Rash, C. E., Crowley, J. S., Briley, J. K., and Mora, J. C. 2001. Analysis of azimuth head motion in rotary-wing flight using various helmet-mounted display configurations. Helmet-and Head-Mounted Displays VI, Proceedings of SPIE Vol. 4361, 115-129.

Rostad, R.J., Rash C. E., Crowley, J. S., Briley, J. K., and Mora, J. C. In press. Analysis of head motion in rotary-wing flight using various helmet-mounted display configurations (Part I – Azimuth). Ft. Rucker, AL: U.S. Army Aeromedical Research Laboratory.

Sherk, H. H. 1989. Physiology and biomechanics. In H. H. Sherk, E. J. Dunn, F. J. Eismont, J. W. Fielding, D. M. Long, K. Ono, L. Penning, R. Raynor (Eds.), The Cervical Spine. Philadelphia, PA: J. B. Lippincott.

Szoboszlay, Z., Haworth, L., Reynolds, T., Lee, A. 1995. "Effect of field-of-view restriction on rotorcraft workload and performance – Preliminary results," in Helmet and Head-Mounted Displays and Symbology Design Requirements II, Ronald Lewandowski, Wendall Stephens, Loran A. Haworth, Editors, Proc. SPIE 2465, pp.142-153.

U.S. Army Aviation Troop Command. 1994. "Aeronautical design standard, handling qualities requirements for military rotor craft," ADS-33D.

Verona, R.W., Rash C. E., Holt, W. R., and Crosley, J. K. 1986. Head movements during contour flight. Ft. Rucker, AL: U.S. Army Aeromedical Research Laboratory. USAARL Report No. 87-1.

Zangemeister, W. H., and Stark, L. 1981. Active head rotations and eye-head coordination. Annals of New York Academy of Sciences. 374:541-59.

Zuckerman, J. 1954. Perimetry. Philadelphia: Lippincott.

Appendix A.

Elevation position distributions.

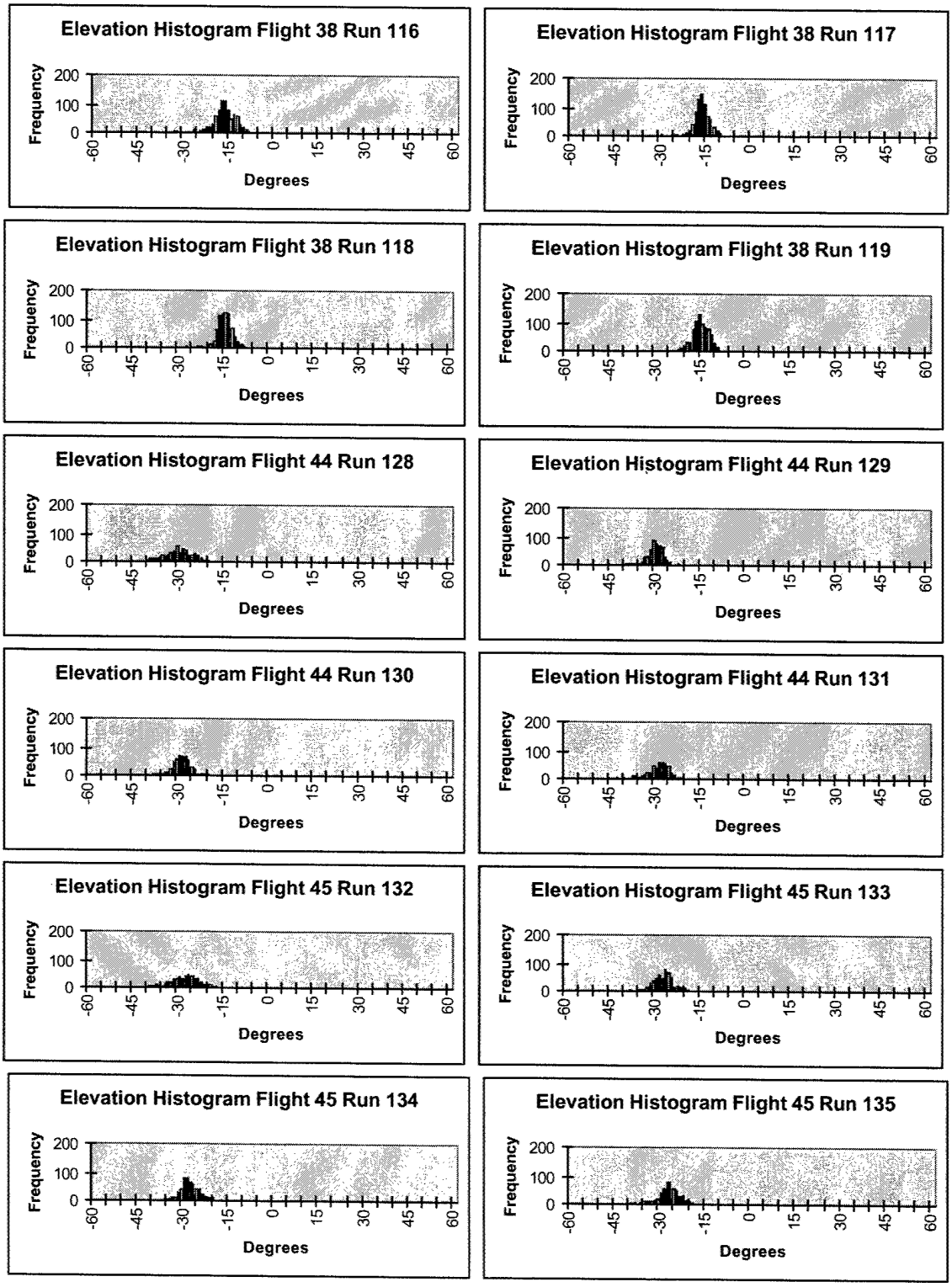

Figure A-1. Subject #1 GVE head position data.

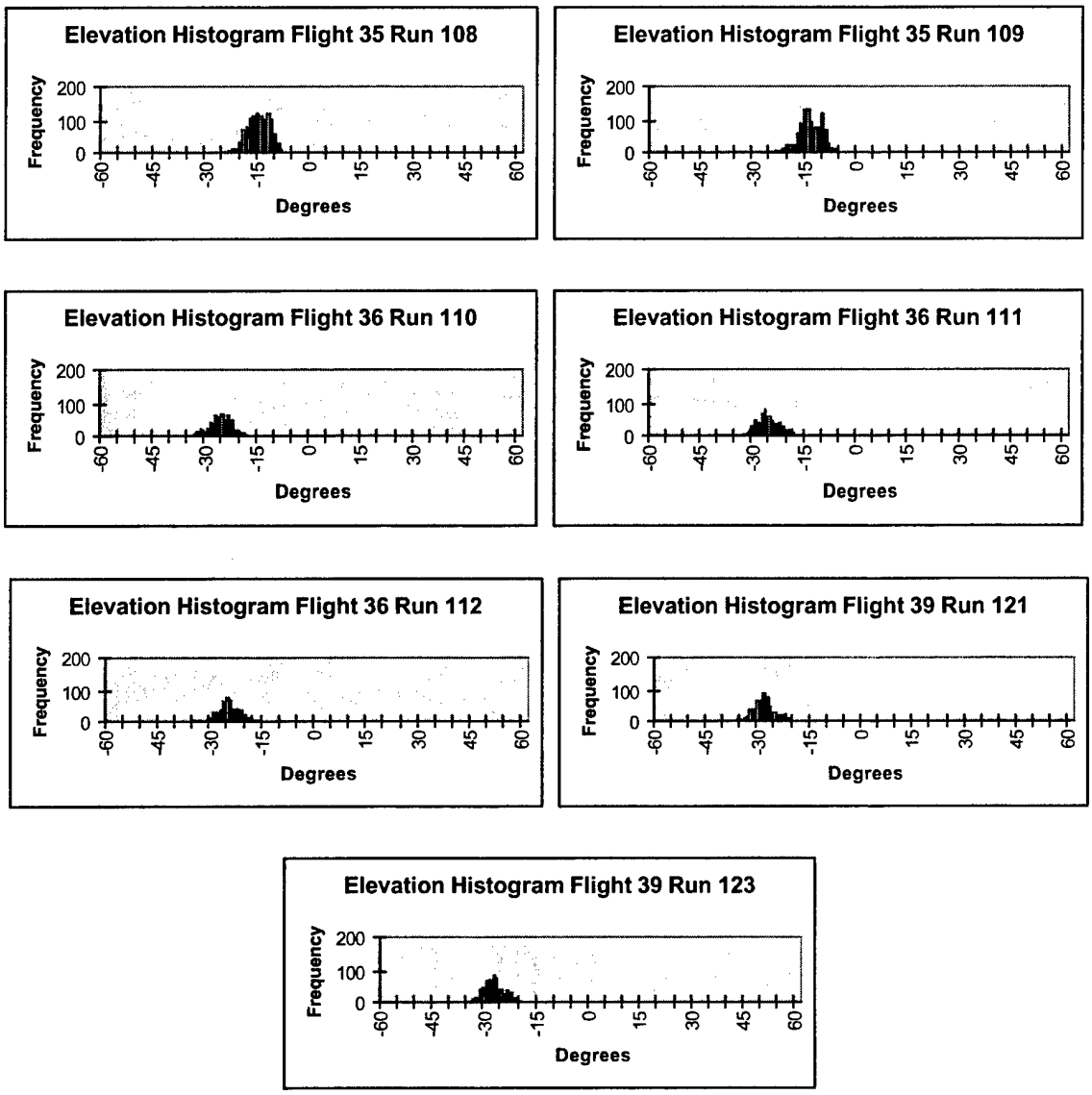

Figure A-2. Subject #1 NVG head position data.

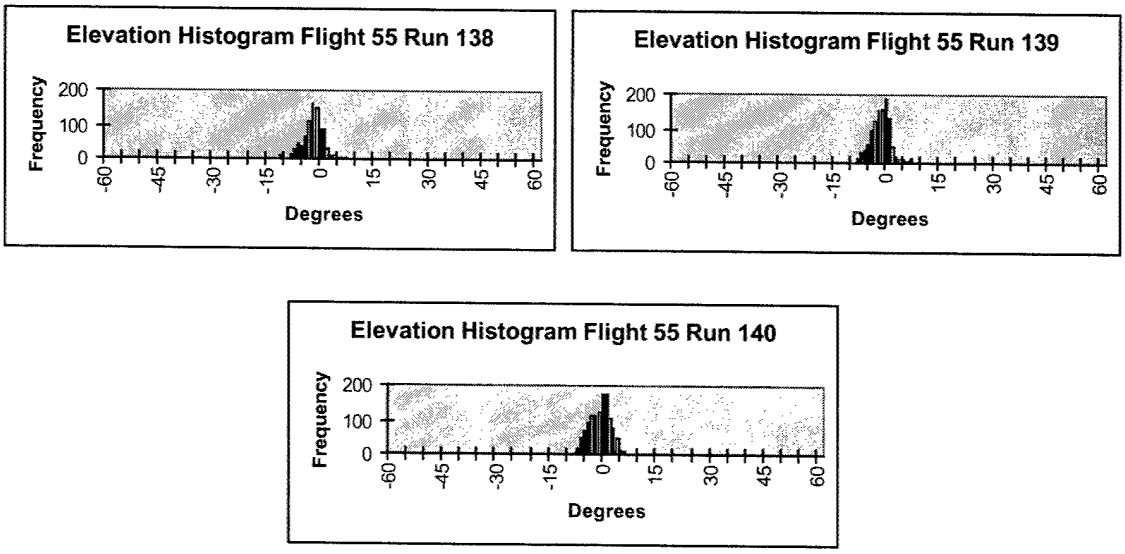

Figure A-3. Subject #1 TIO head position data.

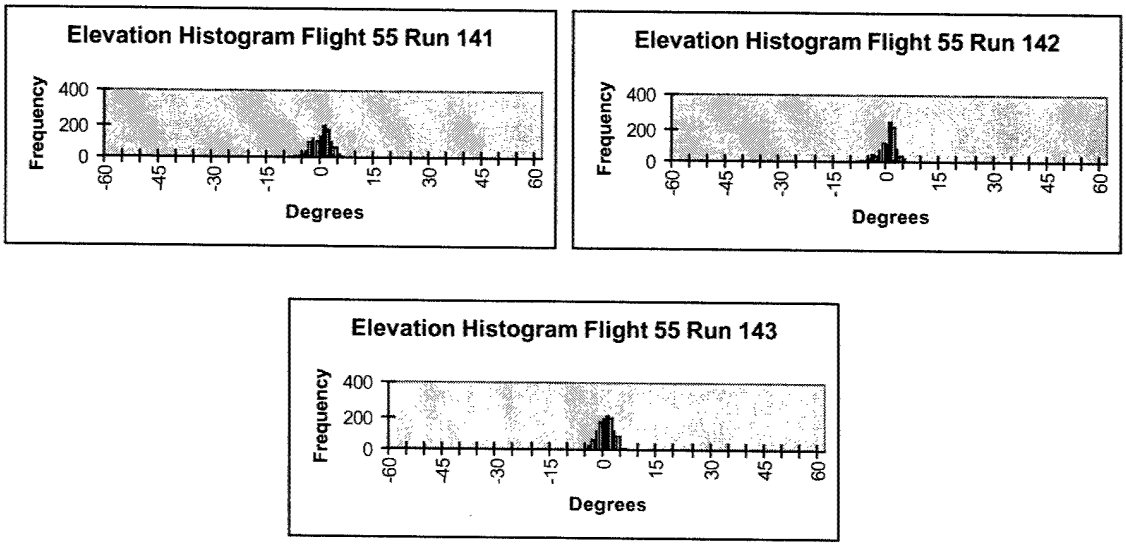

Figure A-4. Subject #1 RWS head position data.

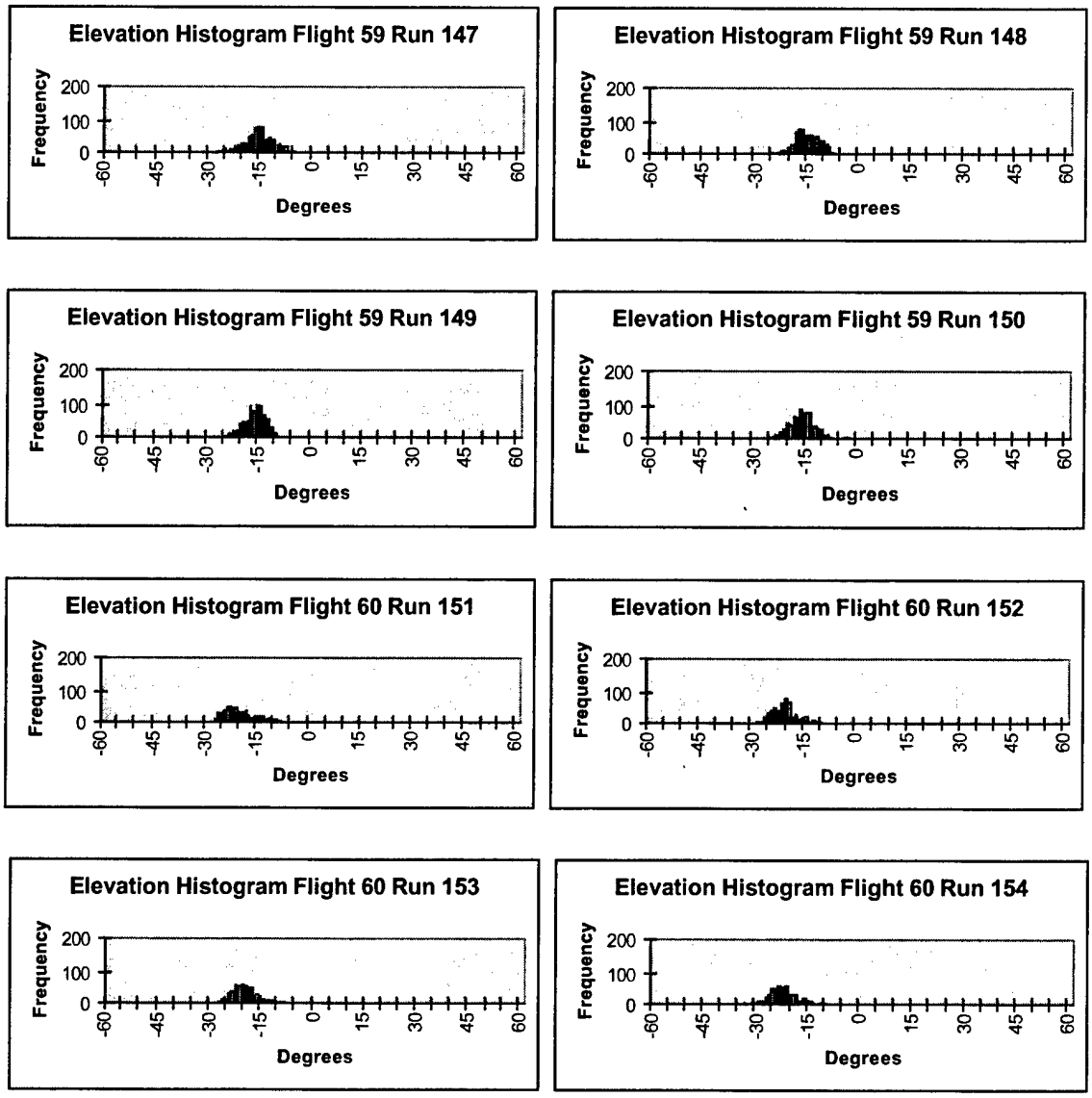

Figure A-5. Subject #2 GVE head position data.

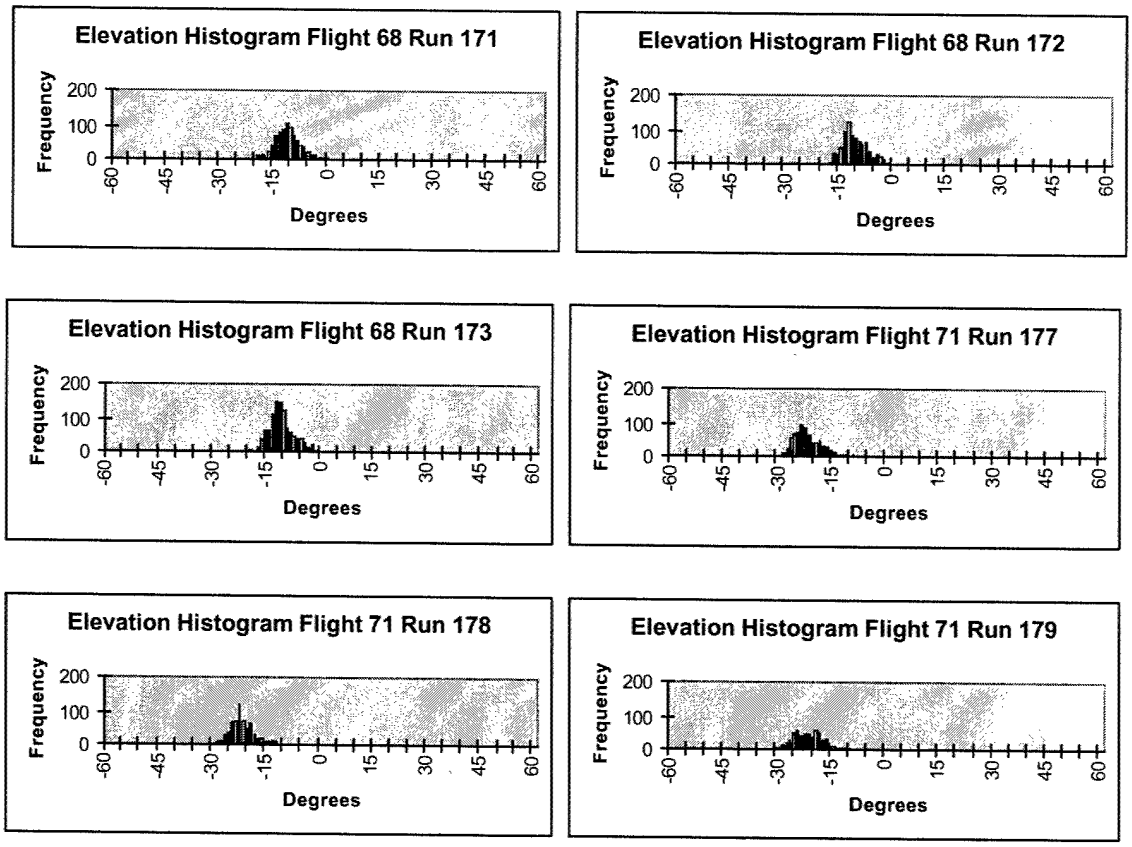

Figure A-6. Subject #2 NVG head position data.

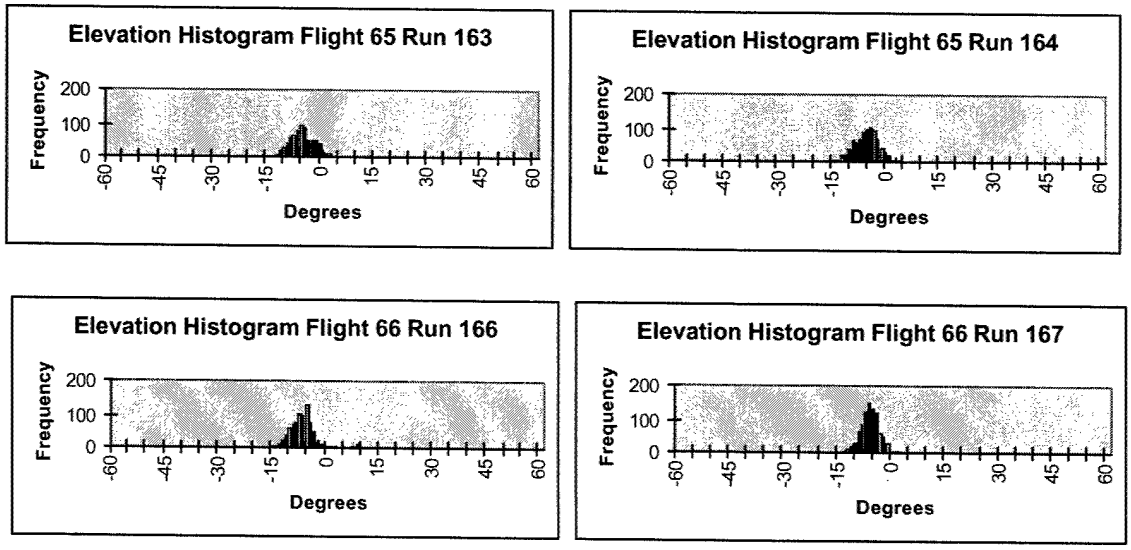

Figure A-7. Subject #2 TIO head position data.

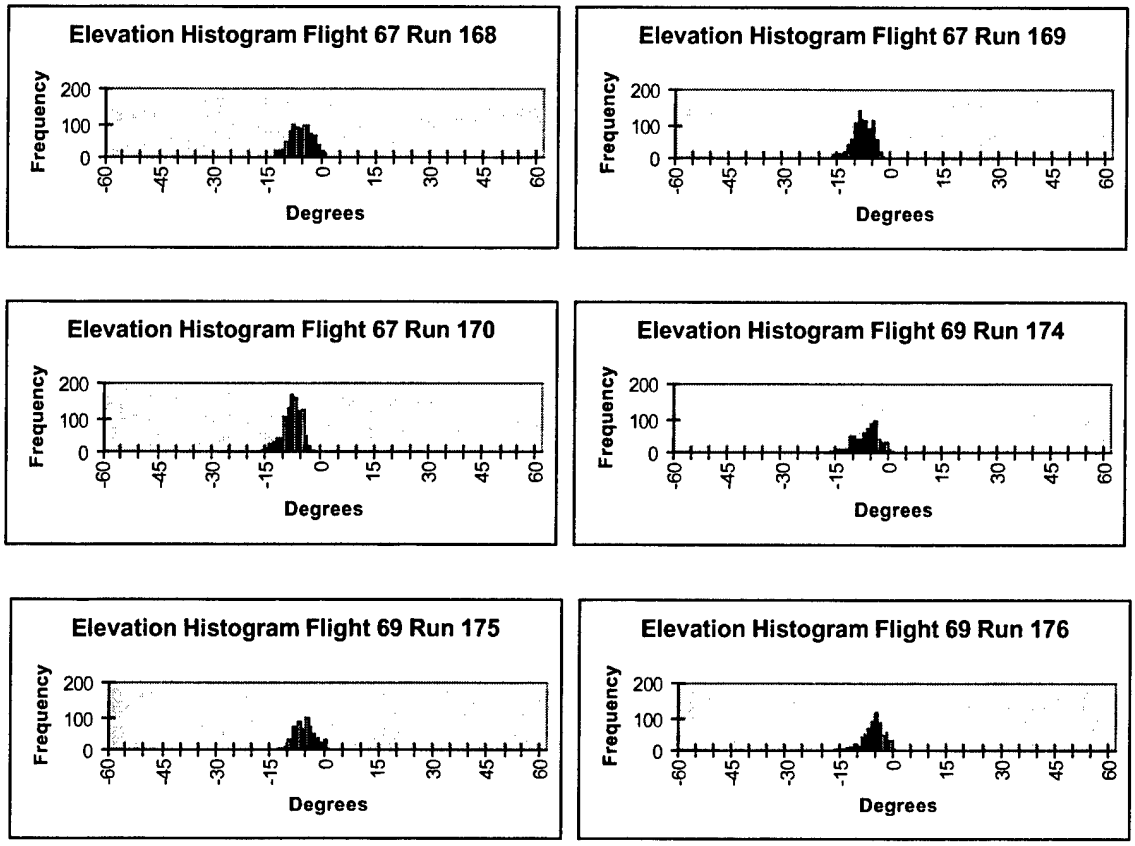

Figure A-8. Subject #2 RWS head position data.

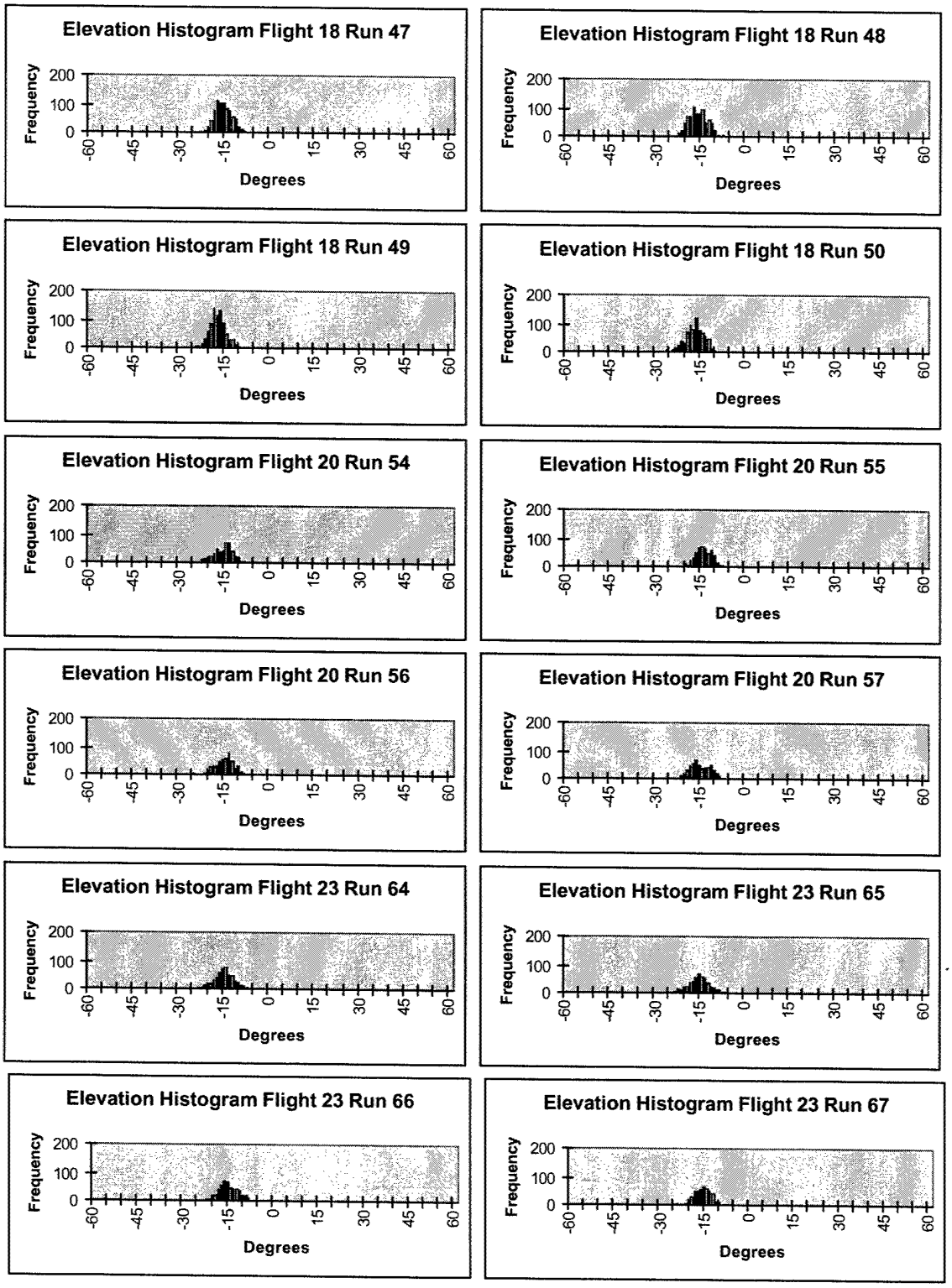

Figure A-9. Subject #3 GVE head position data.

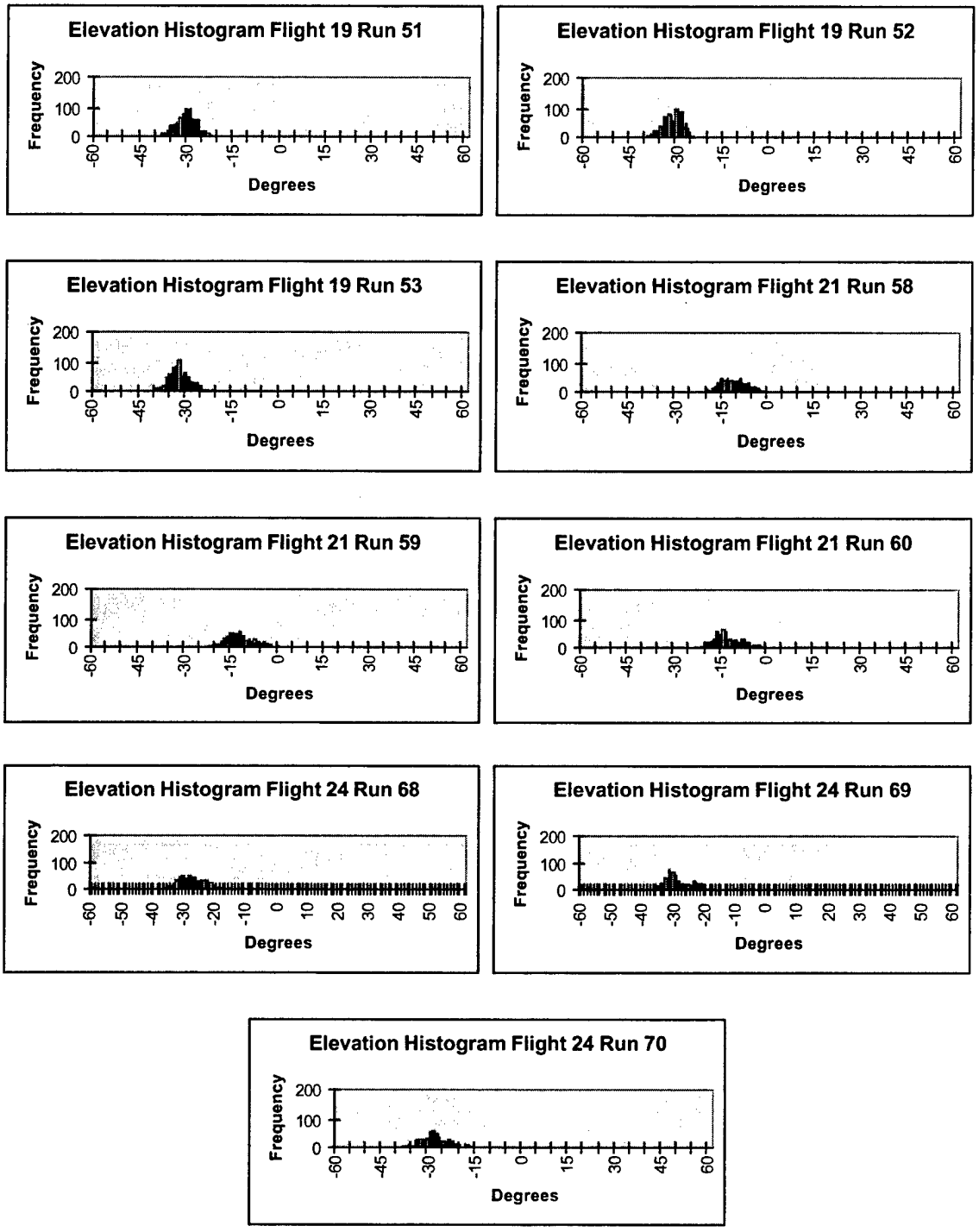

Figure A-10. Subject #3 NVG head position data.

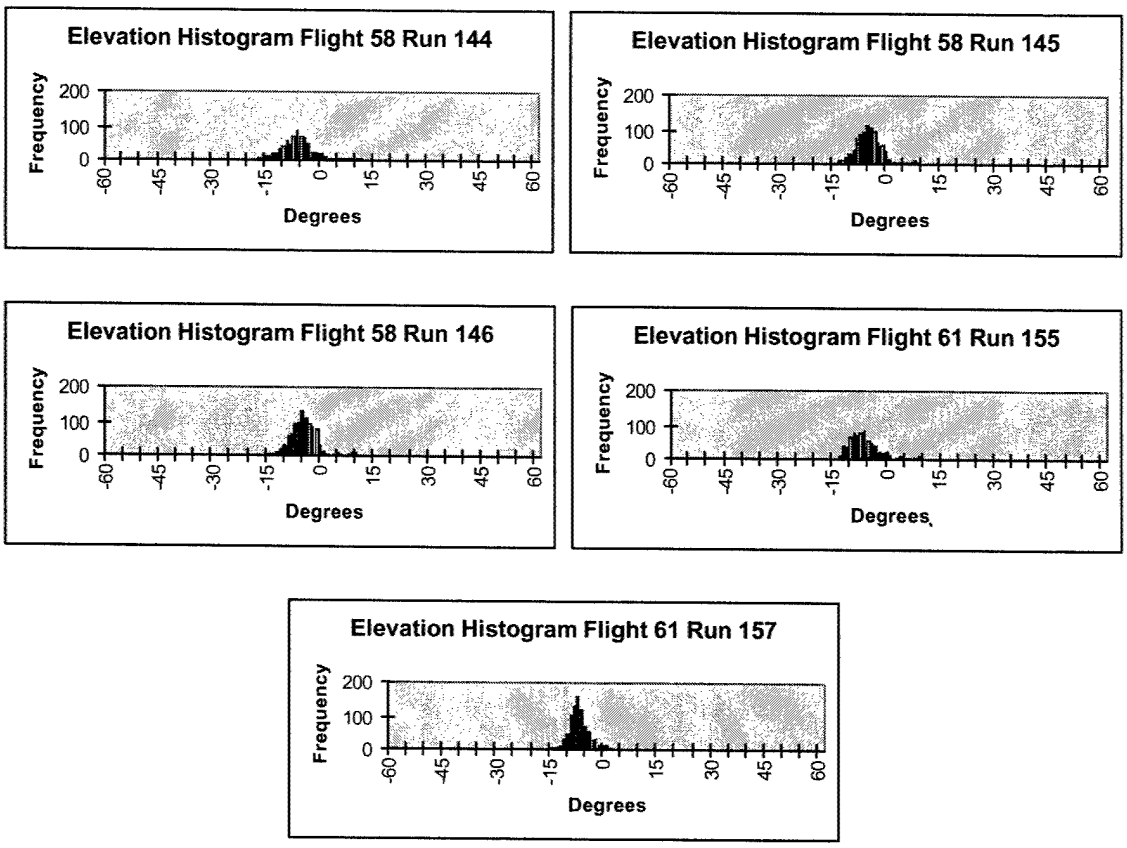

Figure A-11. Subject #3 TIO head position data.

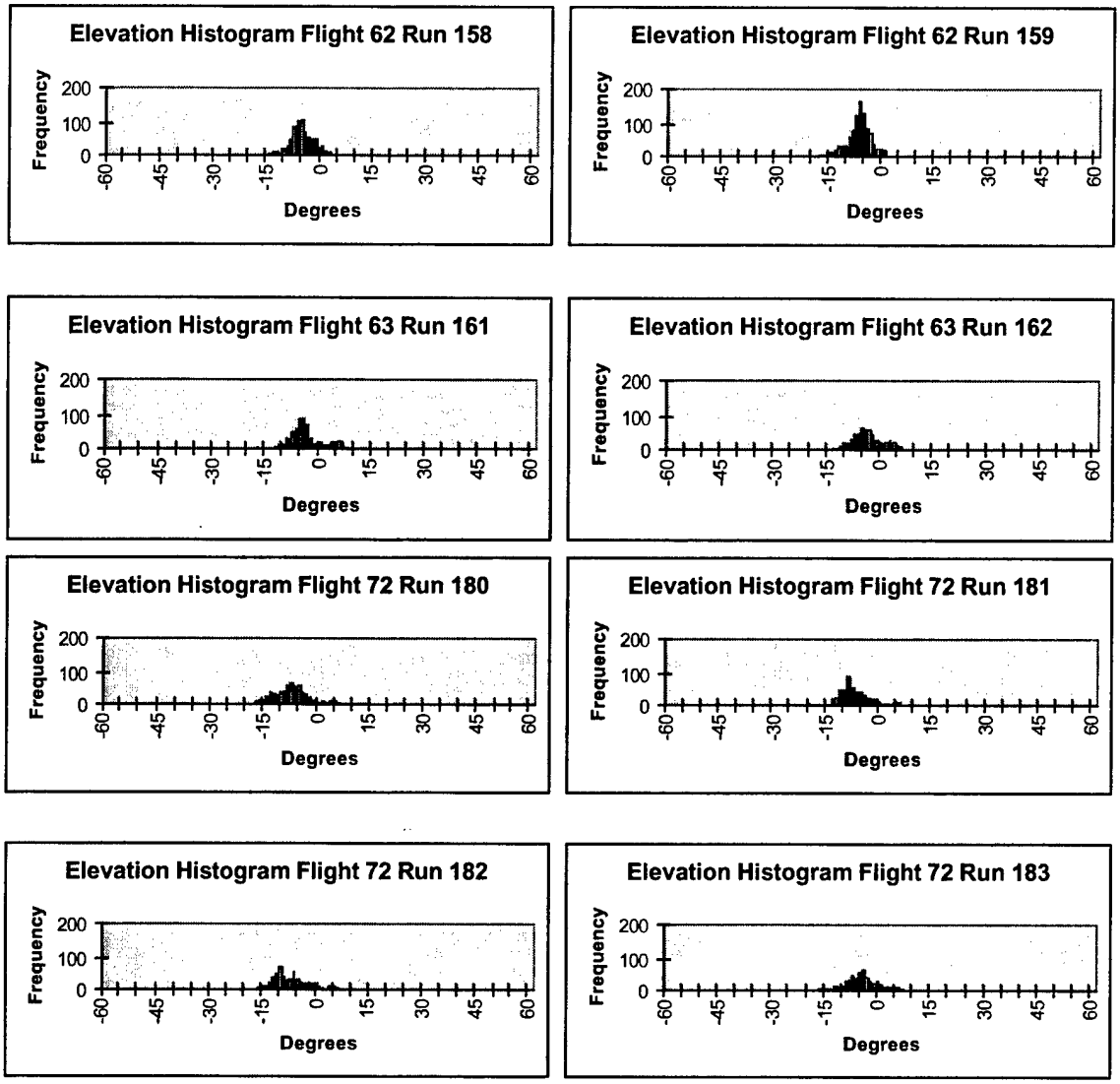

Figure A-12. Subject #3 RWS head position data.

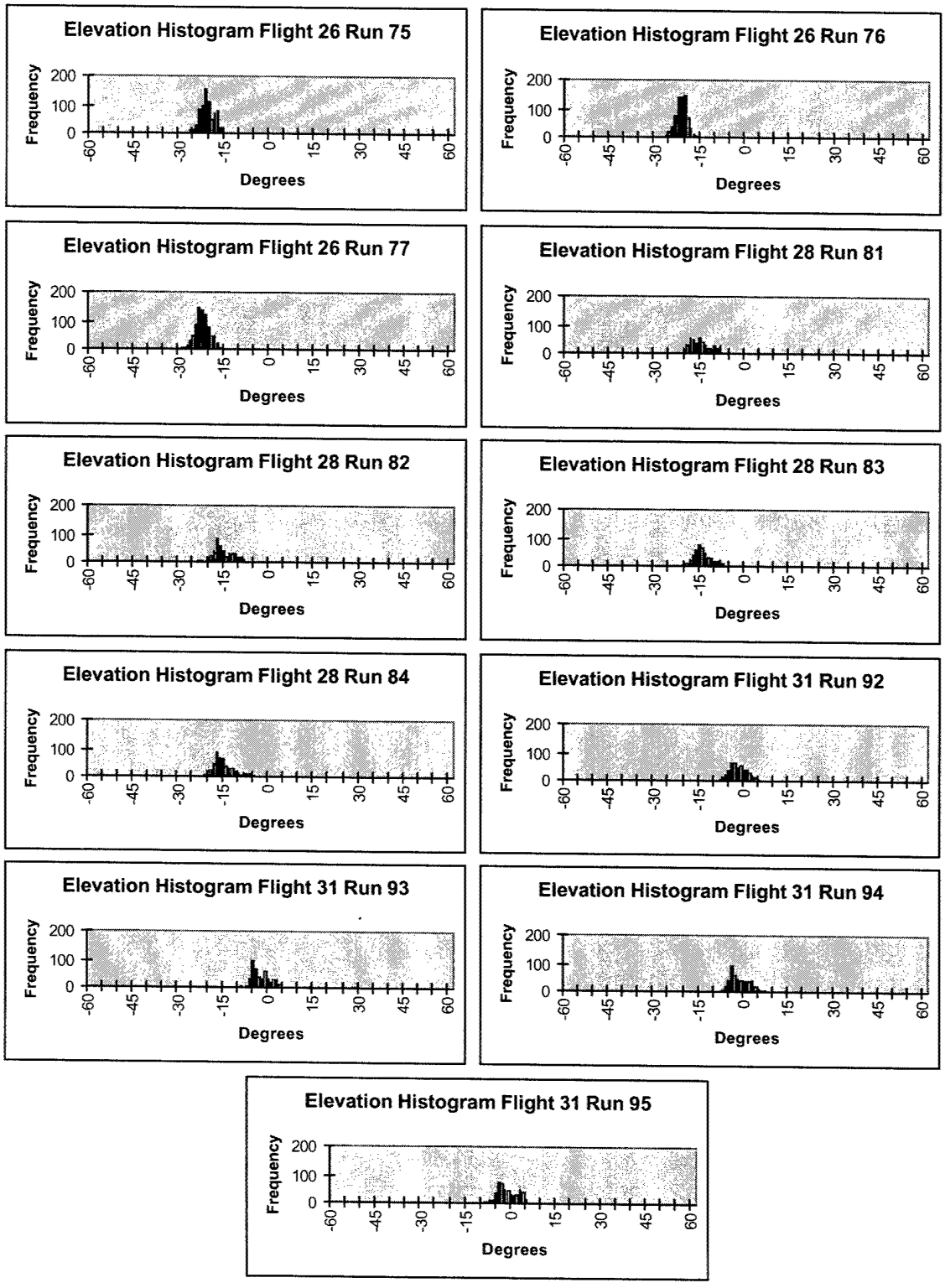

Figure A-13. Subject #4 GVE head position data.

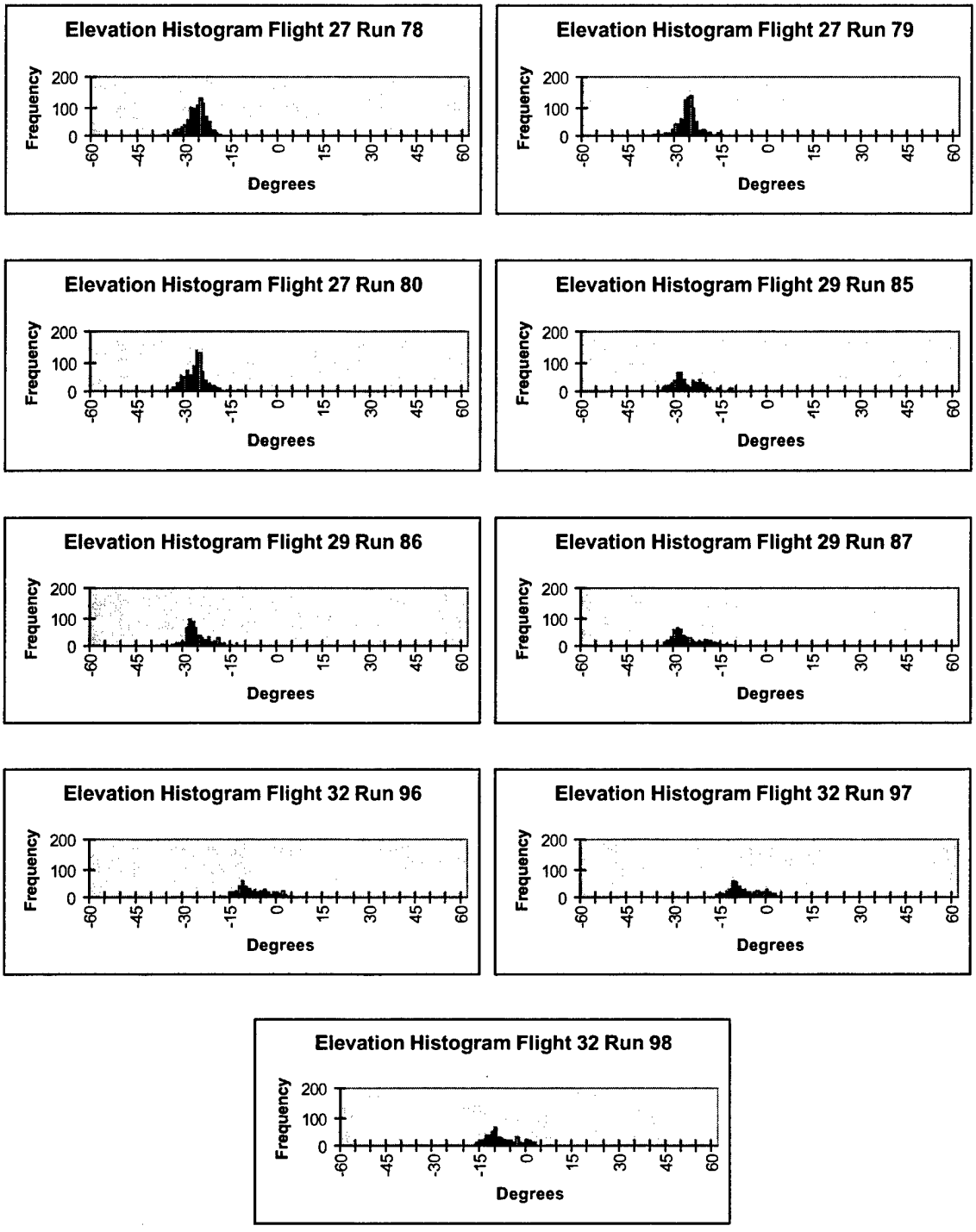

Figure A-14. Subject #4 NVG head position data.

Appendix B.

Summary tables of elevation position distributions by visual environment.

Table B-1.
Summary of moments and statistics for elevation position, slalom course, GVE.
(elevation values expressed in degrees)

Subject	Run	Time	Min	Max	Mean	Median	S.D.	IQR	Skew	Kurt
1	116	76.9	-34.2	-8.1	-16.8	-16.8	3.8	-18.6 to -14.3	-1.1	3.2
1	117	75.7	-33.1	-9.4	-16.6	-16.5	3.1	-17.9 to -15.0	-1.7	6.8
1	118	76.9	-32.3	-8.1	-15.0	-14.8	3.0	-16.4 to -13.3	-1.5	6.2
1	119	76.0	-26.4	-8.6	-15.1	-15.1	2.7	-16.7 to -13.2	-0.4	0.8
1	128	45.2	-42.3	-20.3	-29.9	-30.0	4.4	-32.8 to -26.9	-0.2	-0.4
1	129	48.1	-41.4	-20.4	-29.9	-29.8	2.8	-31.2 to -28.2	-0.6	2.2
1	130	48.6	-39.0	-17.8	-28.9	-28.9	3.1	-30.7 to -27.1	-0.1	1.3
1	131	43.8	-52.7	-19.1	-29.0	-28.3	4.0	-30.8 to -26.4	-1.3	3.7
1	132	45.6	-44.3	-14.8	-28.0	-27.6	4.8	-30.8 to -24.7	-0.4	0.4
1	133	49.8	-42.0	-19.1	-27.4	-27.0	3.4	-29.4 to -25.3	-0.6	1.5
1	134	51.1	-35.9	-18.7	-27.6	-27.8	2.9	-29.5 to -25.8	0.2	0.1
1	135	52.9	-41.2	-14.9	-27.3	-27.0	3.7	-28.9 to -25.0	-0.7	1.3
Combined		**690.6**	**-52.7**	**-8.1**	**-22.9**	**-24.3**	**7.2**	**-28.8 to -16.2**	**0.0**	**-1.1**
2	147	68.4	-27.8	-5.0	-15.6	-15.4	4.4	-18.1 to -12.7	-0.2	0.0
2	148	65.1	-32.3	-4.5	-15.2	-15.4	3.7	-17.7 to -12.6	-0.3	0.8
2	149	71.7	-26.2	-8.6	-16.2	-16.0	3.0	-17.9 to -14.1	-0.4	-0.1
2	150	73.9	-27.3	-2.7	-16.0	-16.0	3.8	-18.5 to -13.7	0.2	0.5
2	151	47.0	-31.5	-8.4	-20.2	-21.3	4.6	-23.6 to -17.3	0.5	-0.4
2	152	52.2	-42.0	-9.1	-21.0	-20.9	4.0	-23.5 to -19.4	-0.2	2.8
2	153	51.7	-40.6	-8.4	-20.0	-20.3	4.0	-22.5 to -17.7	-0.1	2.0
2	154	50.4	-36.4	-10.3	-22.7	-22.8	4.1	-25.3 to -20.3	0.1	0.6
Combined		**480.4**	**-42.0**	**-2.7**	**-18.0**	**-17.7**	**4.7**	**-21.3 to -14.6**	**-0.2**	**0.2**
3	47	74.8	-23.1	-8.0	-15.6	-15.7	2.6	-17.5 to -13.7	0.2	-0.4
3	48	75.7	-25.1	-7.0	-16.1	-16.2	3.1	-18.4 to -14.0	0.2	-0.5
3	49	78.8	-25.5	-10.0	-17.4	-17.4	2.5	-19.0 to -16.0	0.1	0.3
3	50	73.2	-29.7	-9.2	-17.2	-17.0	3.0	-19.0 to -15.1	-0.5	0.6
3	54	44.6	-24.7	-6.6	-15.3	-14.9	3.1	-17.4 to -13.3	-0.3	-0.1
3	55	47.6	-21.1	-7.3	-14.2	-14.2	2.6	-15.8 to -12.0	-0.1	-0.4
3	56	46.5	-25.6	-8.4	-15.0	-14.6	3.0	-16.9 to -13.1	-0.5	0.3
3	57	49.0	-25.0	-8.1	-15.1	-15.4	3.2	-17.5 to -12.4	0.1	-0.8
3	64	50.6	-25.5	-5.4	-15.3	-15.2	3.2	-17.1 to -13.2	-0.2	0.2
3	65	46.8	-24.4	-6.6	-15.1	-15.1	3.4	-17.3 to -13.1	0.0	0.0
3	66	46.7	-23.8	-6.4	-15.1	-15.5	3.0	-17.3 to -13.0	0.2	-0.1
3	67	43.4	-25.7	-7.4	-15.8	-15.7	2.8	-17.7 to -13.9	-0.3	0.6
Combined		**677.7**	**-29.7**	**-5.4**	**-15.8**	**-15.8**	**3.1**	**-17.9 to -13.6**	**0.0**	**0.0**
4	75	72.4	-28.9	-15.7	-21.0	-21.2	2.3	-22.6 to -19.1	0.0	-0.4
4	76	69.0	-27.3	-15.3	-21.6	-21.6	1.8	-22.7 to -20.4	0.0	0.4
4	77	79.8	-29.8	-14.8	-22.5	-22.6	2.4	-23.9 to -21.0	0.1	0.0
4	81	42.0	-22.9	-6.9	-15.0	-15.5	3.4	-17.8 to -12.9	0.5	-0.7
4	82	42.6	-23.4	-7.5	-15.5	-16.3	3.2	-17.8 to -12.8	0.4	-0.6
4	83	46.0	-22.0	-5.0	-14.3	-14.7	3.0	-16.4 to -12.3	0.5	-0.2
4	84	45.0	-22.3	-5.5	-15.2	-16.0	3.4	-17.5 to -13.5	1.0	0.5
4	92	44.4	-9.4	5.2	-2.4	-2.6	2.9	-4.5 to -0.3	0.2	-0.5
4	93	43.6	-10.8	4.0	-2.9	-3.7	3.0	-5.3 to -0.9	0.4	-0.6
4	94	48.0	-7.7	6.7	-1.8	-2.5	3.1	-4.4 to 0.7	0.5	-0.7
4	95	49.2	-9.7	5.6	-1.6	-2.3	3.3	-4.2 to 1.4	0.2	-0.8
Combined		**582**	**-29.8**	**6.7**	**-13.5**	**-16.3**	**8.7**	**-20.9 to -4.8**	**0.4**	**-1.2**
All Subjects		**2430.7**	**-52.7**	**6.7**	**-17.7**	**-17.2**	**7.3**	**-21.9 to -13.9**	**0.1**	**0.7**

Table B-2.
Summary of moments and statistics for elevation position, slalom course, NVG.
(elevation values expressed in degrees, time in seconds)

Subject	Run	Time	Min	Max	Mean	Median	S.D.	IQR	Skew	Kurt
1	108	105.7	-23.8	-6.4	-15.0	-15.0	3.1	-17.4 to -12.6	-0.1	-0.6
1	109	98.2	-23.9	-4.8	-13.8	-14.0	3.3	-15.9 to -11.0	-0.2	-0.1
1	110	51.3	-33.7	-17.7	-25.8	-25.7	3.1	-27.7 to -23.5	-0.1	-0.3
1	111	51.7	-32.5	-17.7	-25.8	-26.1	3.1	-27.9 to -23.7	0.3	-0.4
1	112	51.1	-36.0	-15.7	-24.8	-25.0	3.4	-26.8 to -22.6	-0.1	0.3
1	121	54.0	-46.0	-21.3	-28.7	-28.6	3.5	-30.6 to -26.9	-0.9	3.8
1	123	55.2	-34.3	-20.6	-27.6	-27.8	2.8	-29.6 to -26.0	0.2	-0.4
Combined		**467.2**	**-46.0**	**-4.8**	**-21.3**	**-22.4**	**6.9**	**-27.2 to -15.1**	**0.1**	**-1.1**
2	171	80.0	-19.8	0.4	-11.2	-11.4	3.5	-13.5 to -9.1	0.3	0.3
2	172	80.9	-21.6	-0.3	-10.7	-11.2	3.6	-13.1 to -8.3	0.4	0.0
2	173	103.2	-20.2	-1.5	-11.1	-11.6	3.5	-13.3 to -9.2	0.5	0.1
2	177	70.6	-35.7	-9.1	-22.0	-22.7	3.8	-24.8 to -19.6	0.5	0.8
2	178	63.0	-29.7	-11.8	-21.7	-22.3	3.3	-23.7 to -19.8	0.6	0.6
2	179	54.3	-30.5	-9.7	-21.6	-21.8	3.9	-24.6 to -18.9	0.3	-0.3
Combined		**452.0**	**-35.7**	**0.4**	**-15.5**	**-14.2**	**6.4**	**-21.4 to -10.8**	**-0.2**	**-0.9**
3	51	71.8	-45.5	-20.3	-30.5	-30.3	3.5	-32.7 to -28.1	-0.3	0.5
3	52	73.9	-39.4	-24.1	-31.5	-31.1	3.0	-33.8 to -29.1	-0.3	-0.6
3	53	68.2	-39.8	-21.3	-32.2	-32.6	3.3	-34.5 to -30.2	0.5	0.0
3	58	50.5	-25.2	-1.3	-11.6	-11.8	4.4	-14.9 to -8.5	0.0	-0.4
3	59	51.9	-24.7	-0.3	-12.5	-13.0	4.6	-15.6 to -9.6	0.4	-0.2
3	60	52.6	-21.8	-0.9	-13.0	-13.9	4.5	-16.4 to -9.9	0.5	-0.3
3	68	53.6	-39.5	-14.4	-27.6	-27.8	4.3	-30.8 to -24.3	0.2	-0.2
3	69	53.8	-39.6	-18.2	-28.8	-29.9	4.3	-31.7 to -25.3	0.4	-0.6
3	70	48.8	-40.5	-16.6	-28.1	-28.5	4.5	-31.0 to -25.3	0.2	0.0
Combined		**525.1**	**-45.5**	**-0.3**	**-24.8**	**-28.2**	**9.1**	**-31.8 to -16.8**	**0.7**	**-0.7**
4	78	85.3	-39.1	-19.0	-26.7	-26.4	3.1	-28.5 to -24.6	-0.6	0.7
4	79	81.9	-37.7	-14.8	-26.3	-26.3	3.3	-27.9 to -24.8	0.2	1.9
4	80	83.9	-38.0	-9.8	-26.7	-26.6	4.0	-29.3 to -25.1	0.8	2.5
4	85	52.7	-35.9	-10.9	-26.2	-27.4	4.9	-29.7 to -22.7	0.7	0.1
4	86	56.0	-37.7	-13.0	-26.0	-27.1	4.3	-28.6 to -23.6	0.6	0.8
4	87	49.8	-34.1	-12.5	-26.1	-27.7	5.0	-29.9 to -22.7	0.8	-0.3
4	96	44.6	-18.9	5.7	-7.7	-8.9	5.2	-11.7 to -4.1	0.4	-0.7
4	97	47.0	-17.1	3.8	-7.7	-9.3	5.1	-11.5 to -3.3	0.4	-0.9
4	98	46.1	-16.6	4.2	-7.9	-9.4	5.0	-11.5 to -3.8	0.5	-0.8
Combined		**547.3**	**-39.1**	**5.7**	**-21.7**	**-25.2**	**9.2**	**-28.1 to -14.7**	**1.0**	**-0.1**
All Subjects		**1991.6**	**-46.0**	**5.7**	**-21.0**	**-22.9**	**8.7**	**-28.1 to -13.4**	**0.3**	**-0.8**

Table B-3.
Summary of moments and statistics for elevation position, slalom course, TIO.
(elevation values expressed in degrees, time in seconds)

Subject	Run	Time	Min	Max	Mean	Median	S.D.	IQR	Skew	Kurt
1	138	85.7	-11.9	6.9	-2.4	-2.3	2.7	-3.8 to -0.7	-0.3	1.2
1	139	109.7	-9.5	7.0	-1.9	-1.7	2.7	-3.6 to -0.2	0.1	0.7
1	140	120.4	-8.7	5.5	-1.3	-0.9	2.9	-3.4 to 0.8	-0.2	-0.6
Combined		**315.8**	**-11.9**	**7.0**	**-1.8**	**-1.7**	**2.8**	**-3.6 to 0.0**	**-0.1**	**0.3**
2	163	70.0	-13.7	3.1	-5.4	-5.4	3.2	-7.6 to -3.2	0.1	-0.4
2	164	82.5	-15.1	4.3	-5.5	-5.4	3.4	-7.9 to -3.4	0.0	-0.1
2	166	80.1	-17.3	9.8	-6.7	-6.8	3.7	-9.0 to -5.1	1.2	3.8
2	167	88.1	-15.2	2.3	-6.3	-6.3	2.6	-7.9 to -4.7	0.0	0.5
Combined		**320.7**	**-17.3**	**9.8**	**-6.0**	**-6.0**	**3.3**	**-8.1 to -4.2**	**0.4**	**1.3**
3	144	70.9	-18.1	12.6	-6.0	-6.5	5.1	-9.1 to -4.0	1.0	2.0
3	145	89.3	-14.9	8.8	-5.1	-5.2	3.7	-7.5 to -3.1	0.8	1.8
3	146	97.9	-15.9	10.9	-5.1	-5.3	3.9	-7.4 to -2.9	0.8	2.6
3	155	71.9	-15.9	9.1	-6.7	-7.3	4.3	-9.6 to -4.7	1.2	2.0
3	157	84.4	-16.4	2.0	-7.2	-7.5	2.9	-8.9 to -5.9	0.4	1.0
Combined		**414.4**	**-18.1**	**12.6**	**-5.9**	**-6.4**	**4.1**	**-8.5 to -3.9**	**1.0**	**2.4**
4	None									
All Subjects		**1050.9**	**-18.1**	**12.6**	**-5.0**	**-5.3**	**4.6**	**-8.2 to -1.5**	**0.3**	**0.5**

Table B-4.
Summary moments and statistics for elevation position, slalom course, RWS.
(elevation values expressed in degrees, time in seconds)

Subject	Run	Time	Min	Max	Mean	Median	S.D.	IQR	Skew	Kurt
1	141	106.2	-11.6	5.8	-0.3	0.1	2.6	-2.1 to 1.5	-0.6	0.4
1	142	102.0	-10.4	4.7	-0.2	0.4	2.5	-1.6 to 1.4	-1.0	1.2
1	143	120.0	-8.2	6.1	-0.1	0.1	2.2	-1.6 to 1.5	-0.2	0.0
Combined		**328.2**	**-11.6**	**6.1**	**-0.2**	**0.2**	**2.4**	**-1.7 to 1.4**	**-0.6**	**0.7**
2	168	83.2	-13.9	1.8	-6.4	-6.4	3.1	-8.7 to -4.1	0.0	-.05
2	169	89.1	-19.1	-1.4	-8.5	-8.5	2.8	-10.2 to -6.4	-0.4	0.3
2	170	101.1	-16.8	-2.4	-8.4	-8.2	2.6	-9.9 to -6.5	-0.5	0.2
2	174	63.6	-18.3	0.4	-6.8	-6.5	3.4	-9.3 to -4.5	-0.5	0.0
2	175	65.0	-13.5	0.8	-6.2	-6.1	2.8	-8.4 to -4.3	0.2	-0.5
2	176	63.8	-17.3	-0.6	-6.3	-5.9	3.0	-7.8 to -4.3	-0.8	1.0
Combined		**465.8**	**-19.1**	**1.8**	**-7.3**	**-7.2**	**3.1**	**-9.3 to -5.1**	**-0.2**	**0.1**
3	158	71.2	-15.3	3.2	-5.3	-5.5	3.3	-7.3 to -3.2	-0.1	0.2
3	159	94.8	-20.1	0.9	-6.8	-6.5	3.3	-8.5 to -4.8	-0.4	0.6
3	161	61.2	-19.1	7.5	-4.1	-4.8	4.8	-6.7 to -2.5	0.4	0.6
3	162	55.3	-14.3	6.0	-3.8	-4.3	4.2	-6.6 to -1.2	0.2	-0.4
3	180	59.6	-18.3	5.4	-7.7	-7.7	4.7	-10.9 to -5.0	0.4	0.3
3	181	58.9	-21.4	6.0	-7.5	-8.4	4.4	-10.0 to -5.3	0.6	1.5
3	182	52.9	-19.1	6.1	-7.5	-8.2	4.8	-11.0 to -4.6	0.6	-0.1
3	183	43.9	-20.1	6.9	-4.7	-4.9	4.7	-7.8 to -1.6	0.1	0.2
Combined		**497.8**	**-21.4**	**7.5**	**-6.0**	**-6.1**	**4.5**	**-8.8 to -3.6**	**0.3**	**0.4**
4	None									
All Subjects		**1291.8**	**-21.4**	**7.5**	**-5.0**	**-5.3**	**4.6**	**-8.2 to -1.5**	**0.0**	**-0.4**

Appendix C.

Elevation position box plots.

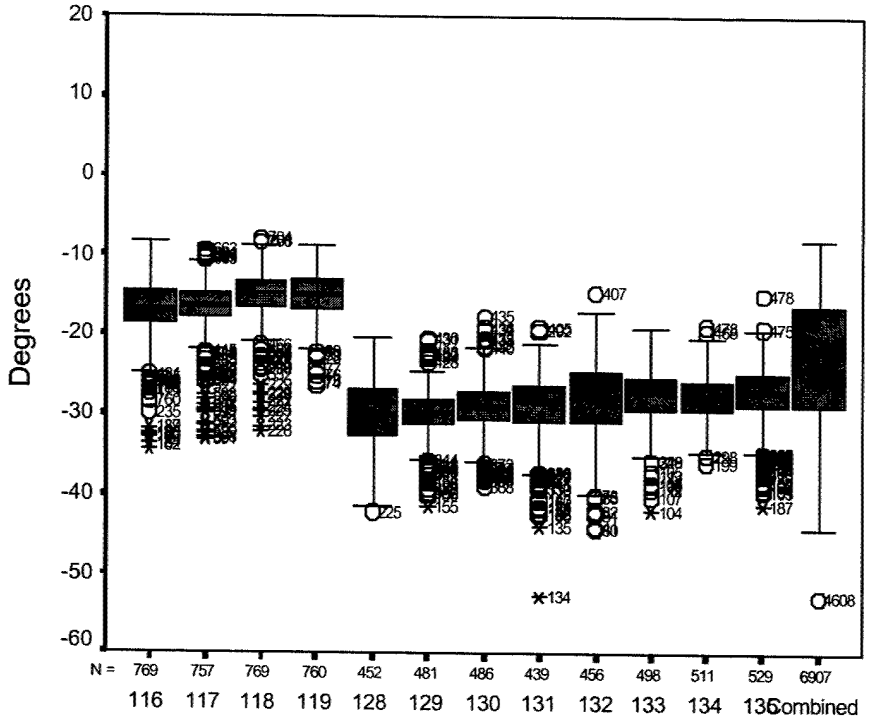

Figure C-1. Subject #1 GVE box plots.

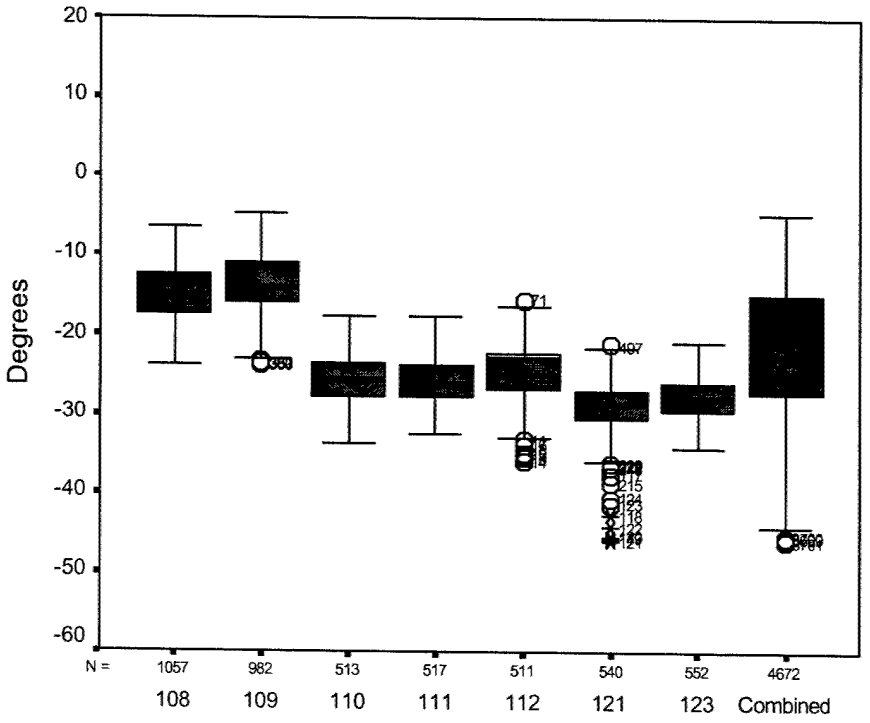

Figure C-2. Subject #1 NVG box plots.

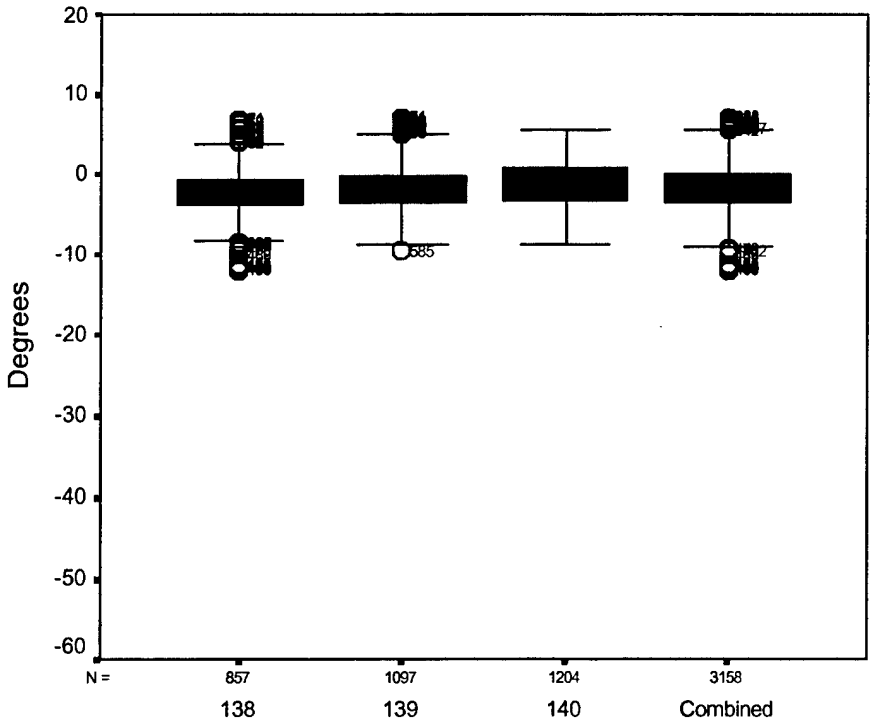

Figure C-3. Subject #1 TIO box plots.

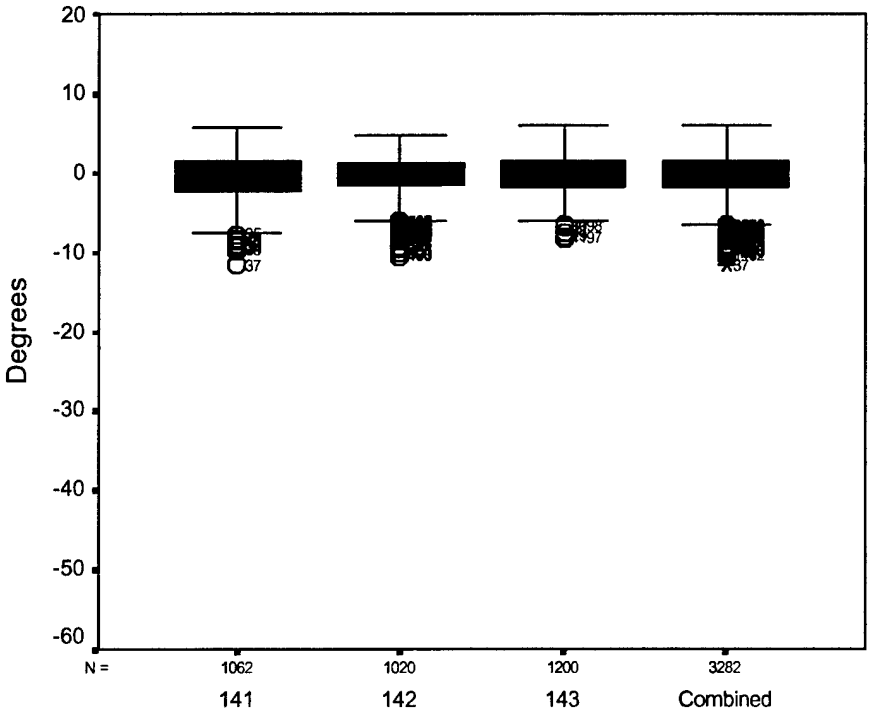

Figure C-4. Subject #1 RWS box plots.

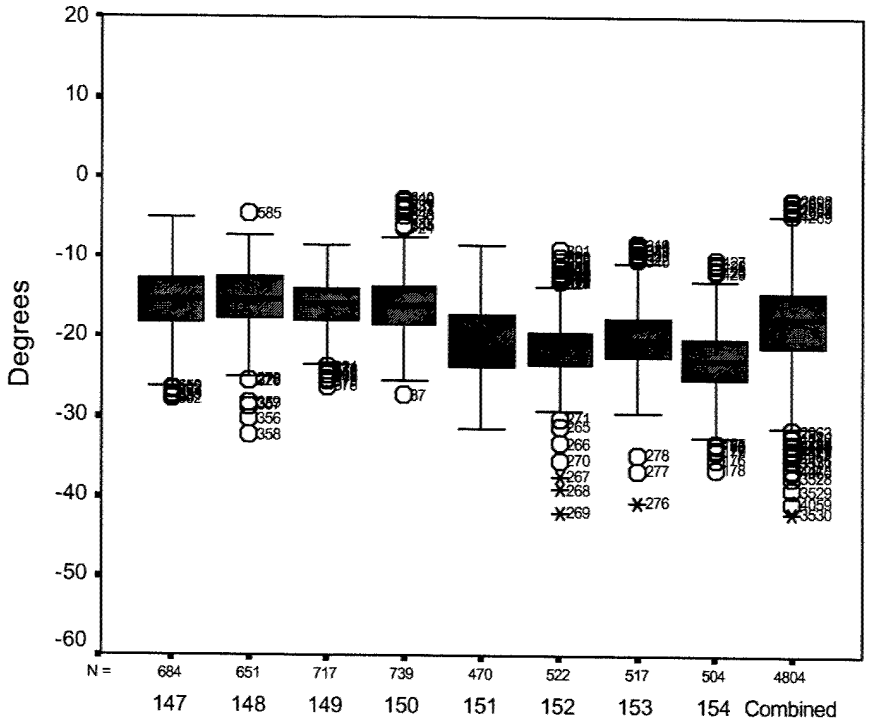

Figure C-5. Subject #2 GVE box plots.

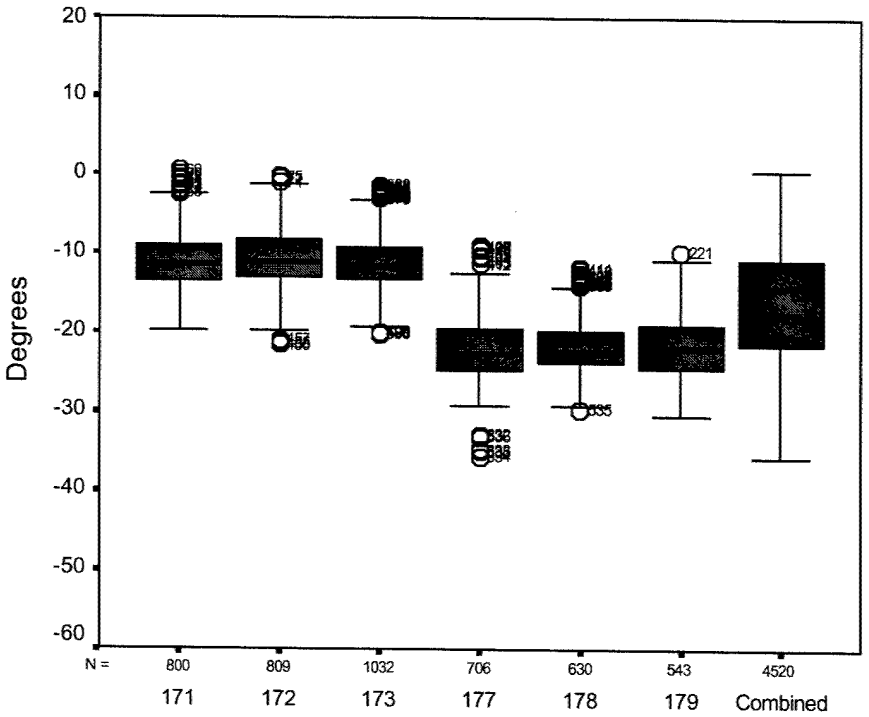

Figure C-6. Subject #2 NVG box plots.

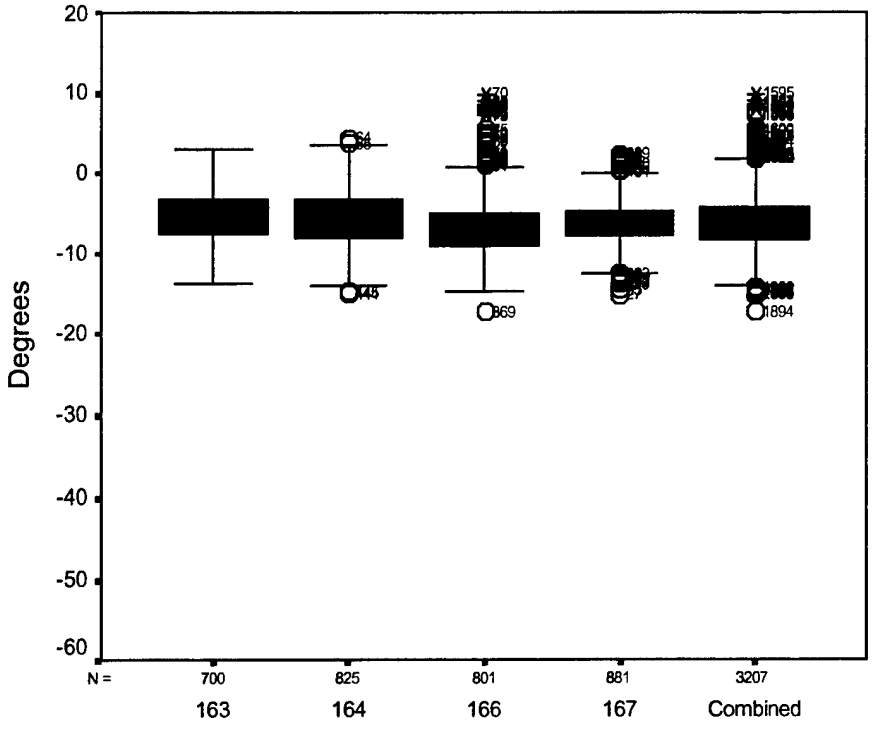

Figure C-7. Subject #2 TIO box plots.

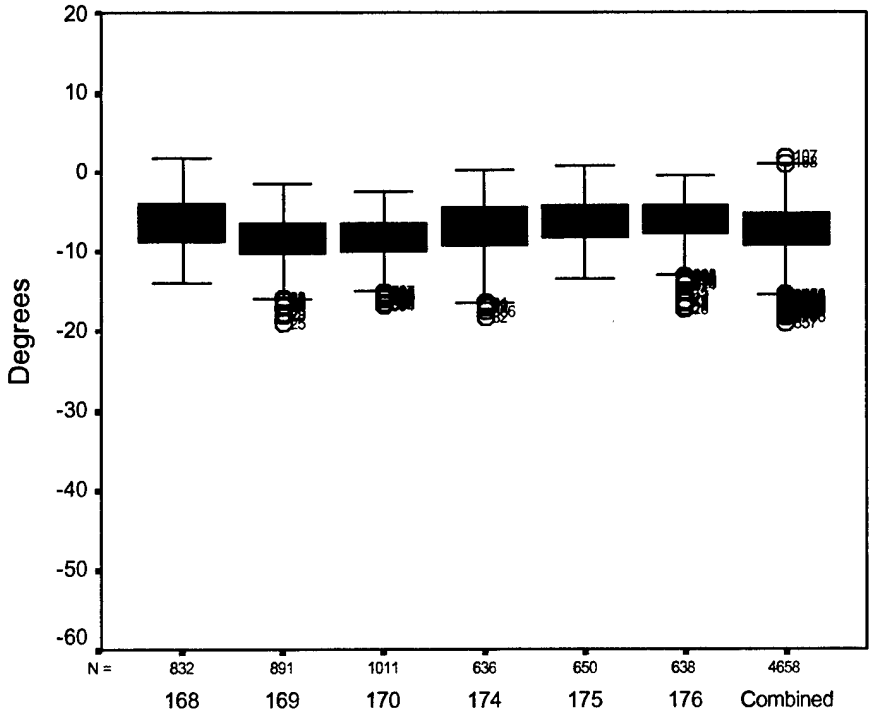

Figure C-8. Subject #2 RWS box plots.

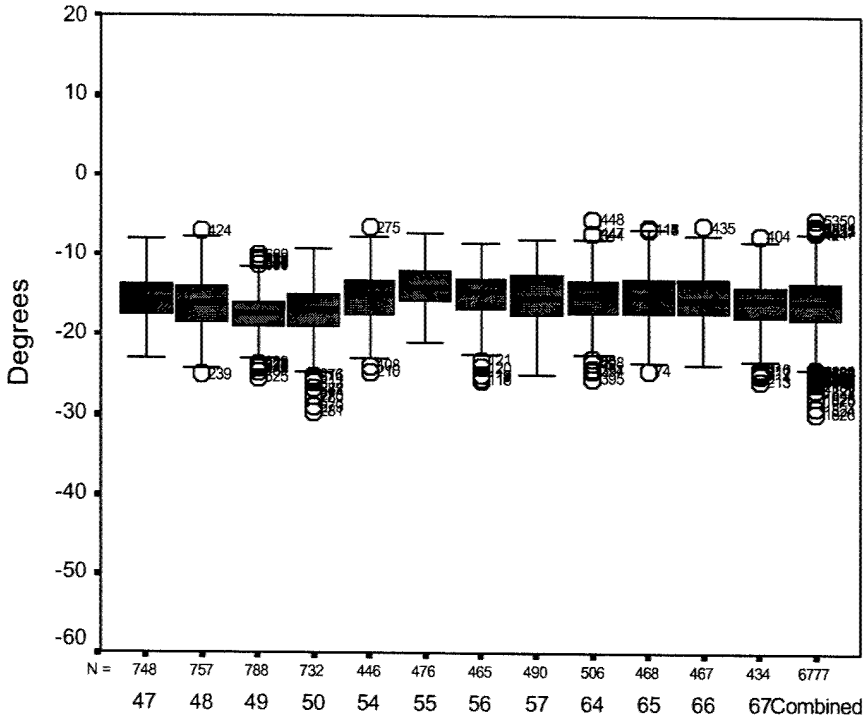

Figure C-9. Subject #3 GVE box plots.

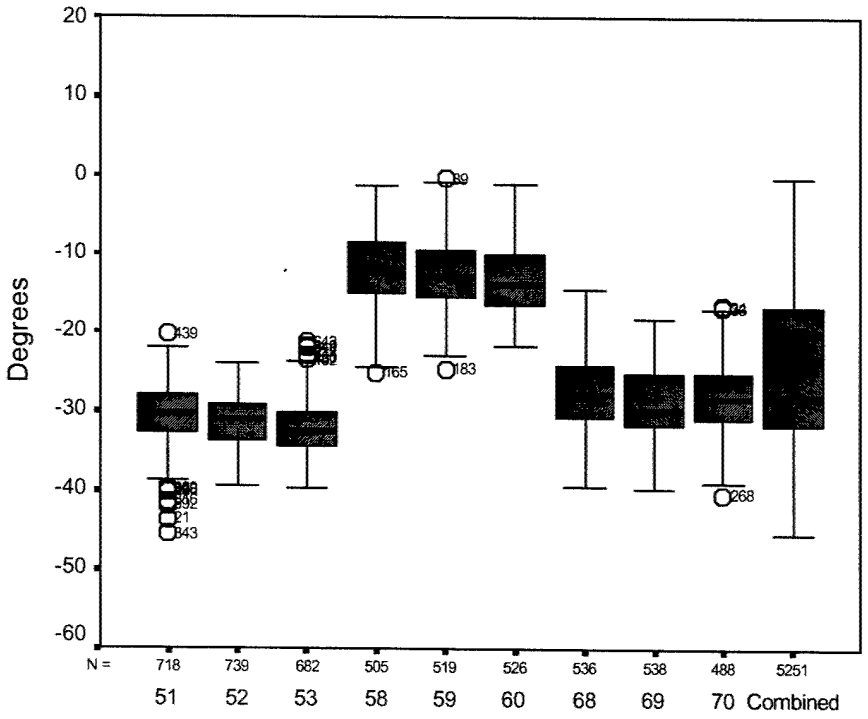

Figure C-10. Subject #3 NVG box plots.

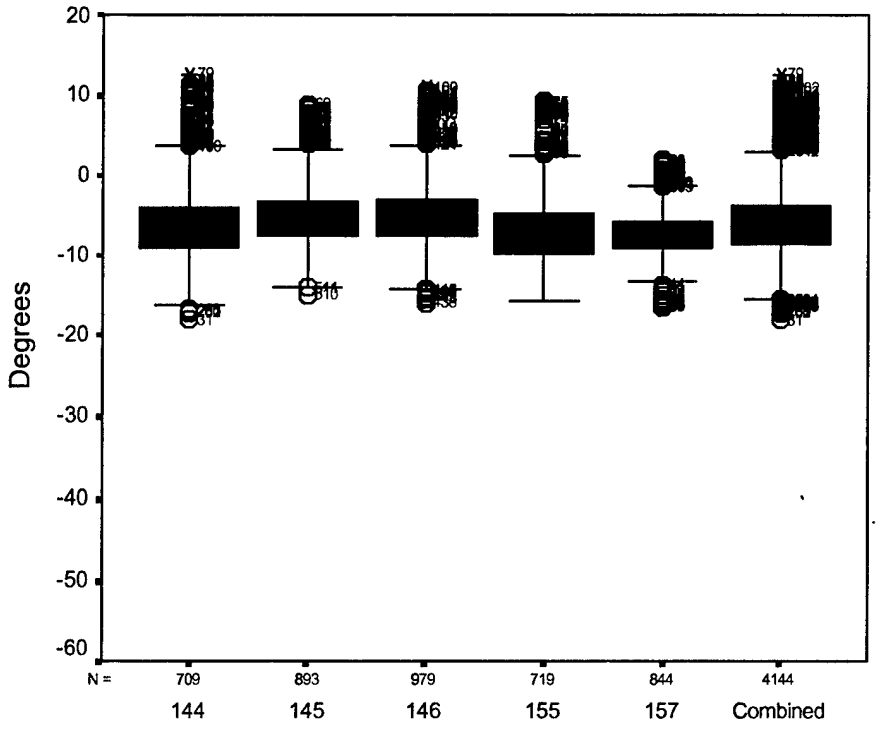

Figure C-11. Subject #3 TIO box plots.

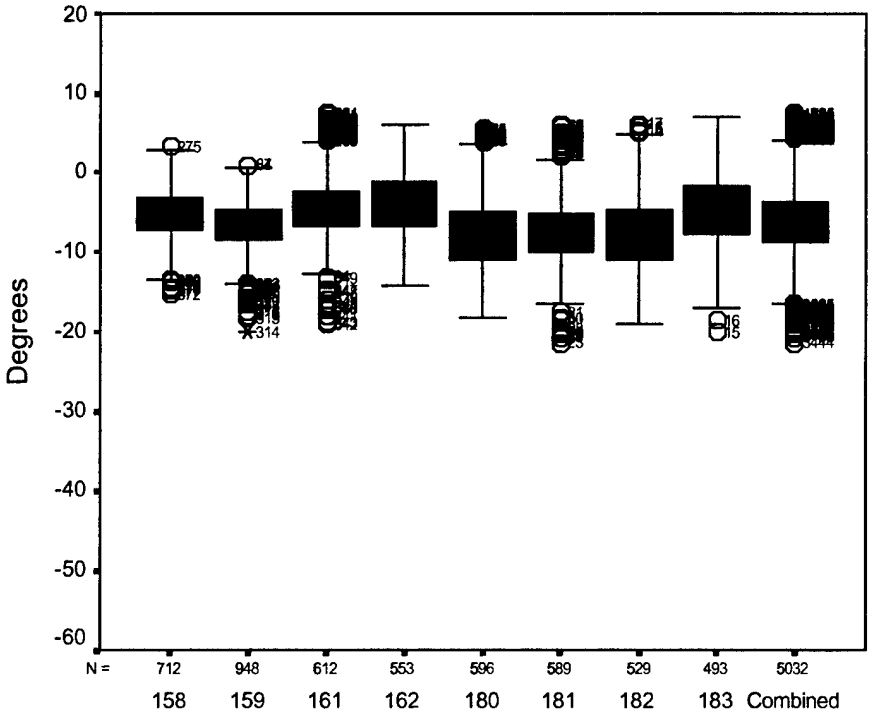

Figure C-12. Subject #3 RWS box plots.

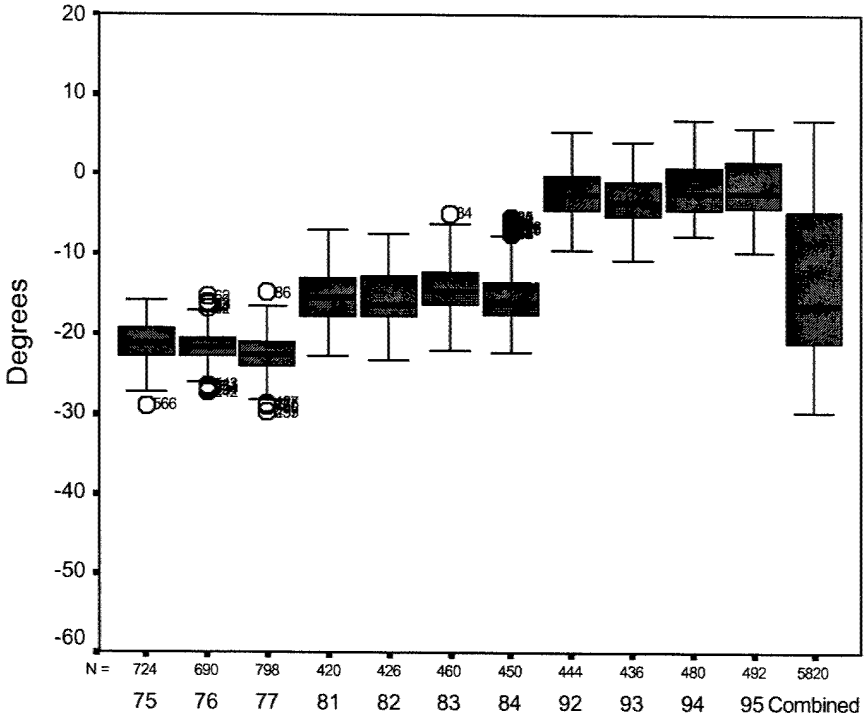

Figure C-13. Subject #4 GVE box plots.

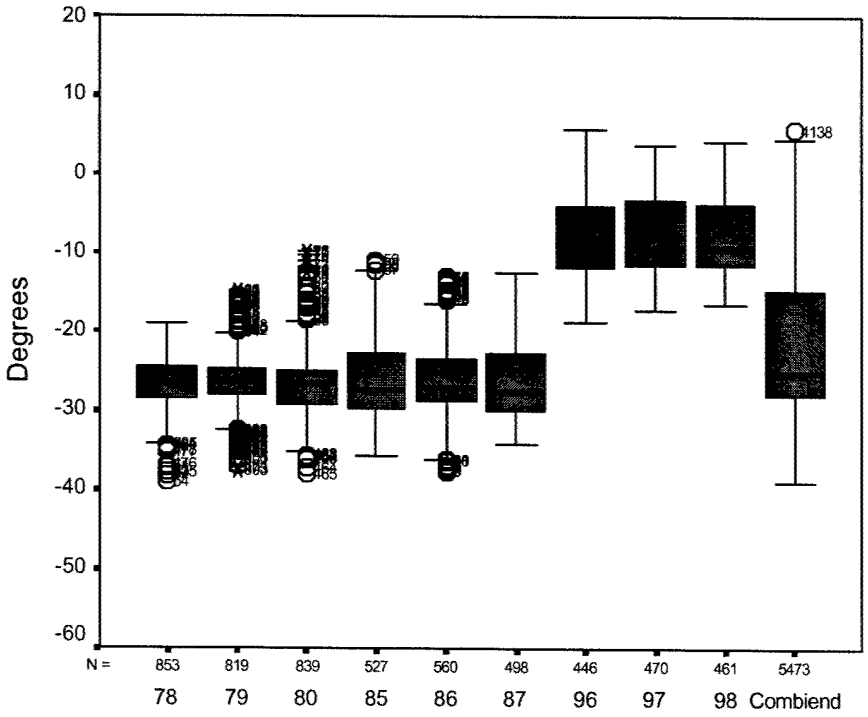

Figure C-14. Subject #4 NVG box plots.

Appendix D.

Elevation reversal summary tables.

Table D-1.
Summary statistics for elevation reversals, slalom course, GVE.
(expressed in degrees)

Subject	Run	Time	# of Reversals	Rev/min
1	116	76.9	47	36.7
1	117	75.7	38	30.1
1	118	76.9	38	29.6
1	119	76.0	35	27.6
1	128	45.2	26	34.5
1	129	48.1	25	31.2
1	130	48.6	31	38.3
1	131	43.8	24	32.9
1	132	45.6	29	38.2
1	133	49.8	22	26.5
1	134	51.1	30	35.2
1	135	52.9	31	35.2
Combined		**690.6**	**376**	**32.7**
2	147	68.4	47	41.2
2	148	65.1	32	29.5
2	149	71.7	39	32.6
2	150	73.9	42	34.1
2	151	47.0	33	42.1
2	152	52.2	32	36.8
2	153	51.7	31	36.0
2	154	50.4	33	39.3
Combined		**480.4**	**289**	**36.1**
3	47	74.8	47	37.7
3	48	75.7	52	41.2
3	49	78.8	51	38.8
3	50	73.2	42	34.4
3	54	44.6	23	30.9
3	55	47.6	23	29.0
3	56	46.5	18	23.2
3	57	49.0	28	34.3
3	64	50.6	33	39.1
3	65	46.8	30	38.5
3	66	46.7	20	25.7
3	67	43.4	29	40.1
Combined		**677.7**	**396**	**35.1**
4	75	72.4	34	28.2
4	76	69.0	32	27.8
4	77	79.8	45	33.8
4	81	42.0	20	28.6
4	82	42.6	16	22.5
4	83	46.0	21	27.4
4	84	45.0	27	36.0
4	92	44.4	17	23.0
4	93	43.6	19	26.1
4	94	48.0	20	25.0
4	95	49.2	17	20.7
Combined		**582**	**268**	**27.6**
All Subjects		**2430.7**	**1329**	**32.8**

Table D-2.
Summary statistics for elevation reversals, slalom course, NVG.
(expressed in degrees)

Subject	Run	Time	# of Reversals	Rev / min
1	108	105.7	67	38.0
1	109	98.2	73	44.6
1	110	51.3	29	33.9
1	111	51.7	38	44.1
1	112	51.1	27	31.7
1	121	54.0	29	32.2
1	123	55.2	27	29.3
Combined		**467.2**	**290**	**37.2**
2	171	80.0	53	39.8
2	172	80.9	46	34.1
2	173	103.2	69	40.1
2	177	70.6	43	36.5
2	178	63.0	40	38.1
2	179	54.3	31	34.3
Combined		**452.0**	**282**	**37.4**
3	51	71.8	40	33.4
3	52	73.9	48	39.0
3	53	68.2	40	35.2
3	58	50.5	30	35.6
3	59	51.9	26	30.1
3	60	52.6	27	30.8
3	68	53.6	32	35.8
3	69	53.8	12	13.4
3	70	48.8	26	32.0
Combined		**525.1**	**281**	**32.1**
4	78	95.3	45	28.3
4	79	81.9	50	36.6
4	80	83.9	50	35.8
4	85	52.7	27	30.7
4	86	56.0	24	25.7
4	87	49.8	19	22.9
4	96	44.6	26	35.0
4	97	47.0	26	33.2
4	98	46.1	14	18.2
Combined		**557.3**	**281**	**30.3**
All Subjects		**2001.6**	**1134**	**34.0**

Table D-3.
Summary statistics for elevation reversals, slalom course, TIO.
(expressed in degrees)

Subject	Run	Time	# of Reversals	Rev /min
1	138	85.7	42	29.4
1	139	109.7	62	33.9
1	140	120.4	71	35.4
Combined		**315.8**	**175**	**33.2**
2	163	70.0	34	29.1
2	164	82.5	46	33.5
2	166	80.1	36	27.0
2	167	88.1	45	30.6
Combined		**320.7**	**161**	**30.1**
3	144	70.9	23	19.5
3	145	89.3	44	29.6
3	146	97.9	47	28.8
3	155	71.9	32	26.7
3	157	84.4	39	27.7
Combined		**414.4**	**185**	**26.8**
4				
All Subjects		**1050.9**	**521**	**29.7**

Table D-4.
Summary statistics for elevation reversals, slalom course, RWS.
(expressed in degrees)

Subject	Run	Time	# of Reversals	Rev /min
1	141	106.2	55	31.1
1	142	102.0	58	34.1
1	143	120.0	69	34.5
Combined		**328.2**	**182**	**33.3**
2	168	83.2	31	22.4
2	169	89.1	43	29.0
2	170	101.1	46	27.3
2	174	63.6	34	32.1
2	175	65.0	31	28.6
2	176	63.8	33	31.0
Combined		**465.8**	**218**	**28.1**
3	158	71.2	25	21.1
3	159	94.8	50	31.6
3	161	61.2	24	23.5
3	162	55.3	27	29.3
3	180	59.6	26	26.2
3	181	58.9	26	26.5
3	182	52.9	17	19.3
3	183	43.9	18	24.6
Combined		**497.8**	**213**	**25.7**
4	None			
All Subjects		**1291.8**	**613**	**28.5**

Appendix E.

Elevation excursion distributions.

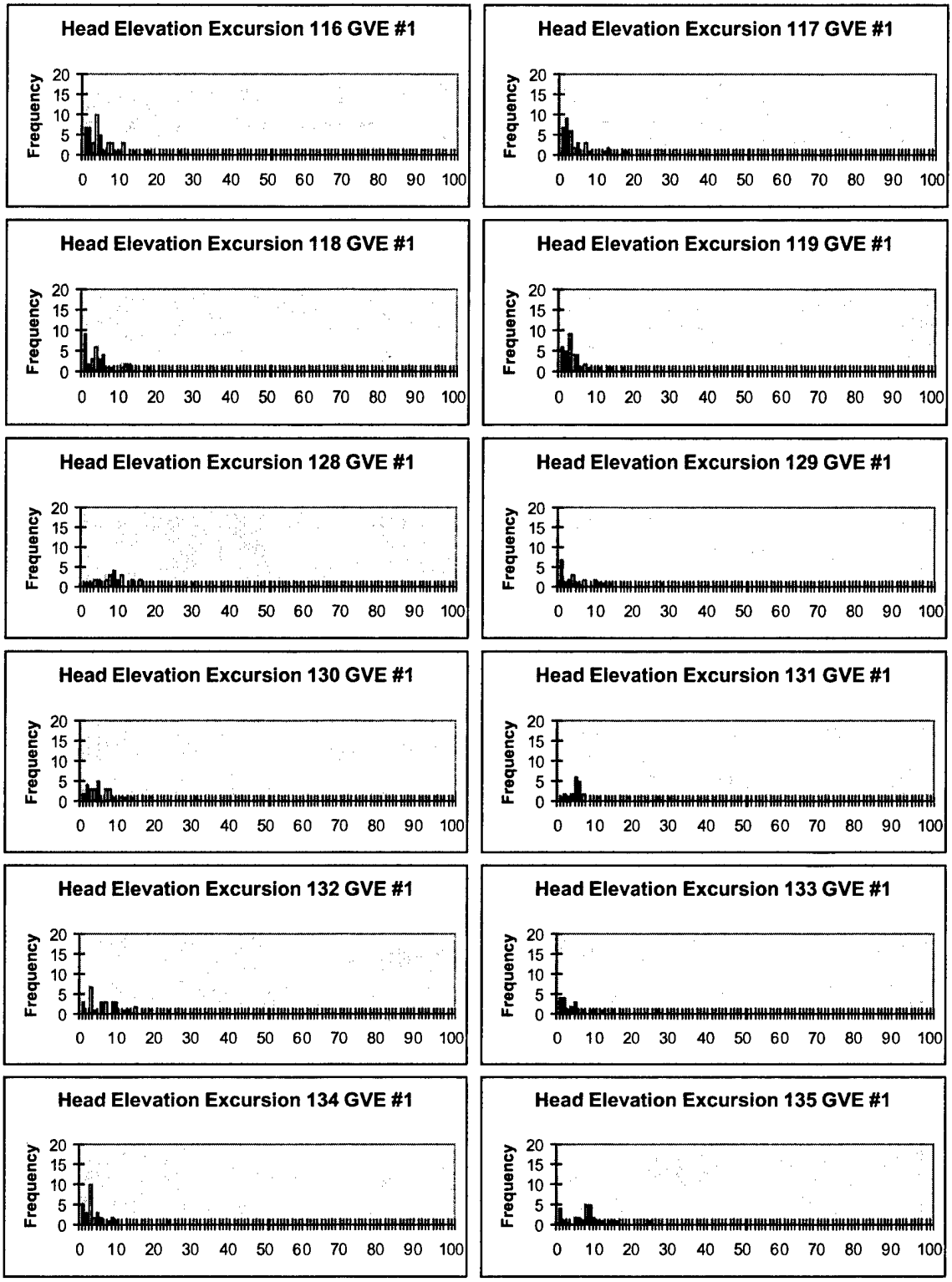

Figure E-1. Subject #1 GVE head position excursion histograms.

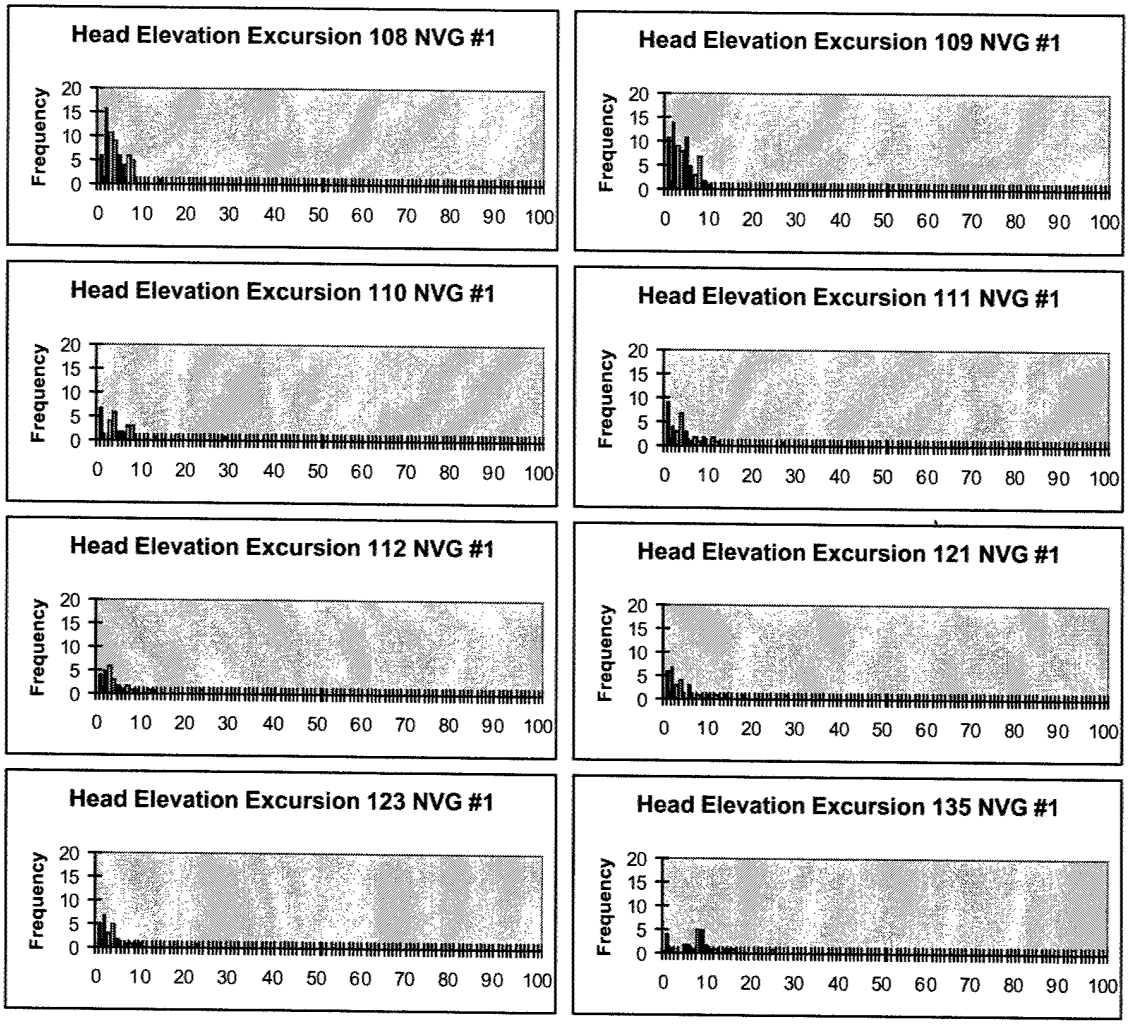

Figure E-2. Subject #1 NVG head position excursion histograms.

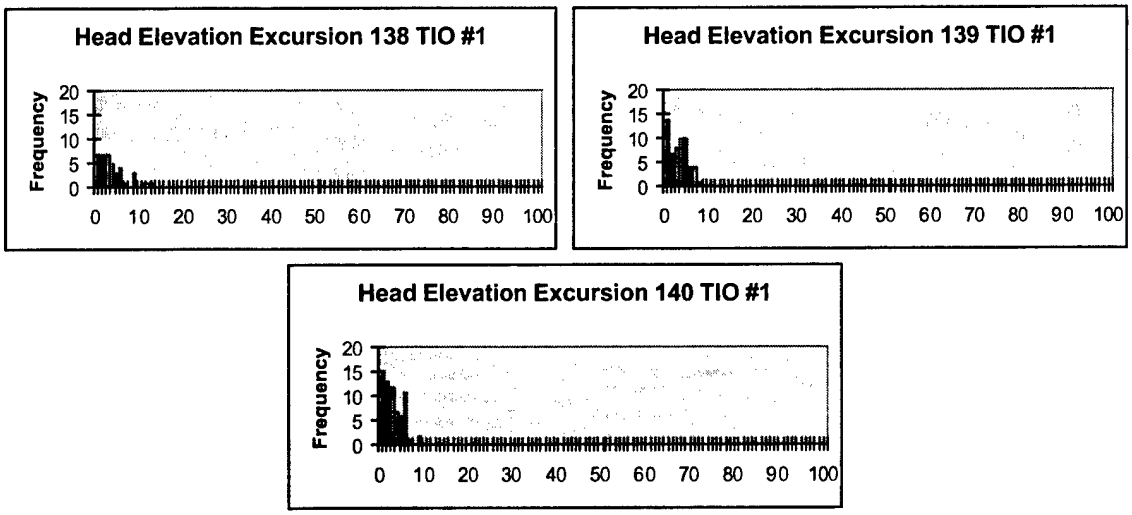

Figure E-3. Subject #1 TIO head position excursion histograms.

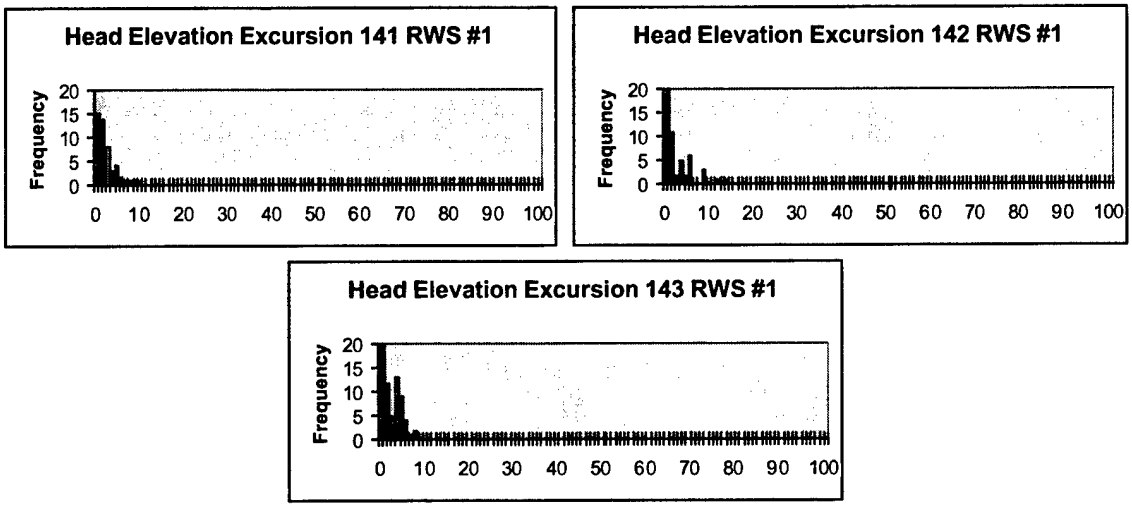

Figure E-4. Subject #1 RWS head position excursion histograms.

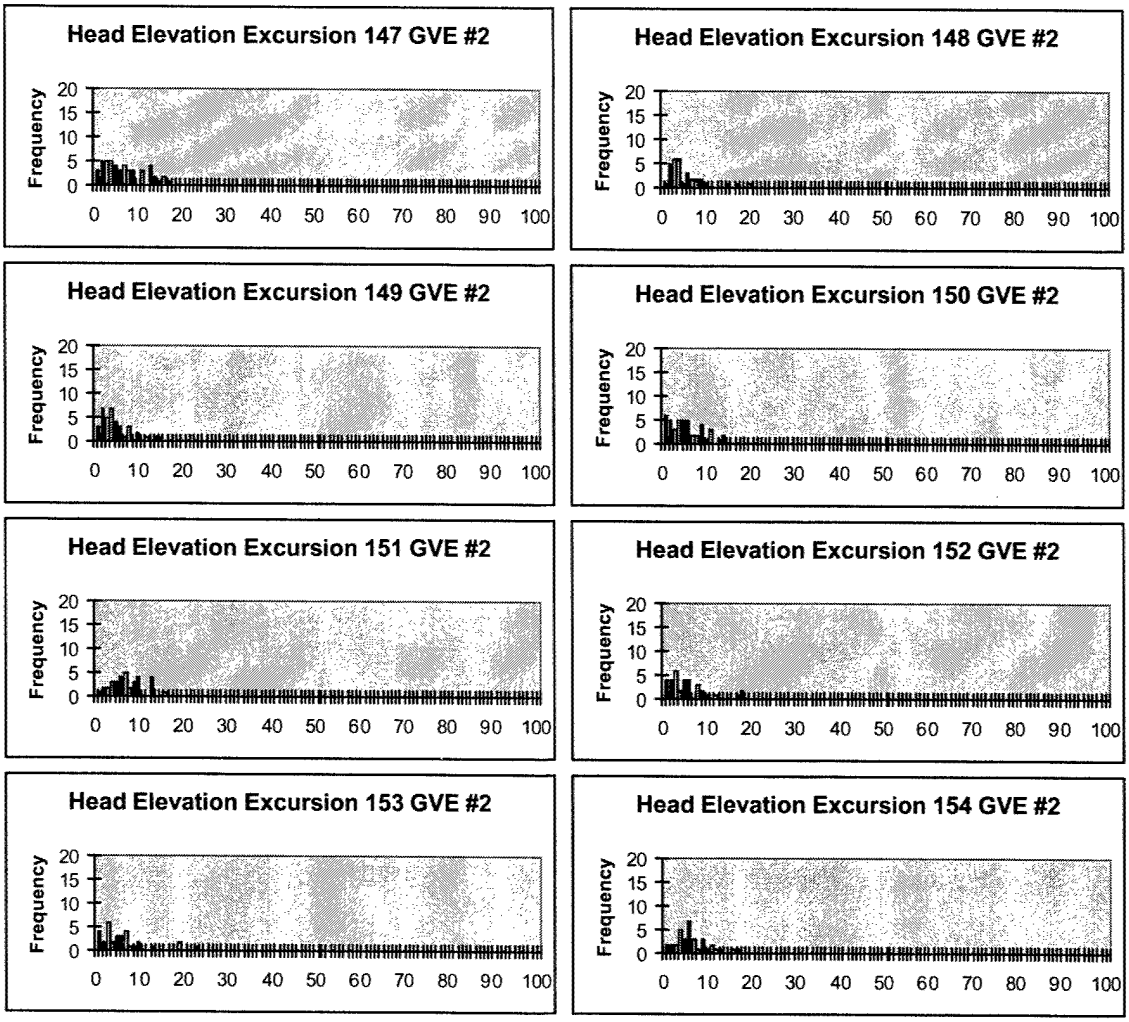

Figure E-5. Subject #2 GVE head position excursion histograms.

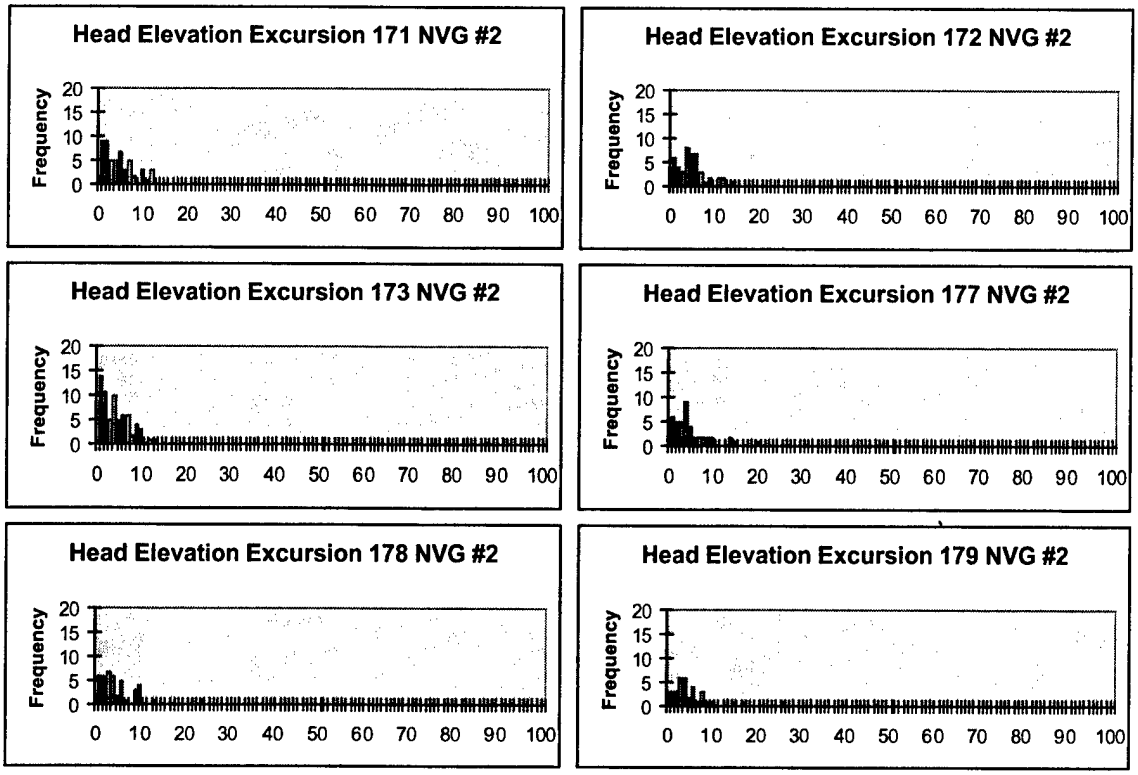

Figure E-6. Subject #2 NVG head position excursion histograms.

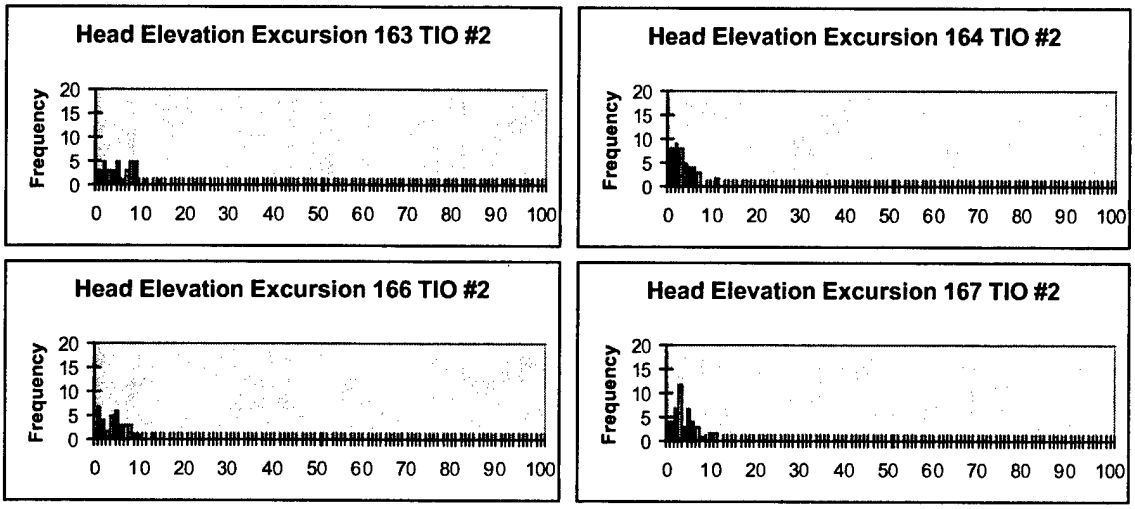

Figure E-7. Subject #2 TIO head position excursion histograms.

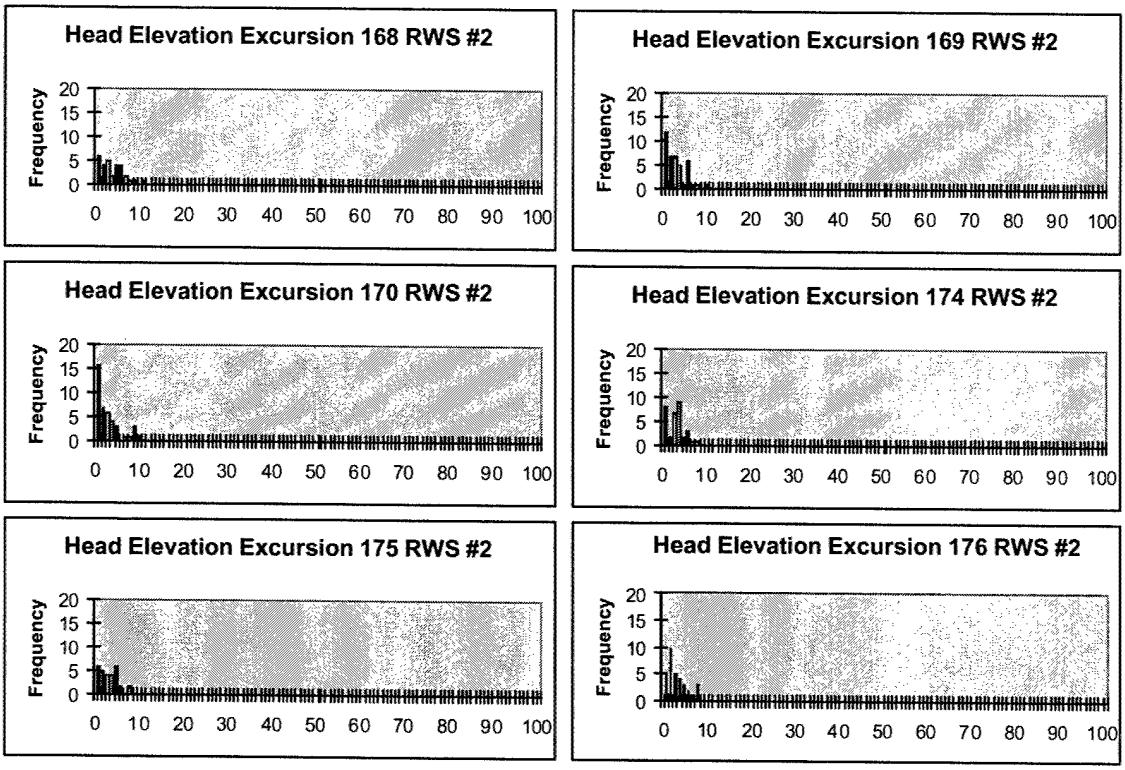

Figure E-8. Subject #2 RWS head position excursion histograms.

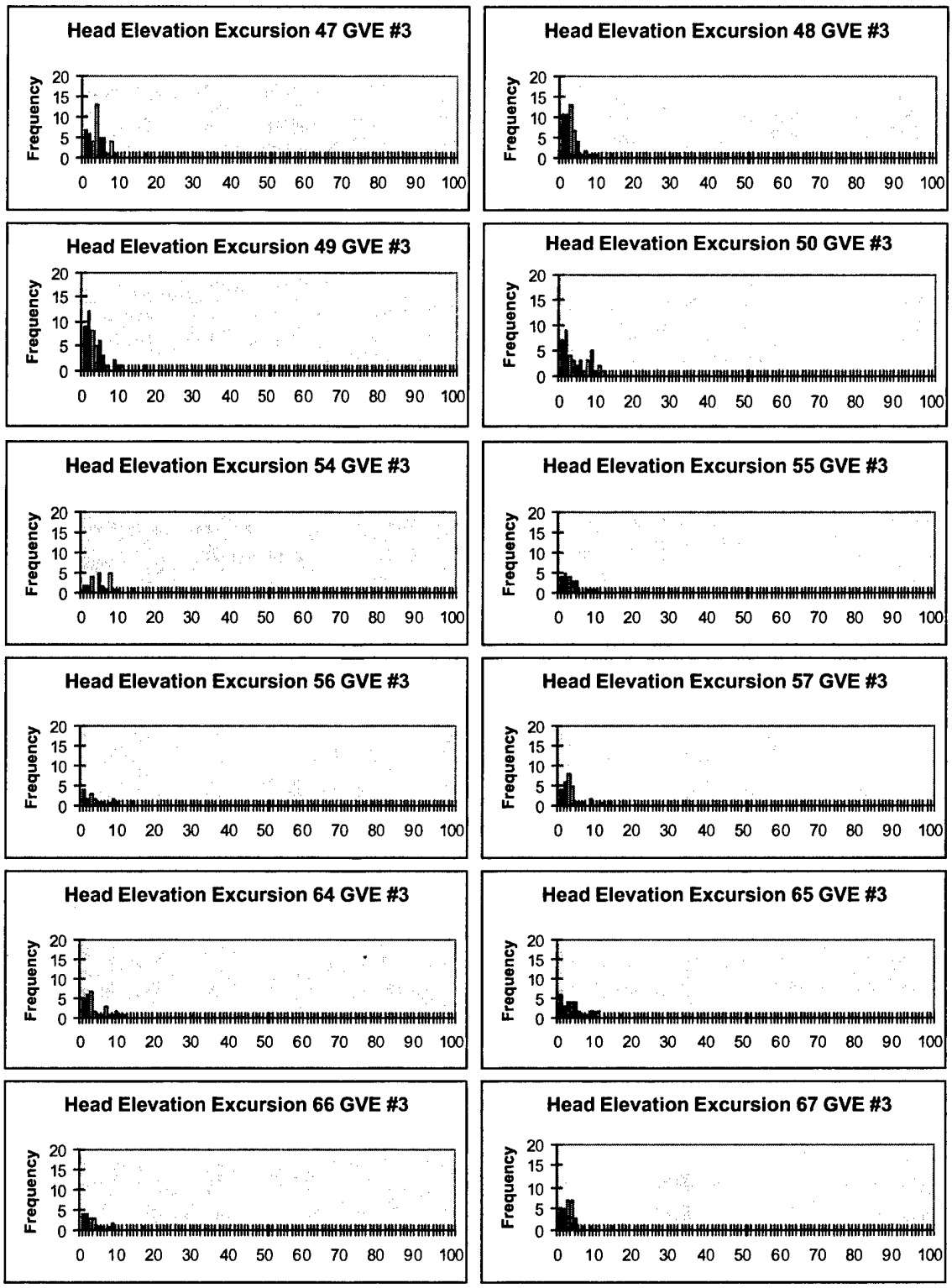

Figure E-9. Subject #3 GVE head position excursion histograms.

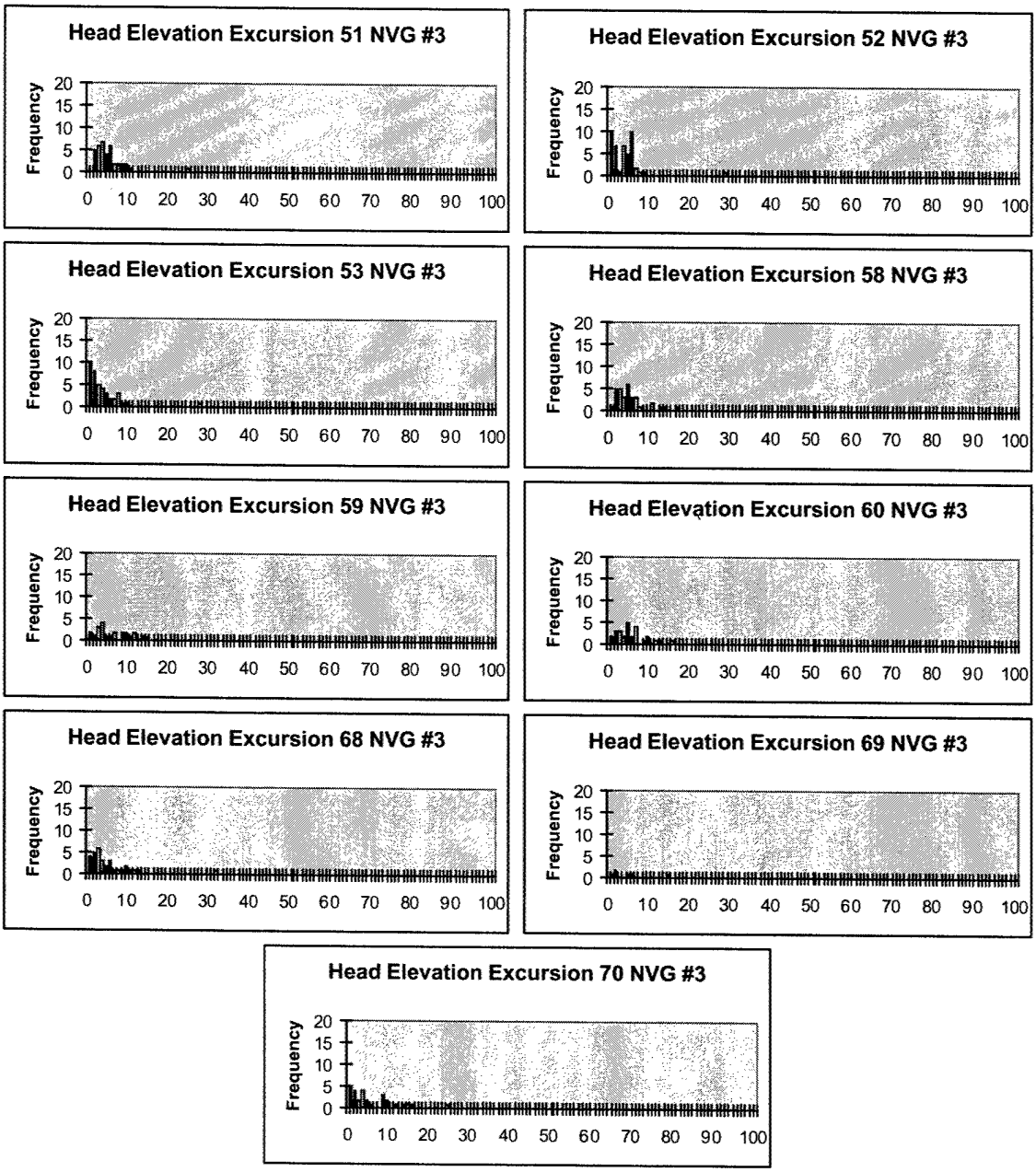

Figure E-10. Subject #3 NVG head position excursion histograms.

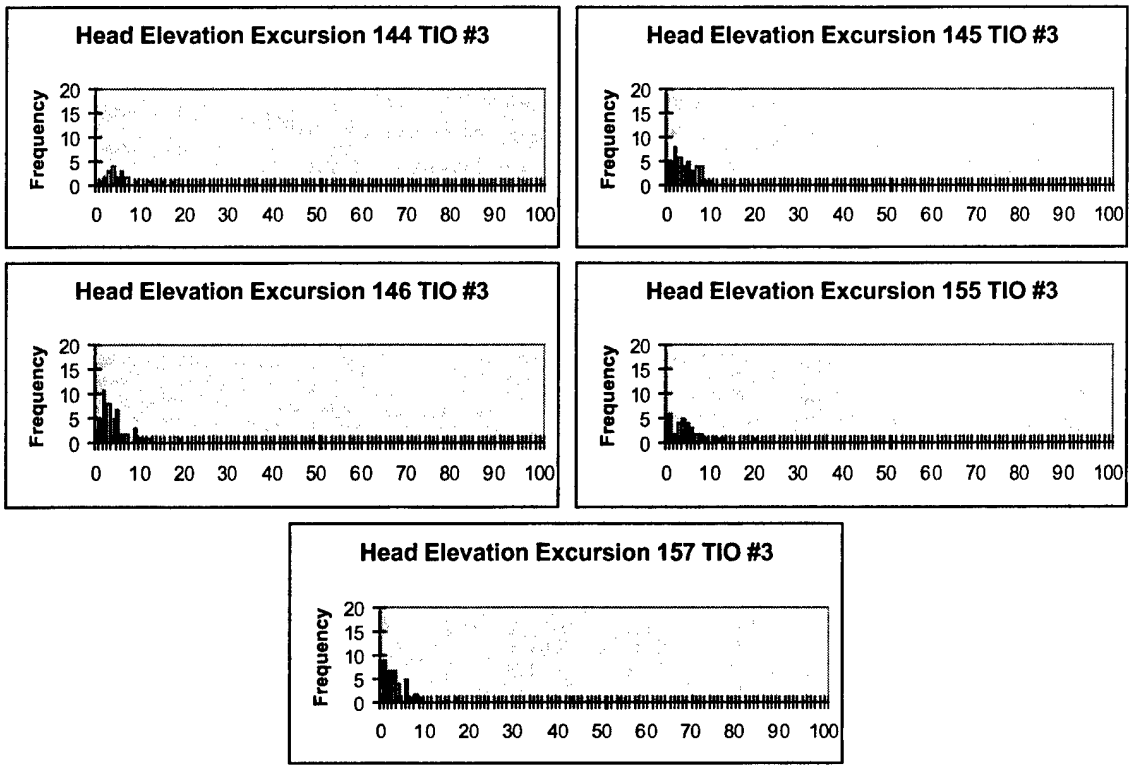

Figure E-11. Subject #3 TIO head position excursion histograms.

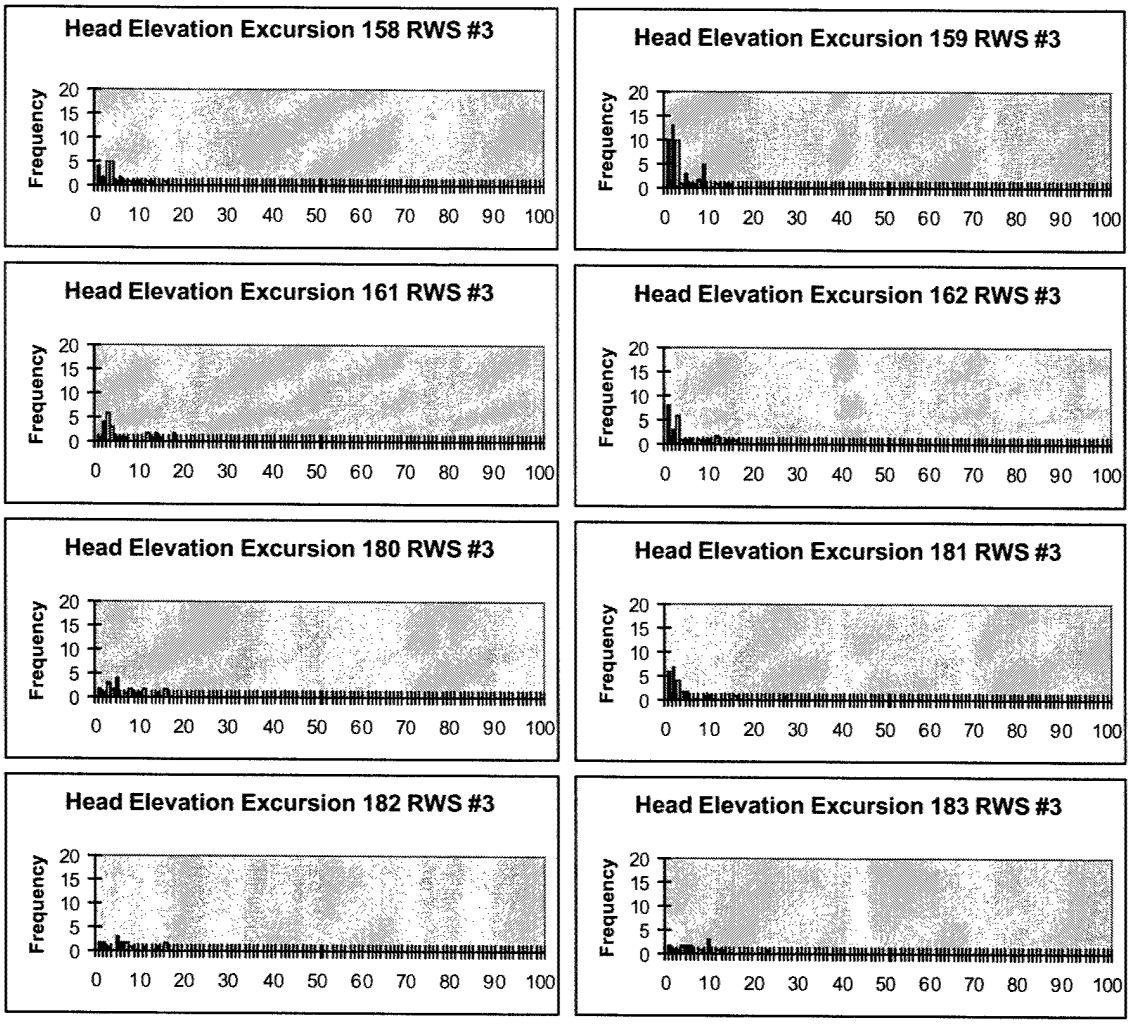

Figure E-12. Subject #3 RWS head position excursion histograms.

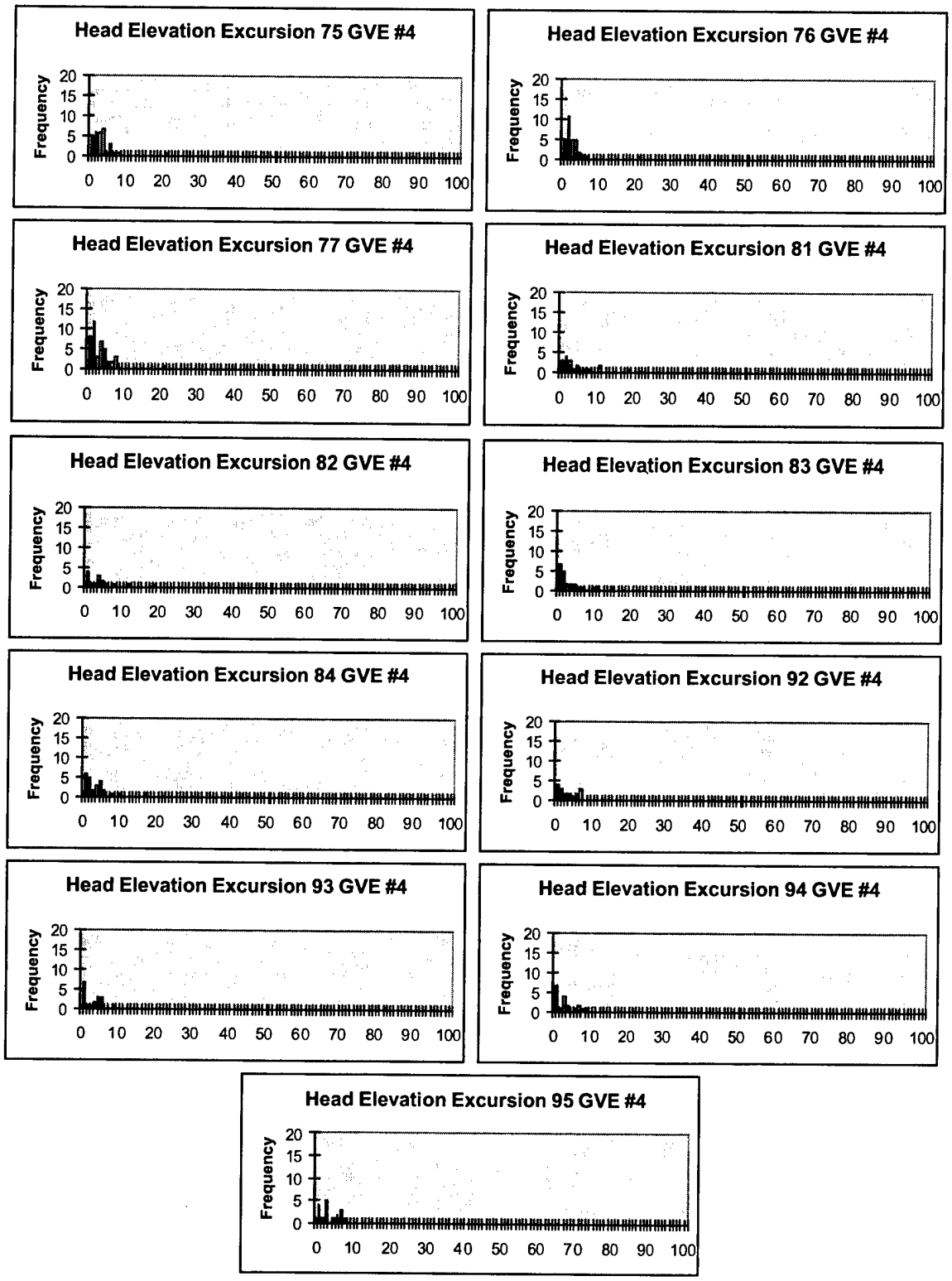

Figure E-13. Subject #4 GVE head position excursion histograms.

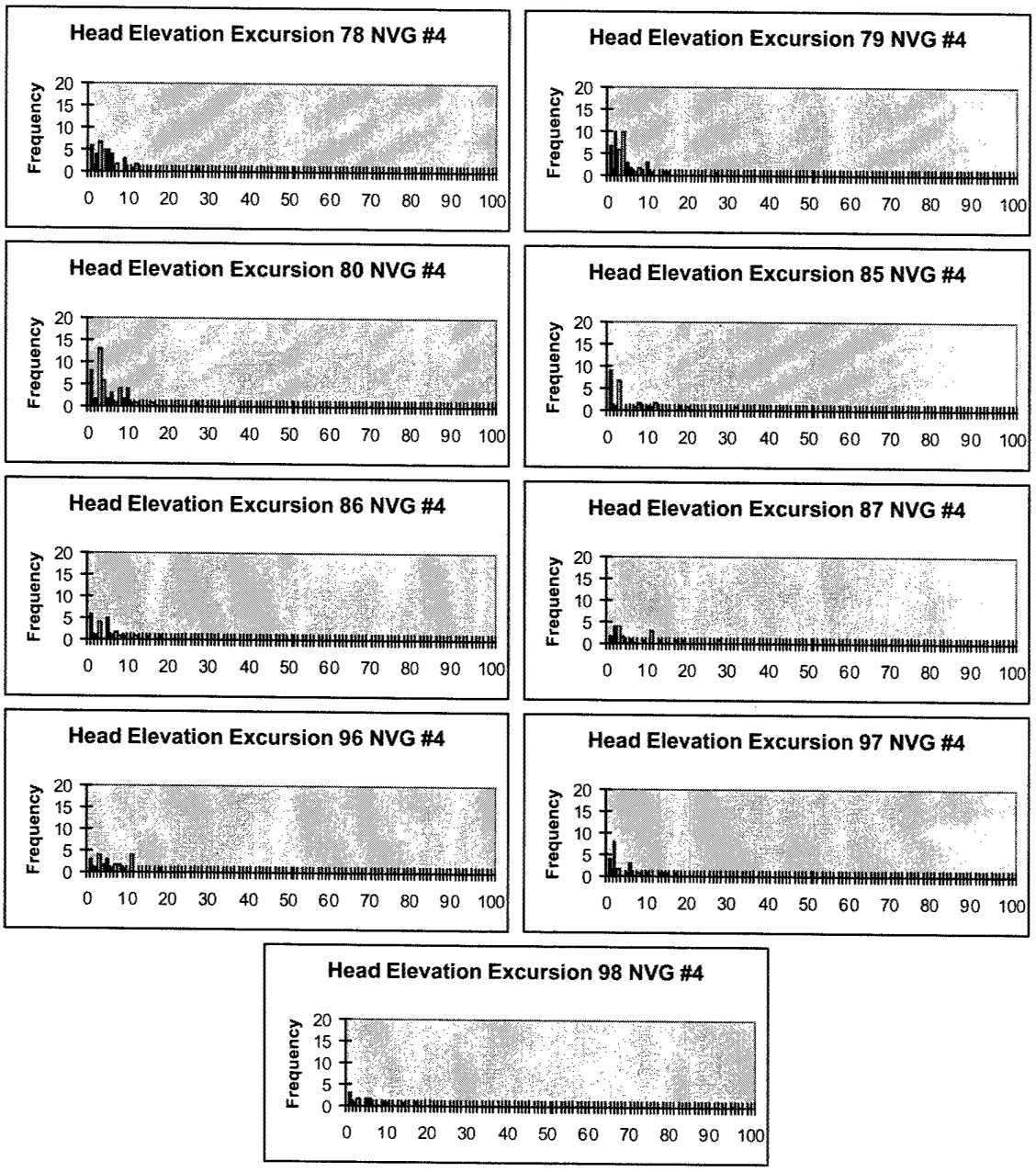

Figure E-14. Subject #4 NVG head position excursion histograms.

Appendix F.

Elevation excursion summary tables.

Table F-1.
Summary statistics for elevation excursions, slalom course, GVE.
(excursion values expressed in degrees)

Subject	Run	Time	# of Excursions	Exc/min	Min	Max	Mean	Median	S.D.	IQR
1	116	76.9	48	37.5	0.1	17.9	5.1	4.0	4.1	2.2-7.1
1	117	75.7	39	30.9	0.1	18.2	4.0	2.3	4.5	1.1-4.6
1	118	76.9	39	30.4	0.0	18.0	4.3	3.6	4.3	1.0-5.9
1	119	76.0	36	28.4	0.1	13.8	3.9	3.2	3.3	1.6-4.7
1	128	45.2	27	38.5	0.6	16.5	8.4	8.7	4.1	1.7-10.8
1	129	48.1	26	32.5	0.0	14.5	4.4	2.6	4.2	1.3-7.0
1	130	48.6	32	39.5	0.1	18.8	5.5	4.8	4.2	2.6-7.6
1	131	43.8	25	34.2	0.3	26.8	6.3	5.1	5.8	3.8-5.8
1	132	45.6	30	39.5	0.5	18.9	7.0	6.4	4.7	3.0-10.0
1	133	49.8	23	27.7	0.4	14.7	4.4	3.4	4.1	1.1-5.0
1	134	51.1	31	36.4	0.7	9.9	3.9	3.2	2.5	2.1-5.3
1	135	52.9	32	36.3	1.1	16.1	7.0	7.9	4.6	2.6-9.4
Combined		**690.6**	**388**	**33.7**	**0.0**	**26.8**	**5.2**	**4.2**	**4.4**	**1.8 - 7.5**
2	147	68.4	48	42.1	0.3	17.1	6.8	6.0	4.6	3.0-9.7
2	148	65.1	33	30.4	0.2	20.3	5.2	3.8	4.4	2.7-6.5
2	149	71.7	40	33.5	0.3	15.0	4.4	3.8	3.3	2.0-5.7
2	150	73.9	43	34.9	0.7	13.9	5.6	4.9	3.7	2.5-8.2
2	151	47.0	34	43.4	0.4	15.8	7.0	6.8	3.8	4.2-9.0
2	152	52.2	33	37.9	0.8	18.4	5.5	4.6	4.3	2.5-7.7
2	153	51.7	32	37.1	0.3	23.4	5.9	5.1	5.1	2.7-6.8
2	154	50.4	34	40.5	0.6	15.9	6.4	6.1	3.4	4.1-8.5
Combined		**480.4**	**297**	**37.1**	**0.2**	**23.4**	**5.9**	**5.0**	**4.1**	**2.9 - 8.2**
3	47	74.8	48	38.5	0.4	9.3	3.9	3.9	2.3	1.8-5.0
3	48	75.7	53	42.0	0.1	9.8	3.2	2.7	2.1	1.7-4.1
3	49	78.8	52	40.0	0.1	10.5	3.3	2.7	2.6	1.6-4.6
3	50	73.2	43	35.2	0.1	11.0	4.3	3.4	3.3	1.6-7.1
3	54	44.6	24	32.3	0.2	10.2	5.1	5.0	2.8	3.2-7.6
3	55	47.6	24	30.3	0.1	8.9	3.0	2.5	2.3	1.3-4.4
3	56	46.5	19	24.5	0.2	14.1	4.0	3.0	3.8	1.2-5.6
3	57	49.0	29	35.5	0.9	12.2	3.9	3.3	2.6	2.0-4.2
3	64	50.6	34	40.3	0.0	10.5	3.7	2.7	3.1	1.3-5.7
3	65	46.8	31	39.7	0.5	10.9	4.7	3.8	3.3	2.1-6.6
3	66	46.7	21	27.0	0.3	9.0	3.3	2.7	2.7	1.4-4.4
3	67	43.4	30	41.5	0.2	9.1	3.1	2.8	2.0	1.6-3.9
Combined		**677.7**	**408**	**36.1**	**0.0**	**14.1**	**3.7**	**3.0**	**2.7**	**1.7 - 5.0**
4	75	72.4	35	29.0	0.0	8.0	2.9	2.6	2.0	1.5-4.2
4	76	69.0	33	28.7	0.1	7.0	2.6	2.2	1.7	1.7-3.6
4	77	79.8	46	34.6	0.1	8.1	3.1	2.4	2.2	1.4-4.6
4	81	42.0	21	30.0	0.0	11.0	3.4	1.9	3.3	1.1-4.5
4	82	42.6	17	23.9	0.0	11.5	3.3	3.4	3.0	1.0-4.5
4	83	46.0	22	28.7	0.6	10.7	3.5	2.2	2.9	1.3-5.1
4	84	45.0	28	37.3	0.3	9.6	3.3	2.7	2.4	1.3-4.9
4	92	44.4	18	34.3	0.5	7.0	3.5	3.2	2.3	1.5-5.7
4	93	43.6	20	27.5	0.0	9.2	3.0	1.9	2.5	1.1-4.9
4	94	48.0	21	26.3	0.2	9.1	3.1	2.2	2.8	0.8-4.2
4	95	49.2	18	22.0	0.3	8.3	3.5	2.7	2.7	1.0-6.2
Combined		**582.0**	**279**	**28.7**	**0.0**	**11.5**	**3.1**	**2.4**	**2.5**	**1.2 – 4.6**
All Subjects		**2430.7**	**1372**	**33.9**	**0.0**	**26.8**	**4.5**	**3.6**	**3.7**	**1.7 - 6.3**

Table F-2.
Summary statistics for elevation excursions, slalom course, NVG.
(expressed in degrees)

Subject	Run	Time	# of Excursions	Exc/ min	Min	Max	Mean	Median	S.D.	IQR
1	108	105.7	68	38.6	0.0	8.4	3.6	3.2	2.3	2.0-4.7
1	109	98.2	74	45.2	0.1	9.3	3.8	3.4	2.4	4.9-5.4
1	110	51.3	30	35.1	0.0	12.9	4.1	3.8	3.0	1.2-5.4
1	111	51.7	39	45.3	0.2	11.6	3.9	3.2	3.2	1.4-4.4
1	112	51.1	28	32.9	0.3	12.9	4.11	3.2	3.2	1.9-4.9
1	121	54.0	30	33.3	0.0	17.9	4.2	2.5	4.3	1.4-3.9
1	123	55.2	28	30.4	0.0	9.7	3.3	2.5	2.6	1.5-5.2
Combined		**467.2**	**297**	**38.1**	**0.0**	**17.9**	**3.8**	**3.2**	**2.9**	**1.6 – 5.2**
2	171	80.0	54	40.5	0.2	11.6	4.2	3.7	3.1	1.6-6.2
2	172	80.9	47	34.9	0.0	14.4	5.0	5.0	3.4	2.3-6.3
2	173	103.2	70	40.7	0.1	12.2	4.1	3.7	3.0	1.6-6.0
2	177	70.6	44	37.4	0.1	20.44	4.9	4.1	1.2	2.0-6.0
2	178	63.0	41	39.0	0.5	12.8	4.6	3.6	3.2	2.3-6.2
2	179	54.3	32	35.4	1.1	16.5	5.3	4.3	3.6	3.0-6.6
Combined		**452.0**	**288**	**38.2**	**0.0**	**20.4**	**4.6**	**3.9**	**3.4**	**1.9 – 6.3**
3	51	71.8	41	34.3	0.3	10.8	4.8	4.2	2.7	3.0-6.1
3	52	73.9	49	39.8	0.1	8.6	3.5	3.8	2.4	1.1-5.8
3	53	68.2	41	36.1	0.0	9.6	3.5	2.7	2.6	1.5-5.0
3	58	50.5	31	36.8	1.4	17.4	5.7	4.7	3.9	3.1-6.6
3	59	51.9	27	31.2	0.0	14.7	5.4	4.1	4.4	1.7-9.1
3	60	52.6	28	31.9	0.1	15.7	5.3	4.9	3.9	2.5-7.3
3	68	53.6	33	36.9	0.5	13.1	4.6	3.4	3.5	2.0-6.1
3	69	53.8	13	14.5	0.0	6.0	1.4	0.4	2.1	0.1-2.3
3	70	48.8	27	33.2	0.7	16.1	5.8	4.2	4.7	2.2-9.2
Combined		**525.1**	**290**	**33.1**	**0.0**	**17.4**	**4.5**	**3.8**	**3.5**	**1.9 – 6.2**
4	78	95.3	46	29.0	0.1	11.9	4.0	3.4	3.2	1.5-5.6
4	79	81.9	51	37.4	0.1	15.1	4.0	3.2	3.5	1.7-4.9
4	80	83.9	51	36.5	0.1	15.8	4.7	3.5	3.6	2.6-7.2
4	85	52.7	28	31.9	0.1	20.2	5.0	3.0	5.4	1.1-7.9
4	86	56.0	25	26.8	0.0	15.4	4.3	3.4	3.8	1.1-6.5
4	87	49.8	20	24.1	0.9	19.0	6.2	3.4	5.5	2.0-10.8
4	96	44.6	27	36.3	0.3	18.3	5.4	4.9	4.3	2.5-7.9
4	97	47.0	27	24.5	0.4	17.4	5.0	2.2	5.1	1.5-6.4
4	98	46.1	15	19.5	0.0	20.2	4.7	3.4	4.2	1.5-6.6
Combined		**557.3**	**290**	**31.2**	**0.0**	**20.2**	**4.7**	**3.4**	**4.2**	**1.5 – 6.6**
All Subjects		**2001.6**	**1165**	**34.9**	**0.0**	**20.4**	**4.4**	**3.6**	**3.7**	**1.7 – 6.2**

Table F-3.
Summary statistics for elevation excursions, slalom course, TIO.
(expressed in degrees)

Subject	Run	Time	# of Excursions	Exc/min	Min	Max	Mean	Median	S.D.	IQR
1	138	85.7	43	30.1	0.0	13.3	4.0	2.9	3.3	1.6-5.5
1	139	109.7	63	34.5	0.1	7.6	3.2	3.1	2.1	1.3-4.8
1	140	120.4	72	35.9	0.2	8.9	3.1	2.7	2.1	1.4-4.8
Combined		**315.8**	**178**	**33.8**	**0.0**	**13.3**	**3.4**	**2.9**	**2.5**	**1.4 – 5.0**
2	163	70.0	35	30.0	0.0	11.0	5.2	5.0	3.0	2.7-7.8
2	164	82.5	47	34.2	0.0	11.2	3.3	3.0	2.6	1.4-4.7
2	166	80.1	37	27.7	0.1	13.0	4.4	4.4	3.1	1.7-5.9
2	167	88.1	46	31.3	0.0	11.3	4.0	3.4	2.7	2.0-5.1
Combined		**320.7**	**165**	**30.9**	**0.0**	**13.0**	**4.1**	**3.6**	**2.9**	**1.7 – 5.6**
3	144	70.9	24	20.3	0.1	16.7	5.1	4.1	4.4	2.2-6.5
3	145	89.3	45	30.2	0.1	9.6	3.9	3.3	2.7	1.7-6.0
3	146	97.9	48	29.4	0.2	18.7	4.3	3.1	3.5	2.0-5.4
3	155	71.9	33	27.5	0.3	20.1	5.1	4.3	4.2	2.1-6.0
3	157	84.4	40	28.4	0.1	16.7	3.3	2.6	3.2	1.6-5.8
Combined		**414.4**	**190**	**27.5**	**0.1**	**20.1**	**4.2**	**3.3**	**3.6**	**1.6 – 5.8**
4	None									
All Subjects		**1050.9**	**533**	**30.4**	**0.0**	**20.1**	**3.9**	**3.3**	**3.0**	**1.6 – 5.5**

Table F-4.
Summary statistics for elevation excursions, slalom course, RWS.
(expressed in degrees)

Subject	Run	Time	# of Excursions	Exc/min	Min	Max	Mean	Median	S.D.	IQR
1	141	106.2	56	31.6	0.0	10.0	2.6	1.8	2.3	1.0-3.4
1	142	102.0	59	34.7	0.0	13.5	2.8	1.5	3.0	1.0-4.1
1	143	120.0	70	35.0	0.0	8.2	2.9	2.2	2.0	1.1-4.3
Combined		**328.2**	**185**	**33.8**	**0.0**	**13.5**	**2.8**	**1.8**	**2.5**	**1.0 – 4.2**
2	168	83.2	32	23.1	0.2	11.1	3.6	3.2	2.7	1.4-5.4
2	169	89.1	44	29.6	0.1	10.0	2.9	2.4	2.2	1.3-4.3
2	170	101.1	47	27.9	0.1	10.0	2.6	1.8	2.4	0.8-3.5
2	174	63.6	35	33.0	0.0	8.0	3.1	3.0	2.0	1.3-4.2
2	175	65.0	32	30.5	0.1	8.4	3.1	2.9	2.2	1.2-5.1
2	176	63.8	34	32.0	0.1	8.3	3.0	2.5	2.1	1.6-4.2
Combined		**465.8**	**224**	**28.9**	**0.0**	**11.1**	**3.0**	**2.6**	**2.3**	**1.2 – 4.5**
3	158	71.2	26	21.9	0.3	15.9	5.0	3.8	4.1	2.5-7.1
3	159	94.8	51	32.3	0.3	15.2	3.8	2.4	3.6	1.4-4.7
3	161	61.2	25	24.5	0.5	18.1	6.7	3.5	5.7	3.1-12.1
3	162	55.3	28	30.4	0.1	16.4	5.0	2.8	5.0	1.3-8.7
3	180	59.6	27	27.2	0.1	15.6	5.4	4.6	4.4	2.2-7.9
3	181	58.9	27	27.5	0.1	27.4	4.2	2.3	5.8	1.5-3.8
3	182	52.9	18	20.4	0.9	15.7	3.2	5.5	4.4	2.7-7.4
3	183	43.9	19	26.0	0.0	23.4	7.0	5.7	5.8	3.2-10.0
Combined		**497.8**	**221**	**26.6**	**0.0**	**27.4**	**5.1**	**3.2**	**4.8**	**1.7 – 7.4**
4	None									
All Subjects		**1291.8**	**630**	**29.3**	**0.0**	**27.4**	**3.7**	**2.6**	**3.5**	**1.3 – 4.8**

Appendix G.

Elevation excursion box plots.

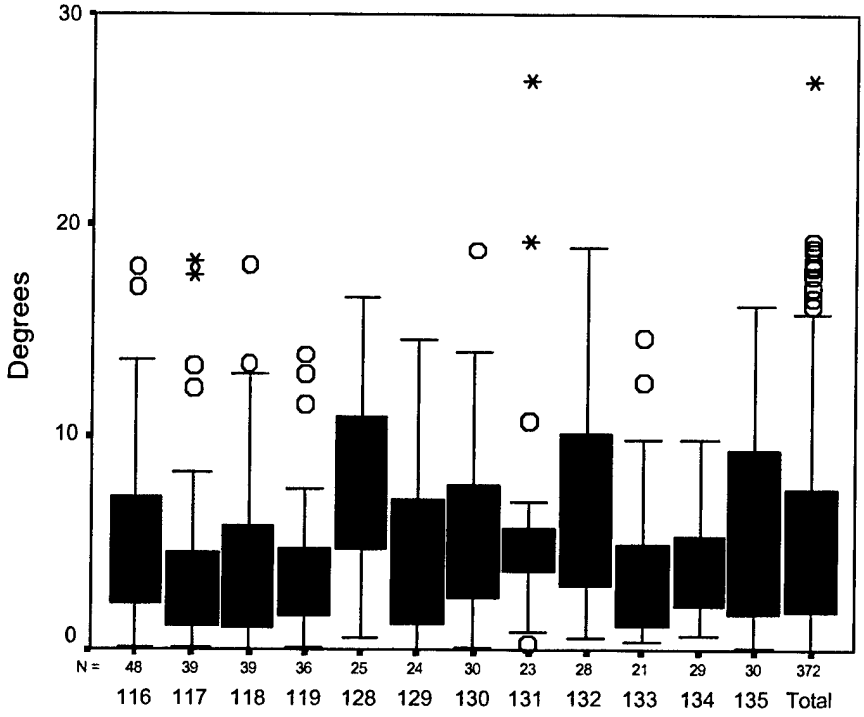

Figure G-1. Subject #1 GVE excursion box plots.

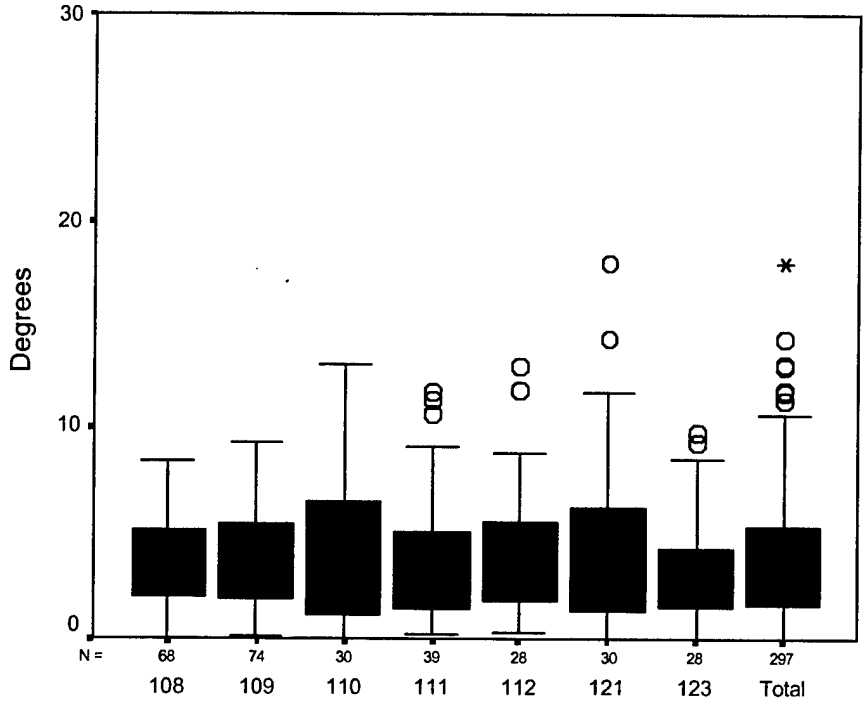

Figure G-2. Subject #1 NVG excursion box plots.

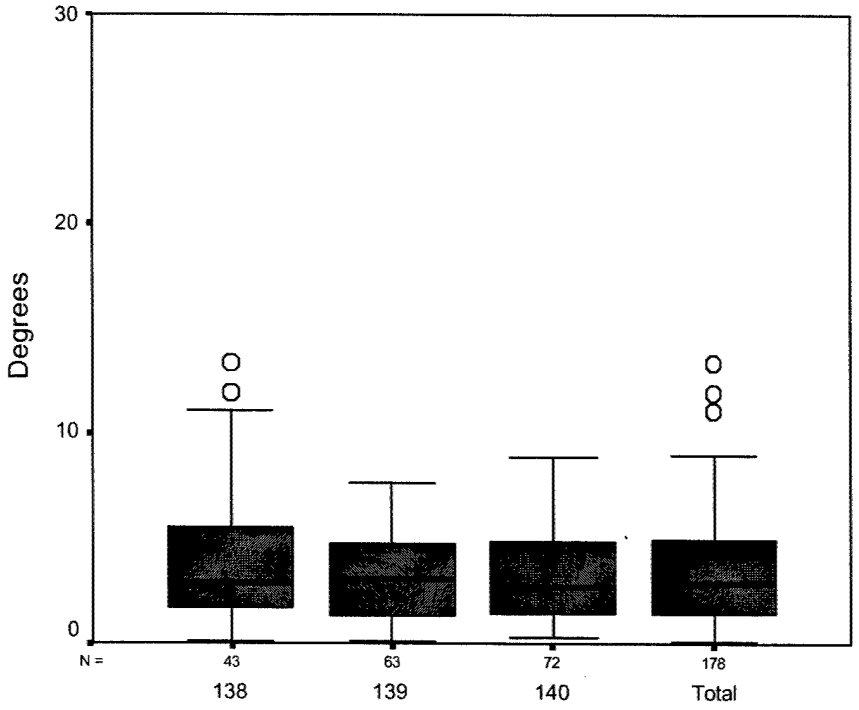

Figure G-3. Subject #1 TIO excursion box plots.

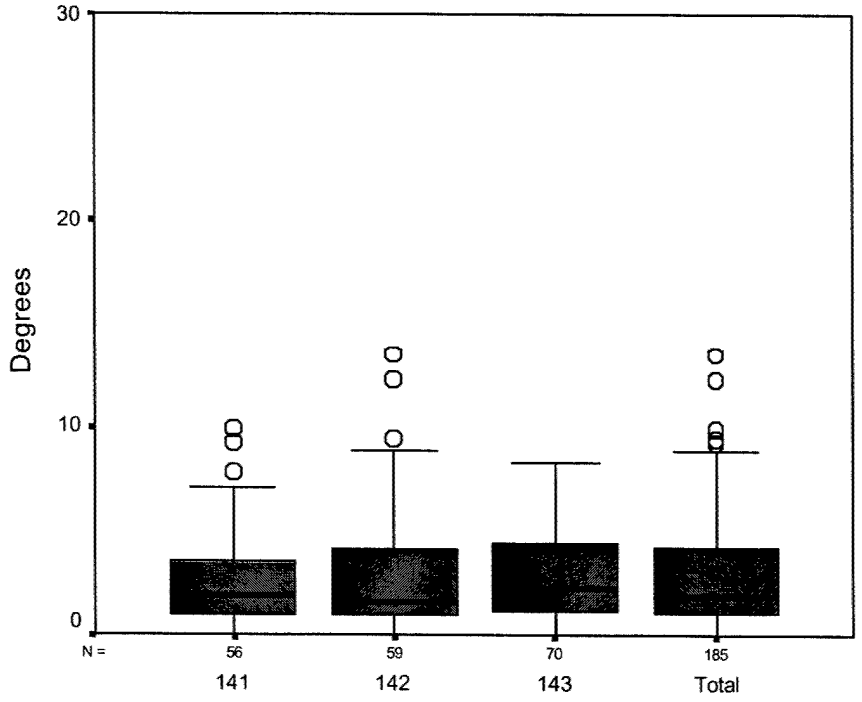

Figure G-4. Subject #1 RWS excursion box plots.

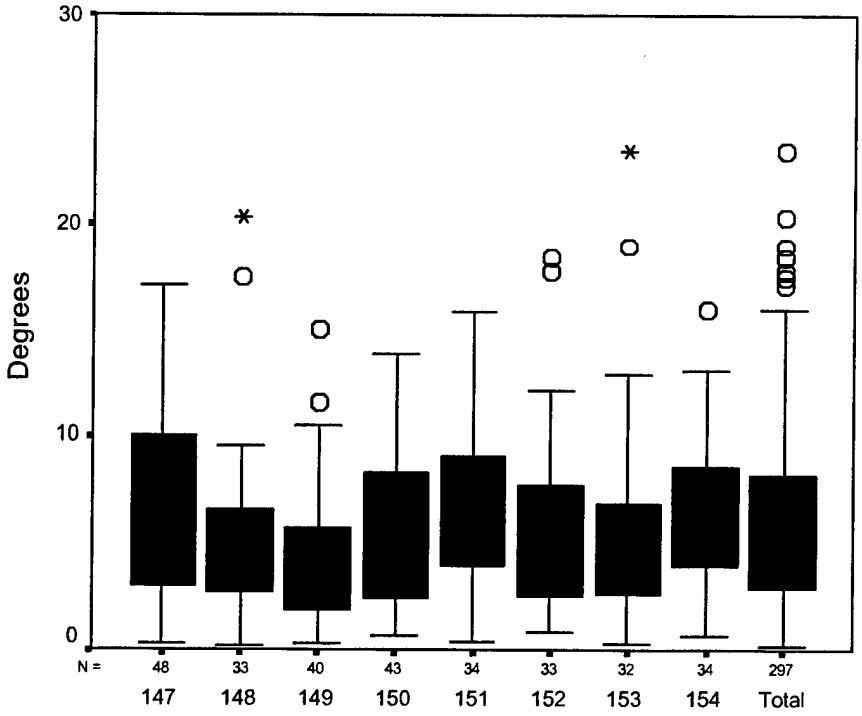

Figure G-5. Subject #2 GVE excursion box plots.

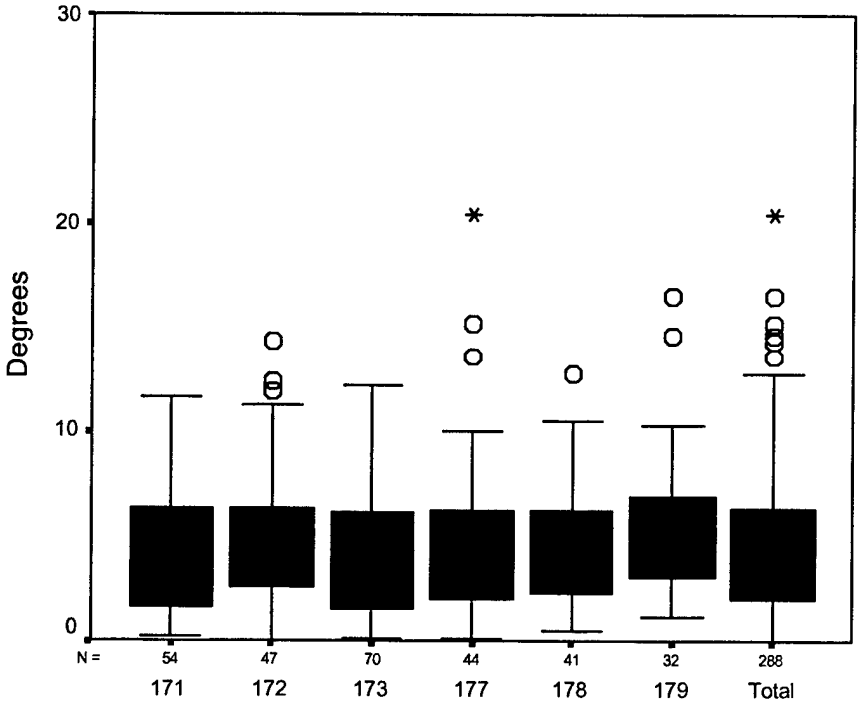

Figure G-6. Subject #2 NVG excursion box plots.

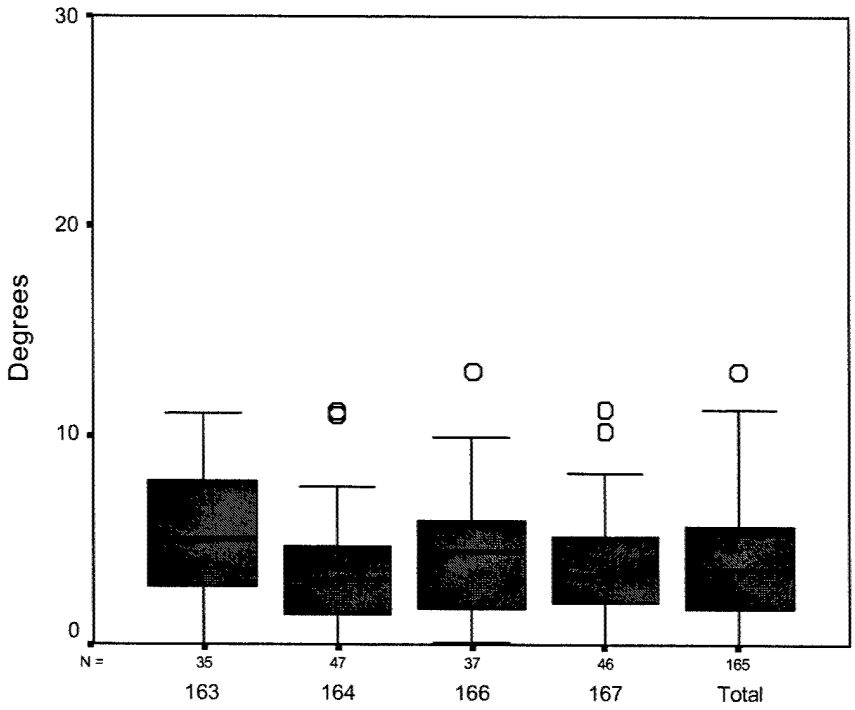

Figure G-7. Subject #2 TIO excursion box plots.

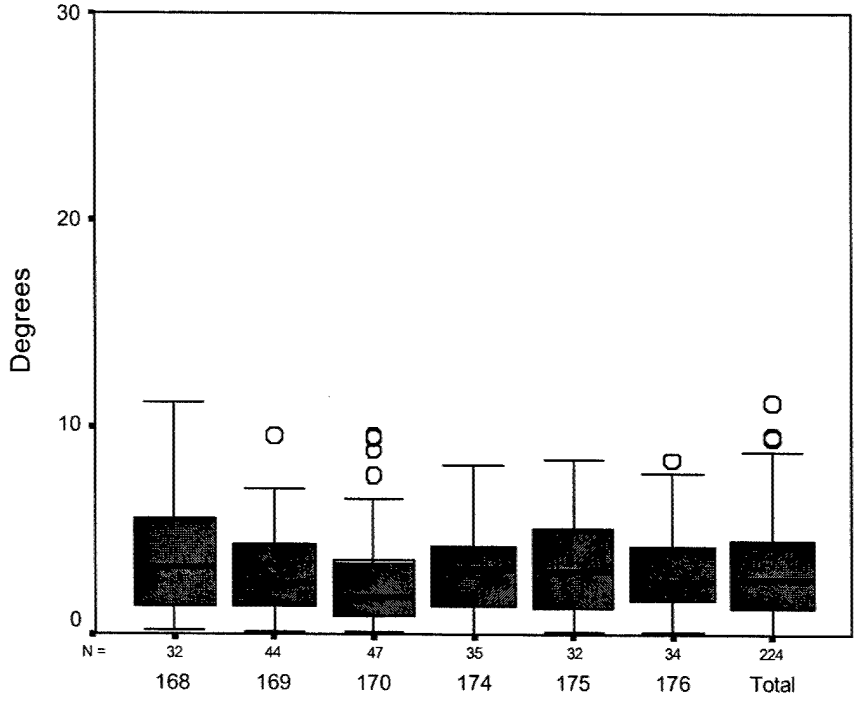

Figure G-8. Subject #2 RWS excursion box plots.

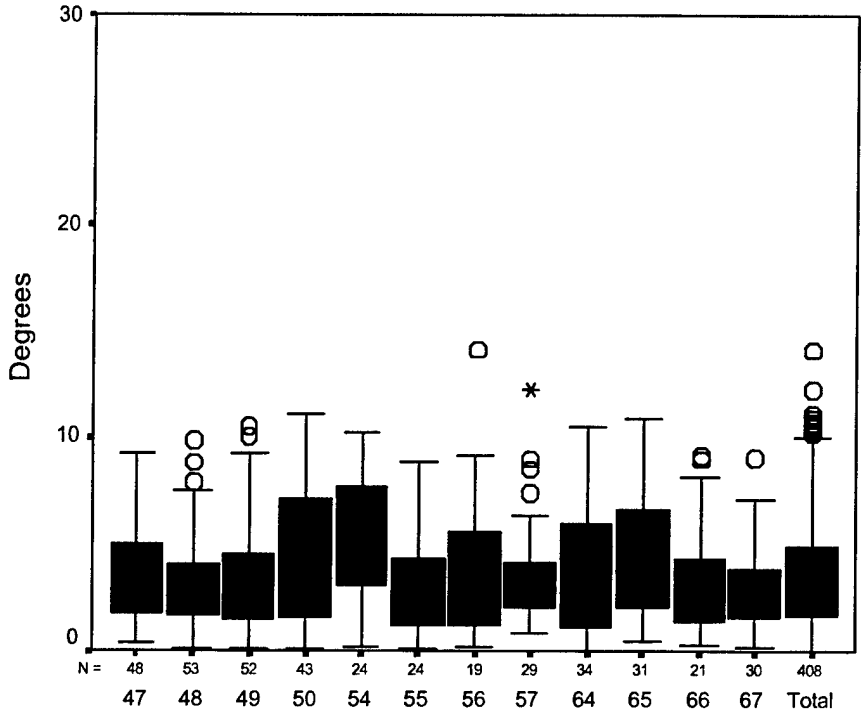

Figure G-9. Subject #3 GVE excursion box plots.

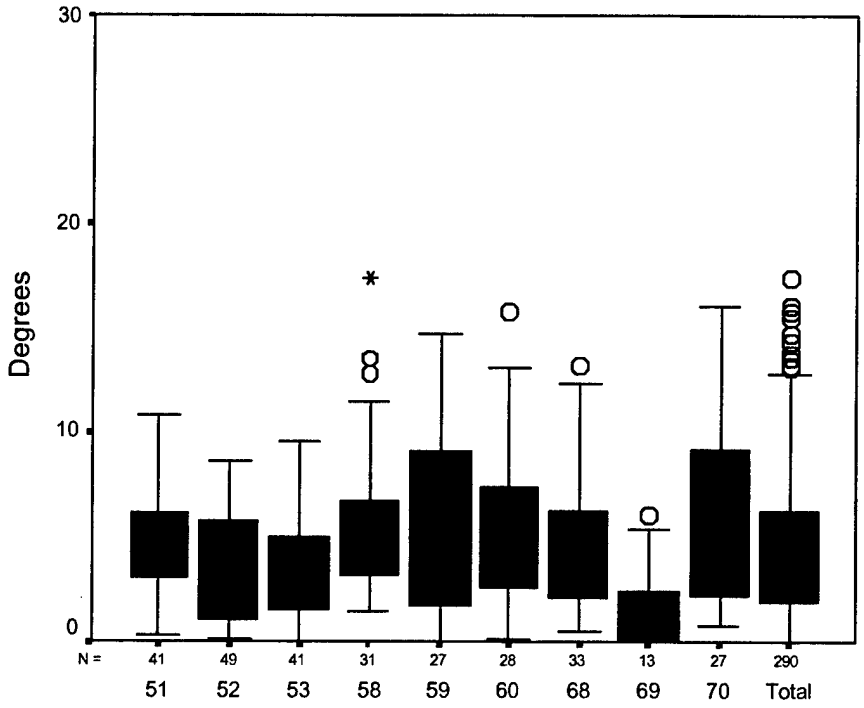

Figure G-10. Subject #3 NVG excursion box plots.

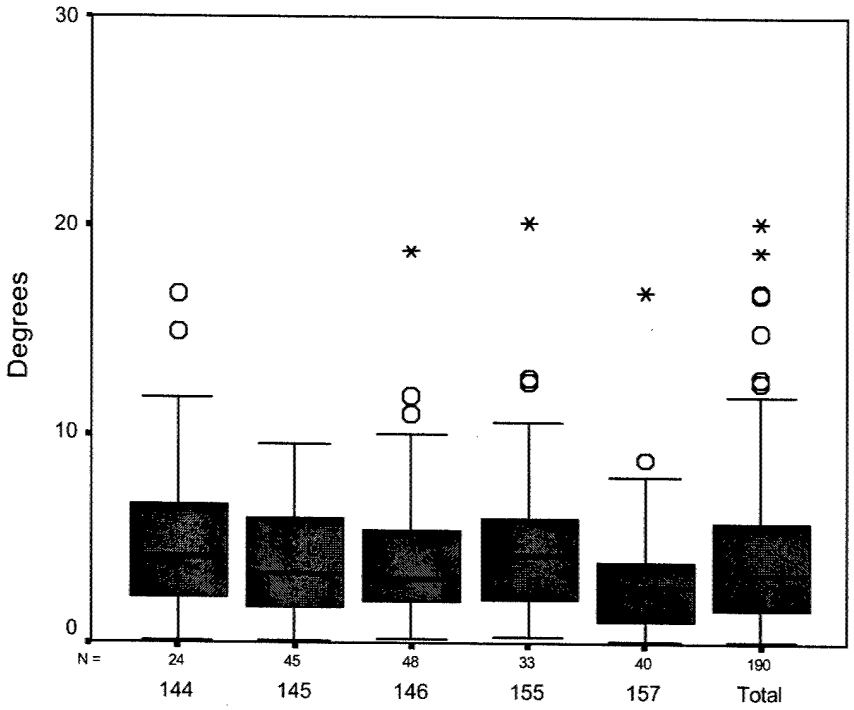

Figure G-11. Subject #3 TIO excursion box plots.

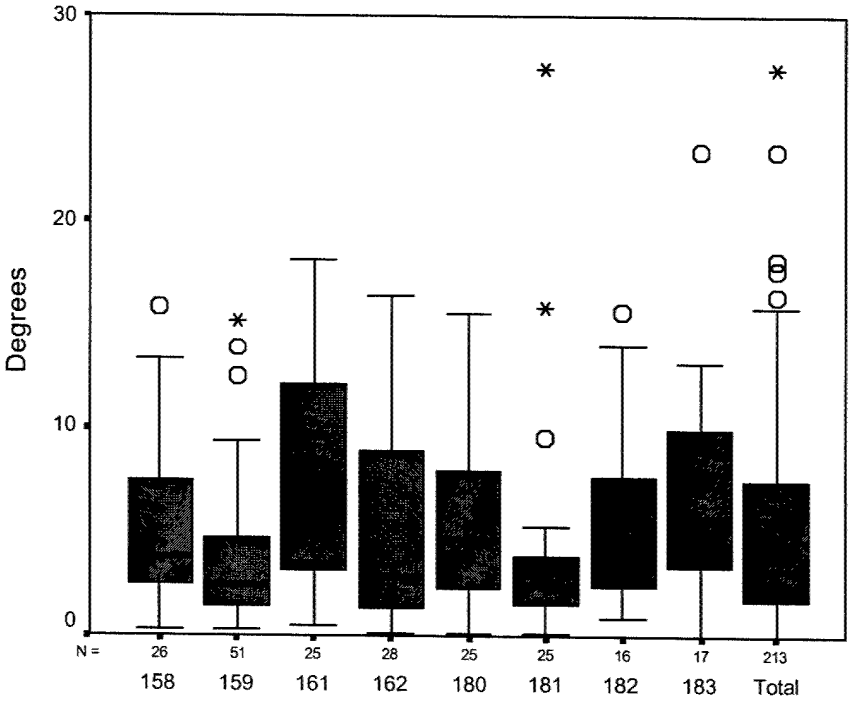

Figure G-12. Subject #3 RWS excursion box plots.

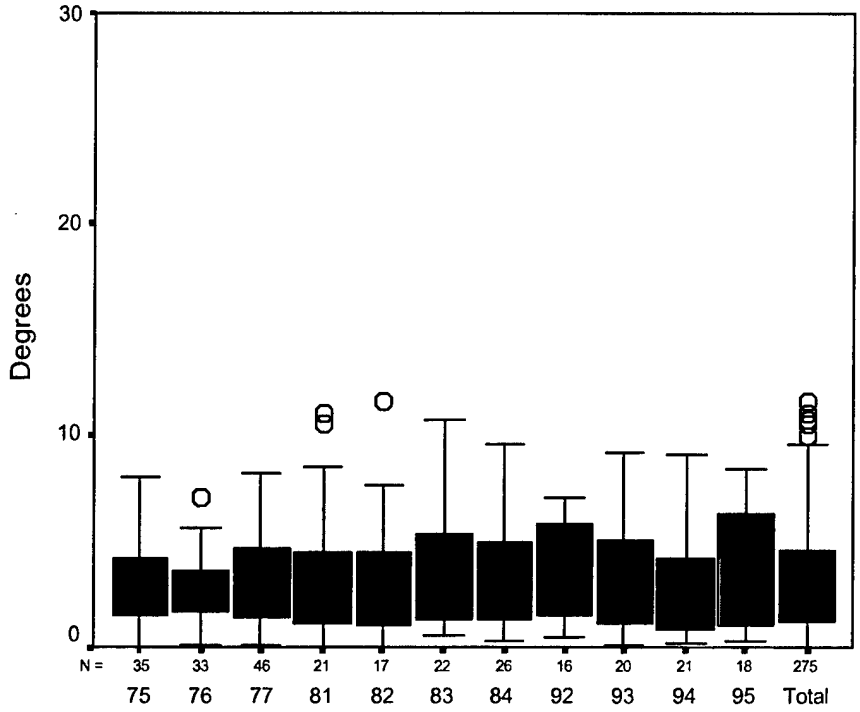

Figure G-13. Subject #4 GVE excursion box plots.

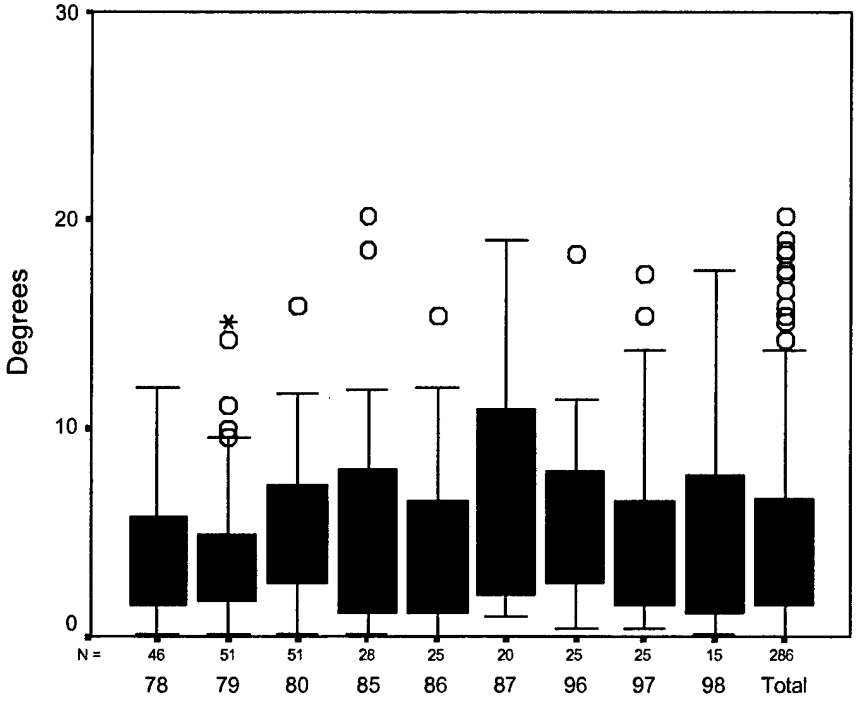

Figure G-14. Subject #4 NVG excursion box plots.

Appendix H.

Elevation velocity distributions.

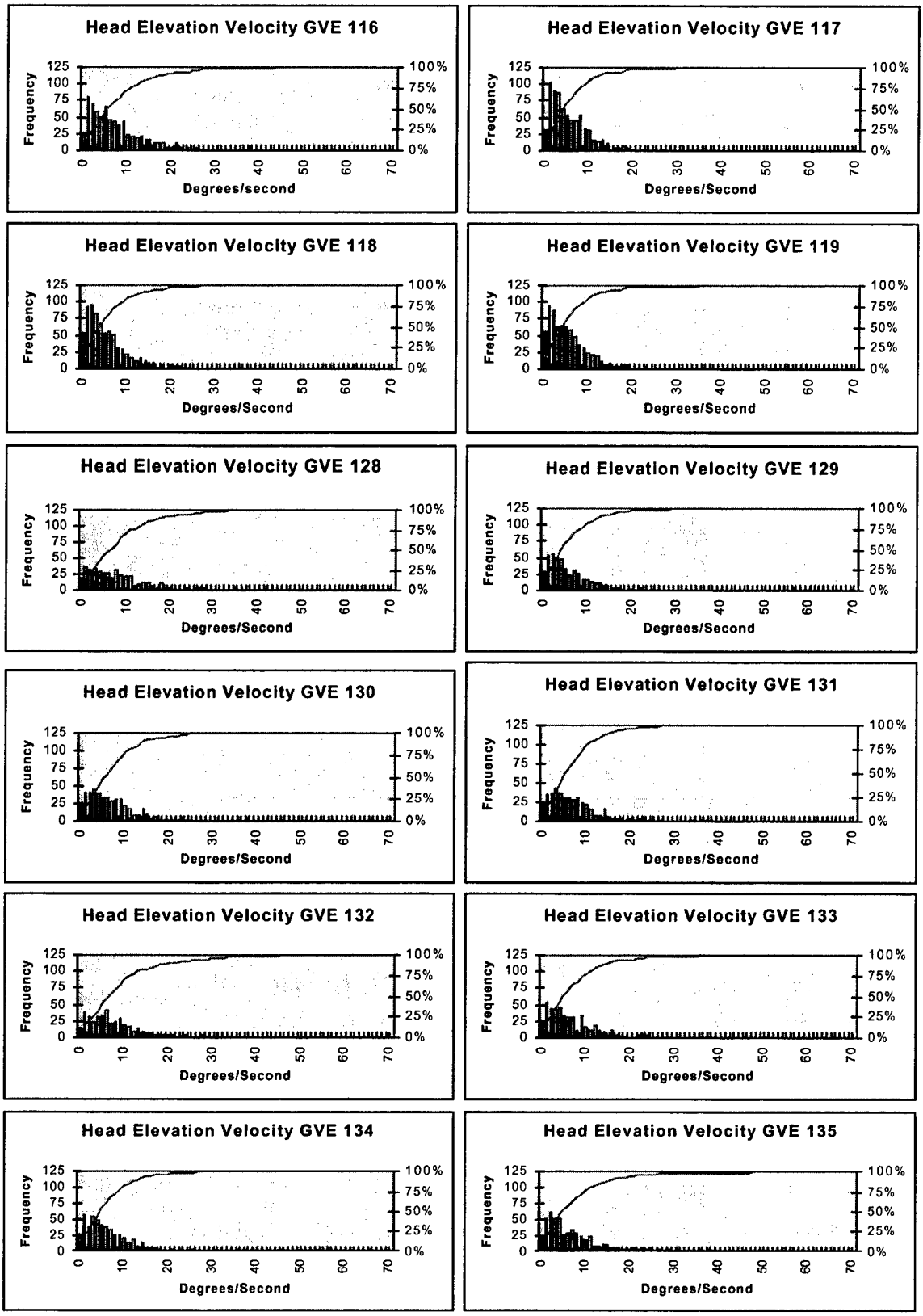

Figure H-1. Subject #1 GVE head velocity distributions with cumulative frequency curves.

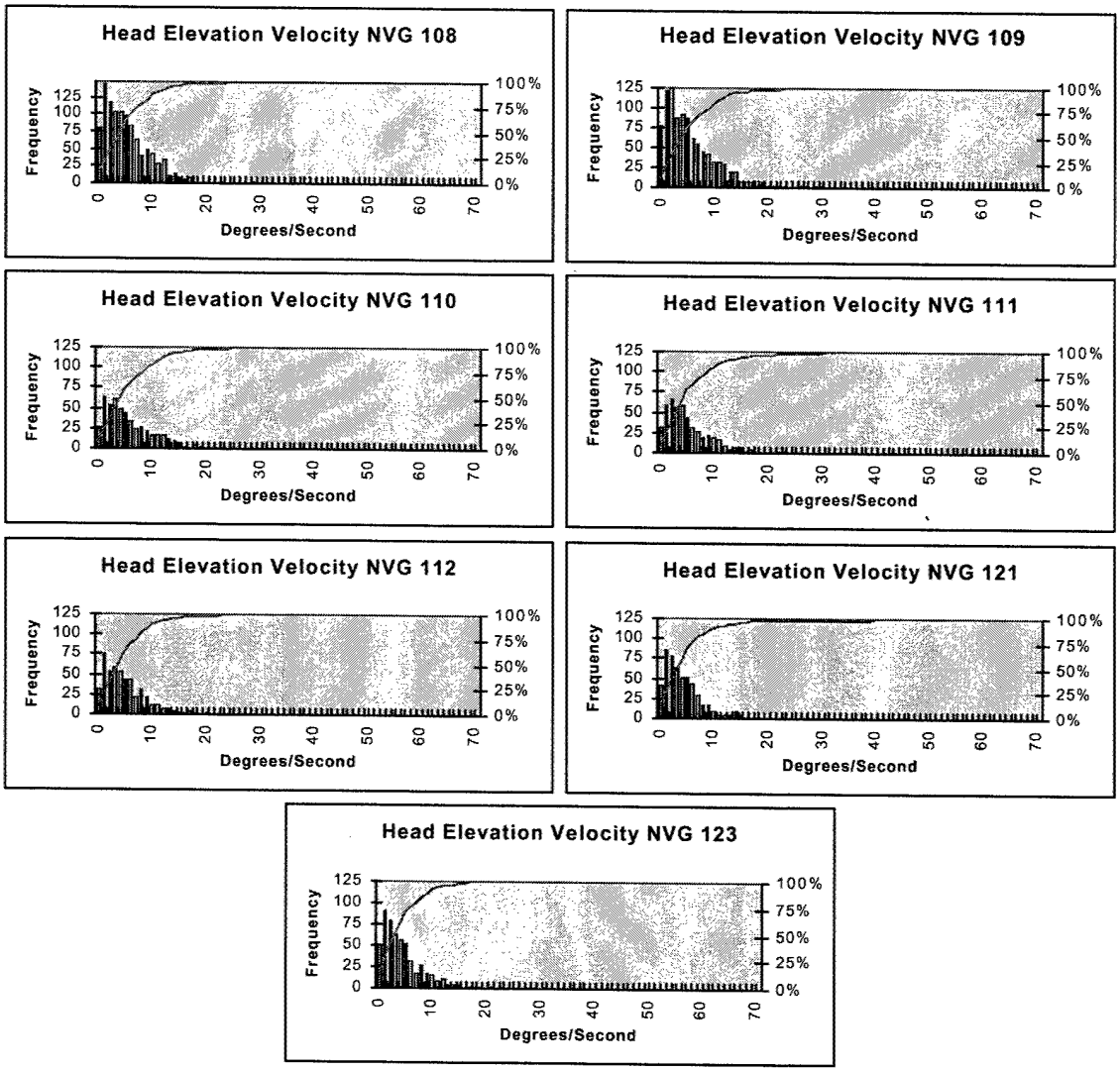

Figure H-2. Subject #1 NVG head velocity distributions with cumulative frequency curves.

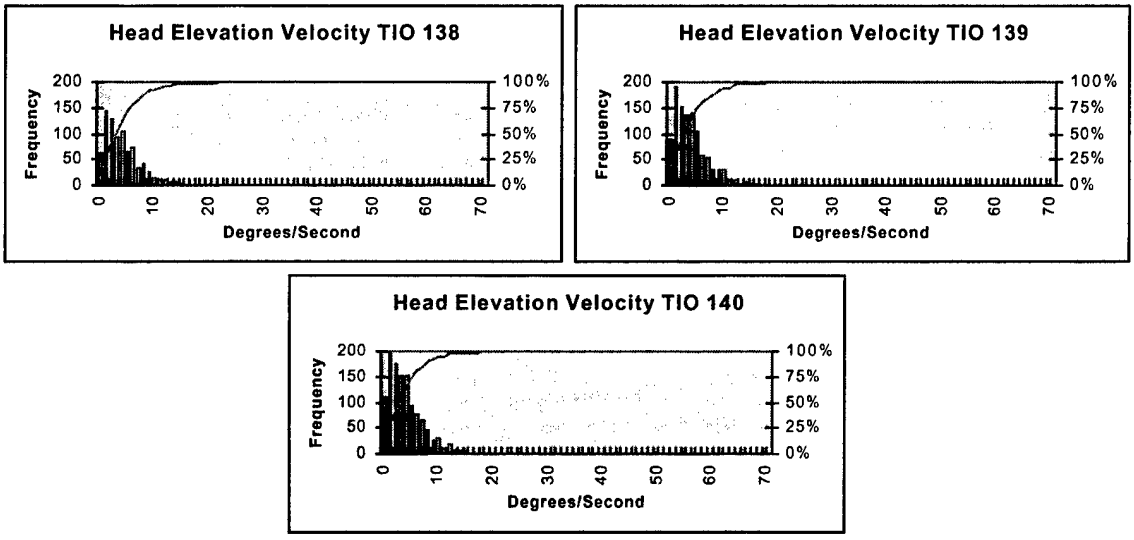

Figure H-3. Subject #1 TIO head velocity distributions with cumulative frequency curves.

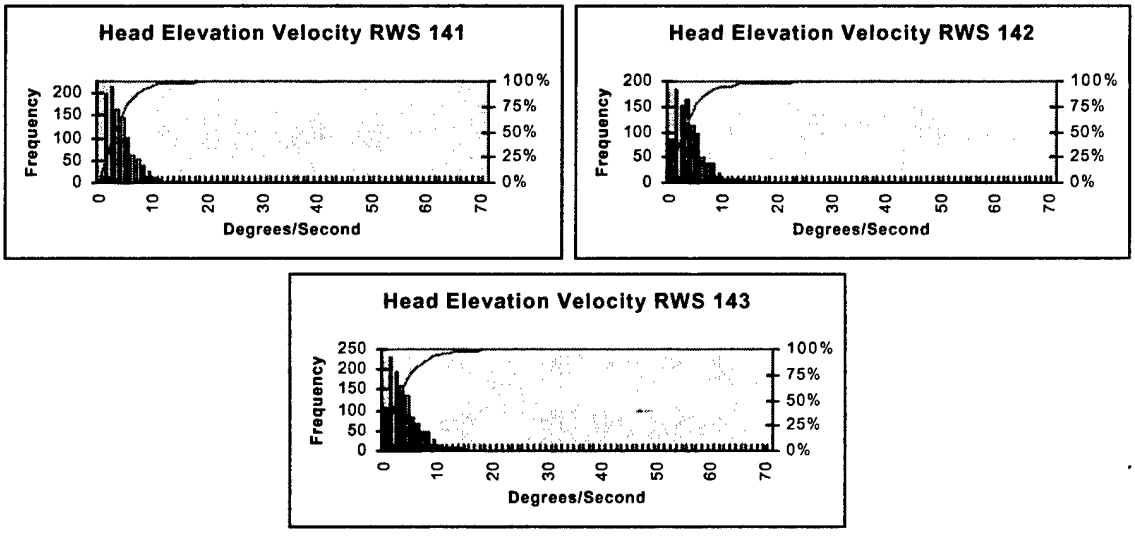

Figure H-4. Subject #1 RWS head velocity distributions with cumulative frequency curves.

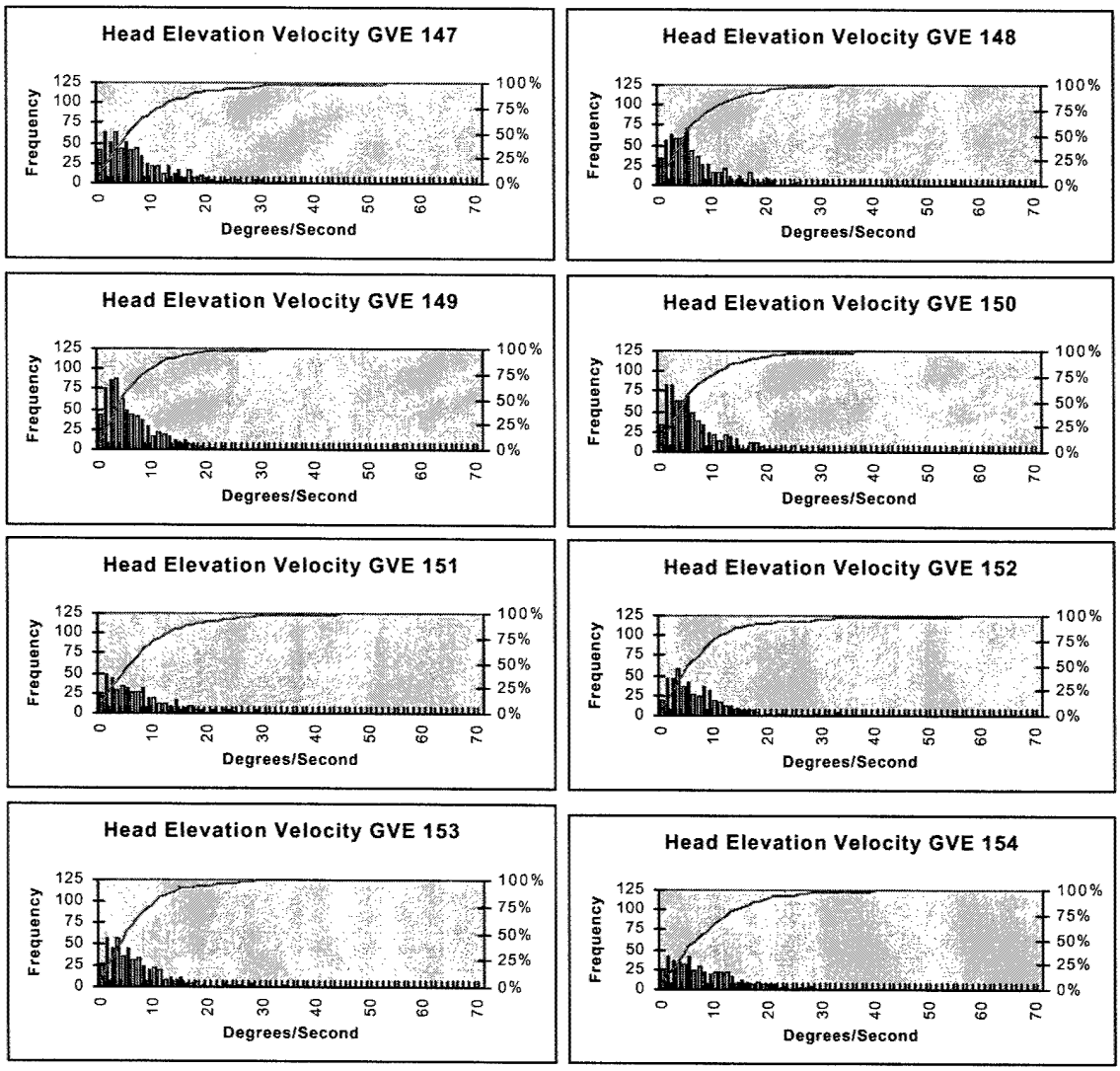

Figure H-5. Subject #2 GVE head velocity distributions with cumulative frequency curves.

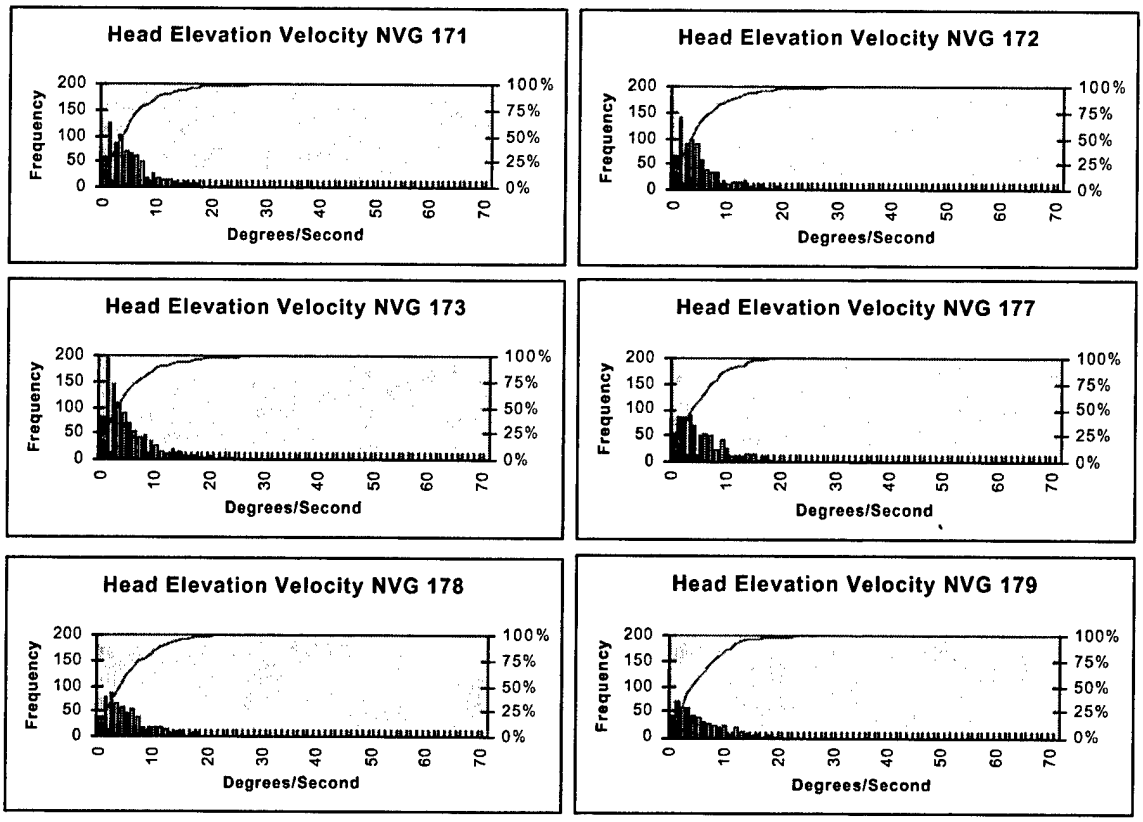

Figure H-6. Subject #2 NVG head velocity distributions with cumulative frequency curves.

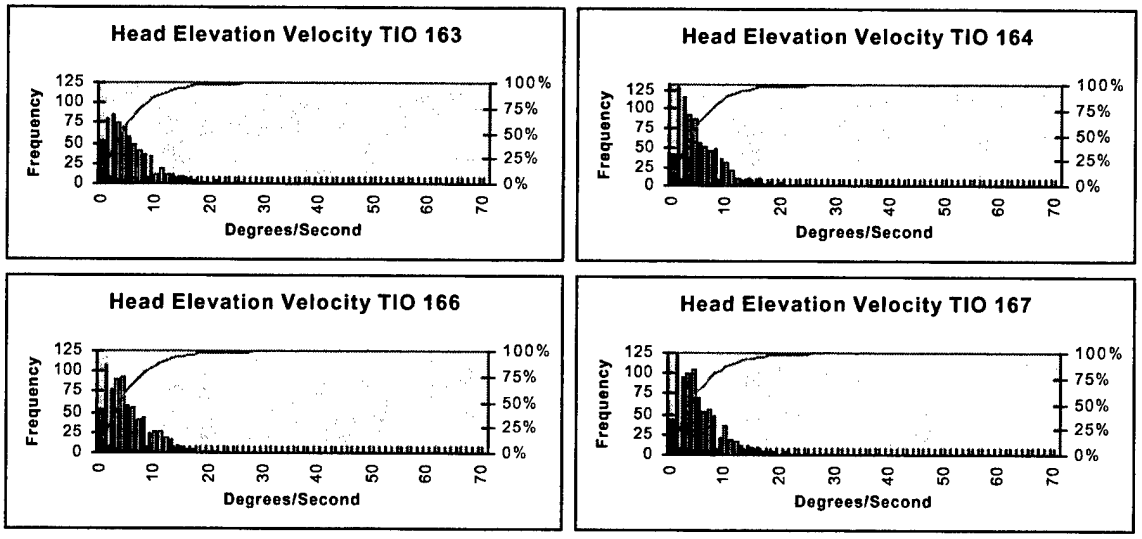

Figure H-7. Subject #2 TIO head velocity distributions with cumulative frequency curves.

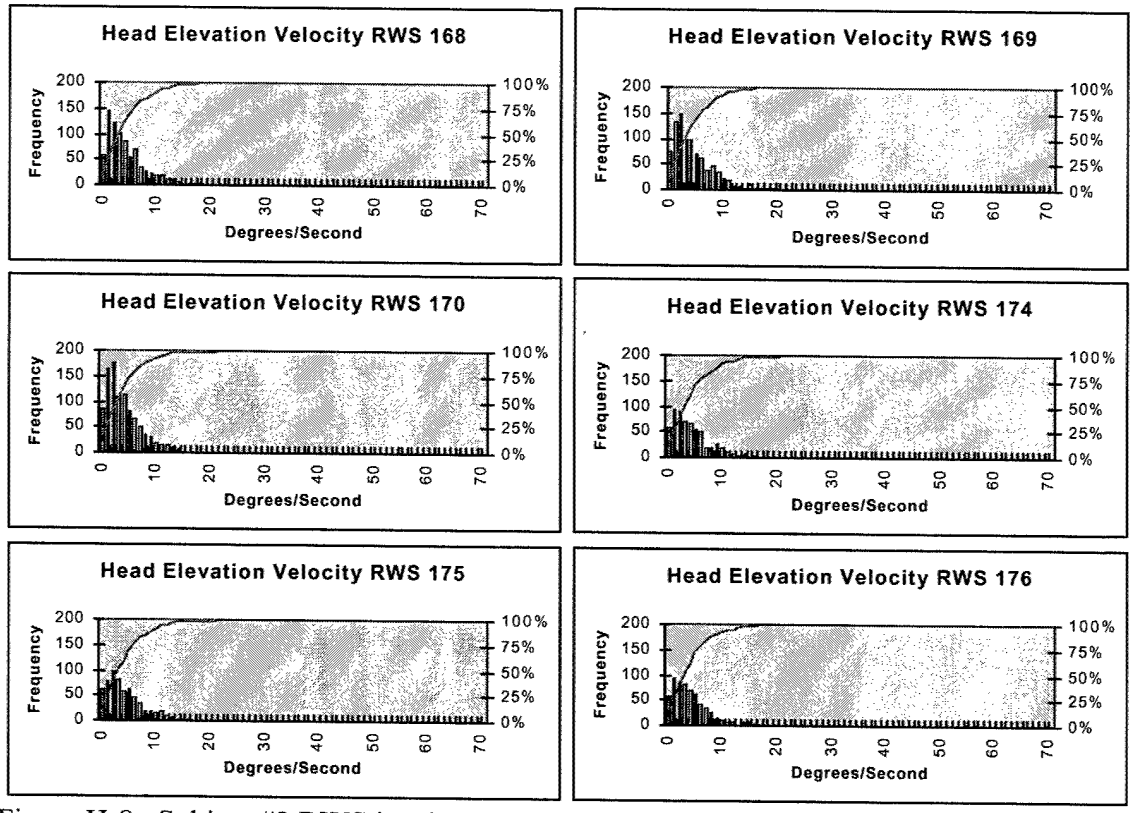

Figure H-8. Subject #2 RWS head velocity distributions with cumulative frequency curves.

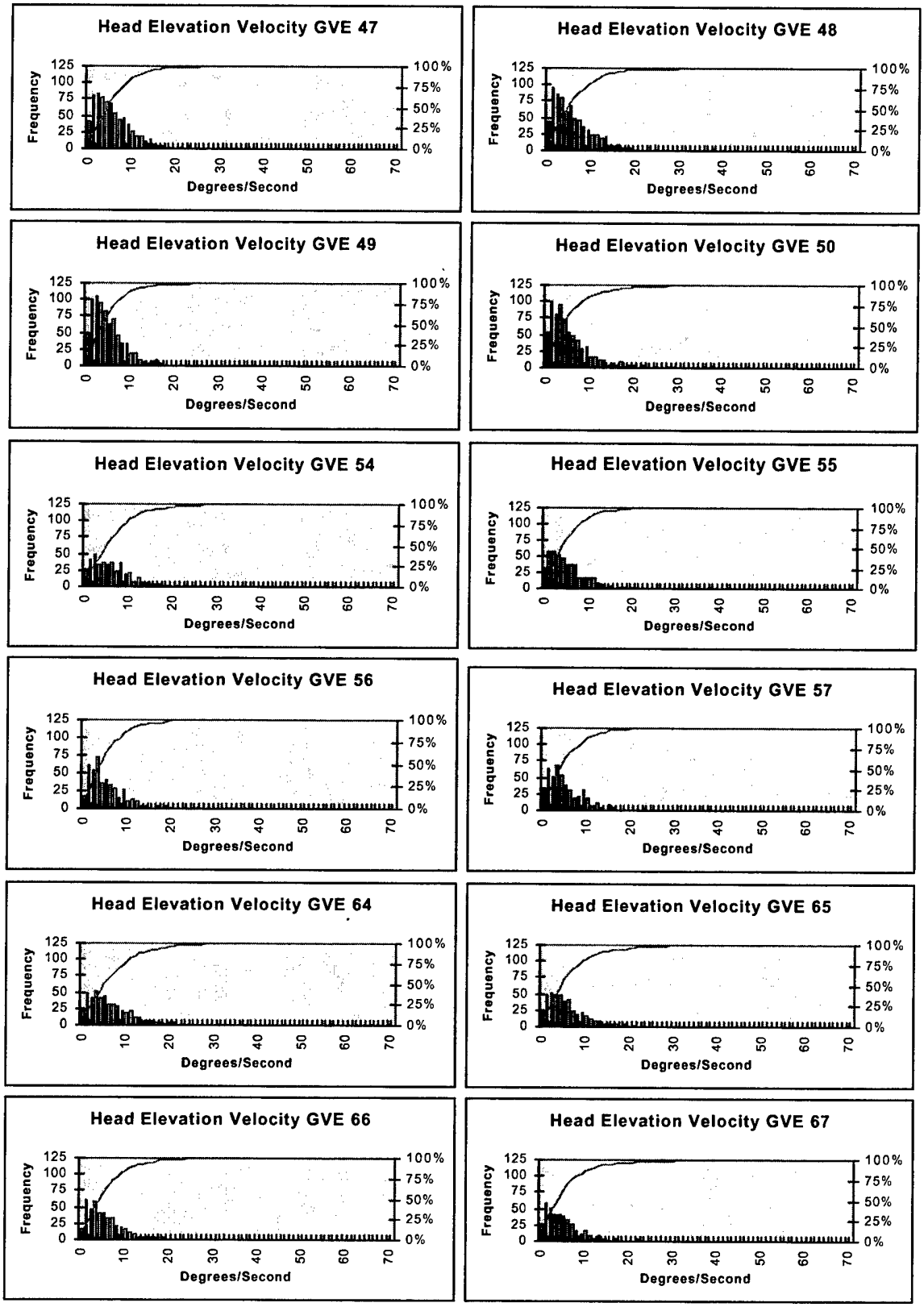

Figure H-9. Subject #3 GVE head velocity distributions with cumulative frequency curves.

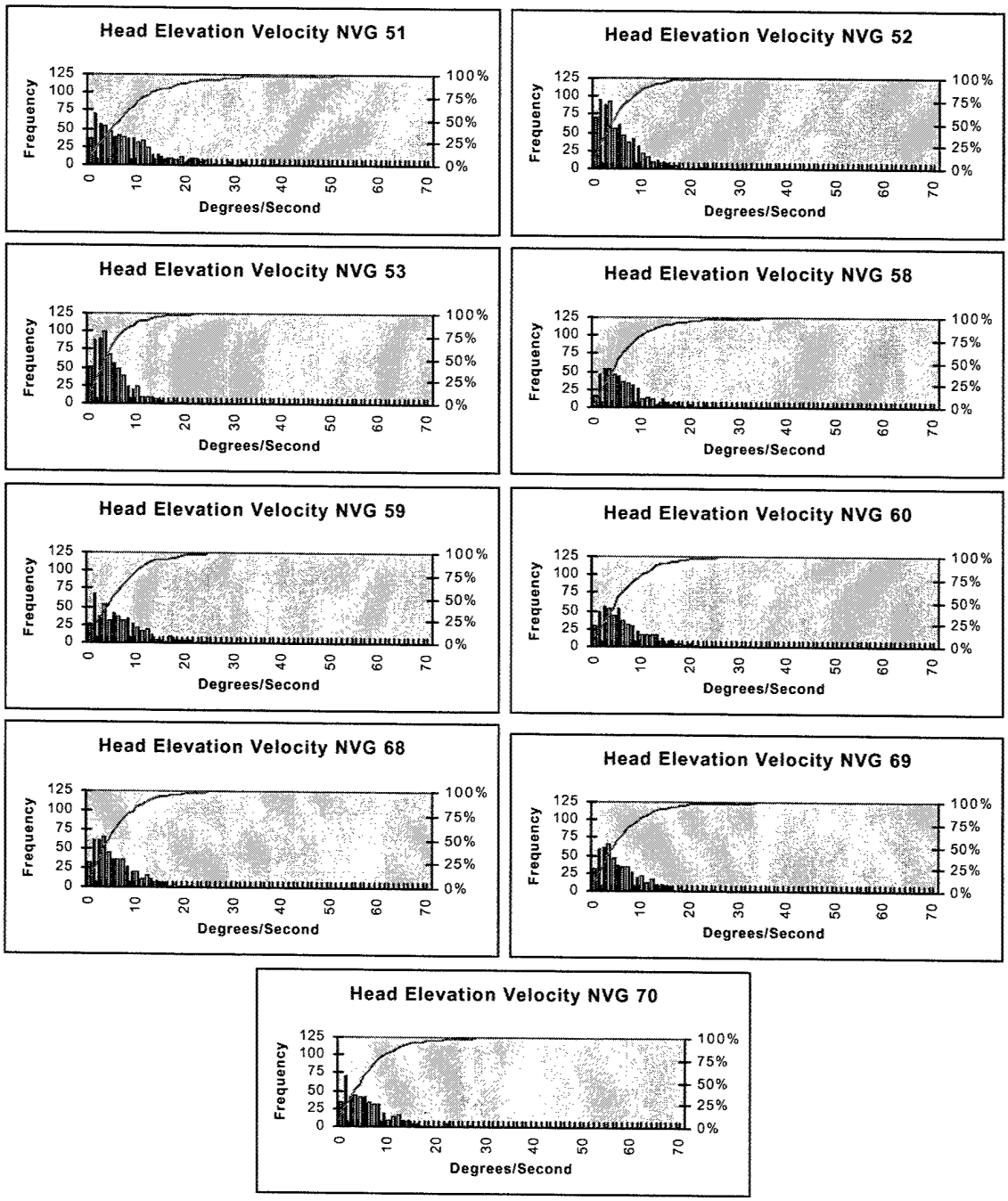

Figure H-10. Subject #3 NVG head velocity distributions with cumulative frequency curves.

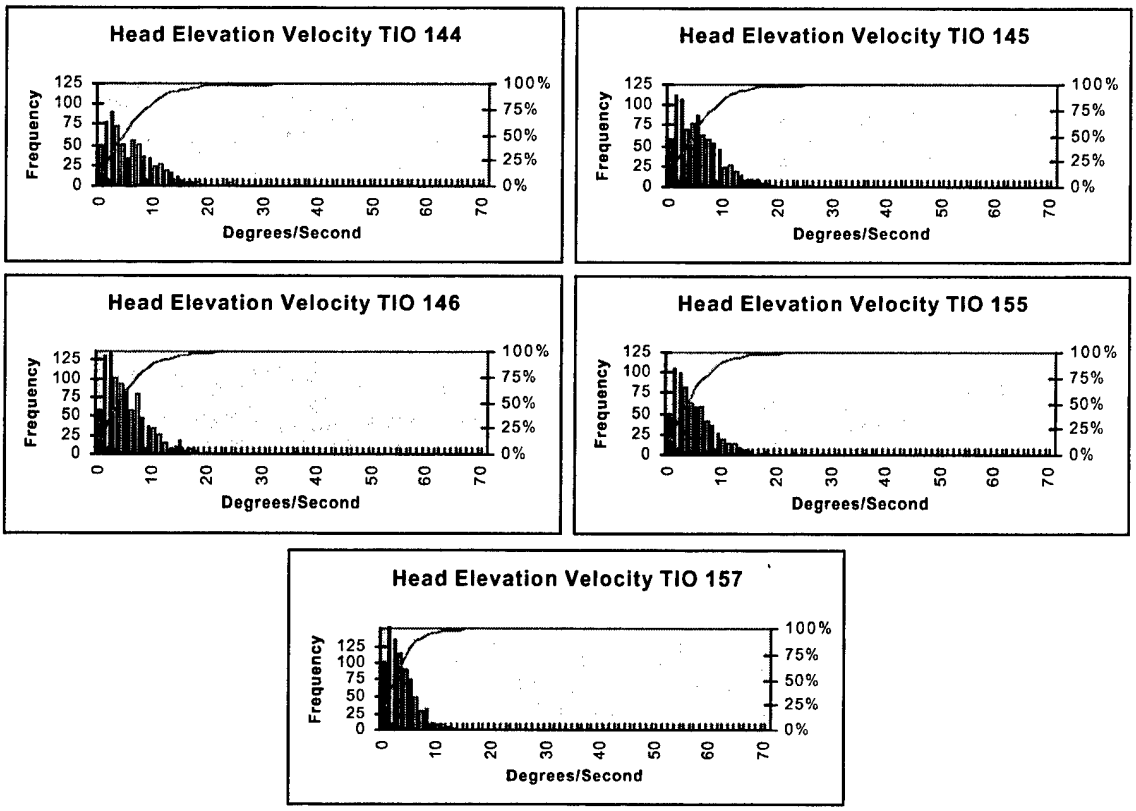

Figure H-11. Subject #3 TIO head velocity distributions with cumulative frequency curves.

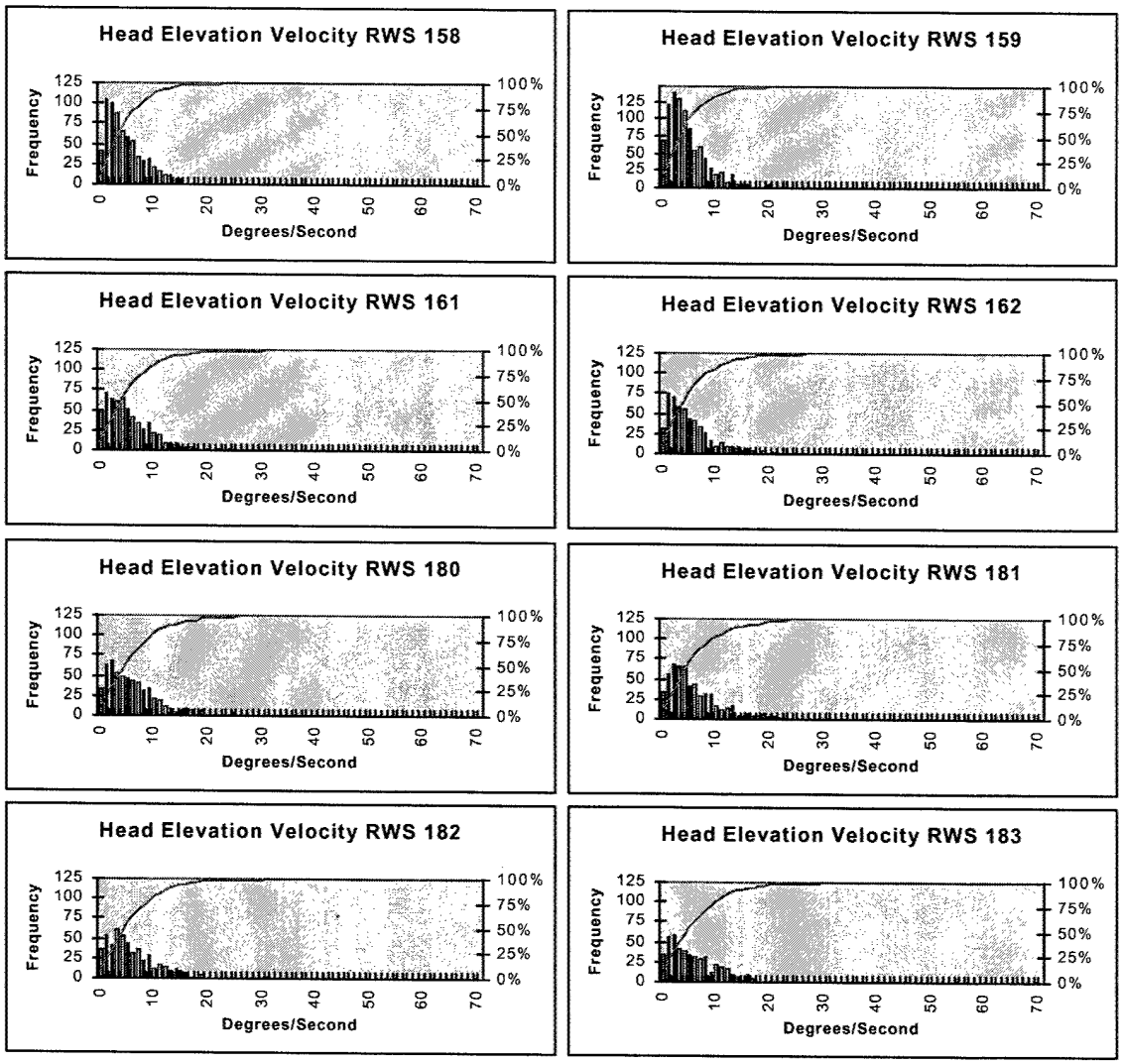

Figure H-12. Subject #3 RWS head velocity distributions with cumulative frequency curves.

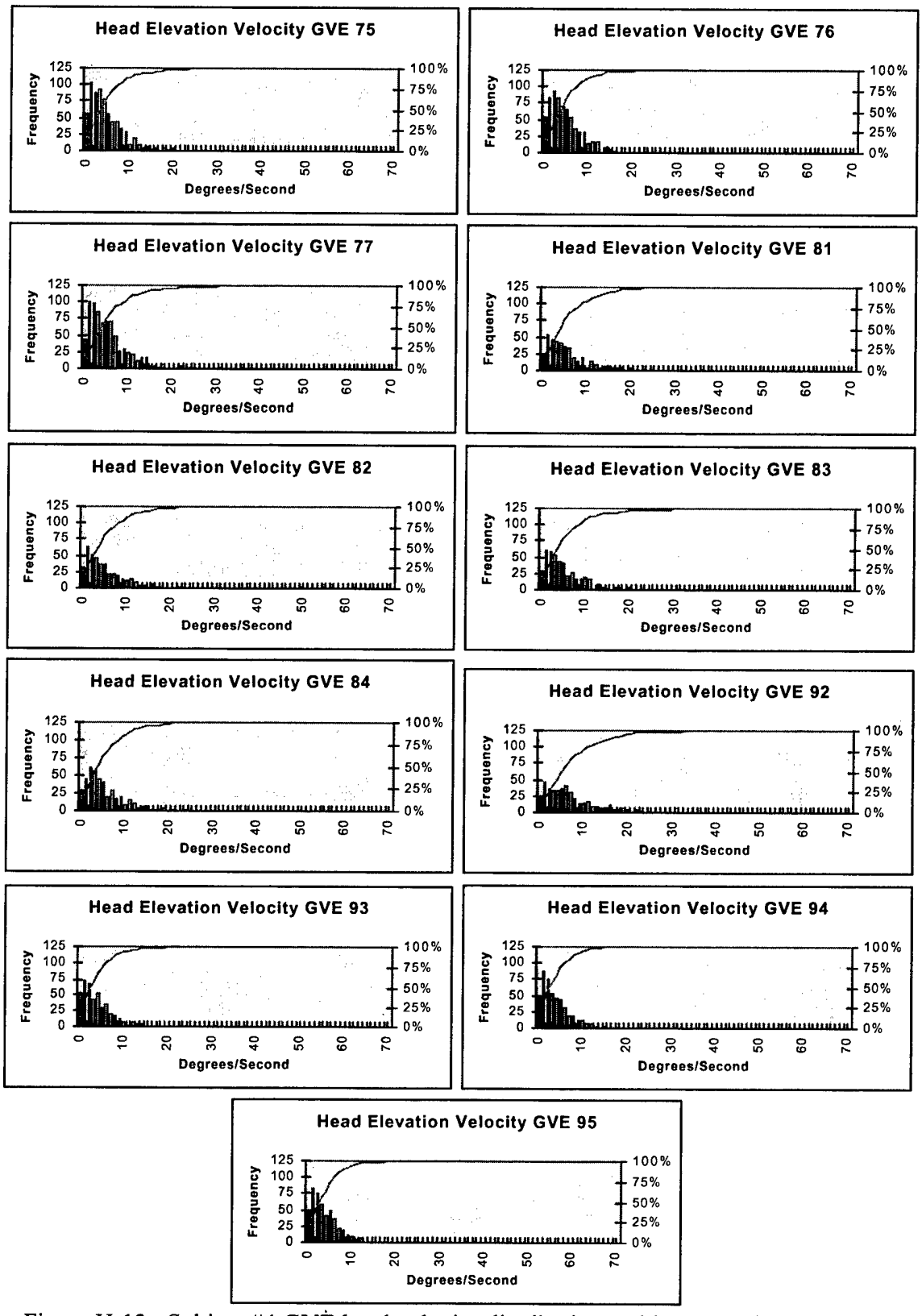

Figure H-13. Subject #4 GVE head velocity distributions with cumulative frequency curves.

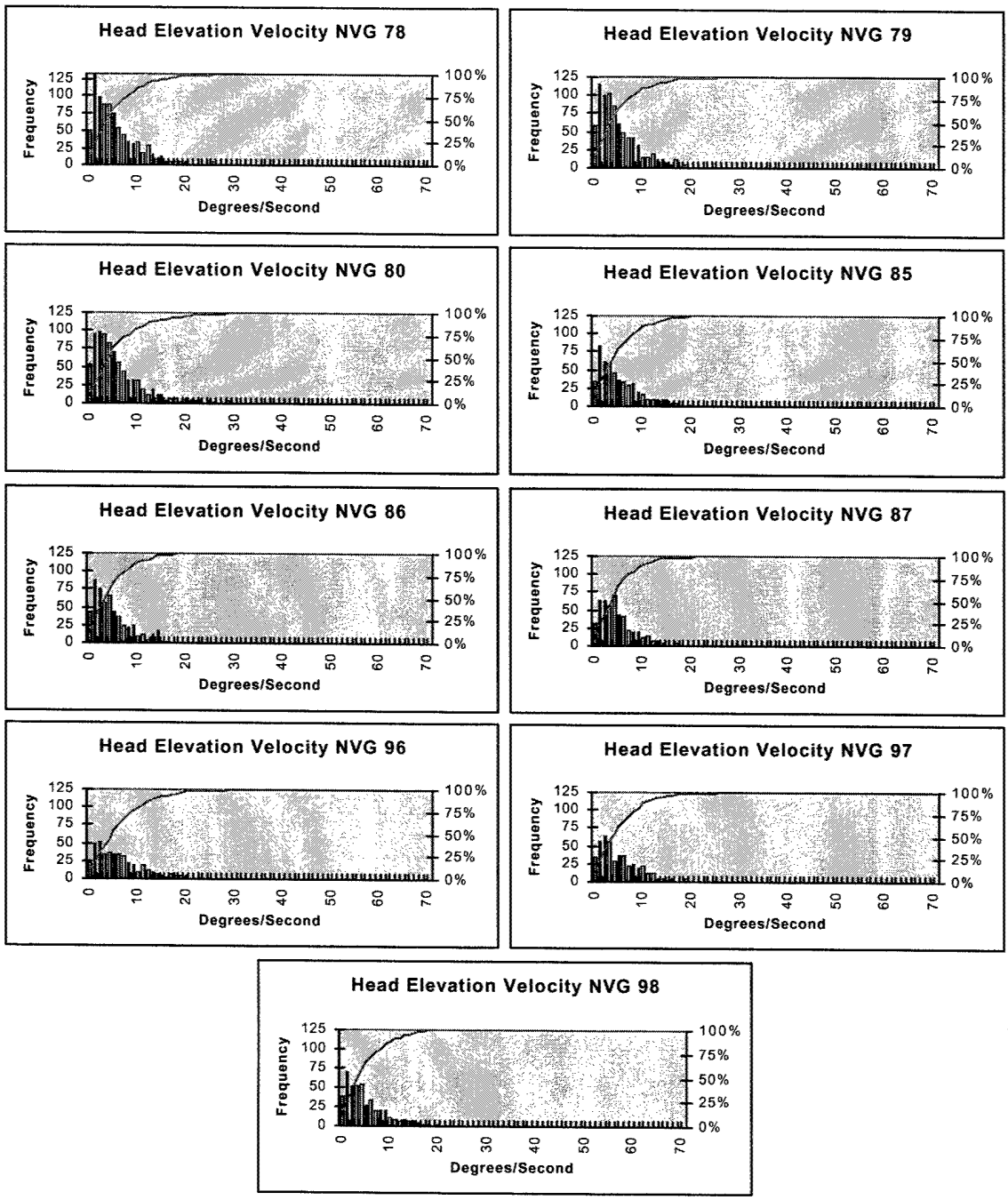

Figure H-14. Subject #4 NVG head velocity distributions with cumulative frequency curves.

Appendix I.

Elevation velocity summary tables for combined distributions.

Table I-1.
Summary statistics for elevation velocity, slalom course, GVE.
(velocity values expressed in degrees/sec, time in seconds)

Subject	Run	Time	Min	Max	Mean	Median	S.D.	Skewness	Kurtosis
1	116	76.9	0	55.0	8.1	6.0	7.7	2.1	6.5
1	117	75.7	0	48.0	5.9	4.0	5.5	2.2	8.5
1	118	76.9	0	52.0	5.9	4.0	5.6	2.2	8.6
1	119	76.0	0	57.0	5.9	5.0	6.0	2.9	14.5
1	128	45.2	0	54.0	8.9	7.0	8.2	2.0	6.1
1	129	48.1	0	36.0	6.0	4.0	5.4	1.7	4.0
1	130	48.6	0	42.0	7.3	6.0	6.1	1.7	4.6
1	131	43.8	0	37.0	7.0	6.0	5.6	1.5	3.3
1	132	45.6	0	53.0	9.3	7.0	8.8	2.0	4.8
1	133	49.8	0	51.0	7.0	5.0	6.5	2.0	6.6
1	134	51.1	0	34.0	6.5	5.0	5.5	1.5	3.2
1	135	52.9	0	54.0	7.5	5.0	7.4	2.2	7.4
Combined		**690.6**	**0**	**57.0**	**7.0**	**5.0**	**6.6**	**2.2**	**8.0**
2	147	68.4	0	58.0	8.5	6.0	8.6	2.2	6.7
2	148	65.1	0	52.0	7.2	5.0	6.8	2.2	7.6
2	149	71.7	0	42.0	6.2	4.0	5.7	1.8	4.9
2	150	73.9	0	51.0	7.0	5.0	6.8	2.0	6.0
2	151	47.0	0	59.0	8.2	6.0	8.0	2.0	6.3
2	152	52.2	0	78.0	8.1	6.0	8.7	3.1	14.1
2	153	51.7	0	111.0	7.2	5.0	8.1	5.3	55.3
2	154	50.4	0	41.0	8.7	7.0	7.5	1.4	2.5
Combined		**480.4**	**0**	**111.0**	**7.6**	**5.0**	**7.5**	**2.7**	**15.1**
3	47	74.8	0	34.0	5.7	5.0	4.8	1.6	4.1
3	48	75.7	0	39.0	5.8	5.0	5.1	1.8	5.8
3	49	78.8	0	29.0	4.9	4.0	4.1	1.7	4.4
3	50	73.2	0	35.0	5.5	4.0	5.3	1.9	4.7
3	54	44.6	0	30.0	6.5	5.0	5.5	1.5	2.9
3	55	47.6	0	33.0	5.3	4.0	4.5	1.6	4.2
3	56	46.5	0	35.0	5.5	4.0	4.8	2.0	5.9
3	57	49.0	0	27.0	5.1	4.0	4.3	1.3	2.1
3	64	50.6	0	29.0	6.9	5.0	5.8	1.3	1.9
3	65	46.8	0	32.0	6.2	5.0	5.5	1.7	3.6
3	66	46.7	0	30.0	5.8	5.0	4.8	1.5	2.9
3	67	43.4	0	41.0	5.6	4.0	5.4	2.3	7.9
Combined		**677.7**	**0**	**41.0**	**5.7**	**4.0**	**5.0**	**1.8**	**4.5**
4	75	72.4	0	39.0	5.0	4.0	4.8	2.2	7.8
4	76	69.0	0	25.0	4.7	4.0	3.9	1.4	2.7
4	77	79.8	0	38.0	5.9	4.0	5.6	2.1	5.6
4	81	42.0	0	24.0	5.7	4.0	4.9	1.3	1.4
4	82	42.6	0	25.0	5.2	4.0	4.7	1.4	2.2
4	83	46.0	0	35.0	5.5	4.0	5.2	2.1	5.8
4	84	45.0	0	33.0	5.5	4.0	5.0	1.8	4.5
4	92	44.4	0	39.0	7.1	6.0	6.1	1.5	3.2
4	93	43.6	0	27.0	4.0	3.0	3.7	1.8	5.6
4	94	48.0	0	20.0	3.8	3.0	3.3	1.3	1.7
4	95	49.2	0	27.0	3.9	3.0	3.5	1.7	5.5
Combined		**582.0**	**0**	**39.0**	**5.1**	**4.0**	**4.8**	**2.0**	**5.8**
All Subjects		**2430.7**	**0**	**111.0**	**6.3**	**5.0**	**6.1**	**2.5**	**12.6**

Table I-2.
Summary statistics for elevation velocity, slalom course, NVG.
(velocity values expressed in degrees/sec, time in seconds)

Subject	Run	Time	Min	Max	Mean	Median	S.D.	Skewness	Kurtosis
1	108	105.7	0	29.0	5.3	4.0	4.5	1.5	3.5
1	109	98.2	0	30.0	5.6	4.0	4.8	1.4	2.7
1	110	51.3	0	28.0	5.7	4.0	4.8	1.3	2.1
1	111	51.7	0	36.0	5.7	4.0	5.4	2.0	5.7
1	112	51.1	0	32.0	5.1	4.0	4.4	1.8	5.5
1	121	54.0	0	46.0	4.8	3.5	5.4	3.7	20.7
1	123	55.2	0	27.0	4.4	3.0	4.0	1.6	3.5
Combined		**467.2**	**0**	**46.0**	**5.3**	**4.0**	**4.8**	**2.0**	**7.0**
2	171	80.0	0	48.0	5.2	4.0	5.2	2.5	11.4
2	172	80.9	0	45.0	5.1	4.0	5.3	2.5	10.5
2	173	103.2	0	34.0	5.0	3.0	5.0	1.9	4.4
2	177	70.6	0	46.0	5.5	4.0	5.0	2.3	10.4
2	178	63.0	0	26.0	5.4	4.0	4.6	1.2	1.4
2	179	54.3	0	40.0	5.6	4.0	5.0	1.8	6.6
Combined		**452.0**	**0**	**48.0**	**5.2**	**4.0**	**5.1**	**2.1**	**8.0**
3	51	71.8	0	66.0	8.8	7.0	8.7	2.2	7.0
3	52	73.9	0	30.0	5.0	4.0	4.5	1.5	3.0
3	53	68.2	0	29.0	4.8	4.0	4.2	1.7	3.9
3	58	50.5	0	39.0	6.8	5.0	6.0	2.0	5.6
3	59	51.9	0	30.0	6.5	5.0	5.3	1.2	1.7
3	60	52.6	0	31.0	6.4	5.0	5.3	1.3	2.1
3	68	53.6	0	36.0	6.1	5.0	5.6	1.9	5.6
3	69	53.8	0	36.0	6.1	4.5	5.6	1.9	5.6
3	70	48.8	0	37.0	6.0	5.0	5.5	1.8	4.4
Combined		**525.1**	**0**	**66.0**	**6.3**	**5.0**	**5.9**	**2.2**	**8.9**
4	78	95.3	0	45.0	5.6	4.0	5.2	2.0	6.7
4	79	81.9	0	38.0	5.2	4.0	4.8	1.9	5.5
4	80	83.9	0	37.0	6.1	4.0	5.7	1.8	3.6
4	85	52.7	0	24.0	5.2	4.0	4.5	1.2	1.2
4	86	56.0	0	29.0	4.7	4.0	4.1	1.4	2.6
4	87	49.8	0	23.0	4.8	4.0	4.0	1.4	2.6
4	96	44.6	0	40.0	6.6	5.0	5.8	1.7	4.5
4	97	47.0	0	34.0	5.3	4.0	4.6	1.7	4.8
4	98	46.1	0	26.0	5.0	4.0	4.5	1.4	2.0
Combined		**557.3**	**0**	**45.0**	**5.4**	**4.0**	**4.9**	**1.8**	**5.0**
All Subjects		**2001.6**	**0**	**66.0**	**5.6**	**4.0**	**5.2**	**2.1**	**8.1**

Table I-3.
Summary statistics for elevation velocity, slalom course, TIO.
(velocity values expressed in degrees/sec, time in seconds)

Subject	Run	Time	Min	Max	Mean	Median	S.D.	Skewness	Kurtosis
1	138	85.7	0	29.0	4.3	3.0	3.8	1.9	6.1
1	139	109.7	0	26.0	4.0	3.0	3.5	1.7	4.8
1	140	120.4	0	24.0	4.0	3.0	3.4	1.4	2.8
Combined		**315.8**	**0**	**29.0**	**4.1**	**3.0**	**3.6**	**1.7**	**4.7**
2	163	70.0	0	29.0	5.4	4.0	4.7	1.5	2.9
2	164	82.5	0	28.0	5.2	4.0	4.5	1.6	3.7
2	166	80.1	0	45.0	5.6	4.0	5.2	2.3	9.6
2	167	88.1	0	39.0	5.5	4.0	5.0	2.0	6.2
Combined		**320.7**	**0**	**45.0**	**5.4**	**4.0**	**4.9**	**1.9**	**6.3**
3	144	70.9	0	41.0	6.0	5.0	5.5	1.9	5.9
3	145	89.3	0	29.0	5.5	5.0	4.6	1.4	2.8
3	146	97.9	0	29.0	5.3	4.0	4.5	1.5	2.9
3	155	71.9	0	34.0	4.9	4.0	4.2	1.7	4.7
3	157	84.4	0	21.0	3.3	3.0	2.9	1.5	3.3
Combined		**414.4**	**0**	**41.0**	**5.0**	**4.0**	**4.5**	**1.8**	**5.3**
4	None								
All Subjects		**1059.9**	**0**	**45.0**	**4.9**	**4.0**	**4.4**	**1.9**	**6.2**

Table I-4.
Summary statistics for elevation velocity, slalom course, RWS.
(velocity values expressed in degrees/sec, time in seconds)

Subject	Run	Time	Min	Max	Mean	Median	S.D.	Skewness	Kurtosis
1	141	106.2	0	24.4	3.4	2.7	3.0	2.0	6.1
1	142	102.0	0	47.0	3.9	3.0	3.9	3.5	23.4
1	143	120.0	0	28.0	3.8	3.0	3.5	1.9	6.1
Combined		**328.2**	**0**	**47.0**	**3.7**	**3.0**	**3.5**	**2.7**	**15.1**
2	168	83.2	0	22.0	4.4	3.0	3.8	1.3	1.8
2	169	89.1	0	30.0	4.5	3.0	4.1	1.9	5.7
2	170	101.1	0	27.0	4.2	3.0	3.8	1.9	5.4
2	174	63.6	0	39.0	4.5	3.0	4.2	2.6	13.8
2	175	65.0	0	29.0	4.6	3.0	4.0	1.7	4.4
2	176	63.8	0	24.0	4.2	3.0	3.6	1.4	2.8
Combined		**465.8**	**0**	**39.0**	**4.4**	**3.0**	**3.9**	**1.8**	**6.1**
3	158	71.2	0	31.0	4.9	4.0	4.3	1.8	5.2
3	159	94.8	0	28.0	4.6	4.0	3.9	1.5	3.1
3	161	61.2	0	51.0	5.8	4.0	5.5	2.5	11.4
3	162	55.3	0	32.0	5.5	4.0	4.9	1.7	3.8
3	180	59.6	0	35.0	6.3	5.0	5.4	1.6	3.2
3	181	58.9	0	32.0	6.1	5.0	5.3	1.5	2.5
3	182	52.9	0	35.0	6.2	5.0	5.5	1.7	4.3
3	183	43.9	0	33.0	6.2	5.0	5.5	1.6	3.4
Combine d		**497.8**	**0**	**51.0**	**5.6**	**4.0**	**5.0**	**1.8**	**5.5**
4	None								
All Subjects		**1291.8**	**0**	**51.0**	**4.7**	**4.0**	**4.3**	**2.1**	**7.5**

Appendix J.

Elevation velocity box plots.

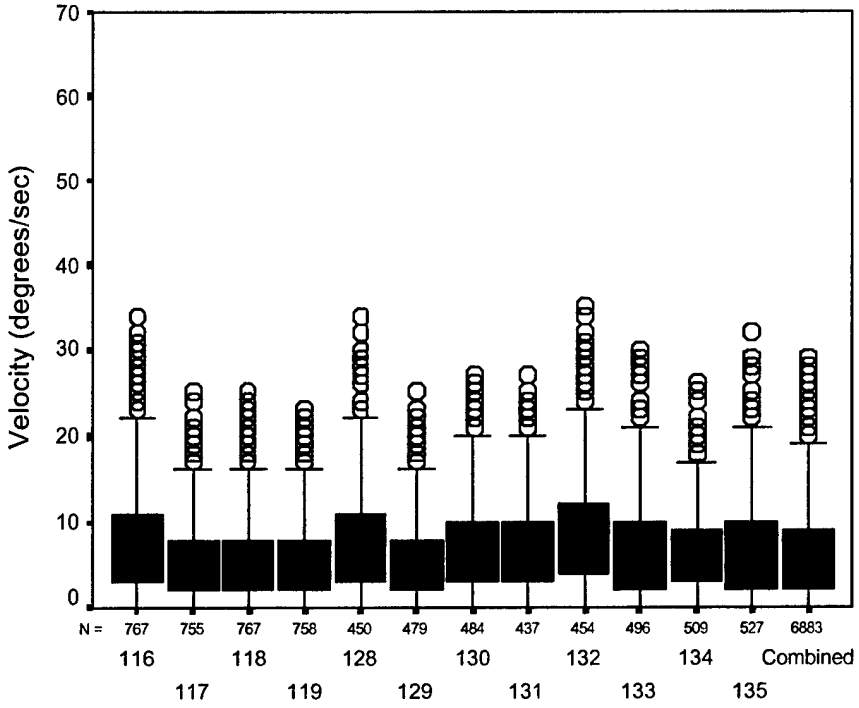

Figure J-1. Subject #1 GVE head velocity box plots.

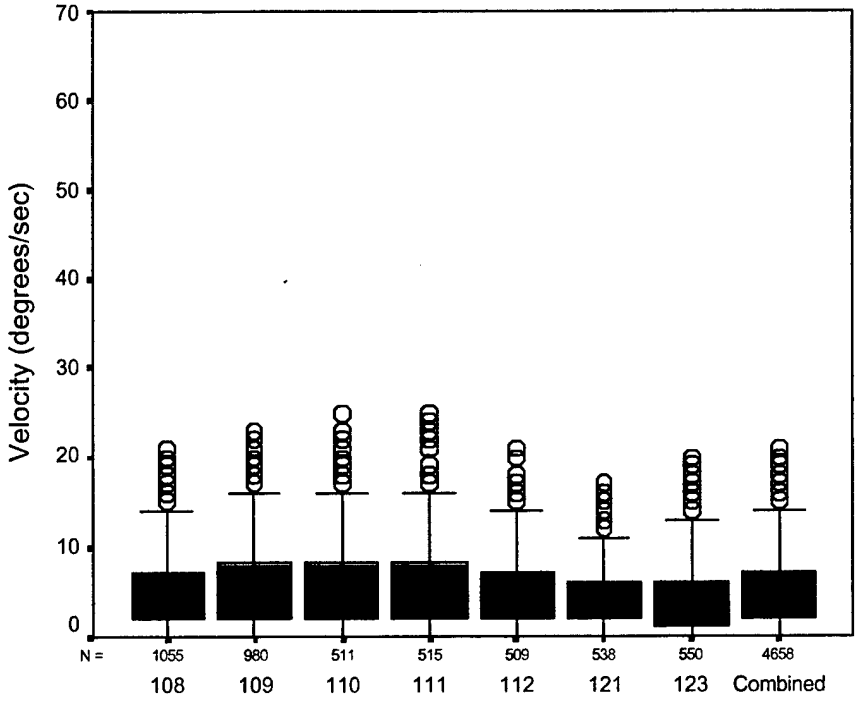

Figure J-2. Subject #1 NVG head velocity box plots.

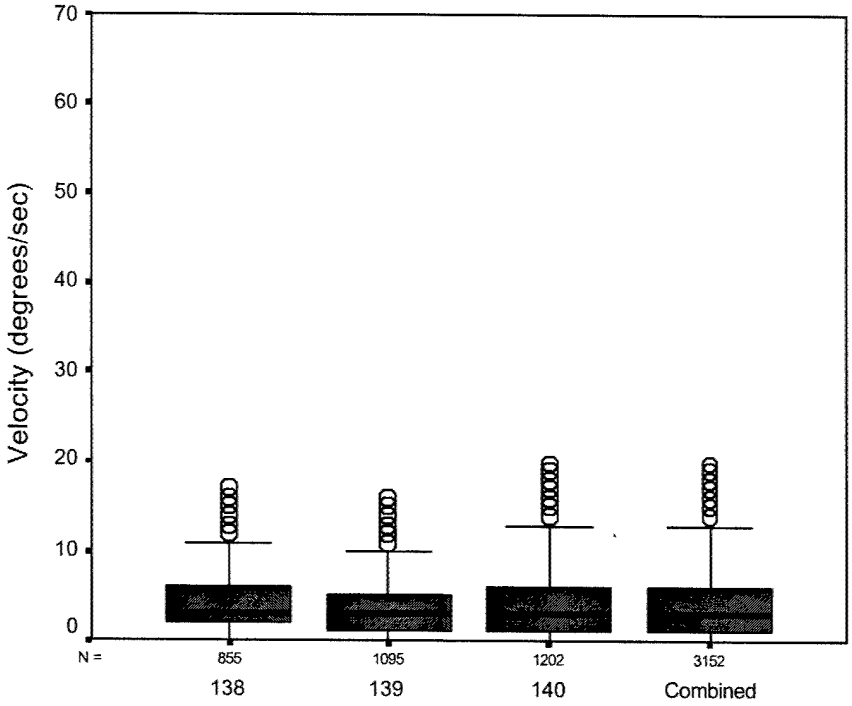

Figure J-3. Subject #1 TIO head velocity box plots.

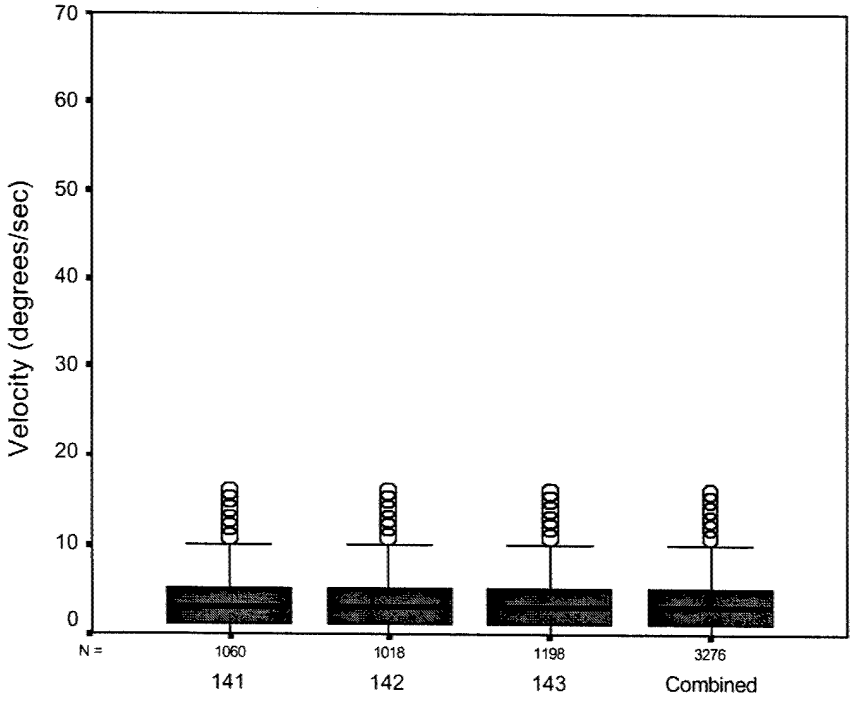

Figure J-4. Subject #1 RWS head velocity box plots.

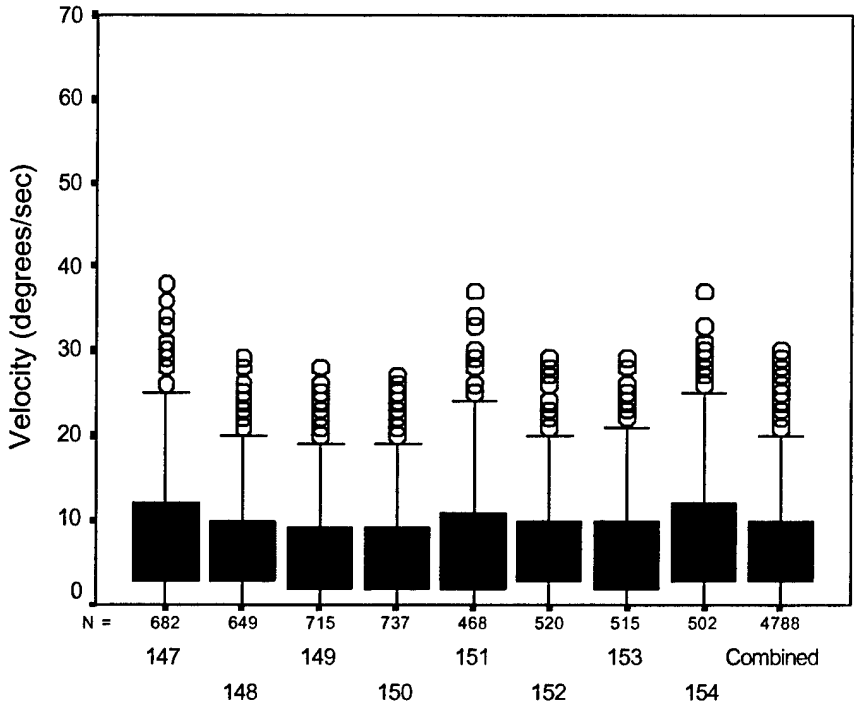

Figure J-5. Subject #2 GVE head velocity box plots.

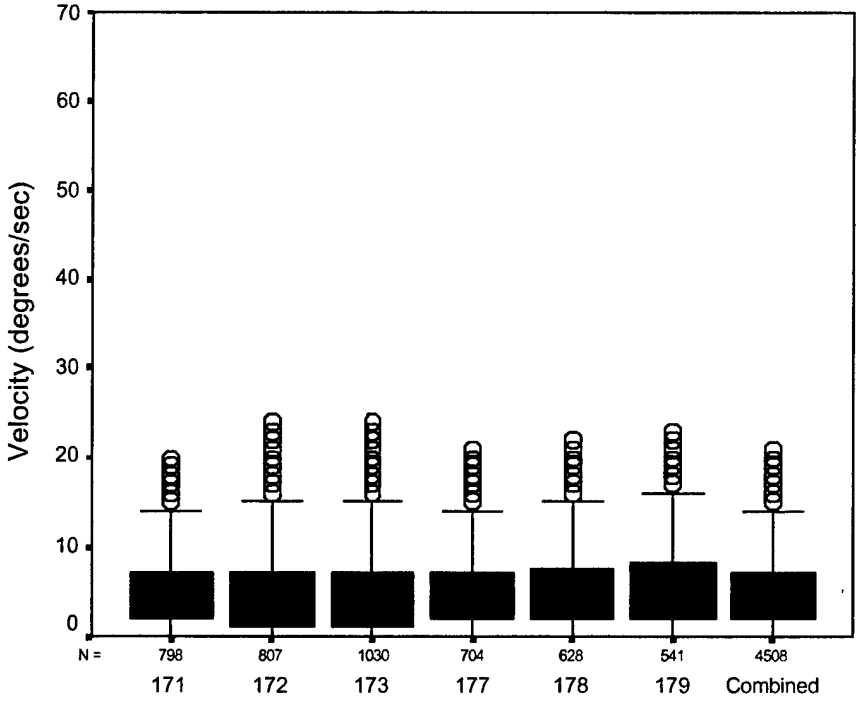

Figure J-6. Subject #2 NVG head velocity box plots.

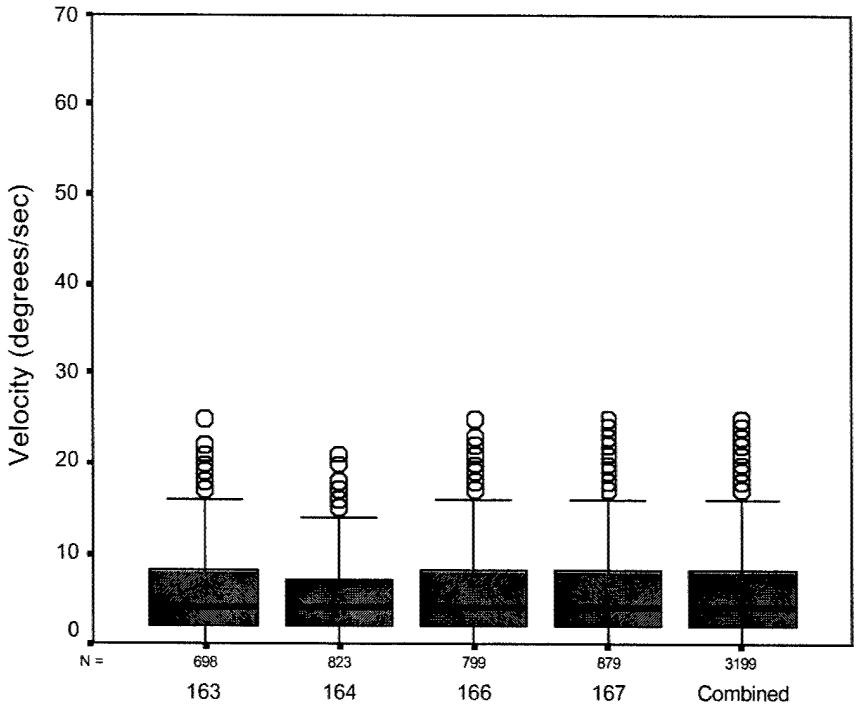

Figure J-7. Subject #2 TIO head velocity box plots.

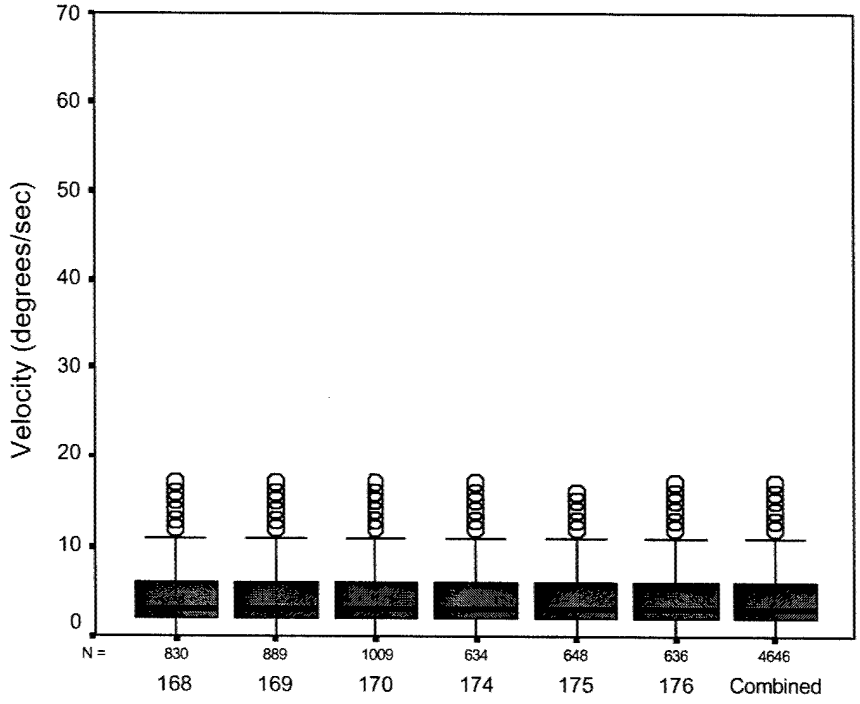

Figure J-8. Subject #2 RWS head velocity box plots.

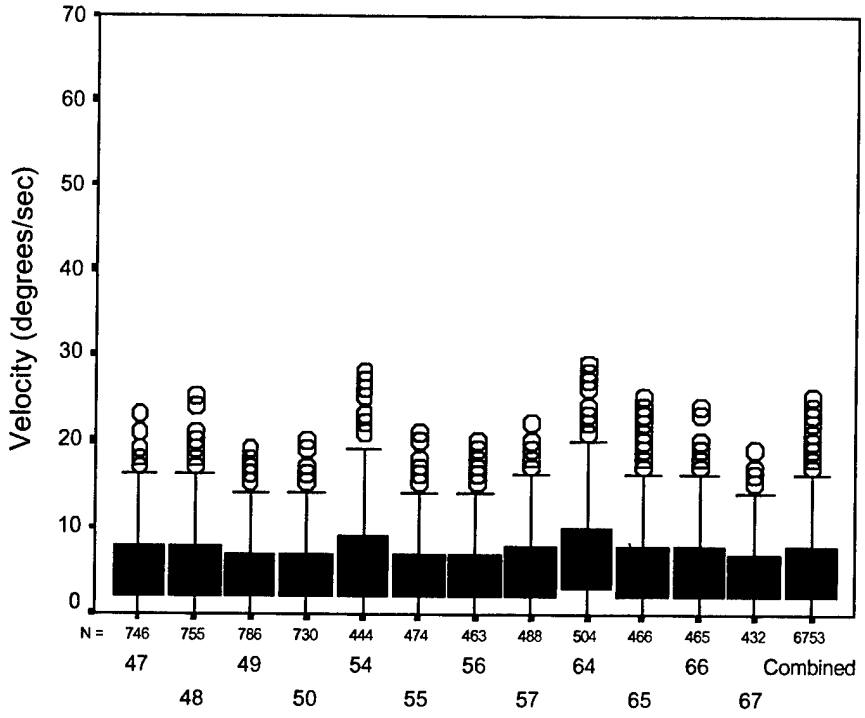

Figure J-9. Subject #3 GVE head velocity box plots.

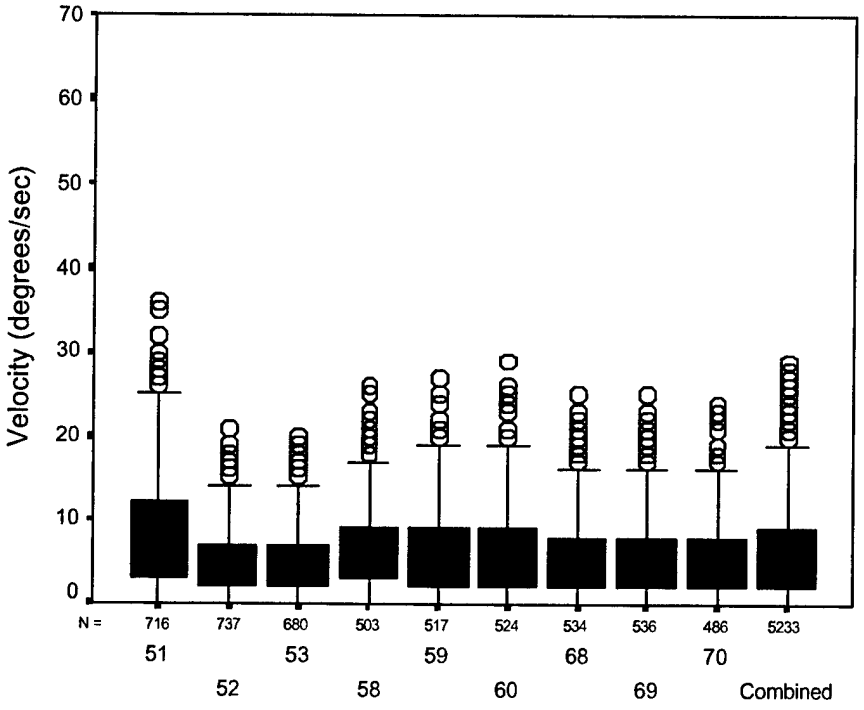

Figure J-10. Subject #3 NVG head velocity box plots.

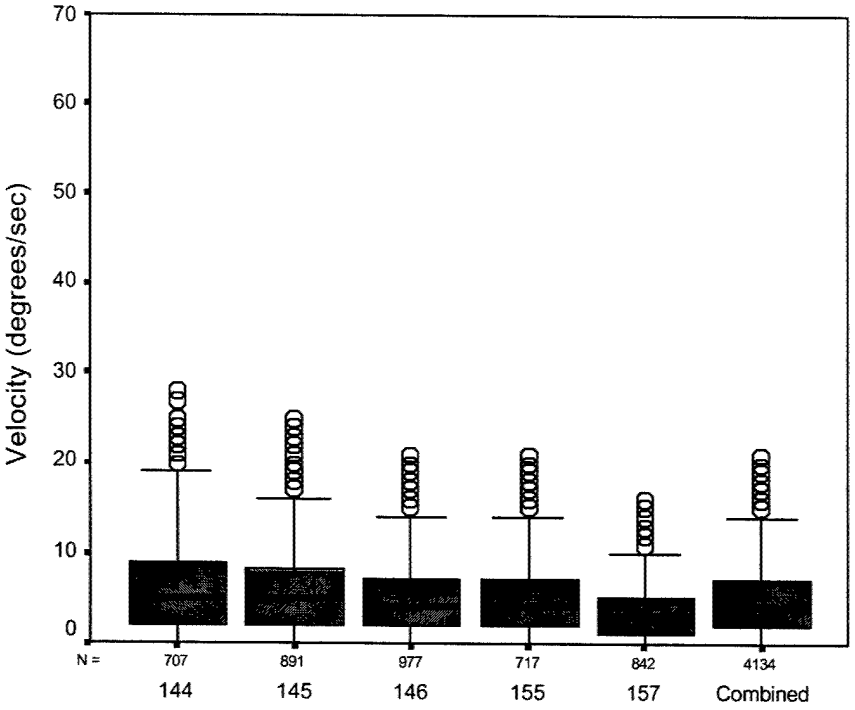

Figure J-11. Subject #3 TIO head velocity box plots.

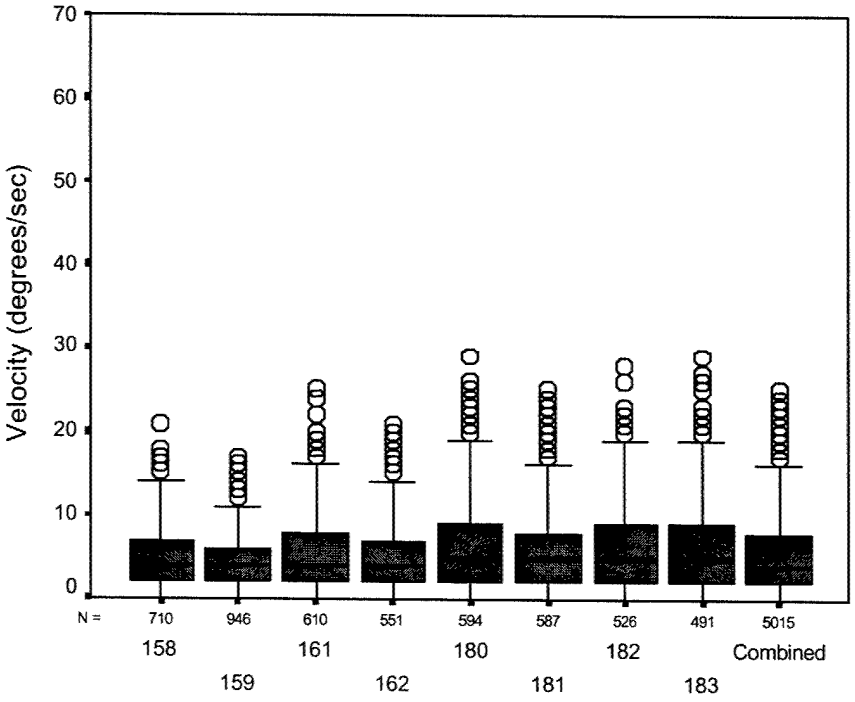

Figure J-12. Subject #3 RWS head velocity box plots.

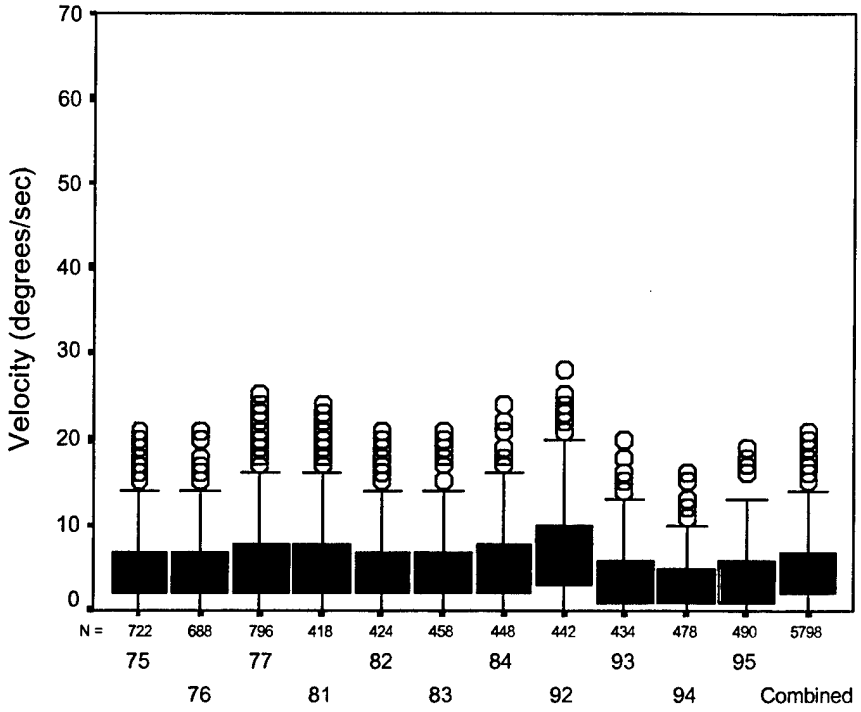

Figure J-13. Subject #4 GVE head velocity box plots.

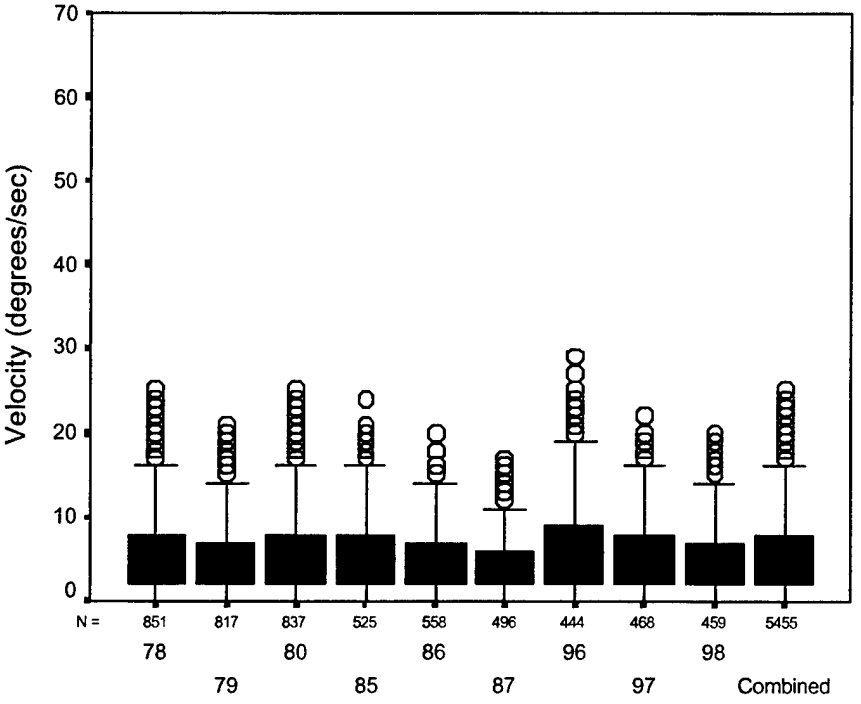

Figure J-14. Subject #4 NVG head velocity box plots.